Declaration

I declare that this thesis has been composed by myself, describes my own work and has not been submitted in any other application for a higher degree.

Henry McSorley
April 2008

Acknowledgements

This PhD would not have been possible without the constant help and support of the whole Maizels group. Rick Maizels has been an excellent supervisor, and has given me every opportunity during my time in the lab to take my research in new directions and further my career. Matthew Taylor's advice in the laboratory on immunology, and outside the laboratory on rock-climbing, was extremely valuable. In the (increasingly crowded) Maizels office, a chat was never too far away and the excellent atmosphere got everyone through many a long hard day. Yvonne Harcus and Janice Murray carried out the largely thankless task of running the parasite and mosquito lifecycles, were always around to lend a helping hand, and without them my PhD (as well as many other Maizels group student's) would not have been possible. Kara Filbey prevented me from having to work more hours than there are in a day by always happily lending a helping hand. John Grainger and James Hewitson are some of the best scientists (and hardest workers) I met during my PhD, and their high standard is something I tried to aspire to. I'm going to miss working in the Maizels lab, I'm leaving some good friends behind.

Outside of the lab, I couldn't have managed without the support of my friends. Gary, Laura, Alex and Lidia have been great friends to me, and I owe them more than a pint in return.

Finally I owe the most thanks to my family. Mum and Dad have always supported me in every way, Claire knows exactly what a PhD can be like, and Louise has always helped me with sorting my life out. They've been great, and I'm very lucky to have them.

Abstract

Many helminth parasites are able to survive for long periods in immunocompetent hosts. It has been suggested that the successful establishment of helminths is in part due to the induction of regulatory T cells (Tregs) which suppress anti-parasite immune responses. A possible mechanism by which parasites induce Tregs would be production of TGF-β, which can induce immunosuppressive Treg cells and also directly suppress immune responses. TGF-β homologues have been identified in parasitic nematodes including *Brugia malayi*, *Schistosoma mansoni* and *Ancylostoma caninum*. The *B. malayi* TGF-β homologue, Bm-TGH-2, has been demonstrated to signal through the mammalian TGF-β receptor, which indicates the TGF-β homologues may have a function in the host. We hypothesised that Treg induction through parasite-derived TGF-β could be a potent method by which parasites could evade the host immune system.

To address this, molecular techniques were first used to identify and characterise the transcription of novel TGF-β homologues from the intestinal parasites *Haemonchus contortus*, *Heligmosomoides polygyrus*, *Nippostrongylus brasiliensis* and *Teladorsagia circumcincta*, showing that TGF-β homologues are present in a wide range of parasites. TGF-β activity was then shown in products from both *S. mansoni* and *H. polygyrus*, and indeed the *H. polygyrus* products were found to induce Tregs through the TGF-β pathway. Antiserum against bacterially expressed *H. polygyrus* TGF-β homologue (Hp-TGH-2) was produced, and used to probe *H. polygyrus* excretory/secretory products, showing that Hp-TGH-2 is secreted. Attempts were also made to express recombinant Bm-TGH-2 (*B. malayi* TGF-β homologue) in insect cells, however the purified protein proved not to be functional.

In vivo mouse models of *B. malayi* infection were tested to examine the phenotype of T cell responses at the site of infection. An accumulation was found of $CD4^{+}Foxp3^{+}CD25^{+}CTLA\text{-}4^{hi}CD103^{+}$ T cells, which resemble activated natural Tregs, and which were suppressive *in vitro*. This proportion of Tregs at the site of infection diminishes over time, however CD103 expression (which is associated with activated Tregs) is increased on Tregs present at all timepoints up to day 21 post-infection, indicating that although a growing effector response may outgrow Tregs over time, the Treg population remains activated. Using an adoptive transfer model, it was shown that the Treg induction could spread to other bystander responses. In IL-4R-deficient mice, Treg accumulation was unaffected, indicating alternatively activated macrophages (which are absent in these mice) are not required for Treg induction.

Contents

Table of Illustrations

3. TGF-β Homologues from parasites

4. Bm-TGH-2 Insect Cell Expression

5. Treg characterisation in *B. malayi* infection

6. Mechanism of Treg accumulation at the site of *B. malayi* infection

Abbreviations

aa	amino acid
AF700	alexa-Fluor 700
APC	antigen presenting cell *or* allophycocyanin
BLAST	basic local alignment search tool
BES	*Brugia malayi* excretory/secretory products
BMDC	bone marrow – derived dendritic cell
BSA	bovine serum albumin
CD	cluster of differentiation
cDNA	complementary deoxyribonucleic acid
CFA	complete Freund's adjuvant
CFSE	5, 6 - carboxyfluoroscein diacetate succinimidyl ester
ConA	concanavalin A
CPM	counts per minute
D	day
DAPI	4',6-diamidino-2-phenylindole
DC	dendritic cell
DNA	deoxyribonucleic acid
DO11.10	a transgenic TCR specific for ovalbumin
EAE	experimental autoimmune encephalomyelitis
ELISA	enzyme linked immunosorbent assay
FACS	fluorescence-activated cell sorting

Fc	antibody constant region
FCS	foetal calf serum
FITC	fluoroisothiocyanate
Foxp3	forkhead/winged-helix P3
FSC	forward scatter
GM-CSF	granulocyte / macrophage colony stimulating factor
h	hour
HES	*Heligmosomoides polygyrus* adult excretory/eecretory products
HEX	*Heligmosomoides polygyrus* adult homogenate
i.p.	intraperitoneal
i.v.	intravenous
IFN	interferon
Ig	immunoglobulin
IL-X	interleukin-X
IL-XR	interleukin-X receptor
iNOS	inducible nitric oxide synthase
KJ1.26	a monoclonal antibody specific for the DO11.10 TCR
LC	Langerhans cell
LN	lymph node
LPS	lipopolysaccharide
mAb	monoclonal antibody
MACS	magnetically activated cell sorting
MHC	major histocompatibility complex

min	minutes
mRNA	messenger ribonucleic acid
NES	*Nippostrongylus brasiliensis* excretory/secretory products
NFκB	nuclear factor-κB
NK	natural killer cell
NKT	natural killer T cell
OD	optical density
PAGE	poly-acrylamide gel electrophoresis
PAMPs	pathogen associated molecular patterns
PBMC	peripheral blood mononuclear cells
PBS	phosphate buffered saline
PCR	polymerase chain reaction
PE	phycoerythrin
PerCP	peridinin-chlorophyll-protein complex
PL	peritoneal lavage
PMA	phorbol 12-myristate 13-acetate
PNPP	p-nitrophenyl phosphate
PRRs	pattern recognition receptors
RA	retinoic acid
RNA	ribonucleic acid
RT-PCR	reverse transcriptase – polymerase chain reaction
s.c.	subcutaneous
SCID	severe combined immunodeficiency

SDS	sodium dodecly sulfate
SEA	soluble egg antigen from *Schistosoma mansoni*
SSC	side scatter
TCR	T cell receptor
TH1	T helper 1
TH2	T helper 2
TLR	Toll-like receptor
TNF	tumor necrosis factor
WHO	World Health Organisation
WT	wild type

Chapter 1:

Introduction

1. Introduction

1.1. Parasitic infections

The majority of the world population is at risk of parasitic infection, with 740 million people now infected with intestinal parasites such as hookworms, 200 million with schistosomiasis, and 120 million with filariasis (WHO website http://www.who.int). With improvements in hygiene in first world countries, however, the prevalence of parasitic infections has fallen dramatically. Improvements in hygiene have coincided with a dramatic increase in inflammatory gastrointestinal conditions, autoimmunity and allergy, leading to the "hygiene hypothesis", first proposed by in 1989 by Strachan et al (1). The hygiene hypothesis states that the immune system requires infections in early life to develop correctly, and without them the immune system is prone to hyperactivity, characterised by inappropriate immune responses (2).

A clear increase in the incidence of inappropriate immune responses can be seen when comparing first and third world countries (2), but this correlation can also be seen within a single area. Individuals from urban areas have an increased risk of inflammatory gut disorders (IBD) than those from rural areas (3), as do those whose employment bring them into contact with dirty environments (2). A study from Canada comparing individuals from different socio-economic groups showed a positive correlation of higher income with increased prevalence of Ulcerative Colitis (UC) and Crohn's Disease (CD), while increased family size correlated with lower prevalence (4). This indicates that larger families (where children are exposed to their sibling's infections), and low-income families have lower levels of hygiene, and are protected from inappropriate immune responses.

Strong evidence for an environmental role in the incidence of type I autoimmune diabetes comes from studies of transmigratory families, where children of families newly arrived in Britain from undeveloped areas of Asia had low incidence of diabetes, but 10 years later the transmigratory population contained similar incidence of type I diabetes as the native population (5). Similarly to inflammatory gut disorders, the incidence of autoimmune diabetes also correlates to socio-economic status within a single area, and low-income also appears to be a protective factor in autoimmune diabetes incidence (6).

Clearance of gut parasites in children by wide-spectrum anthelmintic drug administration was shown to increase allergen specific skin-test and specific IgE responses, in independent studies in Venezuela (7) and Gabon (8), indicating that gut helminth infection can suppress allergy. Controversy still exists in this area with some studies finding no link, or even a positive association between history of helminth infection and hyperactive immune responses. A recent study in Cuba found that *Ascaris lumbricoides* infection and increased contact with animals correlated with protection from allergic responses, in line with other studies. However, infection with *Trichuris trichuria* had no link to allergic responses, and infection with *Enterobius vermicularis* or hookworms had a positive correlation with allergic responses in the same study population (9). Thus, regulation of inappropriate immune responses by helminth infection may be less straightforward than first proposed, and may also depend on other factors such as parasite species. Animal models of infection, colitis, autoimmunity and allergy may be useful tools for dissecting these mechanisms.

The role of parasitic helminths in the hygiene hypothesis has come under particular scrutiny, as there is strong evidence for immunomodulation in parasitic infections.

1.2. Immunity to parasites

Many parasitic infections are able to survive in the host for long periods (10, 11), however it is clear in some infections that successful immune-mediated clearance is possible. In Severe Combined ImmunoDeficient (SCID) mice (which lack B and T cells), intestinal parasites such as *Nippostrongylus brasiliensis* and *Heligmosomoides polygyrus* cannot be ejected, indicating an adaptive immune response is important for protection from these infections (12). TH2 responses characterised by production of IL-4, IL-5 and IL-13 are often associated with parasitic infections, and IL-4 administration can lead to expulsion of *N. brasiliensis* in SCID mice, and dramatically reduce worm counts in SCID mice infected with *H. polygyrus* (12). IL-4-deficient mice are susceptible to *Trichinella spiralis* infection, indicating this cytokines critical role in anti-parasite responses (13).

A strong TH2 response is required for expulsion of most intestinal helminth infections, however there is a range of requirements for components of the TH2 pathway in parasitic expulsion. IL-4 receptor (IL-4R) expression is required for expulsion of the intestinal parasites *N. brasiensis* and *T. spiralis* (14, 15) or protection against the blood-dwelling trematode *Schistosoma mansoni* (16), but differing requirements for the cells on which it is expressed can be seen. *N. brasiliensis* expulsion requires IL-4R expression on non-bone-marrow derived cells only (such as the smooth muscle cells of the intestine) (17), protection from acute *S.*

mansoni infection requires IL-4R expression on bone-marrow derived cells only (such as the cells of the immune system) (16), while *T. spiralis* expulsion requires IL-4R expression on both bone-marrow derived and non-bone-morrow derived cells (17).

TH2 responses are also important in human intestinal parasite infection, as a recent study showed that increased IL-5 and IL-13 responses to parasite antigens inversely correlated with parasite load in *A. lumbricoides* and *T. trichiura* infection, as assessed by fecal egg counts. Reinfection with intestinal parasites 8-9 months after anti-helminthic drug treatment also inversely correlated with TH2 cytokine-dominated responses (18), thus indicating protection against intestinal parasitic infection is conferred by strong TH2 responses in humans.

TH2 responses clearly have a role in ejection of intestinal parasites, however there also appears to be a role for TH1 responses in some non-intestinal parasitic infections such as schistosomiasis and filariasis (10). This will be discussed in sections 1.4 and 1.5.

As a potent immune response is clearly capable of ejecting parasites, chronic parasites must suppress these responses in order to persist in the host. Downregulation of the host immune response is evident in many parasitic infections, as will be discussed in the following section.

1.3 Intestinal Nematodes

Chronic human gut nematodes include roundworms, such as *A. lumbricoides*, pinworms, such as *E. vermicularis*, and hookworms, such as *Necator americanus*. Some models of these parasites in mice show immunosuppression, such as in *H.*

polygyrus, a natural chronic intestinal parasite of mice (19), which has been extensively used as an experimental model (20). In this infection the early TH2 response is downregulated as infection progresses to later timepoints, (21).

Interestingly, *H. polygyrus* infection suppresses house dust mite allergic responses (22) and colitis in an IL-10-deficient mouse model (23), indicating suppression of responses to bystander antigens, and highlighting the probable role of intestinal nematodes in the hygiene hypothesis. Transfer of mesenteric lymph node (MLN) cells can transfer suppression in both the allergy and colitis models (22, 23), indicating an induction of regulatory cells. *H. polygyrus* can also suppress responses to other pathogens, as coinfection with *Citrobacter rodentium* and *H.polygyrus* leads to reduced immunity to *C. rodentium* and increased bacterial titres (24).

In humans, evidence that gut nematode infection can lead to suppression of inappropriate immune responses is mounting. Suppression of inflammation of the gut was seen in patients with Inflammatory Bowel Disease (IBD) given *Trichuris suis*, a pig intestinal nematode which is tolerated for a few weeks in humans (25).

1.4. *Schistosome* Infection

In *Schistosoma mansoni* infection, granulomas form around eggs deposited in the liver. These granulomas are downregulated in size later in infection, indicating an active downregulation of the immune response (26). In endemic areas, individuals who appear immune to the parasite have higher antigen-specific responses than those who are infected, and drug-cure of infected individuals increases their antigen-specific responses, indicating an active suppression dependent on live parasites (10). A correlation can also be seen in infected individuals between high egg output, and

low antigen-specific proliferation (10), indicating individuals with the highest worm burdens are the most suppressed, or least able to control the infection.

The immunosuppression seen in Schistosome infection, as well as in other chronic helminth infections, may benefit both the parasite and the host, as it limits immunopathology. *S. mansoni* infection of IL-10-deficient mice showed that IL-10 is important for controlling the magnitude of the response to parasite antigens in both vaccination (27) and primary infection (28) experiments. IL-10-deficient mice developed strong mixed TH1/TH2 responses to *S. mansoni* antigens, resulting in increased protection to an irradiated cercariae vaccine (27), and increased mortality in primary infection, due to increased fibrosis around eggs deposited in the liver (28).

Infections of IL-4/IL-10 and IL-12/IL-10 double-deficient mice led to increased mortality in primary infection. In IL-4/IL-10 double deficient mice, strongly polarised TH1 responses developed, resulting in acute mortality after egg deposition due to liver damage, lack of containment of the products released from the deposited egg, and cytokine-induced shock. Conversely, IL-12/IL-10 double-deficient mice developed highly polarised TH2 responses, which led to gradual wasting and eventual death due to increased collagen deposition around deposited eggs and fibrosis in the liver (28). In *S. mansoni* infection of mice lacking the IL-4R, which are unable to make TH2 responses, acute pathology was seen due to an inflammatory TH1 response around deposited eggs (29). Thus protection against *S. mansoni* infection depends on a mixed TH1/TH2 response, and immunopathology is controlled by downregulating both arms of this response via IL-10.

1.5. Filarial Infection

One of the best characterised examples of parasite-related immunosuppression is in filarial infections, of which *Brugia malayi* is the best understood laboratory model. *B. malayi* is a member of a family of lymphatic filarial nematodes, which also includes *Brugia pahangi* and *Wuchereria bancrofti*. These parasites are transmitted as L3 larvae by mosquitoes of the *Aedes*, *Anopheles*, *Culex*, or *Mansonia* genera. Following entry into humans, the L3 larvae migrate to the lymphatics, where they moult twice into adults which reproduce sexually to produce the transmissible stage called microfilaria (Mf) which circulate in the bloodstream, as summarised in Figure 1.1.

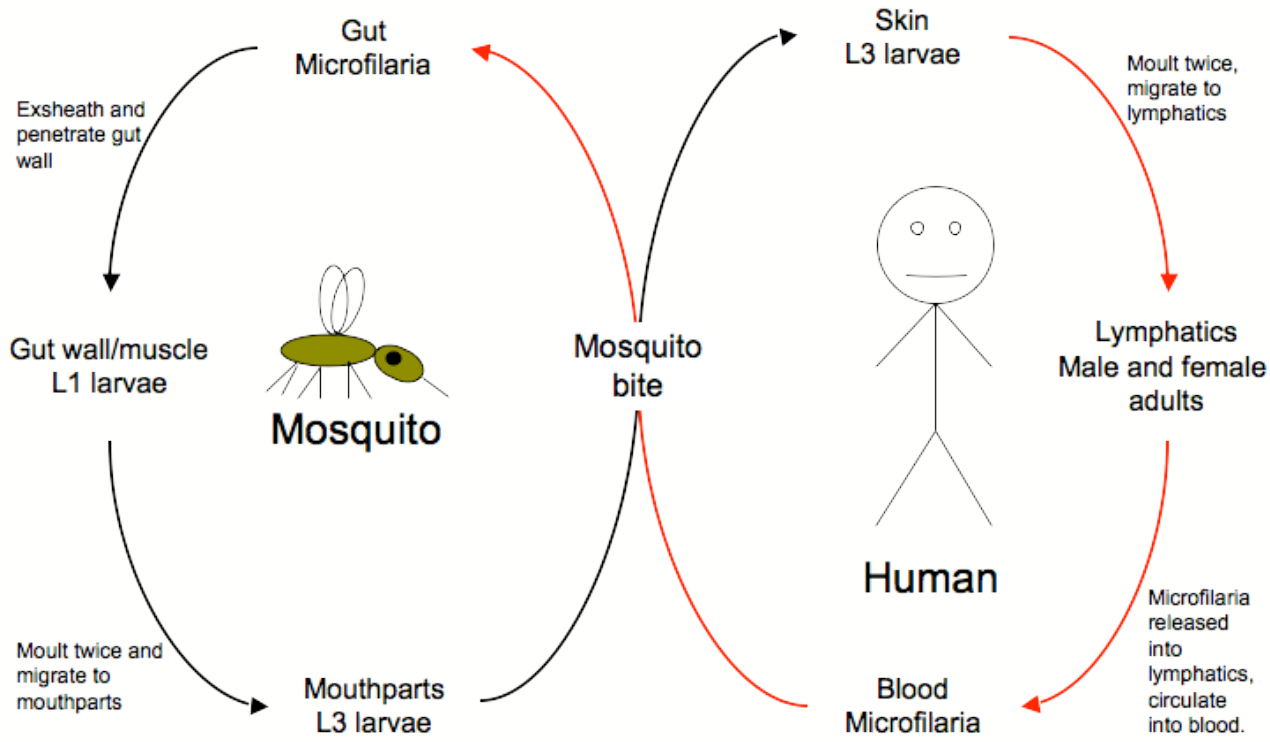

Figure 1.1: Lifecycle of *Brugia malayi*.

Brugia and *Wuchereria* infect approximately 120 million people worldwide (*Wuchereria* infecting 100 million, *Brugia* infecting 20 million), 44 million of whom show overt pathology: the most severe form being elephantiasis, characterised by a

gross swelling of the affected limb, leading to fibrosis and secondary infection. Filarial pathogens have a large economic impact in affected areas; principally sub-Saharan Africa, South America and Asia (see Figure 1.2) due to an inability of sufferers to work. The WHO has identified filariasis as the second-leading cause of significant/long-term disability worldwide (30).

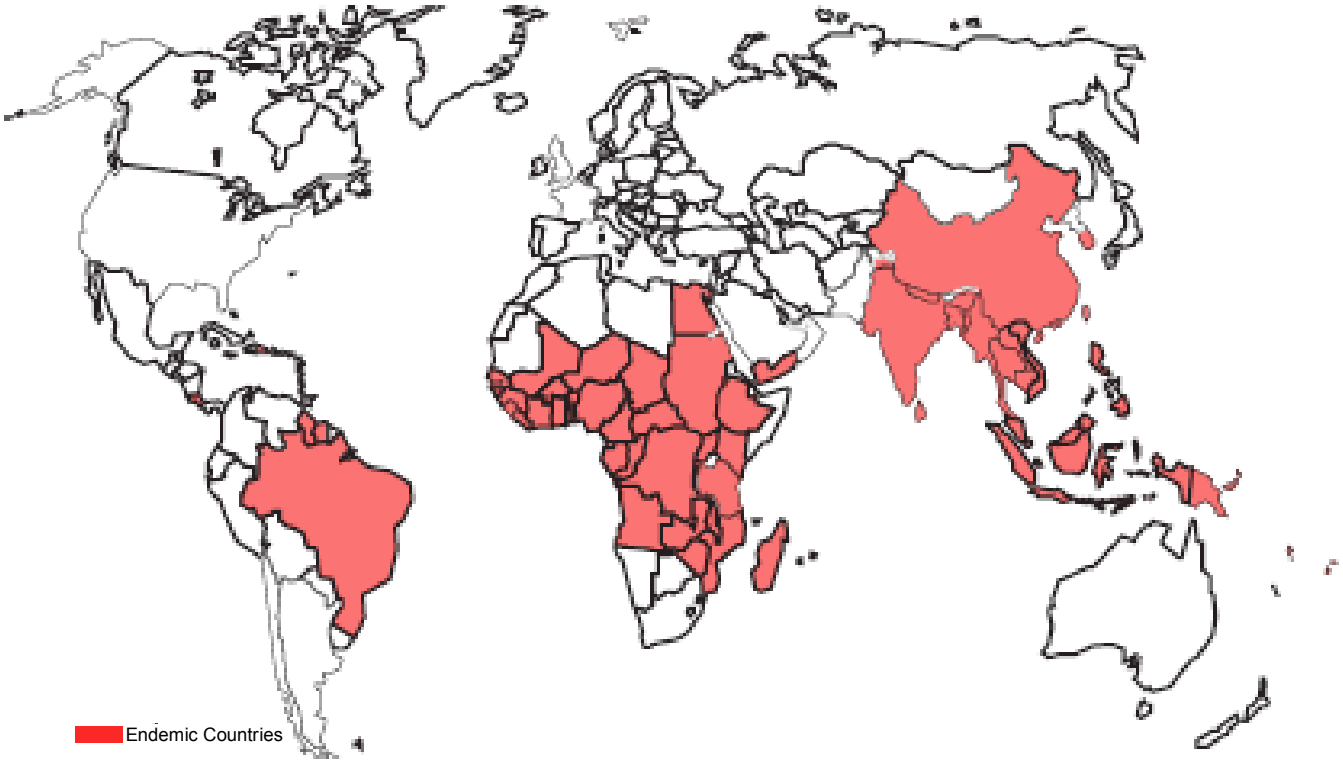

Figure 1.2: Areas affected by filariasis. (Adapted from WHO website, www.who.int/en)

Individuals in areas where filarial infection is endemic can be divided into three groups – endemic normal, chronic pathology and microfilaraemic. Endemic normal individuals have strong TH2 responses to parasite antigens, with circulating IgE antibody, and are thus thought to have produced a productive response and cleared the infection. Individuals with chronic pathology have strong inflammatory responses to the parasite, and will often also have cleared the infection. The difference between these individuals and endemic normals is that immune responses

in chronic pathology are TH1 dominated, and cause damage to the lymphatics where the adult parasites reside. This leads to occlusion of the lymphatic vessels, leading to oedema of the affected limb. This swelling results in the characteristic disability in lymphatic filariasis (known as elephantiasis), and can also cause debilitating secondary infections (30).

The last group, microfilaraemia, is the most common outcome of infection and is most intriguing immunologically. It is characterised by productive infection with microfilariae circulating in the blood and adults detectable in the lymphatics. However, despite this high antigen load, the immune response to parasite antigen in microfilaraemic individuals indicates a very muted TH2 response, reflecting active immunosuppression. This effect can be passed on from mother to child, as filarial infected mothers are more likely to have filarial-infected children, who also show suppressed TH2 responses (31). The suppressed TH2 responses evident in microfilaraemic individuals are characterised by low levels of proliferation to parasite antigen, and antibody responses dominated by the IgG4 isotype (32). It was initially thought that acquired immunity to filarial infection developed over time, as a study showed a negative correlation between age and infection (33), however a subsequent wider analysis showed that infection remains constant through the lifespan of the affected individuals (34). Therefore it seems no immunity to the parasite develops in microfilaraemic individuals.

Treg activity in filariasis is evident in many experimental systems, as will be discussed in more detail later. In human populations in endemic areas, endemic normals have stronger antigen-specific immune responses than those who have microfilaraemia, and chemotherapy using the microfilaricidal agent

diethylcarbamizine has shown recovery of antigen-specific proliferation (35-39), similarly to schistosomiasis (10). This indicates that immunosuppression in microfilaraemics is active and may be dependent on products released by live parasites.

1.6. Parasite-derived immunomodulators

In an effort to dissect the mechanism of parasite immunosuppression, various *in vitro* approaches have been taken. Immune cells have been cultured with live parasites, parasite homogenate or excretory/secretory products (or fractions of either), and recombinant proteins cloned from parasite genomes. In the following sections, progress in each of these areas is described.

1.6.1. Cultures with live parasites

B. malayi L3 larvae are around 1 mm in length, whereas microfilariae are around 0.1 mm in length, and so both are amenable to microculture with immune cells. Much information about the mechanism of immunosuppression from *B. malayi* has come from this approach. A caveat of these live parasite systems is that both of these stages are highly motile in culture, and so it can be difficult to determine if the effects seen are due to immunosuppression, or from mechanical stimulus of immune cells.

B. malayi L3 larvae, in cultures with human skin explants, inhibited the activation of the chief population of APCs in the skin, the Langerhans cells (LC). Because their activation is inhibited, the LCs migrate to the draining lymph node with an immature phenotype, and are less able to stimulate T cells (40). Stimulation

of T cells with immature APCs has been shown to produce tolerance to presented antigens (41). When the *B. malayi* L3 larvae were cultured with dendritic cells (DCs), DC antigen presentation was inhibited, while inducing their migration to the draining lymph nodes. Contact with live microfilariae (Mf) of *B. malayi* can also induce apoptosis of DCs and T cells (42, 43), and contact with live L3 can induce activation, and subsequent apoptosis of NK cells (44). When PBMCs from individuals from endemic areas were stimulated with live L3 larvae increases in transcription of the Treg markers *foxp3*, *TGF-β*, *CTLA-4* and *PD-1*; the tolerogenic DC marker *IDO*; and the anergic T cell markers *c-cbl*, *Itch*, *GRAIL* and *Nedd4* mRNA were increased in infected individuals compared to exposed, uninfected individuals, indicating a predominant Treg response associated with patent infection (45). Some of the effects of culture with live parasites, such as inhibition of antigen presentation by LCs, remained when transwell cultures were used, indicating that mechanical stimulation was not required and that parasite-derived secreted products may be responsible (40).

1.6.2. Excretory/secretory products

Techniques for culture of parasites *in vitro* have been developed, allowing products produced by either excretion or secretion from the parasite to be collected and purified, in the absence of serum proteins. Excretory/Secretory (ES) products are often concentrated using low molecular weight cut-off spin columns, and used in various assays to show their effect on the immune system. Immunomodulatory properties of ES products from many parasites, including *A. viteae*, *B. malayi*, *H. polygyrus*, *N. brasiliensis* and *S. mansoni* have been tested. A possible caveat of

these systems is that parasites may change the makeup of the products released *in vivo* and *in vitro* due to different stimuli from their environment, and, if concentrated, only molecules in the ES of above the molecular weight cut-off are purified.

B. malayi adults ES (BES) injected into *B. malayi*-infected dogs suppresses antigen-specific restimulation proliferative responses to *B. malayi* antigen, suggesting an immunosuppressive role (46). BES injected intraperitoneally into mice induced a suppressive population, similar to that seen in live adult or L3 larvae intraperitoneal infection (47). These cells could suppress proliferation, but not cytokine production by proliferating T cells, and were subsequently identified as Alternatively Activated Macrophages (AAMacs) (48), as will be discussed in section 1.10.

N. brasiliensis adult ES (NES) when injected into the peritoneal cavity of mice also induced a suppressive population of cells, however these were not as potent as BES-induced suppressive cells (47). NES applied to DCs induced maturation which, when the DCs were used to stimulate T cells, drove TH2 responses (49).

S. mansoni infective cercaria ES suppresses *in vitro* polyclonal proliferation of infected or uninfected human PBMCs, and *S. mansoni* antigen-specific proliferation in infected individuals (50). *S. mansoni* cercaria ES can also induce maturation of DCs to produce TH2 responses (51) similarly to NES.

In our group, *H. polygyrus* adult ES (HES) has been used to induce Tregs *in vitro* by a TGF-β receptor pathway (J. Grainger, submitted). Therefore, ES products from parasites can induce both TH2 responses and immunoregulation.

In order to dissect which molecules released by the parasites are responsible for the effects seen, excretory/secretory products have been fractionated by their physical properties such as size or charge. ES-62, a 62 kDa fraction of the excretory/secretory products of the rodent filarial nematode *Acanthocheilonema viteae*, was shown to be highly active in suppressing both T and B cell responses via partial activation of signalling elements, inducing tolerance rather than activation (52, 53). This activity is largely due to phosphorylcholine (PC) on ES-62 (53). An ES-62 homologue has been found in *B. malayi*, and PC has been shown to be attached to many *B. malayi* proteins, thus *B. malayi* may induce tolerance via a similar pathway (53). *In vitro*, *B. malayi* antigens displaying PC motifs or Bovine Serum Albumin (BSA) conjugated to PC can suppress mitogen-driven proliferation of human PBMCs, indicating PC may be an important suppressive mediator from *B. malayi* (54).

In *S. mansoni*, fractions of adult and egg antigens containing lysophosphatidylserine signalled through Toll-like Receptor-2 (TLR-2), inducing IL-10 production in T cells, indicating either Treg or TH2 cell induction (55).

1.6.3 Parasite Immunomodulatory genes

Many parasitic immune evasion genes have been identified, cloned, transgenically expressed and their function investigated, as reviewed in (56). Bm-GPX-1 (Glutathione peroxidase) and Bm-SODs (Superoxide Dismutases) detoxify oxygen radicals (57, 58), which are produced by immune effector cells such as neutrophils and eosinophils. Oxygen radicals can damage parasites, however

production of these detoxification enzymes appears to protect *B*. malayi from oxidative stress to a large extent (59).

B. *malayi* encodes two homologues of human MIF (Macrophage Inhibitory Factor), Bm-MIF-1 and Bm-MIF-2. Bm-MIF appears to have similar chemotactic activity for monocytes and macrophages *in vitro* as host MIF (60). *In vivo*, injection of Bm-MIF-1 into the peritoneal cavity recruits a population of eosinophils, and induces expression of the alternatively activated macrophage marker Ym-1 in recruited peritoneal lavage macrophages (61). This data indicates Bm-MIF is a potent inducer of TH2-associated innate cells.

The antigen presentation pathway is also interfered with by parasite-encoded proteins. *B. malayi* Bm-CPI-2 is a cystatin which suppresses MHC class II presentation by interfering with peptide degradation and loading (62). Cystatins are an evolutionarily conserved family of proteins and as such are also encoded by the free-living nematode *C. elegans*. However, in contrast to *C. elegans* cystatins, *O. volvulus* and *A. viteae* cystatins can suppress the proliferation of polyclonally stimulated human PBMCs and mouse splenocytes respectively, indicating their immunomodulatory role (63). They can also induce production of IL-10 by antigen presenting cells, adding to the suppression of T cell proliferation due to their role in preventing antigen presentation (64).

S. mansoni secretes a 28 kDa protein which catalyses the production of PGD2, a lipid mediator which is responsible for delaying of Langerhans cell migration from the skin in early infection (65), thus delaying an effective immune response until the parasite has migrated away from the site of infection.

Both *S. mansoni* (66) and the filarial parasite *O. volvulus* (67) can produce PGE2, another lipid mediator which induces tolerogenic DCs, suppresses T cells and induces Foxp3 expression in T cells with polyclonal stimulus (68, 69).

With the partial or complete sequencing of parasite genomes including *B. malayi* (70) and *S. mansoni* (71), immune evasion gene identification has accelerated. The *B. malayi* draft genome (70) revealed a number of retinoic acid-binding proteins, which may have an immunomodulatory role as retinoic acid enhances the effect of TGF-β to induce Tregs while suppressing TH17 differentiation (72). Galectin genes were also identified, and mouse galectin-1 has recently been shown to cause apoptosis in TH subsets (73).

Many parasites including *B. malayi*, *Ancylostoma caninum*, *Strongyloides stercoralis* and S. *mansoni* encode homologues of TGF-β (21, 74-78). Their role in the immune system and parasite development will be discussed in the following sections.

1.7. TGF-β structure and function

Transforming Growth Factor-β (TGF-β) was so named for its ability to immortalise and induce proliferation in fibroblasts, as a component of sarcoma growth factor (79, 80). It was first purified from blood platelets, which are a rich source of TGF-β (81). Since its discovery, it has been shown to be active in a large number of biological systems including cell proliferation, development, angiogenesis, apoptosis, tissue repair, fibrosis and the immune response (82-84). TGF-β is a member of a large superfamily of TGF-β-like molecules, including Bone Morphogenetic Proteins (BMPs), inhibins, activins, anti-Müllerian protein and

Growth/differentiation Factors (GDFs), as well as the prototypic TGF-β members of the family. TGF-β family members are identified by a conserved domain at their C-terminus, the presence of highly conserved cysteine residues, a protease cleavage site, a less strictly conserved N-terminal pro-protein region and an N-terminal signal peptide, as summarised in Figure 1.3.

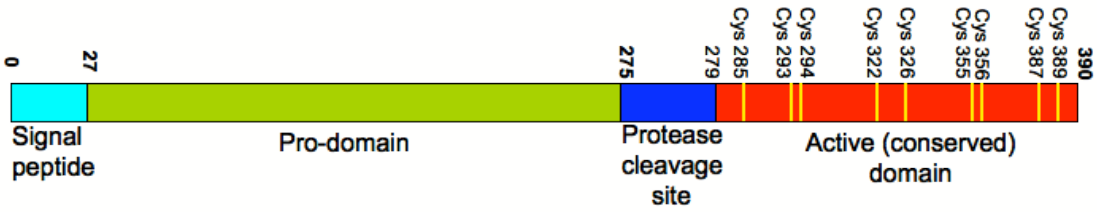

Figure 1.3: Structure of human TGF-β1.

This project was concerned with the prototypic TGF-β members of the superfamily, in humans TGF-β1-3. These isotypes in humans have an active domain which is very well conserved, and a pro-region which is less well conserved, as shown in Figure 1.4. The conserved domain of TGF-β is also very similar in mammals including humans, rats and mice, as shown in Figure 1.5.

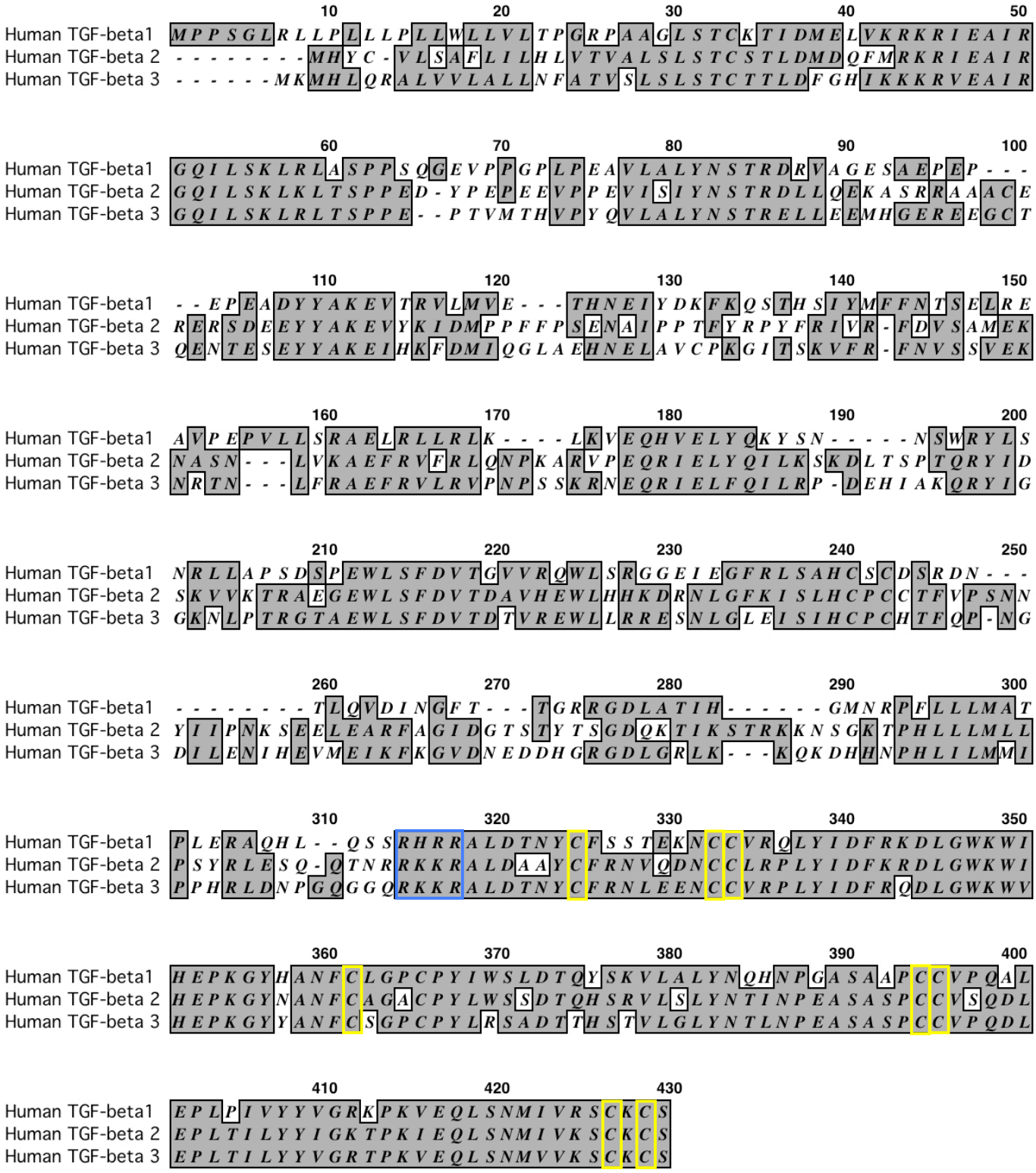

Figure 1.4: Alignment of human TGF-β1, TGF-β2 and TGF-β3 amino acid sequences.
The protease cleavage site is indicated by a blue box, the conserved cysteines by yellow boxes.

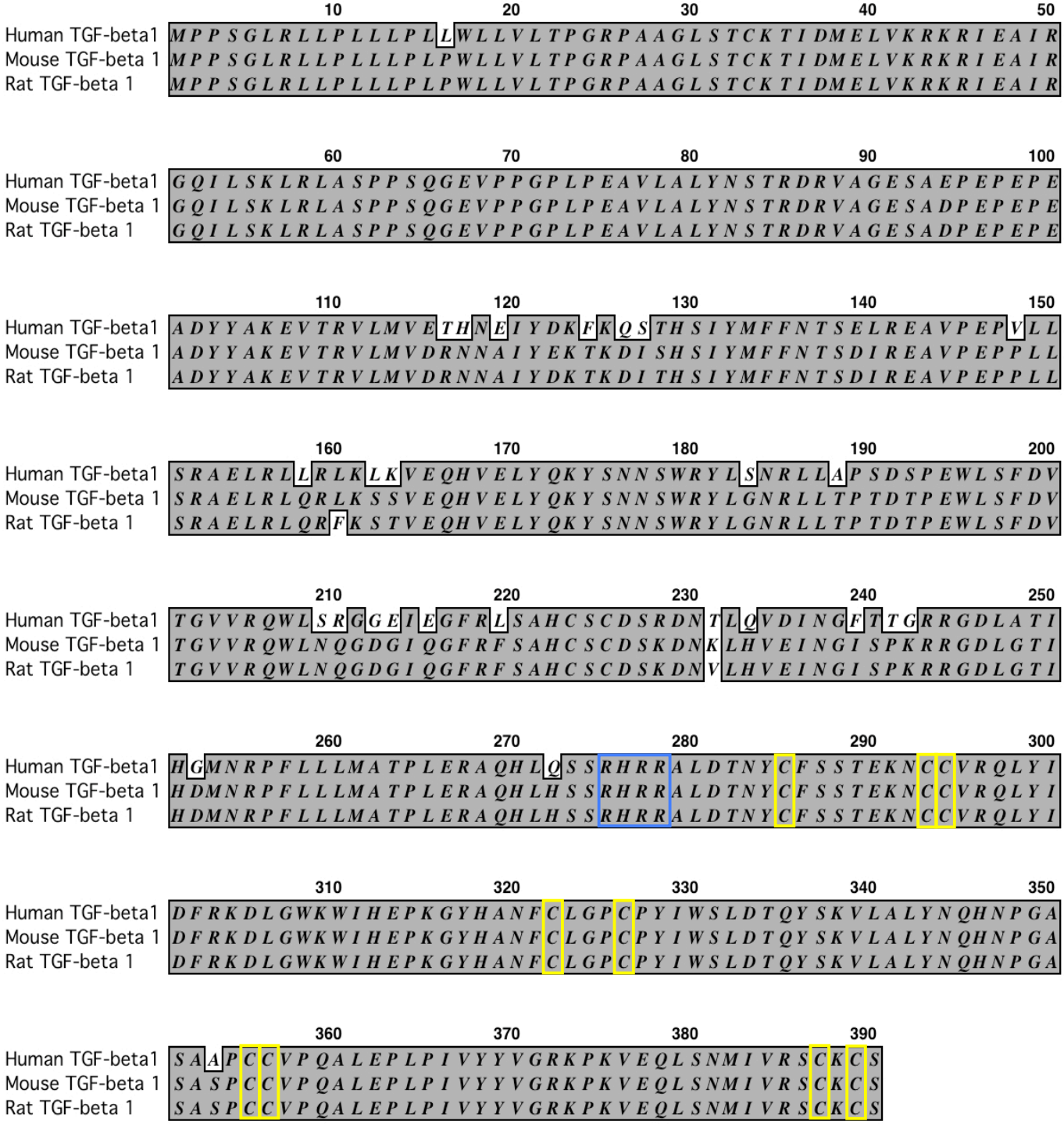

Figure 1.5: Alignment of amino acid sequences of human, mouse and rat TGF-β1.
The protease cleavage site is indicated by a blue box, the conserved cysteines by yellow boxes.

TGF-β family members are present across the metazoan taxon, from humans to fruit-flies and helminths. The TGF-β superfamily can be divided into two groups: the TGF-β/activin/nodal family, which has 9 conserved cysteines in the conserved domain, and the BMP/GDF/MIS family, which has 7 conserved cysteines in the conserved region. These cysteines are essential for correct folding and formation of the latent complex (85).

1.7.1. Release of mature TGF-β

TGF-β is produced as a pre-pro-protein which must undergo a multistep process to release the active cytokine. It is important that inactive cytokine is produced, as TGF-β and the TGF-β receptor are both produced at some level by most cell types. If TGF-β were produced in an active form, it would immediately bind to its receptor, leading to a continual autocrine loop. The TGF-β pre-pro-protein is produced as shown in Figure 1.3, and is directed to the Golgi apparatus by the presence of the signal peptide, which also marks the protein for secretion. The signal peptide is then removed, and the pro-protein is cleaved at the protease cleavage site by furin family proteases. The pro-domain and active domain are now separate peptides, however the pro-domain (now known as LAP – the Latency Associated Peptide) - remains non-covalently associated with mature TGF-β. Latent TGF-β forms a dimer, and in the Golgi body the dimeric latent TGF-β forms disulphide bonds to Latent TGF-β Binding Proteins (LTBP1-4). Members of the LTBP family have specificity for different TGF-β isoforms, and TGF-β isoforms can form heterodimers, thus further increasing the complexity of TGF-β activation (86). The complex of mature TGF-β, LAP and LTBP is known as the Large Latent Complex

(LLC) and is secreted from the cell. The function of LTBP is to attach the LLC to the extracellular matrix (ECM), sequestering latent TGF-β in tissues (85, 87). The LLC is shown in Figure 1.6:

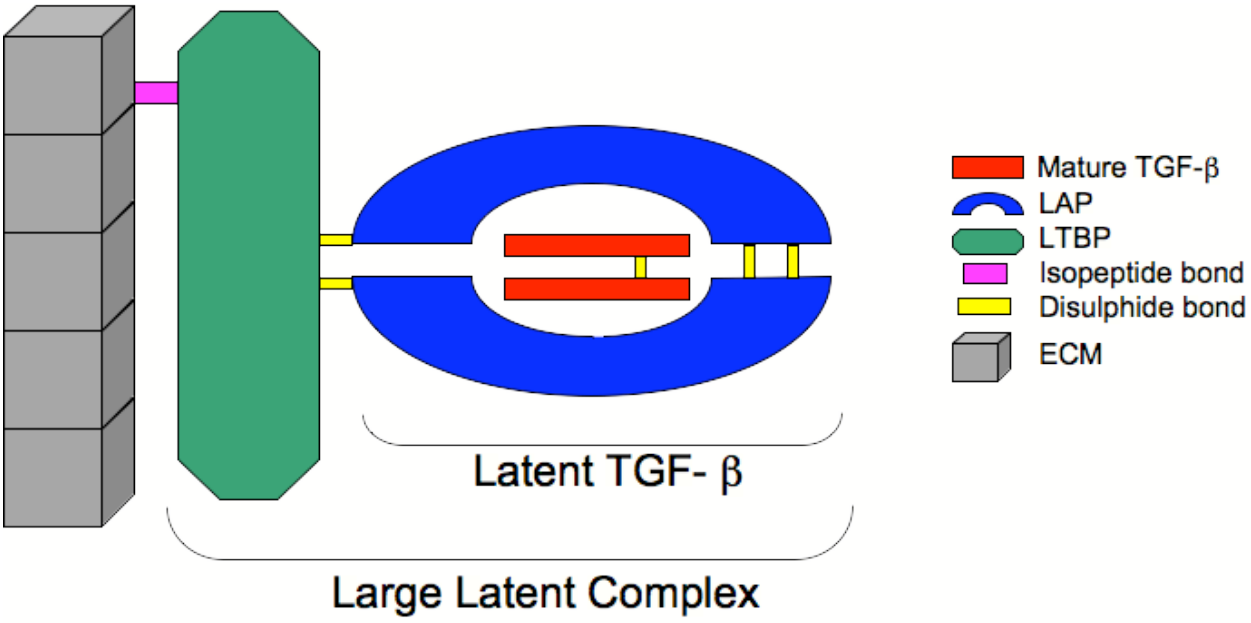

Figure 1.6: The Large Latent Complex (LLC) of TGF-β, bound to the extracellular matrix.

In order for active TGF-β to act on its receptor, LAP must be degraded or conformationally changed to release active TGF-β. Release of active TGF-β can be carried out *in vitro* by heat or acid treatment, which degrades LAP, but a number of other mechanisms may act *in vivo*. A number of processes associated with tissue repair are involved in TGF-β activation, which is logical as TGF-β is itself involved in tissue repair. Reactive oxygen metabolites are often also produced during tissue injury and inflammation, and these can activate TGF-β, possibly by modifying LAP, rendering it unable to stay bound to mature TGF-β (85). Proteases such as plasmin, matrix metalloprotease (MMP) -2 and -9 and thrombospondin-1 (TSP-1) can activate TGF-β, all of which are involved in matrix degradation and tissue repair.

Interestingly, TSP-1-deficient mice develop inflammatory infiltrates in their lungs, similarly to TGF-β-deficient mice, suggesting this TSP-1 cleavage of TGF-β is an important process in mucosal sites (85, 88). Integrins also have a role in TGF-β activation, as both αvβ6 and αvβ8 integrins are able to activate TGF-β *in vitro* in the presence of MT1-MMP protease indicating they may function to hold the LLC on the surface of DC cells, allowing activation by proteases (85). Deletion of the integrin binding domain of LAP resulted in a very similar phenotype to TGF-β-deficient animals (87), so although TGF-β activation *in vitro* is possible in the absence of integrin binding, it seems likely that all TGF-β activation *in vivo* depends on binding to integrins.

αvβ6, the first integrin found to be able to activate TGF-β, is expressed on a subset of epithelial cells, and is upregulated by inflammation, indicating it may activate TGF-β in response to injury. However, αvβ6-deficient mice have only a mild phenotype, not fully replicating TGF-β-deficient mice. (85, 89). αvβ8-deficient mice, by contrast, die shortly after birth due to defects in the vasculature of the brain. αvβ8 integrin is expressed in the immune system on CD4+ T cells and DC cells, but a conditional knock-out of αvβ8 on CD4 cells had no discernable phenotype. An αvβ8 conditional knock-out on $CD11c^{+}$ (DC cells) produced a phenotype indistinguishable from mice deficient in TGF-βR signalling, indicating that αvβ8 on DCs is extremely important for TGF-β activation within the immune system (89). Once mature TGF-β is released by any of the above processes, it must then bind to the TGF-β receptor in order to affect cell fate.

1.7.2. TGF-β Receptor Signalling

TGF-β receptors are expressed by most cell types. They are a family of heterodimeric receptors, with 7 type I receptors (ALK1-7) and 5 type II receptors in humans. TGF-β1-3 binds ALK-5 and TGFBRII, and the signalling pathway activated is summarised in Figure 1.7.

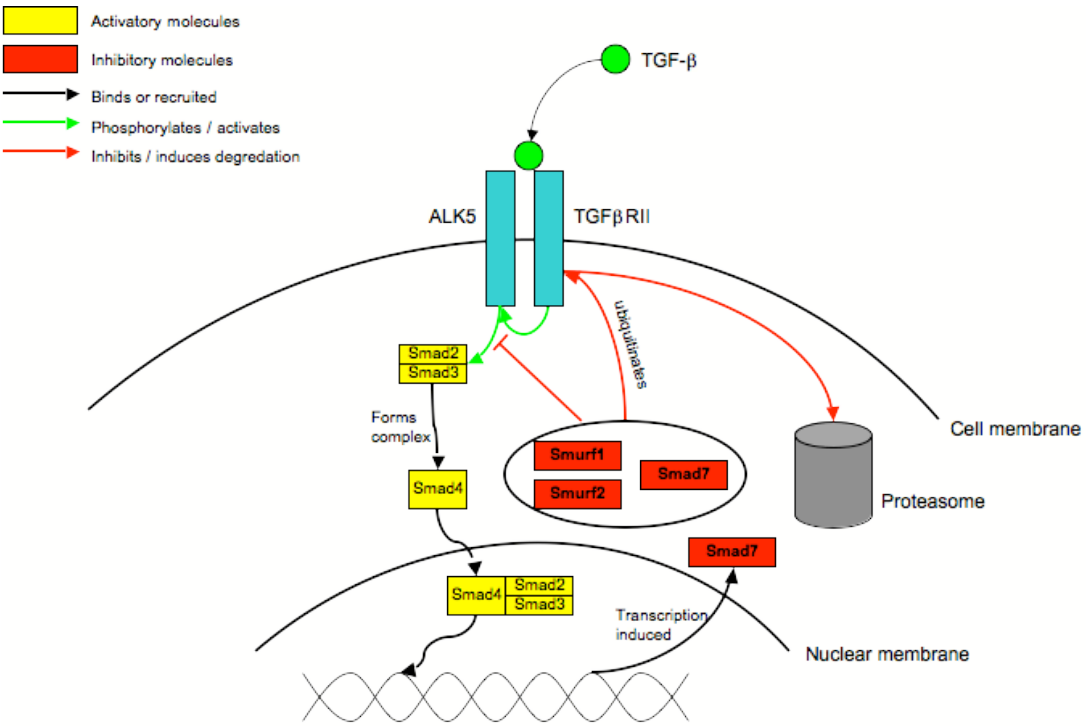

Figure 1.7: The TGF-β signalling pathway.

TGF-β family molecules bind the type II receptor, which then recruits and phosphorylates the type I receptor. The phosphorylated receptor then activates the signalling cascade, dependent on Smad-family proteins. The activated receptor phosphorylates Smad2 and Smad3, which form complexes with Smad4, and enter the nucleus to act as transcription factors (90). Signalling is controlled by Smad7 and Smurf1/2, which induce proteasomal degradation of the receptors, and also compete with Smad2/3 for binding to the receptor. This is a homeostatic process, as Smad7 is

strongly upregulated by TGF-β signalling (91). The TGF-βR can also signal through Smad-independent pathways, such as the extracellular signal-regulated kinase (Erk), mitogen-activated protein kinase (MAPK) and phosphatidylinositol 3-kinase (PI3K)-Akt pathways, through mechanisms not yet elucidated (92).

TGF-β signalling changes expression of a large number of genes, inducing tissue repair, angiogenesis and fibrosis, affecting proliferation and the immune system, as will be discussed in section 1.7.4. TGF-β encourages tissue repair by upregulating extracellular matrix synthesis, downregulating matrix degradation enzymes and upregulating protease inhibitors (82). Thus, application of TGF-β can accelerate the wound healing response; however larger amounts of TGF-β can lead to pathologic fibrosis. In Proliferative Retinopathy (PVR), a disease characterised by fibrosis in the eye leading to blindness, concentrations of TGF-β are three times normal levels, and injection of TGF-β into the eye of healthy mice can lead to PVR-like symptoms (82). Conversely, adenoviral expression of soluble TGF-βR in a model of PVR reduced the severity of the fibrosis (93).

The effects of TGF-β on cell proliferation depends on cell type – in most cell types TGF-β signalling produces growth arrest, by arresting or lengthening the G1 phase of the cell cycle (82). However, as its name suggests TGF-β can also induce transformation of some cell types, and fibroblasts are activated by TGF-β, inducing transformation, leading to fibrosis (83). TGF-β family members also have developmental roles, and are necessary for successful development in metazoans, as discussed in the following section.

1.7.3. Nematode TGF-β family members

Nematode TGF-β family molecules are intimately involved in key developmental events (74, 76-78, 94). Members of the TGF-β family have been found in many nematodes, related to both the TGF-β/activin/nodal family and the BMP/GDF/MIS family, as shown in the phylogeny in Figure 1.8.

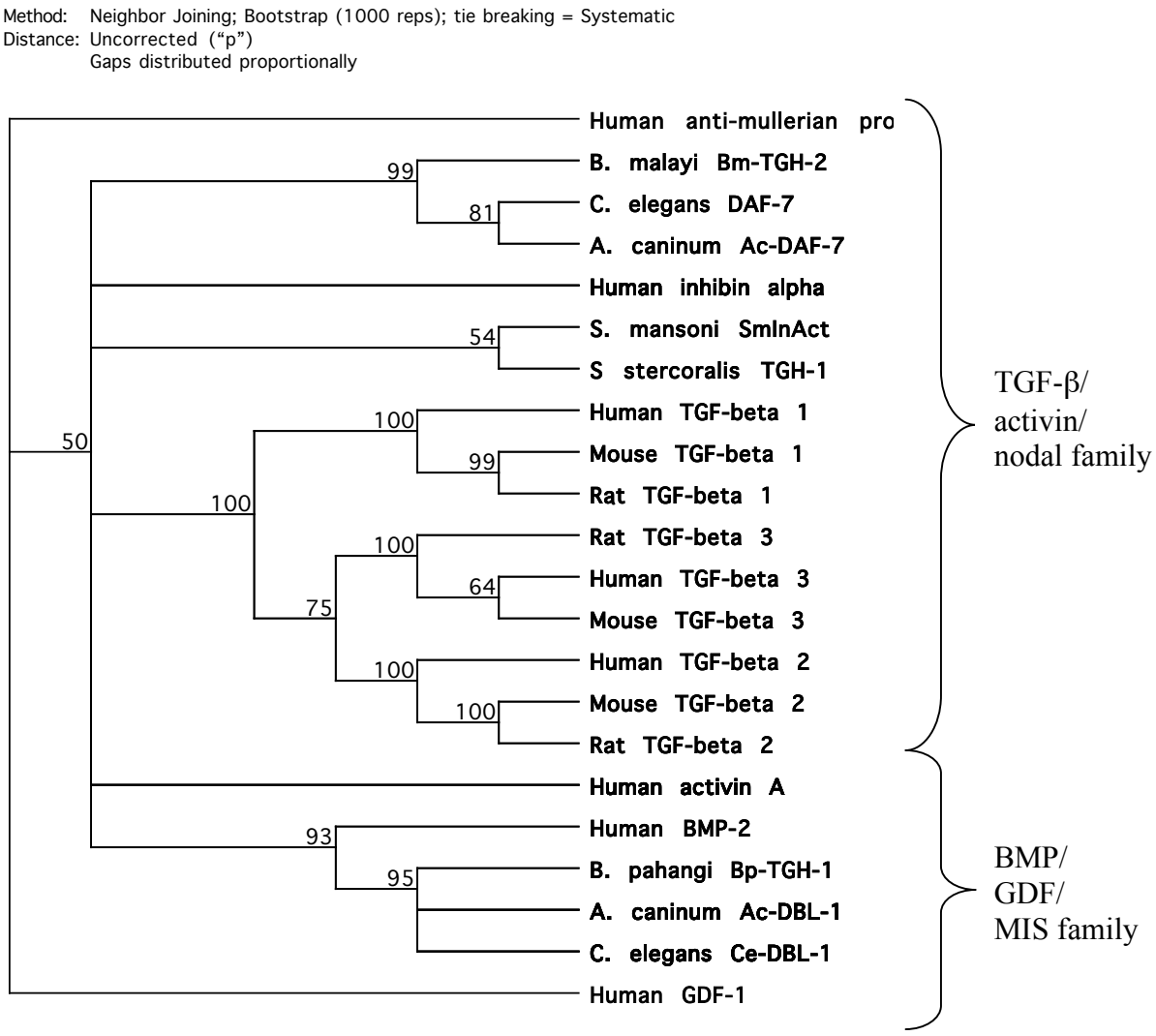

Figure 1.8: Phylogeny of TGF-β family members from mammals and nematodes. Percentages at branch points are based on 1000 bootstrap runs, and are only shown when above 50 %.

C. elegans encodes 5 TGF-β homologues, of which Ce-DAF-7 and Ce-DBL-1 are the best studied. Ce-DAF-7 controls entry to the Dauer state (a resistant stage

entered from the L1 larval stage, which the worm enters in response to adverse conditions), and mutants in Ce-DAF-7 enter Dauer inappropriately and constitutively. Ce-DAF-7 is expressed at highest levels in L1 larvae with a plentiful food supply, which is the stage at which the decision to enter the dauer state is made. Its expression is undetectable in dauer larvae and is upregulated after addition of food and entry into normal development (95). Thus, Ce-DAF-7 expression prevents entry into the dauer stage. Ce-DAF-7 also has developmental roles in other stages as mutants show defective egg-laying (94). Mutants defective in Ce-DBL-1 have smaller body size, whereas overexpression causes larger body size. Ce-DBL-1 is also important in male development, as Ce-DBL-1-defective mutants showed defective male sexual organ development (94).

B. malayi encodes 2 TGF-β family members, Bm-TGH-1 (*B. malayi* TGF-β Homologue-1) and Bm-TGH-2. Bm-TGH-1 is related to Ce-DBL-1, and is a member of the BMP/GDF/MIS family (74), and Bm-TGH-2 is related to Ce-DAF-7 and is a member of the TGF-β/activin/nodal family (96). Bm-TGH-1 has been proposed to be involved in development of the parasite, as its transcription was highest before each larval moult in the host (74). Bm-TGH-2 has been proposed to have an immunomodulatory role, due to high levels of transcription in the microfilarial stage, which is associated with immune suppression, and also as recombinant Bm-TGH-2 could signal through the mammalian TGF-β receptor (96). However, the upregulation of Bm-TGH-2 in microfilariae has also been proposed to have a role similar to that proposed for TGF-β homologues in other parasites, i.e. maintaining developmental arrest (77). Bm-TGH-2, alone among nematode TGF-β homologues

described, has been detected in secretions from the adult parasite, giving credence to the hypothesis it could be an immunomodulatory molecule (96).

Ancylostoma caninum, like *B. malayi*, encodes 2 TGF-β-family molecules, Ac-DAF-7 and Ac-DBL-1, so called due to homology to the relevant *C. elegans* genes. Ac-DBL-1 is expressed at the highest level in male adults, indicating it may have a similar role as Ce-DBL-1 in male development. In contrast, Ac-DAF-7 transcript is highest in the arrested L3 stage. The L3 stage of parasitic nematodes is arrested as the parasites must remain in stasis until they infect the host. Thus arrested parasitic L3 larvae have been proposed to be analogous to the arrested *C. elegans* dauer stage. The high expression of Ac-DAF-7 in the L3 larval stage indicates it could have an opposing role to Ce-DAF-7, i.e. Ce-DAF-7 prevents entry into the arrested state whereas Ac-DAF-7 maintains the arrested state (76). Interestingly, addition of human recombinant TGF-β induces development of *A. caninum* L3 larvae to later stages *in vitro*, indicating the parasite and mammalian TGF-βs are sufficiently similar to both be recognised by the parasite TGF-β receptor (97). This result may contradict the theory that Ac-DAF-7 has a role in maintaining the arrested L3 state, as addition of TGF-β should maintain arrest, not break it. Therefore, although Ac-DAF-7 is expressed at highest levels in L3 larvae, it may not be released and/or activated until the parasite enters the host. Alternatively these results could be explained by host and parasite-derived TGF-β acting on difference parasite receptors, with opposing roles.

Sst-TGH-1, a *Strongyloides stercoralis* TGF-β homologue has been proposed to have a role in maintaining developmental arrest due to its upregulation in the developmentally arrested iL3 stage (77), similarly to Ac-DAF-7.

SmInAct, the *S. mansoni* TGF-β family member, is necessary for successful development, as infertile females show downregulated SmInAct, and the mature form of the protein is only detectable in the egg stage. Using RNAi on adult parasites, SmInAct transcription was knocked down, resulting in the adults producing eggs that would not develop to later stages (78).

Although TGF-β homologues in parasites have a well documented role in developmental pathways, their potential for interaction with the immune system has been neglected, excepting the case of Bm-TGH-2. As TGF-β has an extremely potent and multi-functional role in the immune system, this may be of importance.

1.7.4. TGF-β in the Immune System

TGF-β has multiple roles within the mammalian immune system, summarised in Table 1.1.

Table 1.1: Functions of TGF-β in the immune system.

Cell type	Suppression	Activation	Differentiation
B cells	Suppress proliferation (82).		Induces IgA production (98). Imprints mucosal phenotype (99).
NK cells	Prevents IFN-γ production (100). Prevents accumulation (100).	Chemoattractant (82).	
Dendritic cells / monocytes	Prevents maturation (84). Stimulates apoptosis (84). Prevents TLR signalling (101).	Chemoattractant for monocytes (82).	Induces CD103 expression (99). Imprints mucosal phenotype (99).
$CD4^+$ T cells	Suppresses proliferation (82). Induce apoptosis (102). Suppresses IL-2 production. Suppresses TH1 and TH2 differentiation (92). Low concentrations reduce IL-12 responsiveness (102).	High concentrations increase IL-12 responsiveness (102).	Induces CD103 expression (99). Imprints mucosal phenotype. Promotes IL-10 production (92). TGF-β alone induces Foxp3 (103). TGF-β + IL-6 induces TH17 differentiation (104).
$CD8^+$ T cells	Suppresses proliferation. Suppresses IFN-γ, perforin and t-Bet transcription (105, 106).		

TGF-β in the immune system is often associated with immune suppression. Immune suppressive effects of TGF-β signalling include suppression of transcription of GATA3 (required for TH2 differentiation) and T-Bet, STAT4 and IFN-γ (required for TH1 differentiation), thus suppressing induction of TH2 and TH1 responses

respectively (92). It also suppresses IL-2 production, leading to the suppression of proliferation seen in T cells. TGF-β can therefore suppress the proliferation of naïve T cells (which require IL-2 for proliferation), however activated T cells are less susceptible to suppression, possibly due to downregulation of the TGF-βRII. Some evidence also exists for differential susceptibility to TGF-β suppression by T helper cell subsets: TH1 cell effector cytokine production is downregulated by TGF-β, whereas TH2 cell cytokine production remains unaffected. TGF-β also promotes IL-10 production by T cells, which may further suppress TH1 cells, while not affecting TH2 cells (92).

Other immune cell types affected by TGF-β include $CD8^+$ T cells, in which antigen-specific IFN-γ release and T-Bet transcription (105), as well as perforin expression (106) are suppressed by TGF-β, preventing $CD8^+$ T cells from becoming fully activated and carrying out cytotoxic functions. Using mice expressing dominant negative TGF-βR under the control of the CD11c promoter, the role of TGF-β signalling in DC cells and NK cells could be investigated, as both NK cells and DC cells express CD11c. Transgenic NK cells were at much higher frequency in these mice than wild-type and produced large amounts of IFN-γ, leading to increased TH1 responses (100). Interestingly, DC frequency and production of IL-12 was unaffected in this system, although TGF-β has been shown to prevent DC maturation, antigen-presentation and migration to the draining lymph node, to stimulate DC apoptosis (84), and prevent TLR-signalling (101).

The effects of TGF-β are further complicated by dose- and context-dependency. High concentrations of TGF-β (10-100 ng/ml) increase $CD4^+$ T cell IL-12 responsiveness, whereas low concentrations (below 1 ng/ml) reduced IL-12

responsiveness (102). TGF-β has long been known to have opposing roles in the immune system, suppressing or inducing proliferation depending on dose, cell type and context (83), and accelerating or preventing apoptosis in different conditions (82). It can be inflammatory in some settings as it is a chemoattractant for monocytes and NK cells (82).

TGF-β is also an important differentiation factor. It induces CD103 expression on mucosal homing immune cells (99), and induce class switching to IgA in B cells (98). TGF-β is highly expressed in mucosal tissues, and seems to be involved in imprinting a mucosal phenotype on immune cells (99).

In combination with IL-6, TGF-β was recently shown to be essential for TH17 induction, a highly inflammatory response (104). TH17 cells are intimately involved in disease progression in autoimmune models such as Experimental Autoimmune Encephalomyelitis (EAE) (107), in defence against intracellular bacteria such as *Citrobacter rodentium* (108) and in some models of colitis (109). In *in vitro* cultures, T cells stimulated polyclonally in the presence of TGF-β expressed Foxp3 and became Tregs (103), whereas when IL-6 was also present they produced IL-17 (104). IL-23 is also involved in the TH17 differentiation pathway, however it is not (as first thought) essential, but rather seems to be required for expansion and maintenance of TH17 cells (109). Conversely, the vitamin A metabolite retinoic acid (RA) suppresses TH17 differentiation in the presence of TGF-β and IL-6, and promotes Treg induction (72).

1.8. Treg functions and markers

The possibility that a subset of T cells is involved in suppression of autoimmune responses has long been proposed (110), however it was not until recently that regulatory T cells (Tregs) could be reliably identified and manipulated. The first subset of Tregs discovered, now known as "natural" Tregs, were shown to have a role when it was observed that mice thymectomised between days 3 to 5 after birth develop autoimmune responses directed against the ovaries (111). Therefore, a subset of T cells must develop in the thymus during days 2-4 post-partum that suppress anti-self responses. These thymectomised mice are rescued to a normal phenotype by transfer of $CD4^+CD25^+$, but not $CD4^+CD25^-$, T cells from adult mice, showing that the regulatory cells must be within the $CD4^+CD25^+$ subset (112). Other markers were subsequently found to be associated with Tregs (113), as shown in Table 1.2.

Table 1.2: Markers used to identify Tregs

Marker	Function	Expression	Reference
CD25	Alpha subunit of the IL-2R	Natural Tregs and transiently on activated T cells	(112)
$CD45RB^{lo}$	Isoform of CD45, dephosphorylates src kinases	Natural Tregs and activated T cells	(114)
CTLA-4	Negative costimulatory molecule, binds CD80/CD86	Tregs and activated T cells	(115)
TGF-β (surface-bound)	Suppressive cytokine	May be Tregs only	(116)
GITR	Unknown	Tregs and activated T cells	(117)
FoxP3	Transcription factor	Only in Tregs as nuclear protein	(118)
LAG-3	CD4 family, binds MHC class II	May be Tregs only	(119)
CD103 (αεβ7)	Integrin, binds E-cadherin	Mucosal and skin-homing T cells, correlates with most active Tregs	(120)
PD-1	Inhibitory receptor, binds CD274 (PD-L1)	Transcription upregulated on Tregs	(121)
IL-35	Inhibitory cytokine	Produced by activated Tregs	(122)

CD45RB can be used to separate Tregs from naïve T cells. Transfer of $CD4^{+}CD45RB^{hi}$ cells into *scid* mice results in colitis from uncontrolled immune responses against enteric bacteria. Transfer of $CD4^{+}CD45RB^{lo}$ cells suppressed this colitis, indicating the suppressive population was contained with the $CD4^{+}CD45RB^{lo}$ population (114).

CTLA-4 is also expressed on natural Tregs, and *in vitro* and *in vivo* its expression has been shown to be necessary for suppression. CTLA-4-deficient mice develop a lymphoproliferative disorder, and die within a month of birth (123). Further evidence that CTLA-4 expression is involved in maintenance of tolerance to self is that anti-CTLA-4 treatment in naïve mice results in development of

autoimmunity (115). Moreover, in the autoimmune models of EAE and Insulin-Dependent Diabetes Mellitus (IDDM), anti-CTLA-4 treatment excacerbates disease, as pathogenic autoimmune cells are released from suppression (123, 124). CTLA-4 binds CD80 and CD86 on Antigen Presenting Cells (APCs) with high affinity, leading to DC production of Indoleamine 2,3-dioxygenase (IDO), an enzyme which degrades tryptophan (125). Tryptophan is an essential amino acid for T cell proliferation, and its depletion leads to T cell tolerance and apoptosis (126). As well as being an effector molecule of Treg suppression, CTLA-4 has been shown to be necessary for TGF-β-mediated induction of Tregs, although the mechanism mediating this is unknown (127).

Tregs express surface-bound TGF-β, which they may use to suppress other cells (116). This has been used to explain the conflicting data regarding Treg contact-dependency: natural Tregs cannot suppress in transwell cultures, so must be contact-dependent, however many studies showed that addition of anti-TGF-β ablated suppression, indicating production of soluble immunosuppressive mediators. If the TGF-β used to suppress T effectors is surface-bound on natural Tregs, this explains both results.

GITR (glucocorticoid-induced TNFR family-related receptor) is expressed on all CD4+ T cells at a low level, and although upregulated on activated naïve $CD4^+$ T cells, it is expressed at highest levels on $CD4^+CD25^+$ Tregs. GITR-deficient animals have similar levels of Tregs in the thymus, however levels of Tregs in the periphery are reduced by around a third, indicating GITR signals may be important for maintaining the Treg population (128). Early studies showed that GITR ligation by agonistic antibody resulted in loss of functional suppression by Tregs, and so it was

hypothesised that GITR ligation directly abrogated Treg function (117, 129). However, later studies using coculture of GITR-deficient cells in Treg suppression assays in the presence of agonistic anti-GITR antibody showed that GITR ligation on non-Tregs allows them to overcome Treg suppression (128).

Foxp3 is a transcription factor expressed by natural Tregs, which is necessary for their development. In humans a condition called IPEX (X-linked neonatal diabetes mellitus, enteropathy, and endocrinopathy syndrome) results from mutations in the *Foxp3* gene, and is characterised by fatal systemic autoimmunity. A similar phenotype can be seen in Foxp3-deficient mice, or *scurfy* mice (which lack Foxp3 due to a null mutation) (130). Transgenic expression of Foxp3 in non-regulatory T cells results in development of a Treg phenotype (118). In mice, Foxp3 is entirely specific for Tregs, but in humans Foxp3 is transiently expressed in activated T cells (131). Studies using Foxp3-GFP fusion protein have shown that Foxp3 expression is mostly restricted to $CD4^+$ T cells, with only a small population of $CD8^+$ or $CD4^-$ $CD8^-$ cells expressing Foxp3 (131). The action of Foxp3 as a trancription factor appears to depend upon its binding to NFAT. Complexes of NFAT and AP-1 change expression of genes associated with T cell activation, e.g. upregulation of IL-2. However, Foxp3 can bind NFAT instead of AP-1 in tolerised/regulatory cells, leading to opposing gene regulation, e.g. downregulation of IL2 and upregulation of Treg markers (132).

The CD4-family molecule, LAG-3, is a surface receptor which is reported to be expressed only on activated natural Tregs. Transgenic expression of LAG-3 in naïve T cells induces some suppressive function, and inhibition of LAG-3-expressing cell proliferation. It does not seem to have a dominant role as LAG-3 deficient mice

do not have an autoimmune phenotype, however Tregs from these animals are less suppressive than wild-type Tregs (119). LAG-3 has a related structure to CD4, and binds MHC class II with higher affinity than CD4. Binding to MHC class II is required for its suppressive function, however the mechanism of suppression remains unknown. In order to release proliferating cells from suppression, LAG-3 is cleaved from the surface of the Treg by activation-induced matrix metalloproteases (133).

CD103 is an integrin that, in combination with integrin β7, binds E-cadherin. It may also have costimulatory roles, as agonist antibody enhances proliferation of T cells with suboptimal anti-CD3 (134). This interaction is involved in retaining cells at epithelial surfaces, and CD103-deficient animals have lower numbers of T cells maintained at the mucosal epithelium, and spontaneously develop inflammatory skin lesions (134). Its expression is induced by TGF-β (99), and in naïve animals it is expressed only in mucosal tissues, which have high steady-state levels of active TGF-β (99). $CD103^+$ Tregs are highly suppressive, and are especially active against colitis and inflammatory bowel disease (135). In *Leishmania major* infection, Tregs expressing CD103 accumulate at the site of infection and control the immune response. In CD103-deficient animals, Tregs are not retained at the site of infection and strains which are susceptible to *L. major* infection become resistant, due to an enhanced immune response (120).

PD-1 was identified by subtractive hybridisation as a receptor which was upregulated on apoptotic cells. It is a member of the CD28/CTLA-4/ICOS costimulatory receptor family, and binds its ligands, PD-L1 and PD-L2, which are expressed on APCs and other non-lymphoid tissues. PD-1 is upregulated on activated T cells and on Tregs (136). However a recent report showed that although Tregs

express PD-1, it is stored intracellularly until the Treg is stimulated through the TcR, whereas activated T cells express high levels of PD-1 on their surface (121). Therefore suppression may occur through ligation of PD-1 on effector cells, rather than on Tregs. PD-1-deficient mice have an autoimmune phenotype, however not as severe as that in CTLA-4-deficient mice (136).

IL-35 is a recently-discovered cytokine, which consists of a heterodimer of Ebi-3 and IL-12α (122). It is produced by actively suppressing Tregs (in coculture with effector cells), and its expression is induced by Foxp3. *In vitro*, IL-35 alone can suppress T cell proliferation, indicating its role as a Treg suppressive cytokine. Ebi3 or IL-12α-deficient mice do not have an autoimmune or inflammatory phenotype, and have normal numbers of Tregs in the periphery. As Ebi3 and IL-12α have roles in other cytokines (Ebi3 is a component of the inflammatory cytokine IL-27, and IL-12α is a component of the TH1-inducing cytokine IL-12), mice deficient in either of these genes may have compensating deficiencies in both regulatory and inflammatory capacities. However, Tregs from Ebi3 or IL-12α-deficient mice cannot control pathology in a model of colitis. Thus it appears that although IL-35 is not involved in Treg development, it is required for the highest level of suppressive capacity during inflammatory responses (122).

1.8.1. Development of Tregs

Natural Tregs develop in the thymus, although the signals necessary for the decision to become a naïve T cell or a Treg are still under debate. CD25-deficient or IL-2-deficient mice have around 50% of the normal numbers of Tregs, so signals through the IL-2 receptor are dispensable for Treg development. However, mice

deficient in the common γc, which makes up part of the trimeric IL-2 receptor, as well as many other cytokine receptors (eg IL-4, IL-7, IL-15), have no Tregs, indicating other signals through this receptor are necessary for development (137). IL-15 deficient mice have a similar phenotype to IL-2-deficient mice, showing that IL-15 is dispensable for Treg development. Interestingly, mice deficient in CD122 (the β chain of the IL-2 and IL-15 receptors) or IL-2/IL-15 double deficient mice have no Tregs, so the effects of IL-2 and IL-15 appear to be compensatory in Treg development (138). IL-2-deficient Tregs have normal levels of Treg-associated markers, apart from TGF-β, so the role of TGF-β and IL-2 may be in maintenance of Treg fitness in the periphery (137).

1.8.2. Treg Subsets

There are generally agreed to be two groups of Tregs – natural (nTregs) and adaptive (aTregs). nTregs suppress in a contact-dependent manner and prevent autoimmune reactions (139). They develop in the thymus, populating the periphery and making up around 10% of the $CD4^+$ T cell pool. They express CD4, CD25, CTLA-4 and Foxp3 and are often depleted or purified using antibodies against CD25. It has been suggested that nTregs are specific to self antigens as they police against autoimmune responses (140). Evidence that first suggested this came from mice with transgenic T cell receptors (TcRs) specific to self-antigens, where T cells expressing TcRs with high affinity for self-antigens developed into Tregs, whereas those of low affinity to self-antigens were either deleted or became normal naïve T cells (141). Later studies using mice with transgenic β-chains of the TcR but endogenous α-chains (and thus a limited antigen specificity) confirmed this, as

$CD4^+CD25^+$ and $CD4^+CD25^-$ cells had largely different specificities with little overlap. When TcRs from $CD4^+CD25^+$ cells were transgenically expressed in naïve T cells, they caused a wasting disease indicating an autoreactive specificity (142). However, recently the self-specificity of Tregs has been called into question. Using transgenic mice with a limited repertoire of TcRs, T cells were separated into Tregs and non-Tregs by Foxp3-GFP expression, then and their TcRs were cloned into hybridomas. In this study, neither the Treg nor the non-Treg TcRs responded to self-antigens, indicating all T cells were specific to non-self antigens (143). Clearly further research in this area is needed to clarify this.

aTregs are induced in the periphery either to self or foreign antigens, however their development is less well understood. Whether they originate from naïve T cells, natural Tregs or are a separate subset is still under discussion. Some authorities in the field have proposed two groups of aTregs. These are Tr1 cells and TH3 cells, and their role *in vitro* and *in vivo* has been studied extensively. Tr1 cells produce IL-10 and TGF-β, are $Foxp3^-$ and are created *in vitro* by repeated stimulation in the presence of high concentrations of IL-10 or vitamin D3 and dexamethasone, or by stimulation with tolerogenic DCs (140). They are present in the intestinal epithelium and so are thought to be involved in downregulation of responses to gut flora (92).

TH3 cells resemble activated nTregs in that they express Foxp3 and the surface markers associated with nTregs, but produce high levels of TGF-β, unlike nTregs which express similar levels of TGF-β mRNA to naïve T cells (92). They can be created *in vitro* by polyclonally stimulating T cells in the presence of TGF-β (103, 144), and are thought to be involved in oral tolerance induction *in vivo*. Induction of this subset can also be carried out experimentally *in vivo* as a study showed using

transgenic TGF-β production in the pancreatic islets of diabetes-prone mice led to an accumulation of Tregs, and a suppression of disease (145). Retinoic acid promotes Treg induction by TGF-β, while downregulating TH17 induction, and retinoic acid is involved in imprinting the mucosal phenotype on immune cells (72). TGF-β induction of Tregs is downregulated by TH1 and TH2 cytokines (146), indicating a productive effector response may inhibit the development of tolerance.

Of possible significance to aTreg induction is the finding that PGE2, an arachadonic acid metabolite, can also induce Foxp3 in human T cells similarly to TGF-β (69). PGE2 also induces a tolerogenic phenotype in DCs, resulting in DC upregulation of IDO (68).

1.9. Tregs in Infection

Tregs control autoimmune responses, but they have also come under scrutiny in controlling anti-pathogen responses. Their activity could be of benefit to the host, limiting immunopathology, or of benefit to the pathogen, preventing clearance. Tregs have now been shown to play a role in all classes of pathogens: viruses (147-152), bacteria (153, 154), protozoa (120, 155-157) and helminths (10, 21, 22, 29, 158-165).

1.9.1. Tregs in Viral Infection

Viral infections are often associated with Treg induction, with increased proportions or numbers of Tregs seen in the local tissues or peripheral blood of individuals infected with Friend Virus (150), Human Immunodeficiency Virus (HIV) (166), Hepatitis B Virus (HBV) (151), Hepatitis C Virus (HCV) (152), Herpes Simplex Virus (HSV) (167) and dengue virus (148, 149).

Friend virus infection has been known for some time to produce a suppressed immune response with reduced $CD8^+$ T cell responses. This suppression was later found to be transferable with Tregs (150). $CD4^+$ T cell transfer from chronically infected mice could also suppress tumour immunity *in vivo*, and suppress a mixed lymphocyte reaction *in vitro* (148). Tregs effectively prevent a productive immune response, as Treg ablation produced a reduced viral titre (147).

In HIV, CD25 depletion *in vitro* increased HIV-specific responses in HIV infected individuals (166), and higher frequencies of circulating Tregs correlated with low $CD4^+$ cell counts (148), indicating a role for Tregs in suppressing anti-HIV responses.

In HBV, Treg frequency increased in the blood and liver of chronically-infected individuals and correlated with high viral titre (151), and in HCV Treg frequency and suppressive activity was increased in acute infections, with high Treg induction correlating with increased viral titre and higher probability of progressing to chronic infection (148). HCV liver biopsies also show a correlation between higher Treg accumulation and lower liver damage (26). These data argue for induction of Treg activity in Hepatitis virus infection, leading to chronicity of the infection and control of immunopathology.

Other examples exist of Treg induction in viral infections leading to a more favourable outcome. In dengue virus infection, increased levels of Tregs correlate with milder disease due to a reduction of immunopathology (149).

Host factors may play a role in viral Treg induction. TGF-β is elevated in many viral infections including HIV, SIV, HCV, EBV, CMV, dengue virus, influenza, HTLV-1 and vaccinia virus. IL-10 is also upregulated in many viruses,

and evidence of the importance of its role in viral infection comes from EBV, parapoxvirus and equine herpesvirus 2, all of which encode viral IL-10 homologues (148).

1.9.2. Tregs in Bacterial Infection

Tregs also have a role in bacterial infections. In human *Mycobacterium tuberculosis* infection, Tregs frequencies are increased in the blood of infected individuals, and drug cure of the infection results in return of Treg levels to normal, indicating an active induction of Tregs, dependent on productive infection (153).

There is also evidence of Treg involvement in infection with the chronic stomach-dwelling bacterium *Helicobacter pylori*, the causative agent of peptic ulcers. Depletion of Tregs in an *H. pylori* mouse model results in increased immunopathology but reduced bacterial colonisation (154). In human infection, memory $CD4^+$ T cells from *H. pylori*-infected individuals produced less IFN-γ on antigen restimulation than uninfected individuals. Removal of Tregs from the cultures resulted in increased IFN-γ production in infected individuals only, indicating active suppression (154).

1.9.3. Tregs in Protozoal Infection

Much of our insight into Treg induction in infection has stemmed from work on the protozoal parasites of the *Leishmania* genus. In *Leishmania major* infection, Treg accumulation at the site of infection occurs (157). In adoptive transfer studies, where $CD4^+CD25^-$ or $CD4^+CD25^+$ cells were purified from lesions and transferred to $RAG^{-/-}$ animals, it was shown that transfer of $CD4^+CD25^-$ effector cells resulted in

sterile immunity, while co-transfer of $CD4^+CD25^+$ cells downregulated responses and resulted in survival of a small number of parasites. This effect was partially IL-10 dependent, as infection of IL-10-deficient mice resulted in sterile immunity, and transfer of IL-10-deficient $CD4^+CD25^+$ cells did not suppress immunity as efficiently as wild-type cells. Interestingly, in models where sterile immunity was achieved, the immunity to subsequent infections seen in wild-type mice was lost, indicating that a small number of persisting parasites were necessary for immunity to repeated infections (157). Adoptive transfers using Ly5.1 $CD4^+CD25^+$ cells and Ly5.2 $CD4^+CD25^-$ cells in this model showed that the Tregs present at the site of infection originated from pre-existing natural Tregs, rather than being induced from $CD4^+CD25^-$ naïve cells (120). These Tregs were unusual in that they were not anergic *in vitro*, and would proliferate to *L. major*-infected DCs, while retaining Foxp3 expression and suppressive ability (155). The Tregs at the effector site express CD103, and this is important for suppression as CD103-deficient mice could not recruit Tregs to the infection site, and so susceptible mice became resistant (120).

In another important protozoal parasite, *Plasmodium berghei* (a mouse model of *Plasmodium falciparum*-related cerebral malaria), Tregs have a more complex role in infection. Depletion of Tregs with anti-CD25 prior to infection decreased severity of cerebral malaria. This is surprising as depletion of Tregs usually exacerbates immunopathology such as that seen in cerebral malaria (156). The depletion of Tregs was shown to increase the anti-malarial response, leading to lower early parasitaemia, preventing immunopathology in the brain.

1.9.4. Tregs in helminth infection

1.9.4.1 *Trichinella spiralis*

Trichinella spiralis is a nematode which lives in the lumen of the gut, releasing larvae which migrate through tissues to encyst in the muscle in specially adapted nurse cells. In a mouse model where *T. spiralis* larvae were injected intravenously, IL-10 levels in restimulations were increased and controlled the potentially pathogenic TH1 response. The IL-10 produced was not from TH2 cells as it was unaffected in STAT-6 KO mice, which lack TH2 responses. Increased levels of Foxp3 staining were also seen at the infection site, indicating Treg induction, however ablation of Tregs using anti-CD25 did not result in drecreased worm burden, indicating Tregs may not be the main controlling factor in this model (161).

1.9.4.2. *Heligmosomoides polygyrus*

H. polygyrus infection leads to an induction of a Treg population in the mesenteric lymph node (MLN), with an increase in the proportions and numbers of activated natural Foxp3$^+$ Tregs expressing CD103, CTLA-4 and surface TGF-β in the Mesenteric Lymph Node (MLN), and later the spleen (21, 164). This activated phenotype correlates with increased suppressive ability, as Tregs purified from the infected MLN at later timepoints are more suppressive *in vitro* than naïve controls MLN Tregs (21, 164). At early timepoints after infection, Foxp3$^+$ cells could also be seen to accumulate in the intestinal epithelium, at the site of infection (164). As mentioned previously, transfer of these Tregs is able to suppress both colitis and allergy in recipient animals (22, 23).

1.9.4.3. Schistosome infection

Schistosome infection, or schistosome egg injection, induces a TH2 response, with a small or undetectable TH1 response at later timepoints. However the initial response to infective cercaria is TH1-polarised, which is downregulated at later timepoints as egg deposition occurs (10). It was thought that the suppression of TH1 responses to schistosomes was due to IL-10 released from TH2 cells. However, recent studies have shown that in the absence of TH2 responses (in IL-4-deficient mice), TH1 responses are not greatly increased after schistosome egg injection, but depletion of Tregs greatly increases both TH1 and TH2 responses in an IL-10-independent manner. Tregs in this model expand in the draining LN, and could proliferate to Soluble Egg Antigen (SEA), indicating they may be specific to parasite antigens (29).

In *S. mansoni* infected mouse liver and spleen, *foxp3* transcript levels increase. The Tregs induced in this model are involved in suppression of the pathogenic granuloma around deposited eggs, as retroviral transduction of *foxp3* in infected mice resulted in significant decrease in the size of the granulomas (163). A recent study showed that *S. mansoni* infection did not increase the proportions of $Foxp3^+$ cells in the $CD4^+$ population of infected mice, however their numbers in the liver (at the site of egg deposition) did increase, in concert with $CD4^+Foxp3^-$ cell recruitment (165). However, the phenotype of the Tregs changed, with increased expression of CD103 (as seen in the *H. polygyrus* model (21, 164)), indicating an activated phenotype. Interestingly, when Tregs were depleted using anti-CD25, although proportions of IL-4-producing cells did increase, there was no evidence of

increased proliferation, indicating the Tregs in *S. mansoni* infection may control differentiation, but not proliferation of effector cells (165).

The role of TGF-β in relation to Tregs in this model is yet to be elucidated, although it has been shown that the fibrosis which occurs in the liver of *S. mansoni*-infected mice is unaffected by the absence of TGF-β signalling (168).

1.9.4.4. Filariasis

As mentioned previously, filarial-infected individuals show an antigen-specific hypoproliferative defect, indicating the presence of antigen-specific Tregs. Recently, more direct evidence of Treg induction in filarial infections of humans and model animals has come to light.

In *Onchocerca volvulus*, the filarial nematode which causes river blindness, antigen-specific hyporesponsiveness is present in generalised oncocerciasis (GEO) individuals (those who have productive infections, similarly to microfilaraemic individuals in lymphatic filariasis), which is absent in putative immune individuals. The hypoproliferative defect was specific to *O. volvulus* antigen, as normal responses were seen to *Ascaris suum* antigen, another nematode endemic in the population studied. When T cell lines were made from a GEO individual's PBMCs, the majority of clones which proliferated to *O. volvulus* antigen did not produce IL-2, but instead produced either IL-10 or TGF-β, with four clones producing both, indicating antigen-specific Treg induction. In putative immune individuals (comparable to lymphatic filariasis endemic normals), no Treg-resembling clones could be isolated, supporting the notion that antigen-specific Tregs are controlling the immune response to filariasis in chronically infected individuals (162).

In *Wuchereria bancrofti*, the most widespread causative agent of lymphatic filariasis, CTLA-4 expression is increased on T cells from microfilaraemic individuals, and these CTLA-4^{hi} cells are also $CD4^{+}CD25^{+}$, indicating an increase or activation of Tregs. Blocking CTLA-4 in *in vitro* restimulation cultures led to increased production of filarial antigen-specific IL-5, indicating the CTLA-4-expressing Tregs are suppressing filarial-specific TH2 responses (158).

The *Litomosoides sigmodontis* model of filarial infection has been instrumental in establishing a role for Tregs in filarial infection. *L. sigmodontis* is a filarial nematode which naturally infects cotton rats (*Sigmodon hispidus*), but in the laboratory can complete its lifecycle within gerbils and some strains of mice (169). Infection with *L. sigmodotis* in mice elicits a TH2 response, which leads to rejection of the parasite by a neutrophil-dependent pathway in resistant mouse strains (170). A productive TH2 response is essential, as anti-IL-5 administration prevents parasite clearance (32), similarly to IL-4-deficient mice (170). However, similarly to Schistosome infection, a TH1 component also appears to be involved in rejecting *L. sigmodontis*, as IL-5/IFN-γ double deficient mice have an increased worm burden compared to IL-5 single-deficient animals (171, 172).

L. sigmodontis-infected animals show a similar hypoproliferative defect to that seen in filarial-infected humans (173, 174), indicating a role for antigen-specific Tregs in this model. Tregs are induced in response to *L. sigmodontis* infection, with increases in expression of Foxp3, CTLA-4, and GITR at the site of infection. Administration of anti-IL-10 had no effect in this model, indicating suppression was IL-10-independent. However, administration of anti-CTLA-4 and anti-GITR together resulted in a reduced worm burden and ablation of the hypoproliferative defect, due

to blocking of Treg suppression (blocking CTLA-4), while costimulating suppressed TH2 cells (GITR stimulation) (160). If *L. sigmodontis* Mf alone are injected, they are rejected, however if adult parasites are also introduced, or adult ES is injected, the Mf are tolerated, arguing for a suppressive effect dependent on the secretions of adult parasites (174).

Early experiments using a model of *B. malayi* infection in jirds (Mongolian gerbil *Meriones unguiculatus*), showed a similar hypoproliferative defect to that seen in human infection. These experiments showed a major defect in proliferation of T cells stimulated with parasite antigens, with a smaller defect when stimulated with mitogens, compared to uninfected controls (175). This effect was dependent on adherent cells in the spleen of the jirds, and subsequently a similar population of suppressive adherent cells has been found in the spleens of mice infected with *Brugia pahangi*, a closely related parasite to *B. malayi* (176).

There is also evidence for Treg induction in *B. pahangi* infection of mice. L3 larvae or microfilaria (Mf) were injected subcutaneously, and splenocytes restimulated with adult antigen before analysis for Treg markers. L3 larvae infection, but not Mf injection led to a production of IL-10 and TGF-β by $CD4^+$ T cells. The T cells responding to antigen also upregulated expression of CD25 and CTLA-4, with an upregulation of Foxp3 and IL-10 transcription, all indicating an antigen-specific Treg induction (159).

These results indicate an antigen-specific suppression dependent on live parasites. The mechanisms keeping the immune response in check may involve Treg suppression, parasite-derived immunomodulatory molecules and/or suppressive macrophages.

1.10. Alternatively Activated Macrophages

Early data in the jird *B. malayi* model showed that adherent cells in the spleen were actively suppressing T cell responses, and when the adherent population was removed proliferative suppression was partially abrogated (175). Later work using the mouse peritoneal implant model (where adult worms are directly implanted into the mouse peritoneal cavity, as the full lifecycle cannot develop within the mouse) also showed a suppressive population of adherent cells in the peritoneal lavage (47, 48, 177). This adherent population appears to be composed of alternatively activated macrophages, and much work has been done to characterize these cells (48, 177).

Activated macrophages can be divided into two categories: classically activated or M1 macrophages, and alternatively activated, or M2 macrophages (178), summarized in Figure 1.9.

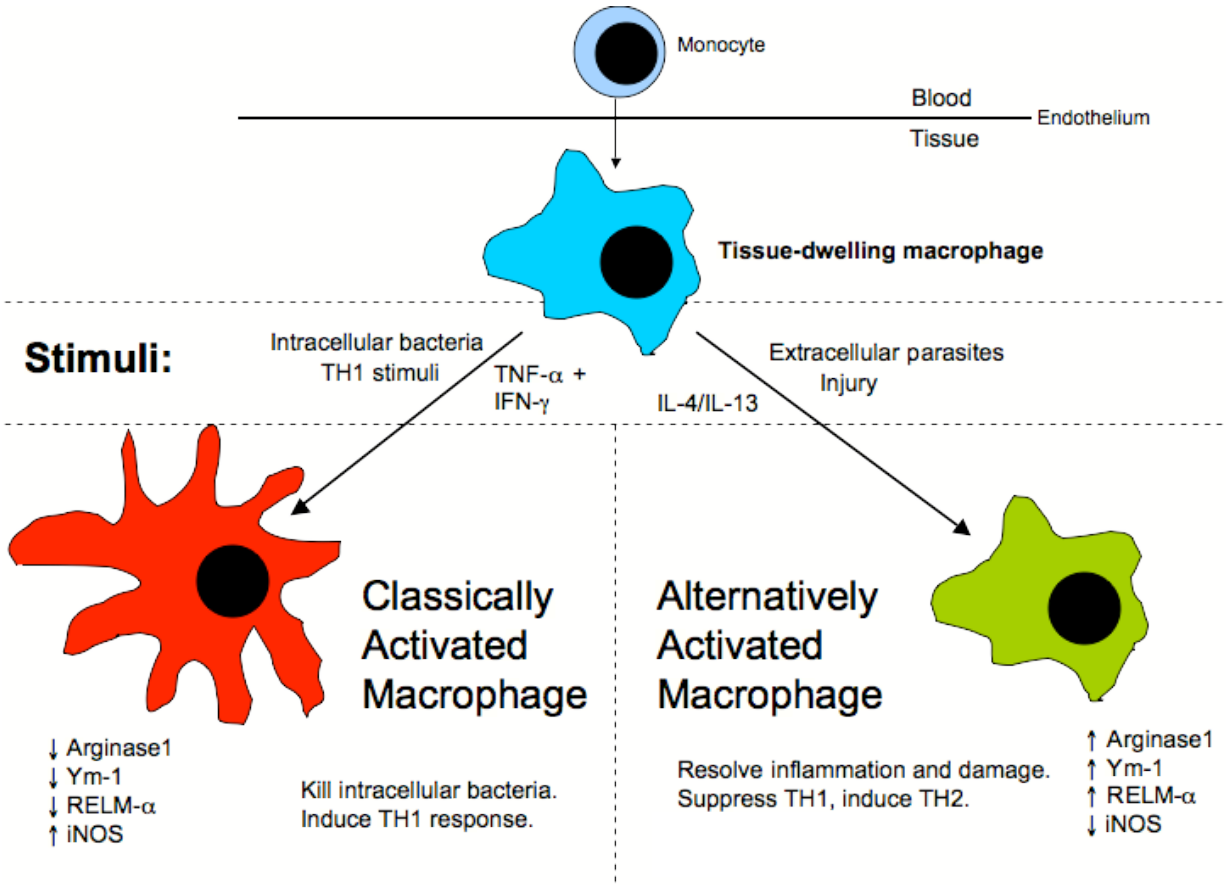

Figure 1.9: Macrophage activation.

Classically activated macrophages are induced by TH1 cytokines such as IFN-γ and TNF-α, or signaling through Toll-Like Receptors (TLRs) by bacterial Pathogen Associated Molecular Patterns (PAMPs). Alternatively activated macrophages (AAMacs) are induced by the TH2 cytokines IL-4 and IL-13 (178, 179). They downregulate the classically activated macrophage maker iNOS, while upregulating Arginase1, Ym1 and RELM-α (180), and these are now used as AAMac markers.

AAMacs are recruited to sites of injury, and are proposed to have roles in tissue repair (181) and suppression of tumour immunity (182). Their effector function in immune responses appears to be to expel parasitic infections, and AAMacs are induced in *B. malayi*, *S. mansoni*, *N. brasiliensis* and *H. polygyrus* infection (178). In a secondary challenge *H. polygyrus* infection, AAMacs accumulate around the L4 larvae in the intestinal wall, and pre-depletion of macrophages prevented immunity to a challenge infection (183) indicating their importance in anti-parasite TH2 effector functions. In filarial infection of mice, AAMacs are induced at the site of infection, are highly suppressive and can induce TH2 differentiation by a partially TGF-β-dependent pathway (184). Mice which lack the IL-4R specifically on macrophages cannot produce AAMacs and succumb to acute schistosomiasis due to a lack of immunoregulatory AAMacs around deposited eggs (185).

Interestingly, it was recently shown that human Tregs can induce alternative activation of macrophages *in vitro*, suggesting a link between Tregs and alternatively activated macrophage induction (186).

1.11. Infection models of filariasis

In order to investigate parasite-mediated Treg induction, in this project I used a mouse model of *B. malayi* infection. *Brugia* infection has also been experimentally modelled in cats (187), dogs (46), gerbils (188), mice (189), rats (190) rhesus monkeys (191) and even humans (192). The mouse model is most often used in immunological studies as the murine immune system is the best characterised, and reagents for manipulating and assessing immune responses are more freely available for mice than for other model systems (193). This model involves either injection of L3 or Mf stage parasites, or surgical implant of adult worms. The major limitation of the mouse model is that the full lifecycle cannot take place, and the parasites are not tolerated indefinitely, in contrast to other animal models (e.g. gerbils, cats and dogs). In the mouse, L3s injected s.c. or i.p. survive between 10 and 60 days, dependent on the strain used (194). Mfs injected i.p. last around 28 days or injected i.v. will circulate for 65 days (193). Adult worms implanted i.p. will survive for 90 days and produce Mfs (193). The rejection of the parasite in mice is mediated by the adaptive immune system as nude (athymic) or *scid* mice tolerate the entire *B. malayi* lifecycle (193, 195). However, although parasite rejection does take place in immunocompetent mice, a similar proliferative defect to that in jirds can be seen, indicating that some suppressive mechanisms, possibly including Treg induction, occur (48, 177). A wide range of cytokine gene targeted mice, as well as monoclonal antibodies, have been used to manipulate *B. malayi* infection in the mouse model, as shown in Table 1.3:

Table 1.3: Immunological manipulations of the *B. malayi* mouse model

Modification	Background	*Brugia* stage used	Outcome	Reference
IL-4 -/-	BALB/c	L3/Mf i.p.	Tolerance of all mammalian lifecycle stages in the Rajan laboratory, increased levels of Mf only in the Devaney laboratory	(196, 197)
IL-4 -/-	C57BL/6	Adults i.p.	Loss of proliferative defect in peritoneal lavage cells	(177)
IL-5 -/-	C57BL/6	L3 i.p.	Higher worm burdens and decreased eosinophilia in primary infection	(198)
IL-10 -/-	C57BL/6	Adults i.p.	No change in proliferative defect	(177)
α-IL-10 treatment	BALB/c	L3 s.c.	Increased proliferation of Ag-stimulated splenocytes	(199)
α-IL-10 treatment	CBA/Ca + C57/BL6	Mf i.v.	Mf cleared more rapidly than controls	(200)
IFN-γ -/-	BALB/c	L3 i.p.	Increased tolerance of L3 at early timepoints	(196)
IgM -/-	C57BL/6	L3 s.c.	Decreased IL-5 and IL-10, increased IFN-γ of Ag-stimulated splenocytes	(199)
SCID	C57BL/6	L3 i.p.	Tolerance of all mammalian lifecycle stages	(196)

Rejection of the parasite is dependent on neutrophil recruitment and requires both the TH1 and TH2 arms of the immune system, as both IL-4 or IFN-γ-deficient mice have increased tolerance to *B. malayi*, similarly to *L. sigmodontis* (170). IL-4 has an intriguing role in *B. malayi* infection as loss of IL-4 leads to increased tolerance, but also reduces the hypoproliferative defect, as both effects may be dependent on TH2 response-induced AAMacs (177). Infections of mice with different stages of the *B. malayi* lifecycle shows that infection with L3 larvae or adults induces a TH2 response, with production of IL-4 in the draining LN, whereas infections with Mf leads to production of the TH1 cytokine IFN-γ (193).

Interestingly, IL-4 is produced in the draining LN at early timepoints to L3 infection by $CD4^-CD8^-$ double-negative $CD3^+$ cells, followed by IL-4 production by conventional $CD4^+$ T cells at later timepoints (201). The early IL-4-producing cells in L3 infection were later characterised as NK T cells (202), and this early IL-4 production may be important for initiating the TH2 response seen in filarial infection.

Regulation of the response by IL-10 is also important, as anti-IL-10-treated infected mice clear Mfs more quickly (200), and anti-IL-10-treatment in *in vitro* restimulation cultures allows proliferation to live L3 larvae (203). B cells may be involved in regulating the TH2 response as in IgM knock-outs (which have no B cells), there is a decreased IL-5 and IL-10 response, and an increased IFN-γ response, indicating a switch to a TH1 phenotype (199).

Genetic differences between mouse strains may also have relevance to the immune-mediated rejection of *B. malayi* from mice. The relative tolerance of various mouse strains to intraperitoneal L3 *B. malayi* infection is shown in Table 1.4:

Table 1.4: Tolerance of mouse strains to *B. malayi* L3 larvae

Strain	No of L3 i.p.	Larvae at 2 weeks post-infection	Reference
AKR	100	3%	(204)
BALB/c	100	6%	(204)
BALB/cByJ	50	40%	(194)
C_3H	100	0.5%	(204)
C57BL/6J	50	<1%	(194)
NZB/NIHJ	100	15%	(204)

There also appear to be differences in tolerance due to high or low dose rates, as can be seen above with the data from different labs comparing 100 or 50 L3 infected i.p. into BALB/c mice.

Therefore *B. malayi* infection of mice represents a non-tolerant model of human filariasis, which may be very useful as both the regulatory and the effector arms of the immune response can be studied with reference to individual stages of parasite infection (193).

1.12. Project Hypothesis

I hypothesised that TGF-β homologues may be expressed by many helminth worms, and that these TGF-β homologues could be responsible for Treg induction in helminth infection.

To investigate this, I used molecular methods to search for novel TGF-β homologues in the intestinal helminths *H. contortus*, *H. polygyrus*, *N. brasiliensis* and *T. circumcincta*. I also expressed the *B. malayi* TGF-β homologue, Bm-TGH-2, in insect cells to assess its impact on the mammalian immune system. To investigate Treg induction in filarial infection, I infected mice with L3 or adult *B. malayi*, and assessed expression of Treg markers. We then used a range of interventions in this model to investigate the mechanism of Treg induction and the specificity of the Tregs induced.

Chapter 2:
Materials and Methods

2. Materials and Methods

All chemicals are from Sigma unless otherwise stated.

2.1. Parasite lifecycles

2.1.1 *Brugia malayi* lifecycle

Brugia malayi L3 larvae were taken from crushed infected *Aedes aegypti* mosquitoes in Grace's insect medium (Invitrogen) by allowing larvae to settle through a metal filter, and separating from mosquito material manually with a Pasteur pipette, with several washes into RPMI 1640 (Invitrogen). 50 L3 were injected intraperitoneally using a 21-gauge needle. L3s were killed as controls by heating to 65°C for 10 min. Adult *B. malayi* parasites were retrieved from the peritoneal cavity of patently (infected 3-12 months previously) infected jirds. Adult *B. malayi* were separated into groups of 4 females with 1 male. When dead adults were required, parasites were frozen at -20°C overnight, then thawed at 37°C prior to implantation. Adult parasites were then surgically implanted into the peritoneal cavity, or controls were cut open, RPMI 1640 injected into the peritoneal cavity, and stitched closed (sham surgery).

2.1.2. *Heligmosomoides polygyrus* lifecycle

The *Heligmosomoides polygyrus* and *Nippostrongylus brasiliensis* lifecycles were maintained by Y. Harcus. L3 larvae of both parasites were obtained from cultures of infected mouse or rat faeces respectively by Baermannisation (section 2.1.5).

200 *H. polygyrus* L3 larvae were orally gavaged into CBA x C57BL/6 F1 mice, and adults obtained at day 14 post-infection by opening the intestines, picking adults and washing into RPMI 1640 medium with 100 U/ml penicillin, 100 μg/ml streptomycin, 2mM L-glutamine and 1 % glucose and cultured at approximately 50 worms/ml at 37°C. After 24 h, a sample of supernatant was taken and centrifuged at 1,500 *g* for 5 min to collect eggs. The adult worms were cultured for 21 days during which time supernatants were collected every 3-4 days and replaced with fresh media. At the end of the 21-day period supernatants were pooled and concentrated over a 3,000 molecular weight filter to 0.5 mg/ml.

2.1.3 *Nippostrongylus brasiliensis* lifecycle

4000 *N. brasiliensis* L3 larvae were injected subcutaneously into SD strain rats (Harlan). L4 larvae were dissected from the lungs and the gut 48 h post-infection, and adult parasites were taken from the gut at day 6 post-infection by Baermannisation (section 2.2.5) by Y. Harcus.

2.1.4 *Haemonchus contortus* and *Teladorsagia circumcincta* lifecycles

Haemonchus contortus and *Teladorsagia circumcincta* lifecycles were maintained as described in Knox et al, 1990 (205), and were carried out by members of the Knox group (Moredun Research Institute, Penicuik, UK). Briefly, infective larvae (L3) were obtained by culturing the faeces of sheep harbouring experimental infections, 21 days post-infection. L3 larvae were exsheathed in 8% sodium hypochlorite solution and following four washes in 0.85% physiological saline at 38°C for up to 90 min. Fourth stage larvae and adult parasites were harvested 8 days

and 21 days respectively after infecting worm-free sheep (7-12 months old) with 50,000 L3 of either *T. circumcincta* or *H. contortus*. Parasites were harvested from the abomasa as described (205) and washed five times in PBS, then stored in TRIzol reagent (Invitrogen) at -80°C, until ready for RNA extraction.

2.1.5. Baermannisation

To collect motile parasites from tissue or faeces, material was added to a coarse nylon mesh in a funnel draining into a 15 ml tube, and immersed in Hanks Buffered Salt Solution (Invitrogen). This Baermann apparatus was then incubated at 37°C for 2 h or until parasites were visible collected in the 15 ml tube.

2.2 Molecular techniques

2.2.1 RNA purification

Approximately 50 µl packed volume of parasites in 1 ml of TRIzol (Invitrogen) were homogenised on ice using a glass homogeniser, and 200 µl chloroform added. This mixture was incubated at room temperature for 2 min before centrifugation at 12,000 *g* for 15 min at 4°C. The aqueous layer (approximately 200 µl) was then removed, added to 500 µl isopropanol, incubated at room temperature for 10 min, and then centrifuged at 12,000 *g* for 10 min at 4°C. The RNA pellet was then resuspended in 500 µl 70 % ethanol, pelleted again, the supernatant removed and the pellet air-dried. The RNA was resuspended in 20 µl DEPC water. The DNA-free kit (Ambion) was used to degrade any remaining DNA: 2 µl of DNAse with 2.4 µl DNAse buffer was added, and incubated at 37°C, 30 min. 5 µl of the DNA-free kit's DNAse inactivation reagent was then added, incubated at room temperature for

2 min, spun down briefly, and supernatant recovered. The concentration of RNA in this supernatant was determined by spectrophotometry at 260 nm using the extinction coefficient for RNA: 25 ul/ug/cm.

2.2.2 Reverse Transcription

Reverse transcription was performed with 500 ng of RNA, 2 μl 10X reverse transcriptase buffer, 2 μl 25 mM dNTP mix, 1 μl 50 U/μl MMLV reverse transcriptase (Stratagene), 0.5 μl 40 U/μl RNAsin (Promega), 1 μl 0.4 μg/ml oligo dT primer (Promega) and DEPC-treated water to 20 μl. The reaction was then performed on a PCR block at 20°C for 10 min, 37°C for 60 min and 99°C for 5 min.

2.2.3 Conventional PCR

Polymerase Chain Reactions (PCRs) were performed on a MJ Research DNA Engine under a variety of conditions. In general, cycles entailed denaturing at 94°C for 1 min, annealing at 55-65°C for 1 min (depending on primers and product), and extending at 72°C for 0.5-2 min (depending on length of product). Reaction mixes were used with 0.2 μl 5 U/μl Taq (QIAGEN), 0.2 μl 25 mM dNTP mix, 2 μl 10 X PCR buffer (QIAGEN), 1 μl forward and reverse primers (10 μm each), 1 μl template (cDNA, colony pick or plasmid miniprep) and water to 20 μl.

2.2.4 5’ and 3’ RACE

The 5’ and 3’ RACE (Rapid Amplification of Complementary DNA Ends) techniques allow amplification of the ends of genes for which a fragment of sequence is known. The 3’ terminus of the sequence is amplified by reverse

transcribing RNA using an oligo-dT primer with an additional sequence at the 3' end of poly-thymidine tract. This means that all cDNA created using this technique contains a specific sequence after the poly-T tail.

To amplify the 5' terminus of the sequence, it is first necessary to ligate a second specific primer to the 5' end of the RNA molecule prior to reverse transcription. This is achieved by first dephosphorylating the RNA, then degrading the 5' cap structure of the mRNA molecule, which exposes a single free phosphate group at the 5' end of the mRNA molecule. The 5' RACE primer is then ligated to the only free phosphate group on the molecule, which is at the 5' end of the gene. Thus, when the mRNA molecule is reverse transcribed, resulting in "RACE-ready" cDNA, specific primers are added to both the 5' and 3' ends of the sequence, allowing amplification of either end.

The Generacer core kit (Invitrogen) was used to carry out 5' and 3' RACE, following the manufacturer's protocols. Briefly, 5 μg RNA was dephosphorylated using Calf Intestinal Phosphatase (CIP), phenol:chloroform precipitated, decapped using Tobacco Acid Pyrophosphatase (TAP), again precipitated, and the GeneRacer RNA oligo was ligated to the free 5' phosphate group. The sequence of the oligo is shown below:

5'-CGACUGGAGCACGAGGACACUGACAUGGACUGAAGGAGUAGAAA-3'

The RNA was again precipitated, and reverse transcribed using the Superscript III RT kit (Invitrogen), and the Generacer oligo dT, with sequence shown below:

5'-GCTGTCAACGATACGCTACGTAACGGCATGACAGTG$(T)_{24}$-3'

The resulting cDNA was RNAse-treated. The RACE-ready cDNA was then used in PCR with gene-specific and Generacer primers to amplify the 5' and 3' ends.

2.2.5 Cloning

PCR products were run on 1.5 % agarose ethidium bromide gels, and bands excised under UV transillumination. Products were then purified using the QIAGEN gel extraction kit, using the manufacturer's protocols. Purified bands were read on a Biophotometer spectrophotometer (Eppendorf) at 260 nm to determine their concentration, using the extinction co-efficient for double-stranded DNA: 20 µl/µg/cm. Amplified DNA fragments were then ligated into the pGEM-T Easy vector (Promega) (Figure 2.1), at a 3:1 molar ratio of insert:vector. This was calculated using the following formula:

(ng vector X kb length of insert)/kb length of vector X 3 = ng insert

Insert and vector were added to ligation reactions with 1 µl 3 U/µl T4 ligase (Promega), 5 µl 2X ligase buffer and water to 10 µl and incubated at 4°C overnight. The 10 µl ligation reaction was then added to 50 µl heat-competent JM109 cells (Promega) which were transformed by incubating on ice for 20 min, 42°C for 50 sec, on ice 2 min, then 450 µl SOCS medium (Invitrogen) was added and incubated at 37°C for 1 h (to allow transformed plasmid to express the antibiotic resistance gene). A 200 µl sample of the transformation mix was then spread on an LB agar plate containing 50 µg/ml ampicillin (Sigma), and incubated at 37°C overnight. Single colonies were picked into 20 µl SOCS medium, 1 µl of which was then used in a colony screen PCR with vector primers to check for expected size of insert. The remainder of the colony picks of selected clones were then seeded into 5 ml LB medium with 50 µg/ml ampicillin, and placed in a 37°C shaking incubator overnight. Cultures were pelleted at 2,500 *g*, 10 min, and plasmid DNA purified from the

bacterial pellets using the QIAGEN miniprep kit, following manufacturer's protocols.

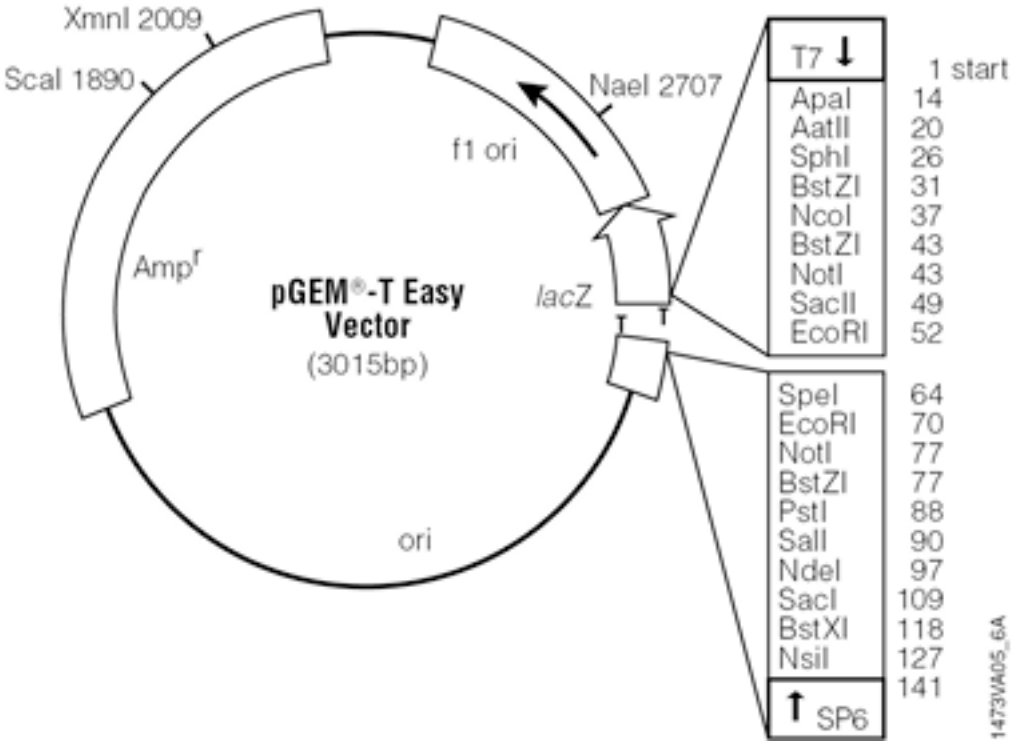

Figure 2.1: pGEM-T Easy vector map
(http://www.promega.com/vectors/t_vectors.htm)

2.2.6 Sequencing

Sequencing was carried out on a ABI3730 automated sequencer, using the BIGDYE 3.0 reagent, with 2 μl BIGDYE 3.0 premix, 2 μl 5X buffer, 1 μl 20 ng/μl vector primer and 1 μl of plasmid miniprep. Sequencing reactions were run at 95°C for 30 sec, 50°C for 20 sec and 60°C for 4 min, for 25 cycles.

2.2.7 Sequence Analysis

Basic Local Alignment and Search Tool (BLAST) searches were used to find similar sequences from all species, using the National Centre for Biotechnology

Information (NCBI) service (www.ncbi.nlm.nih.gov/blast). Sequences were analysed using the MacVector 9 program (MacVector Inc.), and sequences were aligned by the ClustalW function of MacVector, then checked by eye and altered if necessary.

2.2.8 Quantitative Real-Time PCR

Real-time PCR was carried out with 1 μl of a 1 in 10 dilution of cDNA, with 5 μl Platinum SYBR green qPCR supermix (Invitrogen), 0.2 μl of forward and reverse primers (10 μM), and water to 10 μl. Triplicate sample reactions were used. Duplicates of a standard curve of doubling dilutions of a neat mixture of all samples cDNA being assayed was used to find relative levels of expression. The reactions were ran on a Chromo4 real-time PCR machine (Alpha Innotech). Samples to be assayed for SYBR green fluorescence were denatured for 20 sec at 94°C, annealed for 20 sec at 65°C and extended for 20 sec at 72°C for 50 cycles for actin (for all species), *T. circumcincta* β-tubulin, and TGH genes from *H. polygyrus*, *N. brasiliensis* and *T. circumcincta*. For the *H. contortus* TGH, a similar protocol was used, but annealing was carried out at the lower temperature of 55°C.

In all reactions a melting curve analysis was also carried out after the end of the 50 amplification cycles, in which the PCR block was cooled to the annealing temperature, read, then the temperature increased by 0.5°C and read again. This was repeated until the temperature reached 94°C, and the fluorescence profiles allowed determination of whether single or multiple products had been amplified (as a single product denatures at a given temperature, and a second product denatures at another, giving 2 peaks). Reaction products were also run on ethidium bromide gels to confirm that a single product had been amplified.

2.3 Bacterial protein expression

2.3.1 Cloning and expression of *H. polygyrus* Hp-TGH-2

Inserts were amplified using primers with overhanging *Nde*I and *Xho*I restriction enzyme sites, using *Pfu* polymerase (Promega). *Pfu* polymerase reactions were set up as described in section 2.2.2, but using *Pfu* polymerase and buffer instead of *Taq* polymerase and buffer. The product amplified and a plasmid prep of pET21b was digested using *Nde*I and *Xho*I (New England Biolabs) in buffer 2 (New England Biolabs), at 37 °C for 4 h. The insert was then ligated into pET21, transformed in heat-competent BL21 (DE3) cells (Invitrogen) and sequenced as described in section 2.2.5. Clones containing the correct sequence were then seeded into LB medium containing 50 μg/ml ampicillin, in a 37°C shaking incubator. Once the cultures reached an OD600 of 0.4-0.6 (indicating that the bacteria had entered the exponential growth phase), 1 μg/ml IPTG was added, inducing expression of the insert. After a further 3 h of culture, cultures were centrifuged at 10,000 *g*, 10 min. Pellets were resuspended in 6-His Binding Buffer (162 mM Na_2HPO_4, 38 mM NaH_2PO_4, 500 mM NaCl, 10 mM Imidazole, pH 7.4), and centrifuged at 16,000 *g* for 20 min. Supernatants were taken, and the pellet was resuspended in 6-His Binding Buffer containing 8 M urea. The solution was again centrifuged, 16,000 *g* 20 min, and the supernatant was taken. The 6-His-bearing protein was then purified from the supernatant containing 8 M urea using an AKTAprime system (Amersham) with a Ni^{2+}-charged column and sodium phosphate washes, with elution in a rising concentration of imidazole. Multiple fractions collected from AKTAprime were tested for presence of protein by Bradford assay (section 2.3.2) and Coomassie

staining (section 2.3.3). The fractions containing significant amounts of protein were then pooled and dialysed against PBS.

2.3.2 SDS-PAGE gel analysis and Coomassie Staining

One part 4 x LDS sample buffer (Invitrogen) was added to 3 parts of the sample in the presence of 20 mM β-mercaptoethanol (as a reducing agent), then heated to 100°C for 10 min. Reduced samples and the SeeBlue Plus 2 marker (Invitrogen) were then added to wells on a 4-12% Nu-PAGE gel, and run in MES buffer (Invitrogen), at 200 V for 45 min. Gels were incubated overnight at 4°C in Coomassie stain (0.025% Coomassie Brilliant Blue R250 (Amersham), 40% methanol, 7% acetic acid), rocking, then destained in 40% methanol, 7% acetic acid, for 2 h, rocking at room temperature.

2.3.3 Bradford Assay

190 µl of Coomassie Plus protein assay reagent (Pierce) was added to 10 µl of samples and doubling dilutions of BSA standards in PBS (starting concentration of 2 mg/ml). The samples were then read at 595 nm. The concentrations of the samples were then calculated from the standard curve using the SoftMax Pro program (Molecular Devices Corp).

2.3.4 Polyclonal Antibody Generation

To prepare recombinant protein for immunisation, it was mixed with an equal volume of 9 % aluminum potassium sulfate (alum), and a drop of phenol red (Sigma) was added (turning yellow in acidic solution). The solution was neutralised by

adding 1 M sodium hydroxide until the solution became pink. The protein was then allowed to precipitate for 30 min at room temperature, before washing 3 times in phosphate buffered saline (PBS). The precipitated protein with alum was resuspended in PBS, and 200 μg was injected subcutaneously into SD strain rats (Harlan). Four weeks later, a challenge immunisation of 40 μg alum-precipitated protein was administered, and this was repeated a week later. A further week after the second challenge (6 weeks after first immunisation), blood was collected by cardiac bleed from the rats.

The blood was allowed to clot at 4°C overnight, and the fluid phase was centrifuged 12,000 *g* and serum collected. Serum was also collected from naive rats as controls. The immunised rat serum was later IgG purified by adherence to a protein G sepharose column on an AKTAprime instrument. Fractions eluted were assessed for protein concentration by Bradford assay (section 2.3.3) and IgG purity by SDS-PAGE and Coomassie Blue staining (section 2.3.2). Fractions containing IgG were pooled and dialysed in 3,500 MWCO tubing (Spectrum Laboratories) against PBS. The purified IgG was then concentrated using a 5 kDa cutoff spin column (Sartorius), centrifuging at 2,500 *g*, and the final concentration determined by Bradford assay (section 2.3.3).

2.3.5 Western Blots

Samples were run on 4-12% Nu-PAGE gels in MES buffer (Invitrogen) as described in section 2.3.2, then blotted to nitrocellulose membrane (Bio-Rad) in a semi-dry transfer system using transfer buffer (5% 20X transfer buffer (Invitrogen), 10% methanol), at 90 mA for 1 h. The membrane was blocked overnight in 10%

(w/v) dried skimmed milk in TBS, at 4°C, rocking. Membranes were then probed with either 1/2000 anti-6-His antibody in 6-His antibody blocking reagent (QIAGEN), or with specific antisera, or control antibodies at dilutions specific to each antibody, as described in the text. Anti-mouse IgG-HRP or anti-rat IgG-HRP (Cayman Chemicals) secondary antibodies at 1/1000 dilution in 5% (w/v) dried skimmed milk in TBST (TBS with 0.05% Tween, 0.1% Triton-X) were then added, and incubated rocking at room temperature for 1 h. Between each step the membrane was washed 3 times in TBST. In the blot shown in chapter 3, membranes were developed using Chemiglow reagent (Alpha Innotech), and photographed using a FluorChem SP gel imager (Alpha Innotech). In all blots in chapter 4, the membrane was developed using ECL reagent (Amersham) before being exposed to X-Ray film (Amersham).

2.3.6 HES depletion

IgG purified rat antisera or naïve rat IgG (Sigma) at 100 μg/ml was added to 10 μg/ml HES, and incubated at 37°C for 1 h. This was then incubated rotating at 4°C overnight with 50 μl packed protein G sepharose beads. The beads were then pelleted by centrifuging at 12,000 *g* for 5 min at 4°C. The supernatant was then applied to the MFB-F11 TGF-β bioassay (section 2.4.2).

2.4 TGF-β Bioassays

2.4.1 MLEC TGF-β Bioassay

The MLEC TGF-β bioassay uses Mink Lung Epithelial Cells stably transfected with a luciferase gene coupled to the Plasminogen Activator Inhibitor-1

(PAI-1) promoter (a gene strongly upregulated by TGF-β signalling) (82). MLEC cells were grown in RPMI 1640 with 10 % FCS, 100 U/μl Penicillin, 100 μg/ml Streptomycin and 2 mM L-Glutamine in T175 flasks until confluent, then detached using 2 ml 0.05% Trypsin and 0.53 mM EDTA. They were then plated out on 96-well white fluorometer plates at 1.6 x10^4 cells per well in 50 μl medium and allowed to adhere for 4 h at 37°C. Samples in 50 μl medium were then added, and cells were cultured at 37°C for 24 h. To assay the luciferase signal, 100 μl/well Bright-Glo Luciferase Assay reagent (Promega) was added to all wells, incubated at room temperature for 2 min to allow cells to lyse, then read on a LUMIstar luminometer (BMG Biotechnologies).

2.4.2 MFB-F11 TGF-β Bioassay

The MFB-F11 bioassay uses *Tgfb1-/-* mouse fibroblasts which have been stably transfected with a plasmid containing a secreted alkaline phosphatase reporter gene coupled to a Smad-binding element promoter (SBE-SEAP) (courtesy of Tony Wyss-Coray, Stanford University School of Medicine) (206). Cells were allowed to adhere to 96-well tissue culture plates at 4 x 10^4 cells/well in 50 μl DMEM with 10 % FCS, 100 U/ml penicillin, 100 μg/ml streptomycin, 2mM L-glutamine and 15 μg/ml hygromycin B (Invitrogen), at 37°C for 4 h. Plates were then centrifuged at 1,200 g, 5 min, and washed in warm PBS. Samples in 50 μl DMEM without serum was then added to all wells, and incubated at 37°C overnight, after which 10 μl samples of culture supernatant were collected into white 96-well luminometer plates (BMG Biotechnologies). These samples were assayed using the SEAP detection kit

(Clontech) (following manufacturers protocols) and read on a LUMIstar luminometer (BMG Biotechnologies).

2.5 Treg induction assay

Spleen cells from naïve mice were harvested through a nylon strainer, then centrifuged at 1,200 *g*, 5 min. The pelleted cells were then red blood cell lysed in 5 ml red blood cell lysis buffer (Sigma) for 5 min at room temperature. Splenocytes were counted on a haemocytometer, and plated out in RPMI 1640 with 10% Fetal Calf Serum (Invitrogen), 100 U/ml penicillin, 100 μg/ml streptomycin and 2 mM L-glutamine in a 96-well plate, in the presence of 2 μg/ml ConA, and recombinant human TGF-β (R&D Systems) or parasite products as indicated. The cells were then cultured at 37°C in 5 % CO_2 for 72 h, and then stained for flow cytometric staining of CD4, CD25 and Foxp3, as described in section 2.8.1.

2.6 Insect Cell Protein Expression

2.6.1 Insect Cell Culture

The insect cell line SF9 (Invitrogen) was used for amplification of the recombinant virus. The SF21 cell line (donated by A. Alcami, Cambridge University) was used for plaque assays and protein expression. The Hi5 cell line (Invitrogen) was used for attempted expression of the recombinant proteins. Both SF9 and SF21 were derived from the Fall armyworm *Spodoptera frugiperda*, and Hi5 cell line was derived from the cabbage looper *Trichopulsia ni*. All lines were grown at 27°C, either in monolayers or in stirrer flasks. SF9 cells were grown in serum-free Ex-cell 420 media (JRH Bioscience), SF21 cells were grown in TC100

media (Gibco-BRC) containing 10% FCS and Hi5 cells were grown in serum-free Express Five media (Invitrogen). All insect cell media contained 100 U/ml penicillin, 100 μg/ml streptomycin and 2 mM L-glutamine.

2.6.2 Preparation of recombinant baculovirus

All TGF-β homologues were cloned into the pBAC-1 vector (Novagen) (Figure 2.2), and used together with the BacPAK6 viral genome (Clontech) to transfect a SF21 cell monolayer using Bacfectin. This allows homologous recombination between the linearised BacPAK6 viral genome and the engineered pBAC-1 vector, resulting in viable virus expressing the insert gene. Recombinant viruses were then purified by plaque purification (see section 2.6.4) and expression of the relevant homologue tested by Western blotting (see section 2.3.5).

pBAC-1 sequence landmarks	
polh promoter region	1177-1259
polh transcription start	1210-1211
wt polh 5'UTR –1 position	1259
Multiple cloning sites (*Bam*H I - *Xho* I)	1263-1308
His•Tag coding sequence	1309-1326

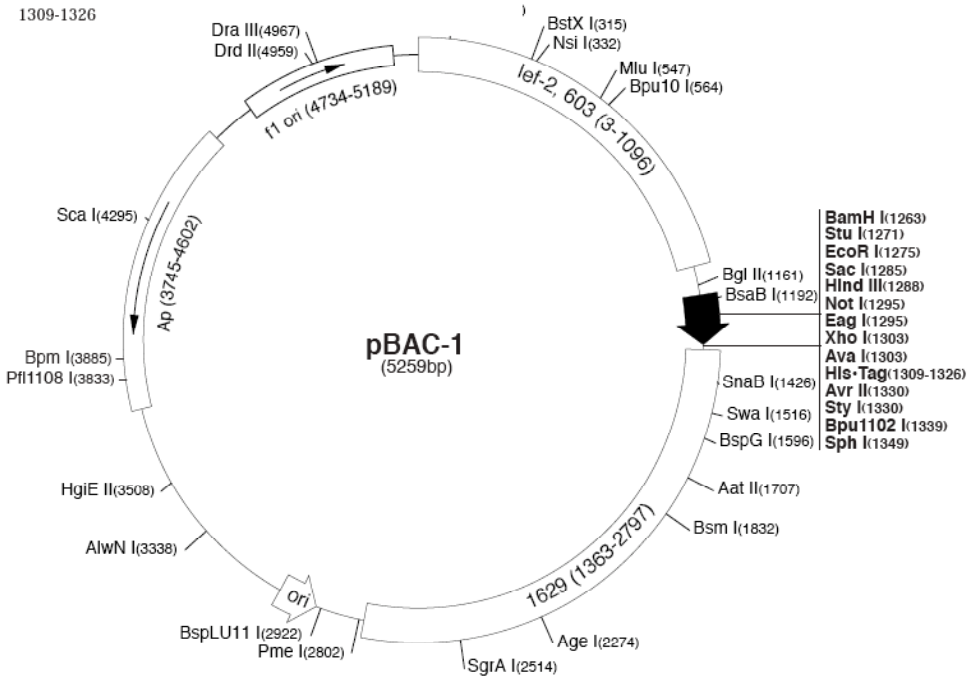

Figure 2.2: pBAC-1 vector map

2.6.3 Amplification of Recombinant Baculovirus

Virus was amplified by infection at a 3:1 virus:cell ratio into SF9 cells in a monolayer until complete cytopathic effect, as judged by a loss of adherence in culture, usually occurring after around 3 days. Media containing virus was then removed, and subjected to centrifugation at 1,200 *g*, for 5 min in order to pellet dead cells. The supernatant was aspirated off and the virus titre calculated by plaque assay (section 2.6.4)

2.6.4 Plaque assay

Virus, at a range of 10-fold dilutions, were infected into monolayers of SF21 cells in 6-well tissue-culture plates, and each well overlaid with 3 ml 3% Seaplaque agarose (Cambrex). The agarose was then overlaid with 2 ml complete TC100 media, and plates were incubated for 4 days at 27°C. The media was removed and 1.5 ml/well 1:13 neutral red (Sigma):PBS solution was overlaid, allowed to diffuse into the agarose and aspirated off. The plate was stored overnight in the dark at room temperature to allow plaques to develop. The visible plaques could thus be counted to give viral titre, or individual plaques picked using a sterile glass pipette.

2.6.5 Insect cell protein expression

Expression of recombinant protein was carried out using SF21 cells, either in 24-well plates in monolayers or in 1,000 ml stirrer flasks (Techne). TGF-β homologue recombinant virus was added at 10 pfu/cell and furin virus added at 20 pfu/cell. Supernatants from small-scale trial expressions were run on Western blots (section 2.3.5). Supernatants from large-scale expressions were dialysed against at

least a 10-fold volume of His binding buffer (162 mM Na_2HPO_4, 38 mM NaH_2PO_4, 500 mM NaCl, 10 mM Imidazole, pH 7.4). The 6-His-bearing protein was then purified from the supernatant containing 8 M urea using an AKTAprime system (Amersham) with a Ni^{2+}-charged column and sodium phosphate washes, and eluted in a rising concentration of imidazole. Multiple fractions collected from AKTAprime were tested for presence of protein by Bradford assay (section 2.3.3) and Coomassie Blue staining (section 2.3.2). The fractions containing significant amounts of protein were then pooled and dialysed against PBS.

2.6.6 Mass spectrometry

Bands were excised from Coomassie Blue-stained gels and sent to the SIRCAMS service (University of Edinburgh) for matrix-assisted laser desorption/ionization (MALDI) Mass Spectrometry analysis. Peptide fragment sizes predicted by the analysis were entered into the ProteinProspector MS-Fit tool (http://prospector.ucsf.edu), and searched against the nonredundant (nr) sequence database in NCBI, to give predicted peptides and blast hits of *B. malayi* genes.

2.7 Animal Models

2.7.1 Animals

BALB/c, C57BL/6, CBA, DO11.10, OT-II, CD4-trophic TGF-βRII dominant negative (C57BL/6 background), and IL-$4R^{-/-}$ (BALB/c background) mice, 6-10 weeks old, were bred and housed according to Home Office guidelines. Male adult jirds (*Meriones unguiculatus*) carrying a patent *Brugia malayi* infection were used as a source of adult worms and microfilariae (Mf).

2.7.2 Preparations of Single-Cell Suspensions from Mice

At indicated time points, mice were sacrificed using terminal anaesthesia and bled out. Ice-cold RPMI 1640 with 10% Fetal Calf Serum (Invitrogen) was then used to recover peritoneal cells by lavage (Peritoneal Lavage: PL). Samples of the peritoneal lavage taken directly *ex vivo* were analysed by flow cytometric staining. The remaining cells were then incubated on tissue-culture grade plastic plates for 1-3 h at 37 °C to allow macrophages to adhere. Non-adherent cells were then removed and stained for flow cytometry, and in some experiments the adherent macrophages were detached by addition of 5 ml 1X PBS, 0.18g/L glucose and 3mM EDTA, and incubation at 37°C for 15 min. The macrophages were then used in the EL-4 suppression assay (section 2.8.7). Where appropriate, L3 larvae recovered from the peritoneum were also counted at this point.

Spleens and mediastinal lymph nodes were also taken in some experiments, and single cell suspensions prepared through nylon filters; splenocyte suspensions were red blood cell lysed (using red blood cell lysis buffer, Sigma) and stained for flow cytometric analysis, or restimulated with *B. malayi* adult homogenate for 72 h at 37°C. Supernatants were then taken and used in cytokine ELISA.

2.8 Immunological Techniques

2.8.1 Flow cytometry

Samples of 2 x 10^5 to 2 x10^6 cells were used for flow cytometric staining, depending on the frequency of the populations examined. Prior to flow cytometric staining 40 μl 100 μg/ml purified naive rat IgG (Sigma) in FACS buffer (PBS with 0.5 % Bovine serum albumin and 0.05 % sodium azide) was added to all samples to

block Fc receptors. Cells were then washed in 200 µl FACS buffer before extracellular staining was carried out.

The following antibodies and reagents were used for flow cytometric staining:

- FITC-conjugated α-GR1 (RB6-8C5) (BD Pharmingen), use at 1/25
- PE-conjugated α-SIGLEC-F (E50-2440) (BD Pharmingen), use at 1/100
- Biotinylated α-F4/80 (BM8) (Biolegend), use at 1/100
- APC conjugated α-CD4 (RM4-5) (BD Pharmingen), use at 1/100
- PerCP conjugated α-CD4 (RM4-5) (BD Pharmingen), use at 1/100
- APC-Cy7 conjugated α-CD4 (RM4-5) (Ebioscience), use at 1/100
- AlexaFluor 700 α-CD4 (GK1.5) (Biolegend), use at 1/100
- Biotinylated α-CD25 (7D4) (BD Pharmingen), use at 1/25
- FITC conjugated α-CD25 (7D4) (BD Pharmingen), use at 1/50
- PE conjugated α-CD25 (7D4) (BD Pharmingen), use at 1/50
- FITC conjugated α-CD103 (M290) (BD Pharmingen), use at 1/25
- Biotinylated α-CD103 (M290) (BD Pharmingen), use at 1/50
- PE conjugated α-CTLA-4 (UC10-4F10-11) (BD Pharmingen), use at 1/10
- FITC, PE or APC conjugated α-Foxp3 (FJK-16s) (Ebioscience), use at 1/50
- FITC conjugated α-GITR (DTA-1) (made in-house), use at 1/250
- APC-conjugated α-IL-4 (11B11) (BD Pharmingen), use at 1/25
- PE conjugated α-IL-10 (JES5-16E3) (BD Pharmingen), use at 1/25
- FITC conjugated α-IFN-γ (XMG1.2) (BD Pharmingen), use at 1/25
- PerCP or APC conjugated streptavidin (Biolegend), use at 1/200

When intracellular cytokines were measured, the cells were first stimulated for 6 h at 37°C, in the presence of PMA (50 ng/ml), Ionomycin (1 µg/ml) and

Brefeldin A (Sigma) (20 μg/ml). They were then stained for surface markers, and permeabilised for 20 min at 4°C in BD Pharmingen Fix/Perm. Intracellular cytokines were stained in BD Pharmingen Perm/Wash.

To stain for Foxp3 and intracellular CTLA-4, cells were first stained for extracellular markers, then permeabilised for between 30 min and 16 h (as advised in the manufacturers protocols – no differences in staining were apparent in this range of permeabilisation times) using the Ebioscience Foxp3 staining kit. Foxp3 and CTLA-4 were stained in 1X Ebioscience Permeabilisation buffer.

Relevant isotype controls were used on all samples. Samples were acquired on a BD Biosciences LSR II flow cytometer and analysed using FlowJo software (Tree Star).

2.8.2 $CD4^+CD25^+$ Suppression Assay

$CD4^+$ cells were isolated from naïve mouse spleens and peritoneal lavage cells from L3 *B. malayi*–infected mice (15 mice pooled), using magnetic bead isolation on MACS columns (Miltenyi Biotech), as per the manufacturer's instructions. $CD4^-$ splenocytes were also collected, irradiated (30 Gy) to prevent proliferation, and used as APCs in suppression assays. $CD4^+$ MACS-purified splenocytes and PL cells were stained with Alexa Fluor 700-conjugated anti-CD4 and PE-conjugated anti-CD25. They were then separated on $CD4^+CD25^+$ and $CD4^+CD25^-$ cells using a BD Biosciences FACSAria. $CD4^+CD25^-$ naïve splenocytes or infected peritoneal lavage cells were then stained with 5 μM CFSE for 5 min, and washed into media. Suppression assay cultures were set up with 5 x 10^4 $CD4^+CD25^-$

splenocytes (responders), 5 x 10^4 $CD4^+CD25^+$ cells and 2 x 10^5 APCs in 96-well round-bottom plates in the presence of 0.1 μg/ml anti-CD3 at 37°C for 4 days.

2.8.3 Adoptive Transfer

Splenocytes were prepared from DO11.10 mice and 5 x 10^6 cells injected i.p. into groups of BALB/c male mice. The following day mice were infected as before with either L3 larvae or adult *B. malayi*, and a further day later 5 x 10^5 mature pOVA-loaded Bone Marrow-derived Dendritic Cells (BMDCs) were injected i.p., then mice were sacrificed 6 days later and PL taken.

2.8.4 BMDC culture

Bone marrow cells were obtained from femurs and tibias of BALB/c mice by flushing the bones with RPMI containing 10% FCS/1% penicillin-streptomycin/1% L-glutamine. Cells were centrifuged and plated out in non-tissue culture Petri dishes at a density of 5 × 10^5/ml in complete RPMI, supplemented with 20 ng/ml GM-CSF. Fresh medium was added 3, 6 and 8 days after the start of culture. After 10 days at 37°C, the cells were washed off into complete media containing 5 ng/ml GM-CSF (Peprotech), 100 ng/ml LPS (Sigma) and 100 μg/ml peptide OVA (323-339), and incubated overnight. Cells were then washed into PBS before injection.

2.8.5 Anti-TGF-β administration

Where blocking antibodies for TGF-β were used, anti-TGF-β was grown in-house (clone 1D11), and 100 μg/mouse antibody in PBS was injected

intraperitoneally on days -1, 1 3 and 5 from infection. Controls of rat IgG (Sigma) were used, as mentioned in chapter 6.

2.8.6 ALK-5 Inhibitor

It was attempted to block ALK-5 signaling using the specific inhibitor SB-525334 (Tocris bioscience). Each mouse was injected with 200 μg of SB-525334 in 1:1 PBS:DMSO, or PBS/DMSO vehicle alone either intraperitoneally or subcutaneously 30 min prior to infection, and 2, 4 and 6 days after infection with *B. malayi*.

2.8.7 Macrophage Suppression Assay

Adherent cells from the PL were prepared as described in section 2.7.2 and 1 x 10^5 cells were cultured with 1 x 10^4 EL-4 cells in RPMI 1640 containing 10 % FCS for 48 h, then pulsed overnight with 1 μCi/well *methyl*-^{3}H-thymidine. Proliferation was measured on a 1450 Microbeta scintillation counter (Trilux).

2.8.8 Cytokine ELISA

Ab pairs used for cytokine ELISAs were: IL-4 (11B11 for capture (grown in-house), BVD6-24G2 for detection), IL-5 (TRFK5 for capture, TRFK4 for detection), IL-10 (JES5-2A5 for capture, SXC-1 for detection), IFN-γ (R4-6A2 for capture (grown in-house), XMG1.2 for detection), IL-13 (38213 for capture (grown in-house), polyclonal rabbit anti-IL-13 (Preprotech) for detection). All antibodies were from BD Biosciences unless otherwise indicated. Capture antibodies were coated onto Maxisorp Immunoplates (NUNC) in carbonate buffer (0.1 M Na_2CO_3, 0.1 M

$NaHCO_3$, pH 9.6) at 4°C overnight, then blocked in 10 % FCS in Tris-Buffered Saline with 0.05% Tween 20 (TBST) at 37°C for 2 h. Samples and standards were then added (40 μl/well), and incubated at 4°C overnight. In some experiments, supernatants were then transferred to a second set of plates to allow quantification of other cytokines using the same supernatants. Secondary antibodies were then added in TBST with 10 % FCS, and incubated at 37°C for 1 h. Extravidin conjugates were then added in TBST with 10 % FCS, and incubated at 37°C for 1 h. Detection reagents were finally added, the plates were allowed to develop at room temperature in the dark, and read at 450 nm. Plates were washed between each step 5 times in TBST, and washed twice in water before addition of the detection reagents.

Recombinant murine IL-4, IFN-, IL-10, IL-13 and IL-5 (Sigma-Aldrich) were used as cytokine standards. Biotin detection Abs were used with ExtrAvidin-alkaline phosphatase conjugate (Sigma) and Sigma FastTM *p*-nitrophenyl phosphate substrate, except in the IL-13 ELISA, where extravidin-horseradish peroxidase (Sigma) and ABTS peroxidase substrate (KPL) was used.

2.9. Statistical analyses

Statistical analyses were carried out using Prism 4.0b (Graphpad Software Inc.). Where 2 groups were analysed, Student's t test was used. Where groups of 3 or more were analysed, One-Way ANOVA was used with a Bonferroni's multiple comparison test. In both cases if variances differed significantly, data was log-transformed to normalise. If the data could not be normalised, non parametric tests were used: Mann-Whitney test for 2 groups, and Kruskal-Wallis with a Dunn's post test for groups of 3 or more.

Chapter 3:
TGF-β Homologues from parasites

3. TGF-β Homologues from parasites

TGF-β homologues have already been found in many nematodes such as *Caenorhabditis elegans* (95), *Brugia malayi* (74, 96), *Ancylostoma caninum* (76) and *Schistosoma mansoni* (78). Molecular techniques were used to search for TGF-β homologues in the intestinal parasitic nematodes *Haemonchus contortus*, *Heligmosomoides polygyrus*, *Nippostrongylus brasiliensis* and *Teladorsagia circumcincta*.

The *A. caninum* TGF-β homologue Ac-TGH-2 was used as a starting point in homology searches, as *A. caninum* is an intestinal parasitic nematode, with a lifecycle similar to those of *H. contortus*, *H. polygyrus*, *N. brasiliensis* and *T. circumcincta*. *A. caninum* is a hookworm parasite of dogs, *H. contortus* and *T. circumcincta* are hookworms of sheep, *H. polygyrus* is a mouse intestinal parasite and *N. brasiliensis* is a hookworm parasite of rats.

The *H. contortus*, *H. polygyrus* and *T. circumcincta* are transmitted via the faecal/oral route, with L3 larvae infecting orally, developing to L4 larvae in the stomach of mice or the abomasum of sheep (the fourth stomach), where they penetrate the gut wall and develop to sexual adults, which emerge into the lumen of the gut, and deposit eggs in faeces. The *N. brasiliensis* lifecycle is slightly different as it infects via the skin, and migrates through the tissues to the lungs where it is coughed up and swallowed, developing to sexual adults in the lumen of the gut, also depositing eggs in the faeces.

3.1. Degenerate primer design

A TGF-β homologue was previously identified in *A. caninum*, Ac-TGH-2 (sometimes known as Ac-DAF-7). The Ac-TGH-2 sequence was used to search *H. contortus* genomic contigs on the Sanger website (http://www.sanger.ac.uk/Projects/H_contortus). The most significant hit was contig016772, which covered part of the conserved domain of Ac-TGH-2, as shown in Figure 3.1. An alignment of nematode TGF-β amino acid sequences was made, and degenerate primers were designed for regions which were best conserved and had lowest degeneracy (Figure 3.2). Where sequences could not be made to match all homologues, they were preferentially matched with that of *H. contortus* contig016722 and *A. caninum* Ac-TGH-2. The primer sequences are shown in Table 3.1 (Y = C/T, R = A/G and N = A/C/G/T):

Table 3.1: Degenerate Primers

Primer name	Nucleotide sequence	Amino acid sequence encoded	Degeneracy
RMM_TGF_for1	5'-TGYATGCCNGARGAYAARGARCC-3'	CMPEDKEP	128-fold
RMM_TGF_for2	5'-GTNGAYTTYCARCARATNGGNTGG-3'	VDFQQ(I/M)GW	512-fold
RMM_TGF_rev1	5'-RTAYTCNGCNGGRTGRCARCACAT-3'	MCCHPAEY	512-fold
RMM_TGF_rev2	5'-RTTRTCNGCRTTCATRTADATCAT-3'	MIYMNADN	64-fold

Combinations of these degenerate primers were used in PCRs with *H. polygyrus*, *N. brasiliensis* and *T. circumcincta* adult cDNA, and products (shown in Figure 3.3) were excised from gels and sequenced. A single 200 bp band was amplified from *H. polygyrus* cDNA using RMM_TGF_for1 and RMM_TGF_rev1 (Figure 3.3A), which showed significant similarity to Ac-TGH-2 by BLASTx

(searching a protein database using a translated nucleotide sequence). Bands at 400 bp and 250 bp were amplified from *N. brasiliensis* cDNA using RMM_TGF_for1 and RMM_TGF_rev1 (Figure 3.3B), of which the 400 bp band showed significant similarity to Ac-TGH-2, but contained putative introns. Bands at 200 bp and 300 bp were amplified from *T. circumcincta* cDNA using RMM_TGF_for2 and RMM_TGF_rev1 (Figure 3.3C), of which the 300 bp band showed significant similarity to Ac-TGH-2, however also contained putative introns. All sequences amplified are shown in Figure 3.4. Putative introns were removed from the sequences of *N. brasiliensis* and *T. circumcincta* to construct TGF-β homologue coding sequence fragments. Introns were identified by regions dissimilar to the Ac-TGH-2 coding sequence which contained in-frame stop codons (Figure 3.4). As intronic regions could only originate from genomic DNA, the *N. brasiliensis* and *T. circumcincta* cDNA must have been contaminated with genomic DNA. Therefore new cDNA was made for both parasites, with DNAse treatment prior to RT-PCR. Subsequent sequences did not amplify intronic DNA.

Non-degenerate primers were designed to the sequences amplified for *H. polygyrus*, *N. brasiliensis* and *T. circumcincta*, and from contig016772 of *H. contortus*. Primers were designed in both directions in each region for some genes to allow nested PCRs to be carried out. Primer sequences are shown in table 3.2:

Table 3.2: Non-degenerate primers

Primer	Forward primer	Reverse primer
H. contortus TGF 5'	5'-ATGTTCATGTCGGTTACGCTGG-3'	None
H. contortus TGF 3'	None	5'-CTCAGCAGGGTGACAGCACATTC-3'
H. polygyrus TGF 5'	5'-CCCGGATGTTGCCTCTACGAC-3'	5'-GTCGTAGAGGCAACATCCGGG-3'
H. polygyrus TGF 3'	5'-GACGCAACTGGAAATCAGGGG-3'	5'-CCCCTGATTTCCAGTTGCGTC-3'
N. brasiliensis TGF 5'	5'-GGTTGCTGTCTCTACGATCTC-3'	5'-GAGATCGTAGAGACAGCAACC-3'
N. brasiliensis TGF 3'	5'-GACGCAACGGGTAACCAAGGG-3'	5'-CCCTTGGTTACCCGTTGCGTC-3'
T. circumcincta TGF 5'	5'-GGGTGATTGTTCTGTGAATCAC-3'	5'-GTGATTCACAGAACAATCACCC-3'
T. circumcincta TGF 3'	None	5'-TCAAGAGCATGTACATTTACGG-3'

3.2. Full sequence of TGF-β homologues

Rapid Amplification of Complementary DNA Ends (RACE) was used to find the 5' and 3' ends of the sequences. RACE-ready cDNA was made using the Invitrogen Generacer Core kit from adult parasites of all 4 species. The products of 5' RACE are shown in Figure 3.5, and the 3' RACE products shown in Figure 3.6. The *H. contortus* and *T. circumcincta* 5' and 3' RACE products were amplified by conventional PCR, while the *H. polygyrus* and *N. brasiliensis* 5' and 3' RACE products were amplified by nested PCR, using first the Generacer primer and the gene-specific primer, followed by the Generacer nested primer and the nested gene-specific primer. Alignments were made of the full nucleotide (Figure 3.7) and amino acid (Figure 3.8) sequences with other TGF-β family members. The novel TGF-β homologues were named after their similarity to Ac-TGH-2 as Hc-TGH-2 (*H. contortus* TGF-β Homologue), Hp-TGH-2 (*H. polygyrus* TGF-β Homologue), Nb-TGH-2 (*N. brasiliensis* TGF-β Homologue) and Tc-TGH-2 (*T. circumcincta* TGF-β Homologue).

The sequences of Hp-TGH-2 and Nb-TGH-2 were amplified independently multiple times from RACE-ready cDNA as they are truncated at the 5' end compared to Ac-TGH-2 (see Figures 3.7 and 3.8). They were also amplified from Expressed Sequence Tag (EST) libraries (courtesy of Y. Harcus), and Hp-TGH-2 was also amplified using a spliced-leader PCR, with a gene-specific reverse and spliced leader forward primer, with the same sequence being found each time (data not shown). The SmInAct gene is also truncated at the 5' end, as can be seen in Figure 3.7 and 3.8, so this is not a feature confined to the *H. polygyrus* and *N. brasiliensis* TGF-β homologues.

3.3. Signal peptide identification

Part of the characteristic TGF-β structure is a signal peptide at the N-terminus, however when the novel TGF-β homologues were entered into the SignalP web-based signal peptide prediction program (http://www.cbs.dtu.dk/services/SignalP/), signal peptides were predicted for *A. caninum* (Ac-TGH-2) and Hc-TGH-2, however neither *S. mansoni* SmInAct nor any of the other novel TGF-βs had predicted signal peptides. The predictions are shown in Table 3.3:

Table 3.3: Signal peptide predictions

Gene	Signal peptide prediction	Cleavage site
Human TGF-β1	0.999 – Signal peptide	29-30 AG-LS
Ac-TGH-2	0.986 - Signal peptide	23-24 AL-FL
SmInAct	0.000 – No signal peptide	None
Hc-TGH-2	0.986 – Signal peptide	23-24 VHT-HN
Hp-TGH-2	0.000 – No signal peptide	None
Nb-TGH-2	0.000 – No signal peptide	None
Tc-TGH-2	0.001 – No signal peptide	None

3.4. Phylogenetic analysis of TGF-β homologues

The conserved domain of a range of human and nematode TGF-β family members were aligned (Figure 3.9). From the conserved region alignment, a phylogenetic tree (Figure 3.10) was constructed. As expected, Ac-TGH-2, along with the novel TGF-β homologues identified here aligned closely in a single group, with significant bootstrap values, forming an intestinal parasite TGF-β homologue family. Their relatedness to the rest of the TGF-β family was more difficult to quantify, as the nematode homologues appear to be only distantly related to the human TGF-β family.

3.5. Real-time PCR analysis

To assess the expression profile of the novel TGF-β homologues, cDNA was prepared from different lifecycle stages of each parasite. For *H. contortus* and *T. circumcincta*, we were supplied with L3 larvae that were either infective, or had been exsheathed, mimicking entry of the L3 larvae into the host. We were also supplied

with L4 larvae obtained from the abomasal wall, and adults from the gut. All *H. contortus* and *T. circumcincta* material was supplied by D. Knox, Moredun. Y. Harcus supplied cDNA from *N. brasiliensis* infective L3 larvae, L4 larvae taken from the lung, L4 larvae taken from the gut, and adults. *H. polygyrus* L3, adults and eggs were prepared in the laboratory. An RT-PCR reaction was carried out to make cDNA from all RNA. Real-time PCRs were then carried out on actin from all parasites and β-tubulin from *T. circumcincta* only, as housekeeping genes to normalise the levels of transcription. Regions of each of the parasite TGF-β homologues were also amplified to assess levels of transcription by real-time PCR. Primers used for real-time PCR are shown in table 3.5:

Table 3.5: Real-time PCR primers

Transcript	Forward primer (binding site)	Reverse primer	Product size
Actin (all species)	5'-TGAGCACGGTATCGTCACCAAC-3' (216-237)	5'-TTGAAGGTCTCGAACATGATCTG-3' (386-364)	171 bp
T. circumcincta β-tubulin	5'-TTCCATTCCCTCGTCTTCAC-3' (773-792)	5'-AGCCATTTTCAATCCACGAG-3' (1092-1073)	320 bp
H. contortus Hc-TGH-2	5'-ATGTTCATGTCGGTTACGCTGG-3' (652-673)	5'-CTCAGCAGGGTGACAGCACATTC-3' (954-932)	445 bp
H. polygyrus Hp-TGH-2	5'-CCCGGATGTTGCCTCTACGAC-3' (589-609)	5'-CCCCTGATTTCCAGTTGCGTC-3' (789-769)	201 bp
N. brasiliensis Nb-TGH-2	5'-GGTTGCTGTCTCTACGATCTC-3' (193-213)	5'-CCCTTGGTTACCCGTTGCGTC-3' (387-367)	195 bp
T. circumcincta Tc-TGH-2	5'-GGGTGATTGTTCTGTGAATCAC-3' (699-720)	5'-TCAAGAGCATGTACATTTACGG-3' (918-897)	220 bp

The levels of TGF-β homologue transcription were then divided by levels of actin or β-tubulin transcription to find the levels of transcription relative to housekeeping genes (Figure 3.11). As the *T. circumcincta* real-time PCR shows, normalisation by actin or β-tubulin gave similar results (Figure 3.11 D and E). β-tubulin is used routinely as a housekeeping gene in the Knox group, as its transcription is stable through all lifecycle stages (D. Knox personal communication). As actin gave similar results to β-tubulin in *T. circumcincta*, we can presume that β-actin is a good housekeeping gene to use in intestinal parasites.

In *H. contortus*, *H. polygyrus* and *N. brasiliensis*, transcription of the TGF-β homologues is highest in the L3 larvae stage, prior to the larvae entering the host. In

these parasites, the transcription is also lowest in the adult stage, when the parasites are in the lumen of the gut, external to the host. Interestingly, this trend is reversed in *T. circumcincta*, where transcription is highest in the adult stage, and lowest in the L3 stage and L4 stages (when the parasite is migrating through the tissue).

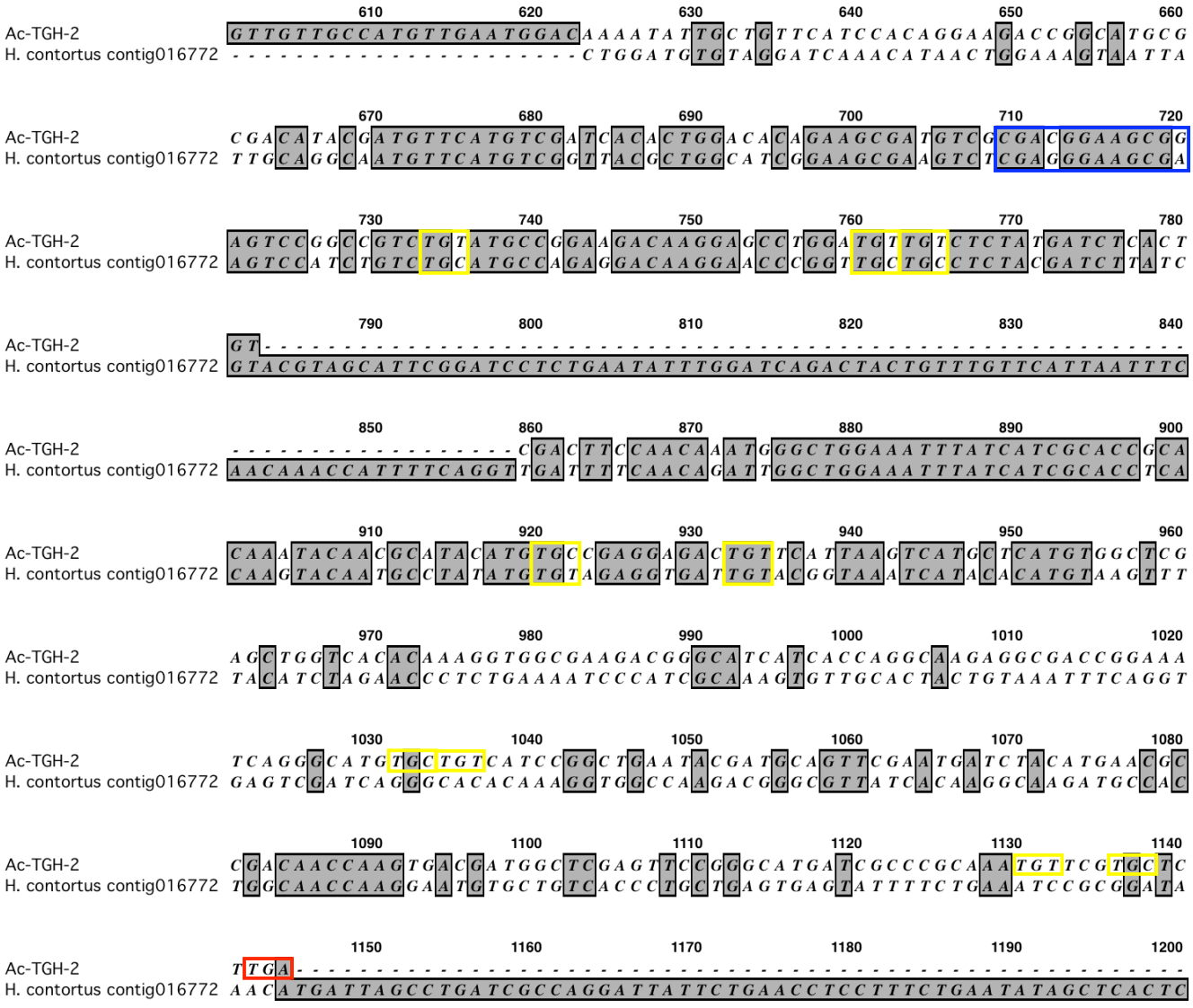

Figure 3.1: *H. contortus* contig016772 aligned with Ac-TGH-2
Part of the Ac-TGH-2 nucleotide sequence (600-1200) aligned with *H. contortus* genomic contig016772. The protease cleavage site is indicated by a blue box, conserved cysteines are indicated by yellow boxes, and the Ac-TGH-2 stop codon is indicated by a red box.

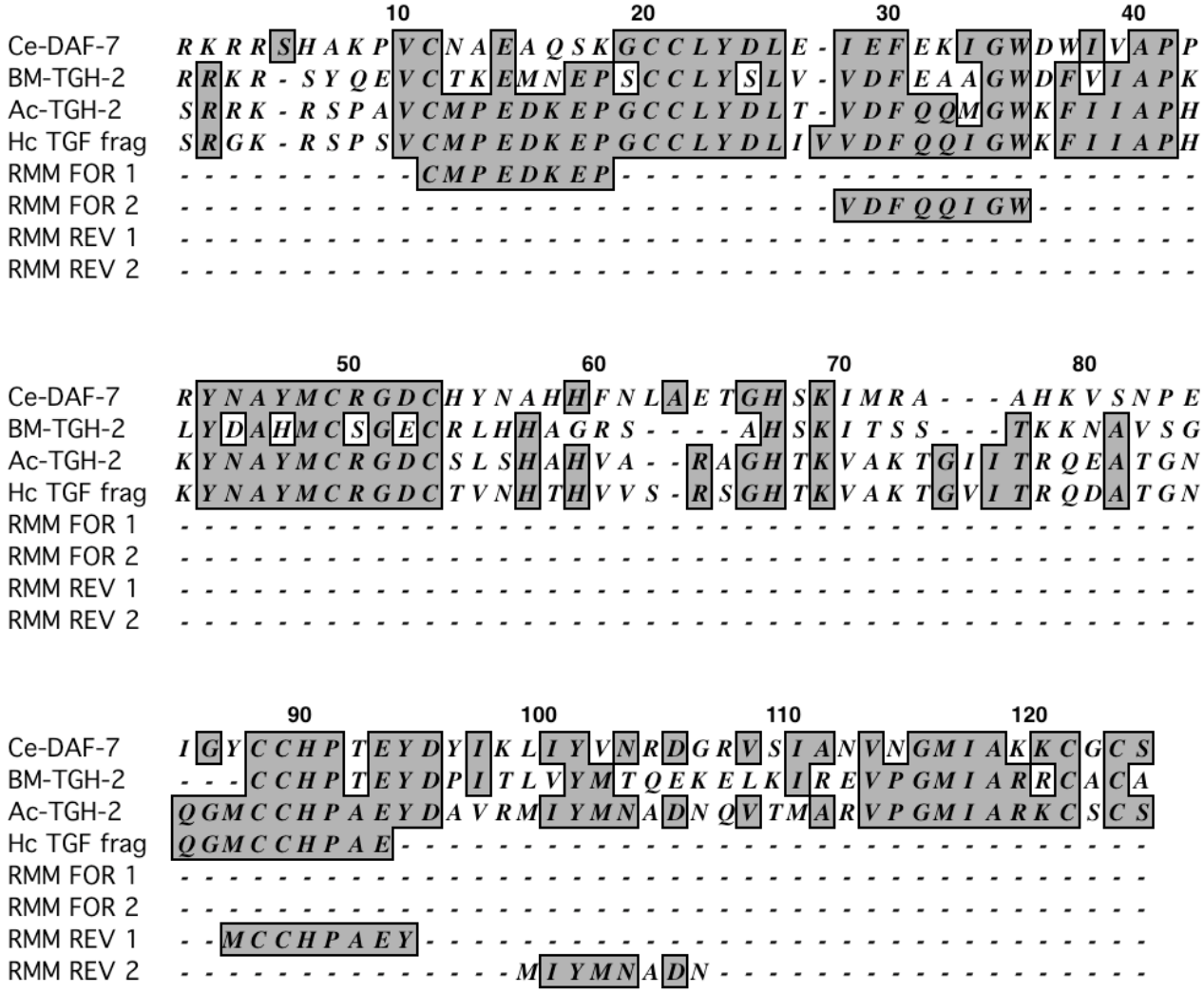

Figure 3.2: Degenerate primers aligned with known TGF-β homologues
Alignment of the active domain of TGF-β family members from *C. elegans* (Ce-DAF-7)*, B. malayi* (Bm-TGH-2)*, A. caninum* (Ac-TGH-2), and contig016772 from *H. contortus* (Hc TGF frag), and the amino acid sequences coded by the degenerate primers designed (RMM FOR/REV 1/2)

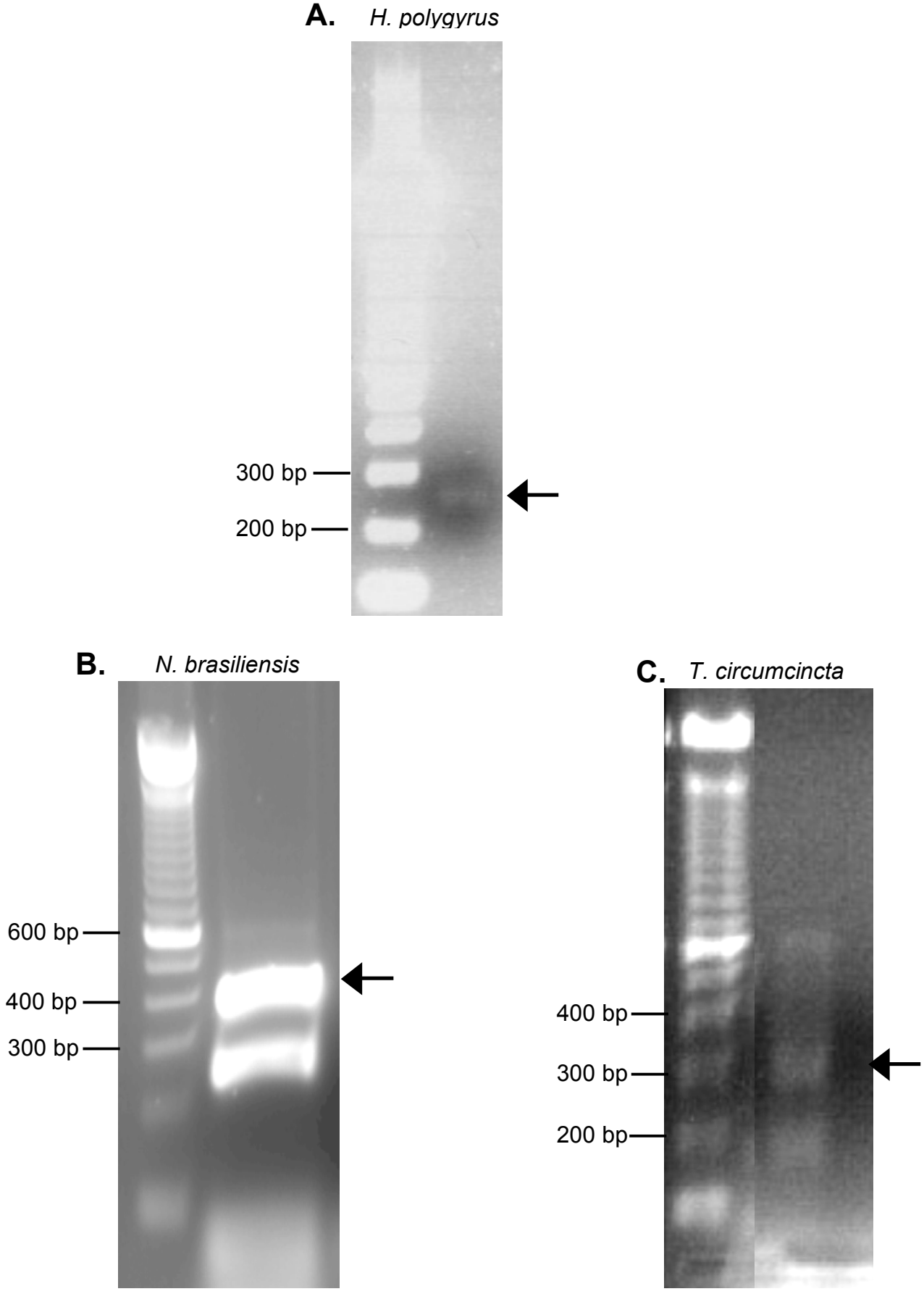

Figure 3.3: Degenerate PCR products
Ethidium bromide gels (1.5% agarose) of degenerate PCR products amplified from *H. polygyrus* (A), *N. brasiliensis* (B) and *T. circumcincta* (C). Arrows indicate sequenced bands. (Composite images)

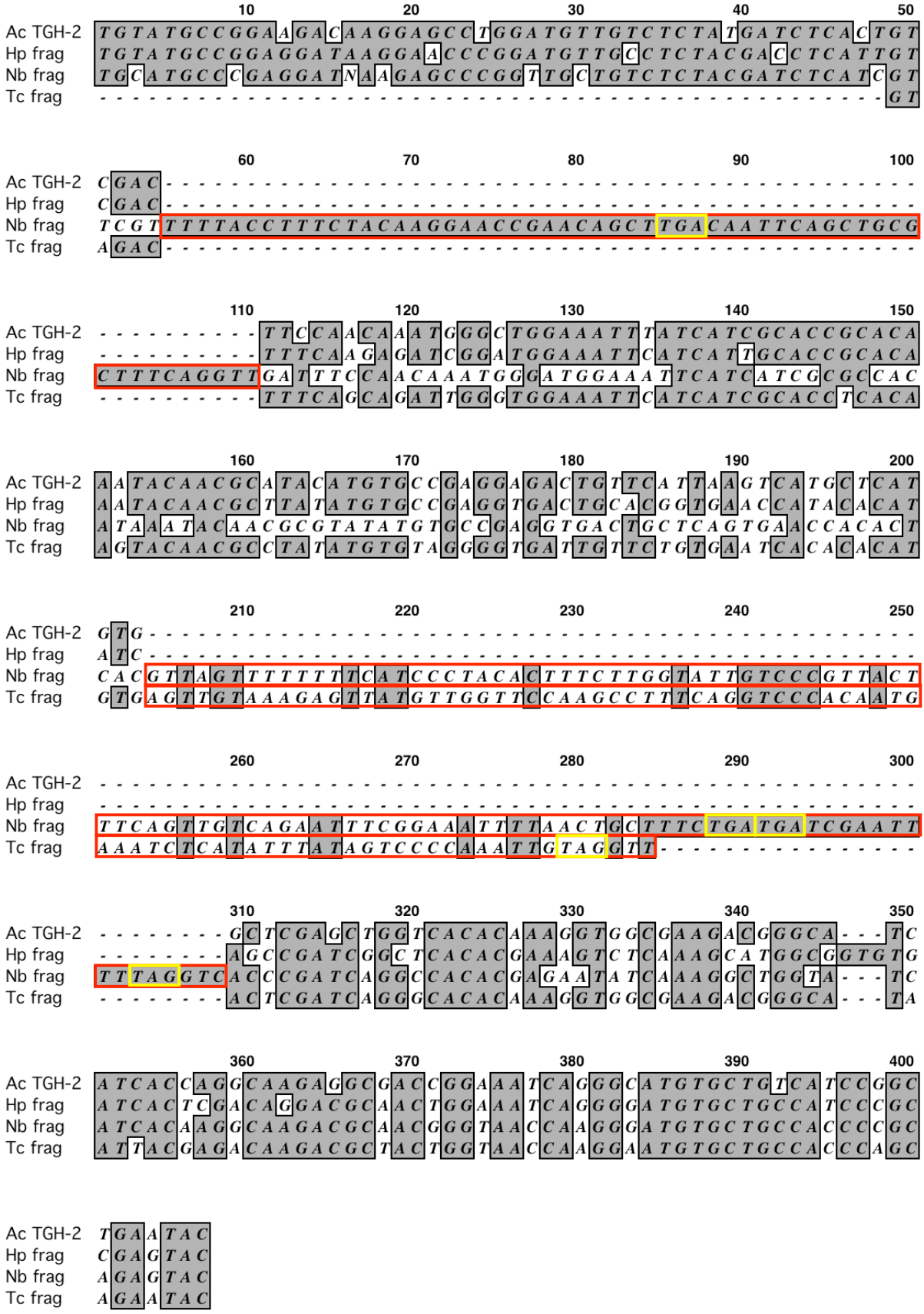

Figure 3.4: Alignment of denegerate PCR products with Ac-TGH-2
Fragment of Ac-TGH-2 coding sequence (777-1203) aligned with fragments amplified by degenerate PCR from H. *polygyrus*, *N. brasiliensis* and *T. circumcincta* cDNA. Red boxes indicate putative intronic regions, yellow boxes indicate in-frame stop codons.

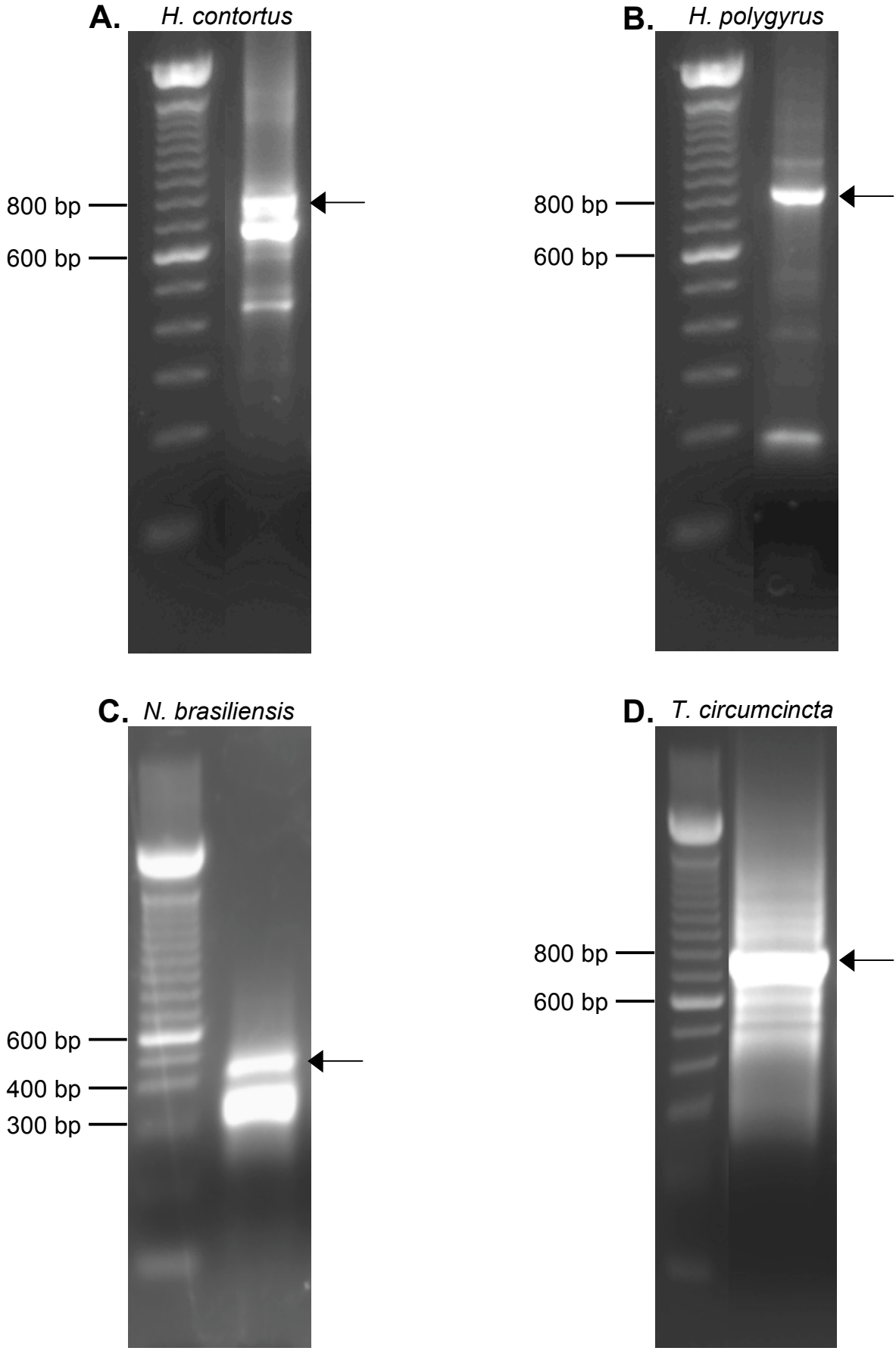

Figure 3.5: Products of 5' RACE
5' RACE products of TGF-β homologues from *H. contortus* (A), *H. polygyrus* (B), *N. brasiliensis* (C) and *T. circumcincta* (D), run on 1.5 % agarose ethidium bromide gels. Arrows indicate bands sequenced. (Composite images)

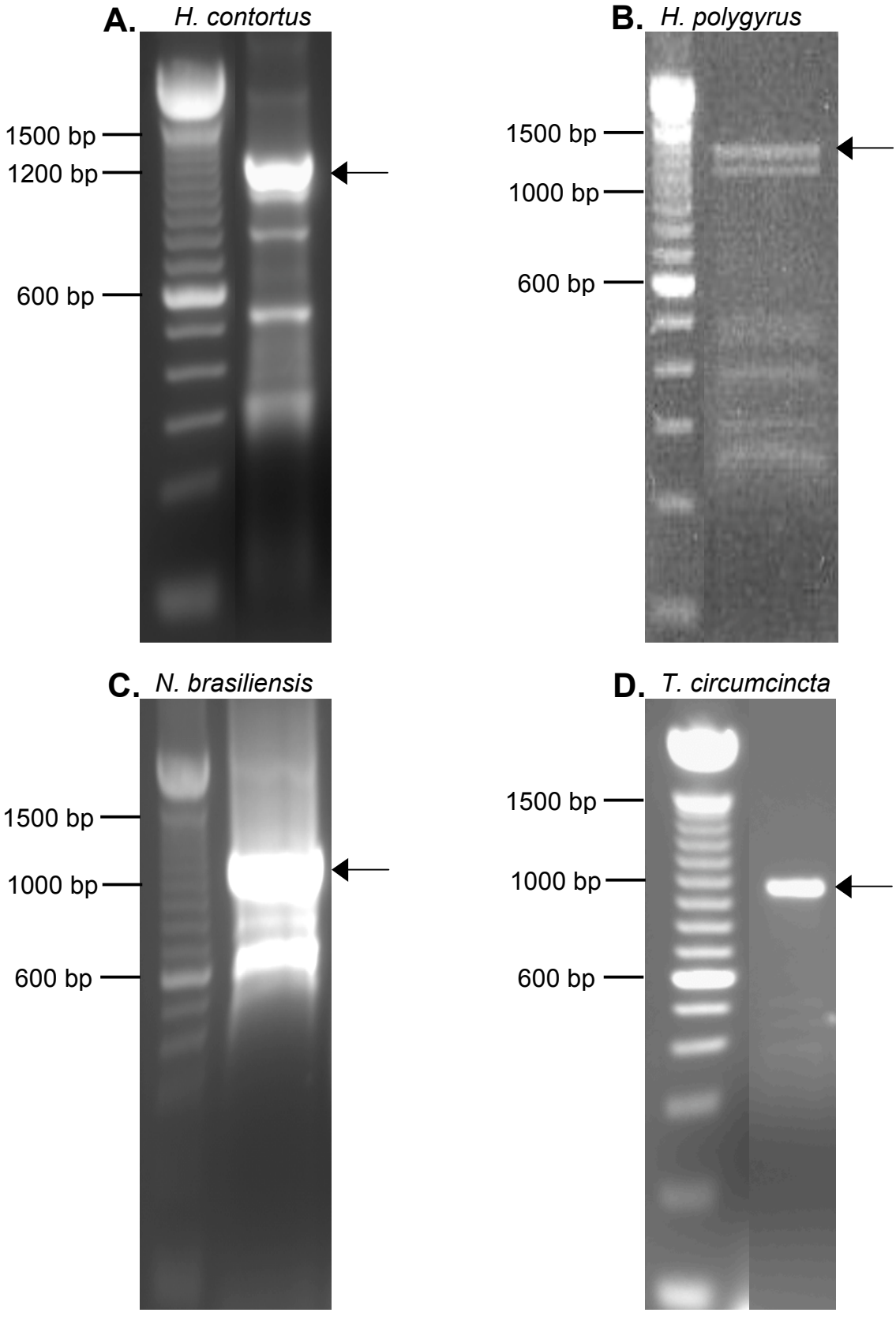

Figure 3.6: Products of 3' RACE
3' RACE of TGF-β homologues from *H. contortus* (A), *H. polygyrus* (B), *N. brasiliensis* (C) and *T. circumcincta* (D), run on 1.5 % agarose ethidium bromide gels. Arrows indicate bands sequenced. (Composite images)

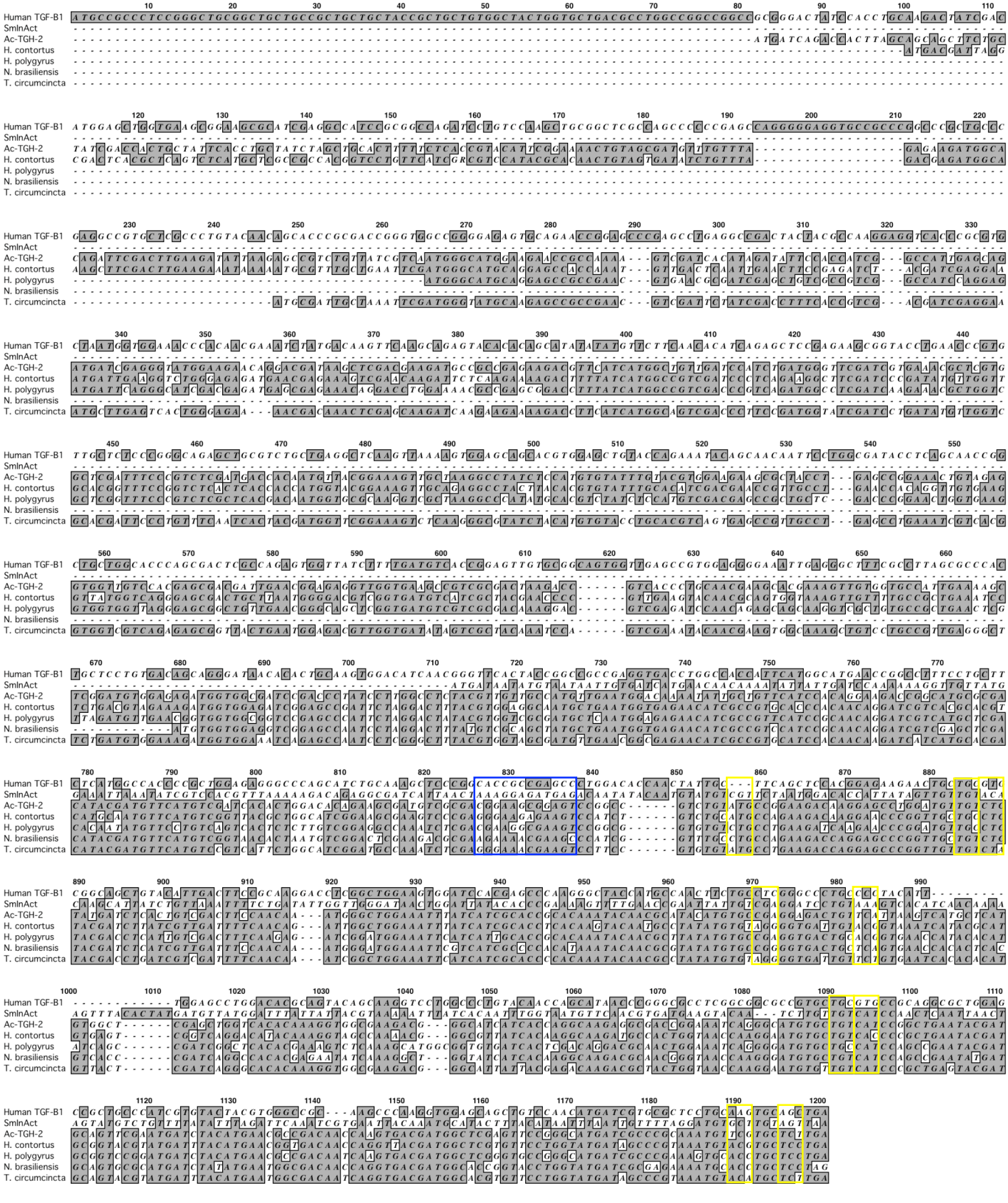

Figure 3.7: Nucleotide alignments of novel TGF-βs with known TGF-βs
DNA alignments of known TGF-βs from Human, *S. mansoni, A. caninum*, and novel TGF-β homologues from *H. contortus*, *H. polygyrus*, *N. brasiliensis* and *T. circumcincta*. Blue box indicates protease cleavage site, yellow boxes indicate conserved cysteines.

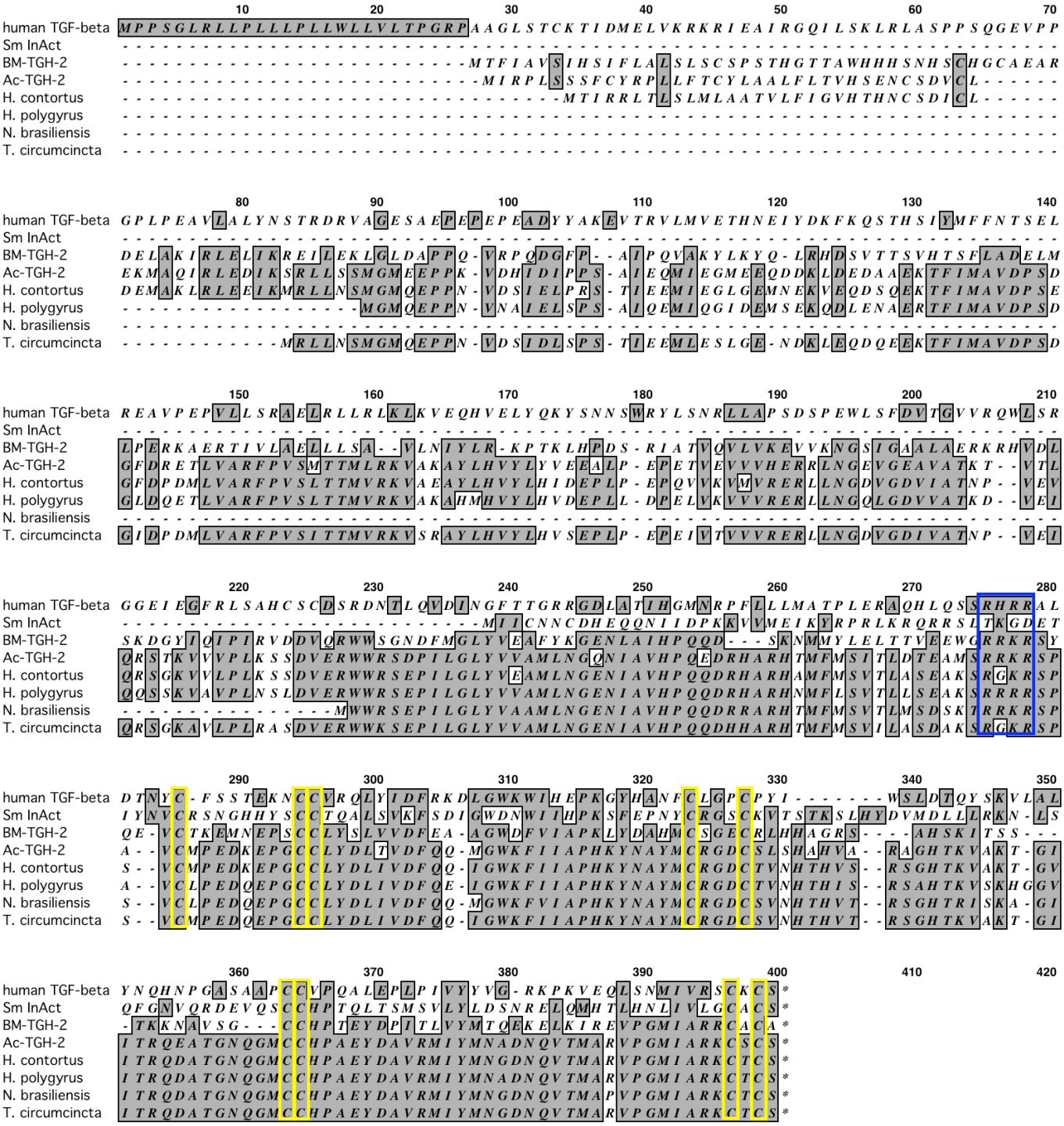

Figure 3.8: Amino acid alignments of novel TGF-βs with known TGF-βs
Protein alignments of known TGF-βs from Human, *S. mansoni, B. malayi*, *A. caninum*, and novel TGF-β homologues from *H. contortus*, *H. polygyrus*, *N. brasiliensis* and *T. circumcincta*. Blue box indicates protease cleavage site, yellow boxes indicate conserved cysteines.

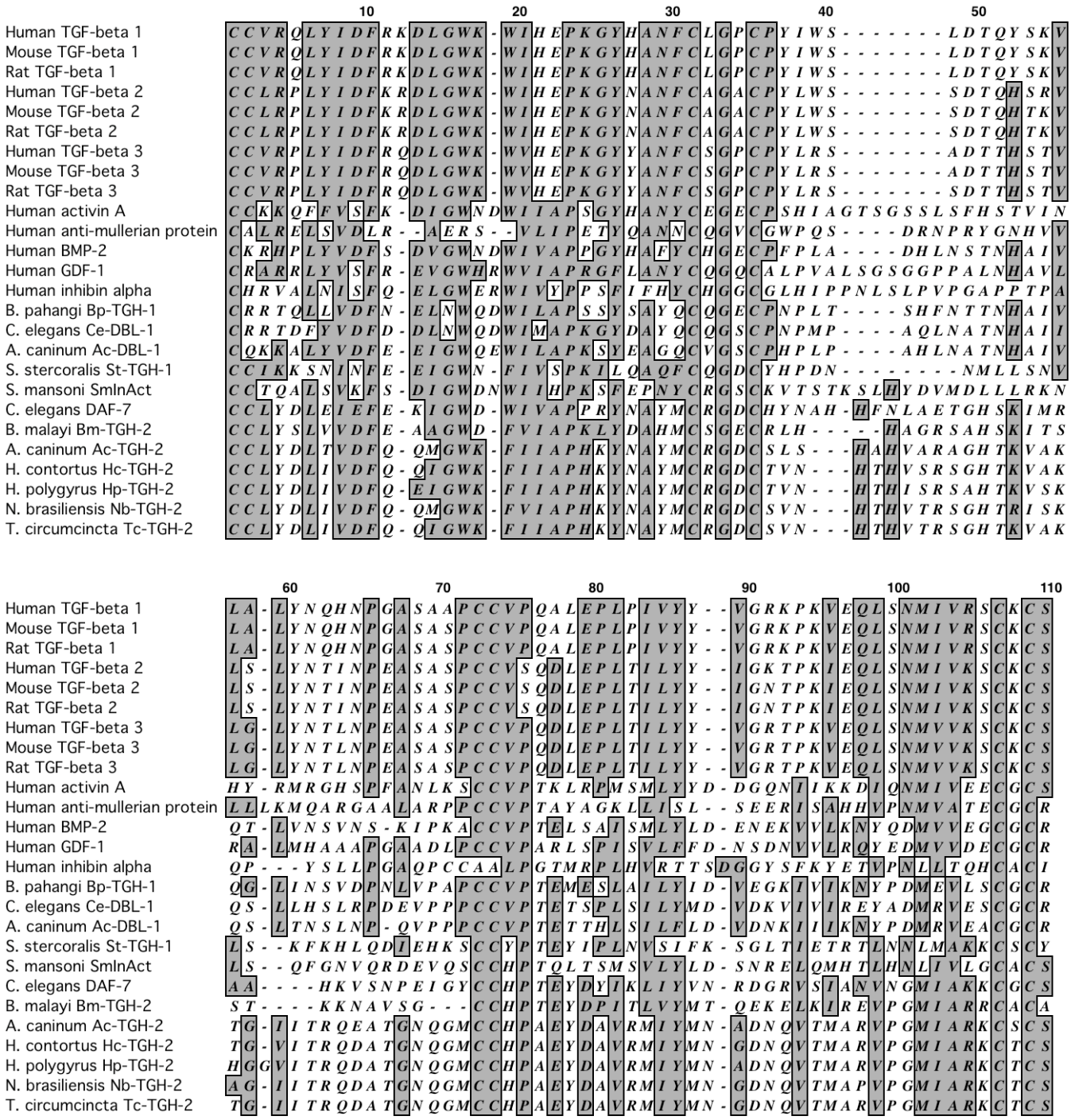

Figure 3.9: Amino acid alignments of conserved region of novel and previously known TGF-βs
Amino acid alignments of conserved region of TGF-β-superfamily members from mammals and nematodes.

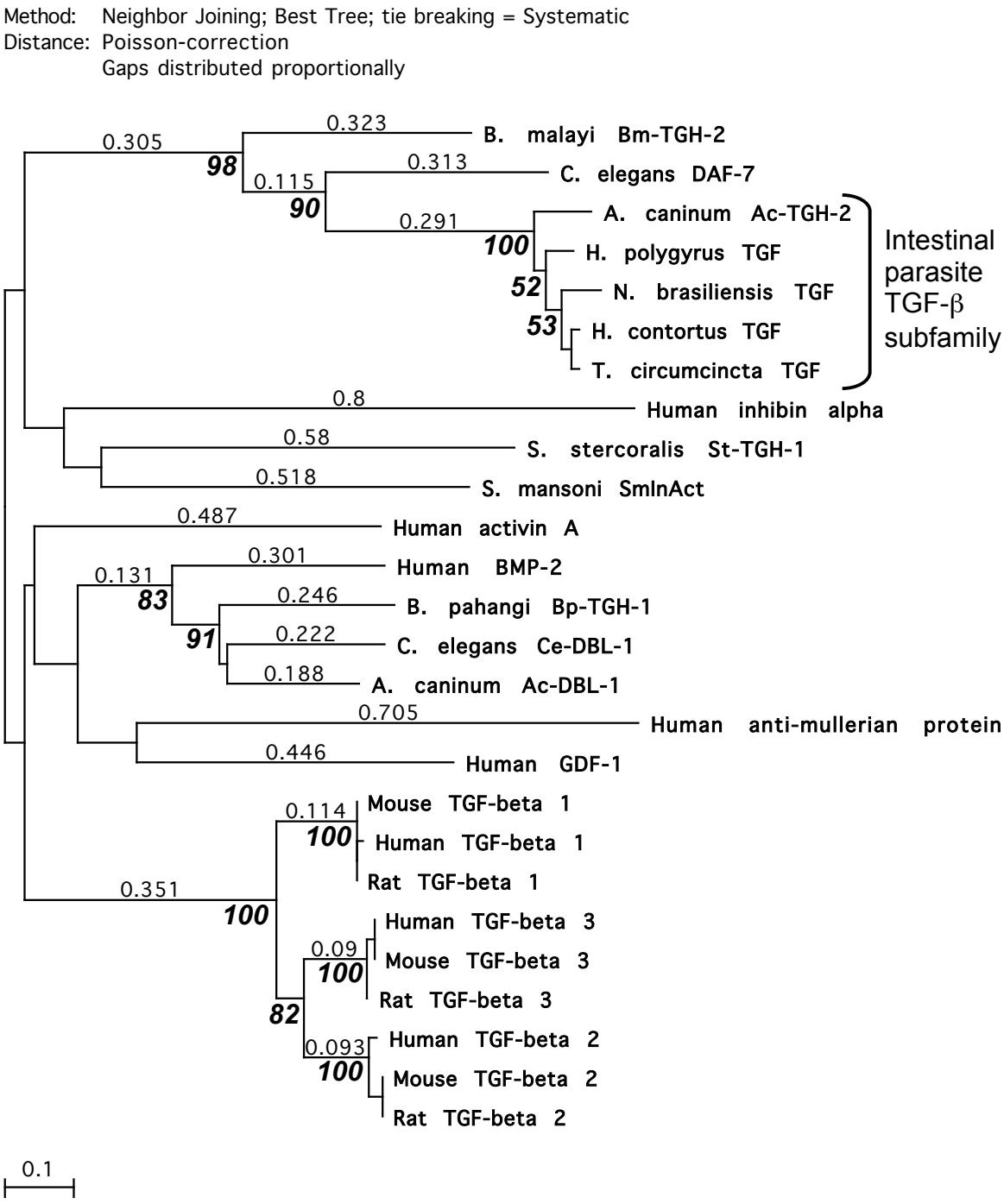

Figure 3.10: Phylogenetic tree of novel and previously known TGF-βs
Best fit tree of TGF-β superfamily members (shown aligned in Figure 9). Values shown in normal type (e.g. 0.093) indicate divergence between sequences, and numbers in bold italics (e.g. ***100***) indicate bootstrap values (percentage of calculated trees which branched as shown, values are representative of 1000 repetitions). Where no values are shown, the bootstrap values are below 50 %.

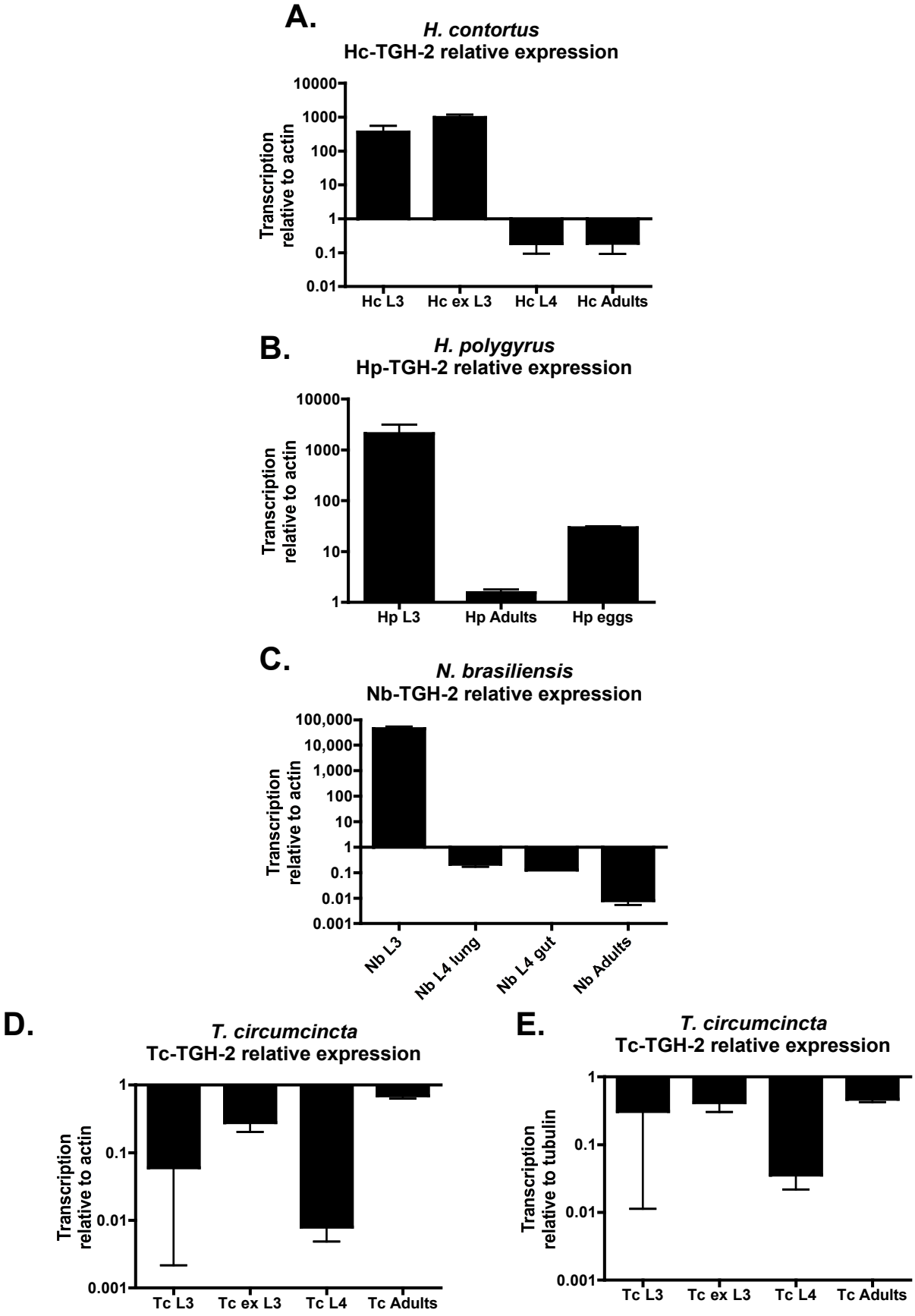

Figure 3.11: Real-time PCR of TGH-2 transcription

Levels of TGF-β homologue, actin and β-tubulin transcription were measured by real-time PCR in different developmental stages of *H. contortus* Hc-TGH-2 (A), *H. polygyrus* Hp-TGH-2 (B), *N. brasiliensis* Nb-TGH-2 (C) and *T. circumcincta* Tc-TGH-2 (D and E). The relative transcription levels were calculated by dividing the relative levels of TGF-β homologue transcription by relative levels of actin (A-D) or β-tubulin (E) transcription. Error bars show standard error of mean, of three technical replicates. This experiment was carried out once.

3.6. *H. polygyrus* Hp-TGH-2 expression

Hp-TGH-2 was selected for expression in bacteria. Only the conserved active domain was expressed as it was hypothesised that antibodies against this region would be most likely to block binding of the active protein to the receptor. The active domain was first amplified using primers specific to the region immediately downstream from the protease cleavage site, and the end of the sequence, with overhanging restriction enzyme sites, to allow sticky-end cloning into the pET21 expression vector. The primers used are shown in Table 3.4 below, with overhanging ends in bold, and restriction enzyme sites in red:

Table 3.4: Primers used to clone Hp-TGH-2 conserved domain

Primer name	Sequence	Binding site on sequence
Hp_cons_NdeI_for	5'-**GGGCCC**CATATGAGTCCGGCGGTGTGTCTGCCT-3'	557-576
Hp_XhoI_rev	5'-**GGGCCC**CTCGAGGGAGCAGGTGCACTTTCGGGCGATC-3'	903-879

The product was digested with NdeI and XhoI restriction enzymes (New England Biolabs), then ligated into NdeI/XhoI-cut pET21 vector (Novagen). The vector map and cloning site is shown in Figure 3.12. The ligated plasmid was then transformed into BL21 (DE3) *E. coli* cells, and expression induced with IPTG. Protein expression was then assayed by Coomassie staining of cell lysates. As is shown in Figure 3.13A, significant levels of expressed protein were only seen in supernatants of cell lysates resuspended in 8 M urea, therefore the protein produced was insoluble in saline. The expression yielded a band at around 14 kDa, which is close to the predicted size of 10.5 kDa. Lysates resuspended in His-purification binding buffer with 8 M urea were then 6-His purified using the AKTAprime.

Fractions eluted are shown in Figure 3.13B. Fractions 12 to 24 were pooled and dialysed against PBS containing 8 M urea.

3.7. *H. polygyrus* TGF-β homologue polyclonal antibody

The expressed conserved domain of Hp-TGH-2 (Hp-TGH-2-cons) was used to immunise SD strain rats (Harlan): the protein was precipitated onto alum, then 200 μg was injected subcutaneously. 4 and 5 weeks later, challenges of 50 μg/ml alum-precipitated protein was given, and serum was prepared from the rats 6 weeks after first immunisation. The serum was used in Western blots against *H. polygyrus* adult excretory/secretory products (HES), *H. polygyrus* adult homogenate (HEX) and recombinant protein (Hp-TGH-2-cons) (Figure 3.14). In HEX, some bands were seen at ~65 kDa and 30 kDa when the blots were probed with naïve serum, which appears to be non-specific binding due to the large amount of protein used (230 μg of HEX on the gel). However, probes using immunised serum showed extra bands at ~50 kDa in HES, and ~35 kDa in HEX. In HEX, a collection of high molecular weight bands were also seen.

The 50 kDa band seen in HES is larger than the predicted mass of latent Hp-TGH-2 of 33.7 kDa, however this difference could be due to glycosylation. The band seen in HEX at around 35 kDa is much closer to the predicted protein mass, and could reflect that the protein is not glycosylated until it is secreted by the parasite. The very large molecular weight bands seen in HEX are intriguing, as latent mammalian TGF-β is known to form the Large Latent Complex (LLC) by covalently binding to Latent TGF-β Binding Proteins (LTBPs). These large latent complexes

have a molecular weight of around 220 kDa (207), and so these type of complexes could explain the bands seen here.

3.8. TGF-β activity in HES and SEA

H. polygyrus excretory/secretory products (HES) can produce a signal on the TGF-β bioassay (Grainger *et al*, in review). When *S. mansoni* Soluble Egg Antigen (SEA) was tested on the bioassay it also produced a signal, and neither the HES nor SEA signal could be blocked by anti-mammalian TGF-β antibody, therefore were not due to contamination from the host (Figure 3.15A). To test whether the Hp-TGH-2 is the source of the TGF-β activity, we attempted to block the TGF-β signal by addition of purified rat anti-Hp-TGH-2-cons. Serum was IgG purified using a protein G-sepharose column, and spin concentrated using a 5 kDa cut-off spin column (Sartorius**).** As can be seen in Figure 3.15B, the signal could not be ablated by addition of antiserum to block the TGF-β signal. Addition of the naïve rat IgG control (bought in from Sigma, rather than purified in-house) increased the HES TGF-β signal, however this appears to be due to contamination of the naïve rat IgG with (most probably rat-derived) TGF-β, as can be seen in the control of naïve rat IgG alone (Figure 3.15B).

The polyclonal antibody was raised against bacterially expressed protein, which do not contain disulphide bonds, and so would not be folded correctly. Antibodies raised against incorrectly folded protein would be less likely to block interaction of the parasite protein with the receptor. Therefore we attempted to deplete the TGF-b homologue from HES prior to addition to the TGF-β bioassay, by incubation with antisera followed by depletion of immunoglobulin with protein G

sepharose beads. Depletion of HES using protein G sepharose beads also did not reduce the TGF-β signal (Figure 3.15C).

Both HES and SEA were used in a Treg induction assay, to see if they could induce Tregs in combination with polyclonal stimulus, similarly to mammalian TGF-β (103). HES was shown by J. Grainger to induce Tregs similarly to TGF-β (Grainger *et al*, in review). In order to test whether HES induces Tregs through the TGF-β pathway, HES was used in a Treg induction assay with wild-type or CD4-trophic TGF-βRII dominant negative (TGF-βRIIDN) splenocytes. TGF-βRIIDN mice contain a transgene producing a truncated TGF-βRII which is able to bind TGF-β and the type I TGF-βR chain (ALK-5) but lacks the ability to signal to the cell. This transgene is under the control of the CD4 promoter (which has been altered to allow expression in $CD4^+$ and $CD8^+$ T cells), so T cells cannot respond to TGF-β. When HES was used on a Treg induction assay on TGF-βRIIDN splenocytes (Figure 3.16), no Treg induction was seen, indicating that functional TGF-β receptor signalling is required for the Treg induction by HES.

As SEA produces a strong signal on the TGF-β bioassay (Figure 3.15A), it was hypothesised that it would, like HES, also induce Tregs. However, when SEA was used in a Treg induction assay, no Treg induction was seen (Figure 3.17A). Interestingly, addition of SEA ablated the Treg induction seen with addition of mammalian TGF-β, indicating an inhibitor of Treg induction is present in SEA. To remove the effect of Toll-Like Receptor (TLR) ligands in SEA, a Treg induction assay was carried out in MyD88-deficient splenocytes, which cannot respond to TLR ligands. As shown in Figure 3.18B, very similar results were seen, therefore the inhibitor of Treg induction does not act through the TLR pathway.

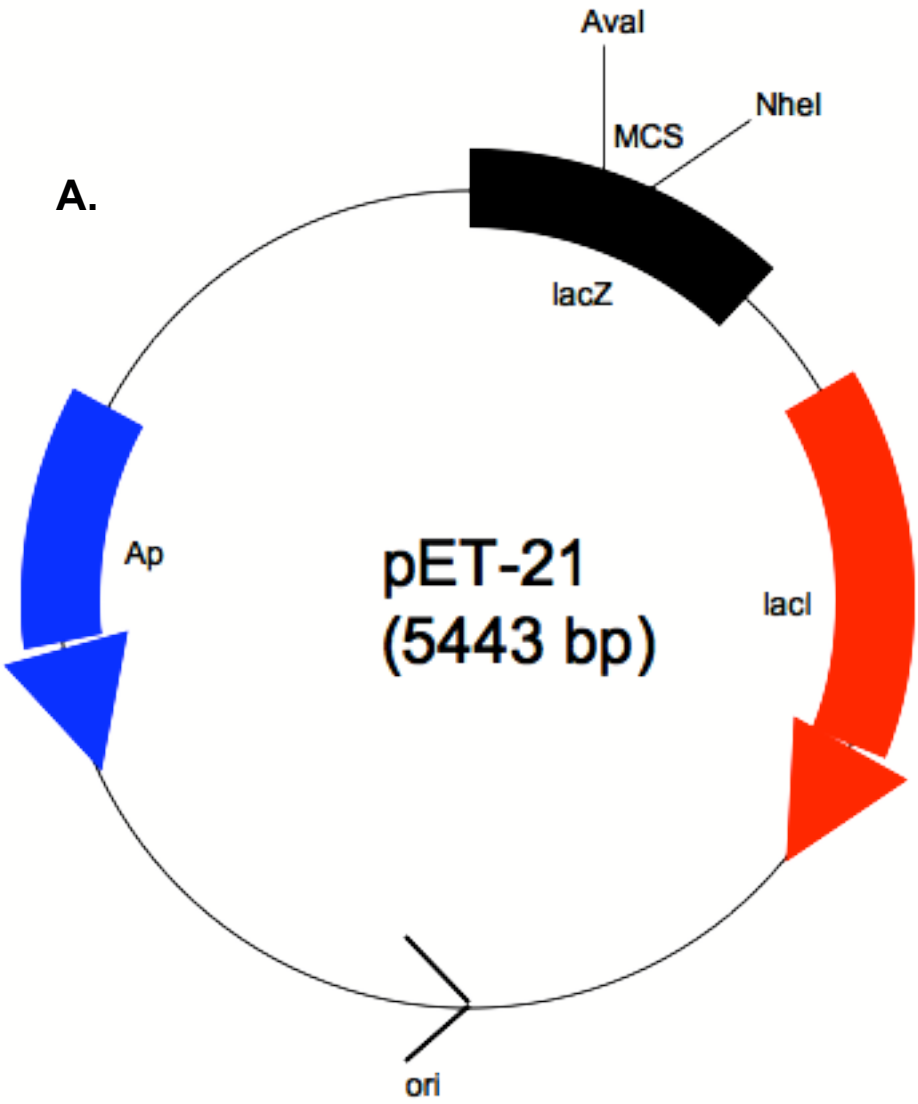

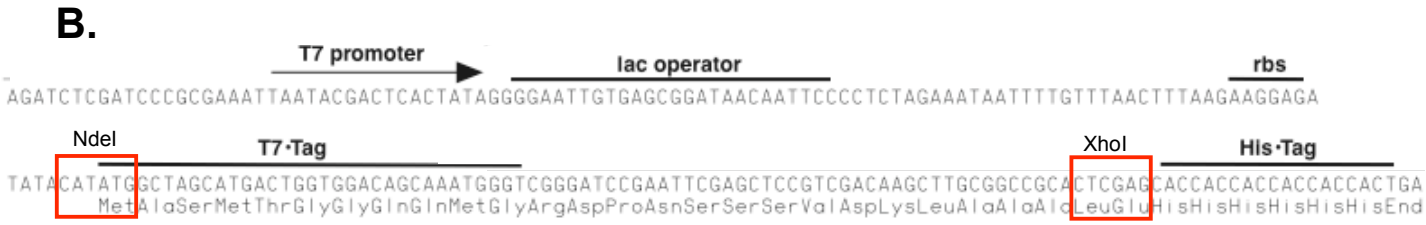

Figure 3.12: pET-21 vector map
Vector map (A) and multiple cloning site (B) of pET-21. Red boxes indicate the NheI and XhoI restriction enzyme sites used for cloning. (Adapted from the Novagen website: http://www.merckbiosciences.com/docs/docs/PROT/TB036.pdf)

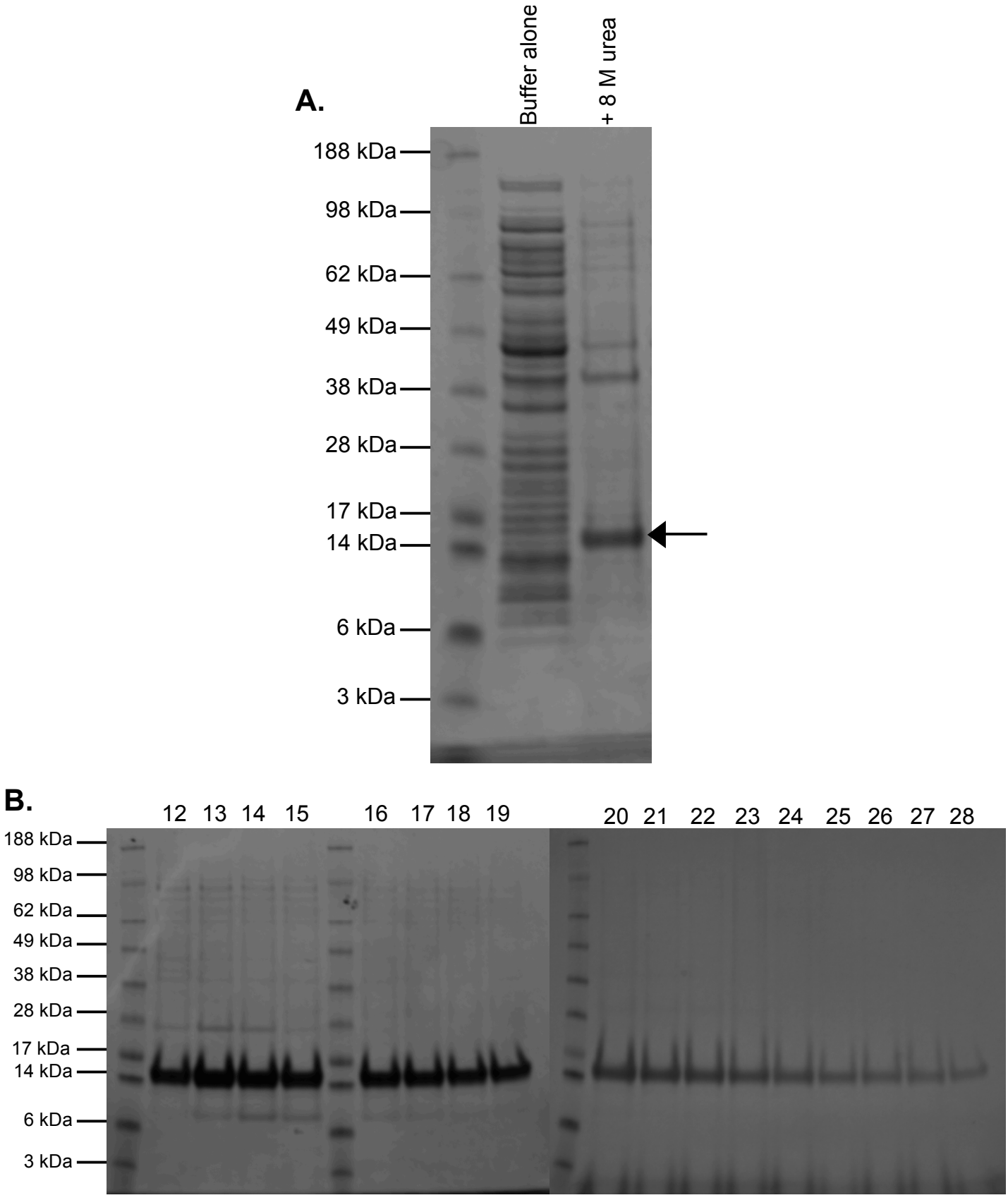

Figure 3.13: Expression of Hp-TGH-2-cons
E. coli containing the pET21-Hp-TGF-cons plasmid were cultured for 3 h in the presence of 1 ug/ml IPTG. Coomassie-stained 4-12 % SDS-PAGE gel in (A) shows supernatant soluble in 6-His binding buffer alone, or soluble in 6-His binding buffer with 8 M urea (arrow indicates ~14 kDa expressed protein). Coomassie-stained 4-12 % SDS-PAGE gels in (B) show fractions of expressed, His-purified Hp-TGF-cons eluted from the AKTAprime.

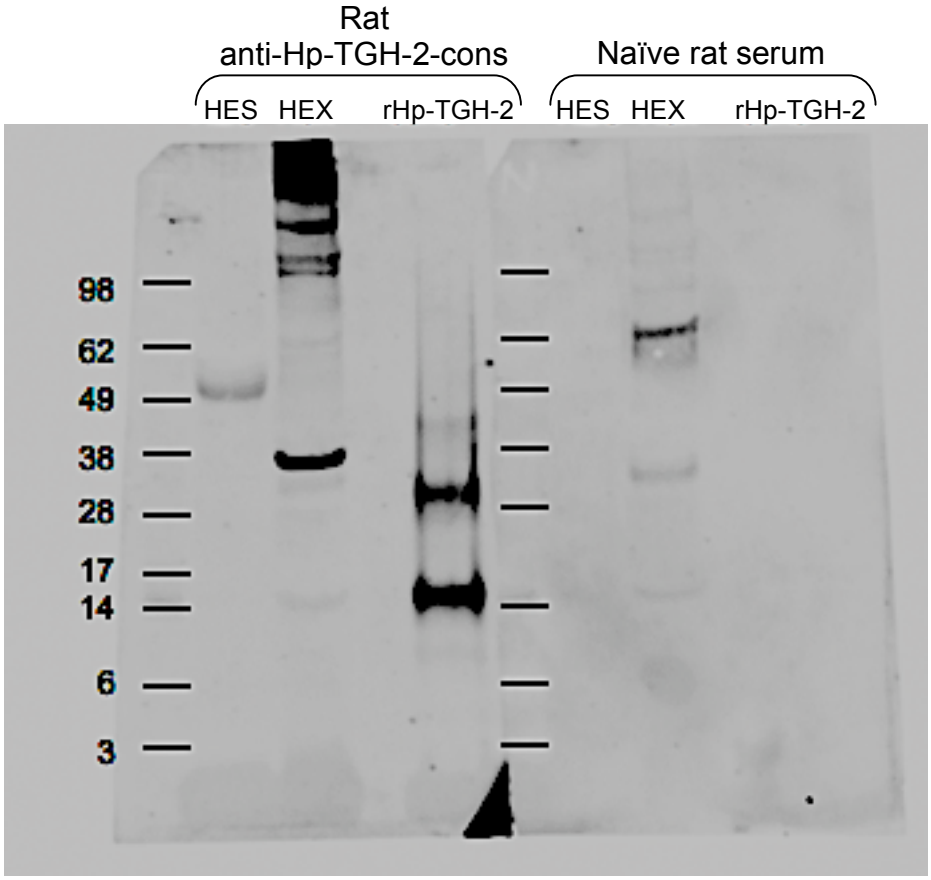

Figure 3.14: Detection of Hp-TGH-2 in *H. polygyrus* products
HES (49 μg), HEX (230 μg) and recombinant Hp-TGH-2-cons (100 ng) were run on a denaturing 4-12 % SDS-PAGE gel, transferred to nitrocellulose membrane and probed with 1/100 rat serum (anti-Hp-TGH-2-cons or naïve), then 1/1000 anti-rat IgG-HRP and developed with Chemiglow reagent (Alpha Innotech), and photographed on a FluorChem SP imager (Alpha Innotech).

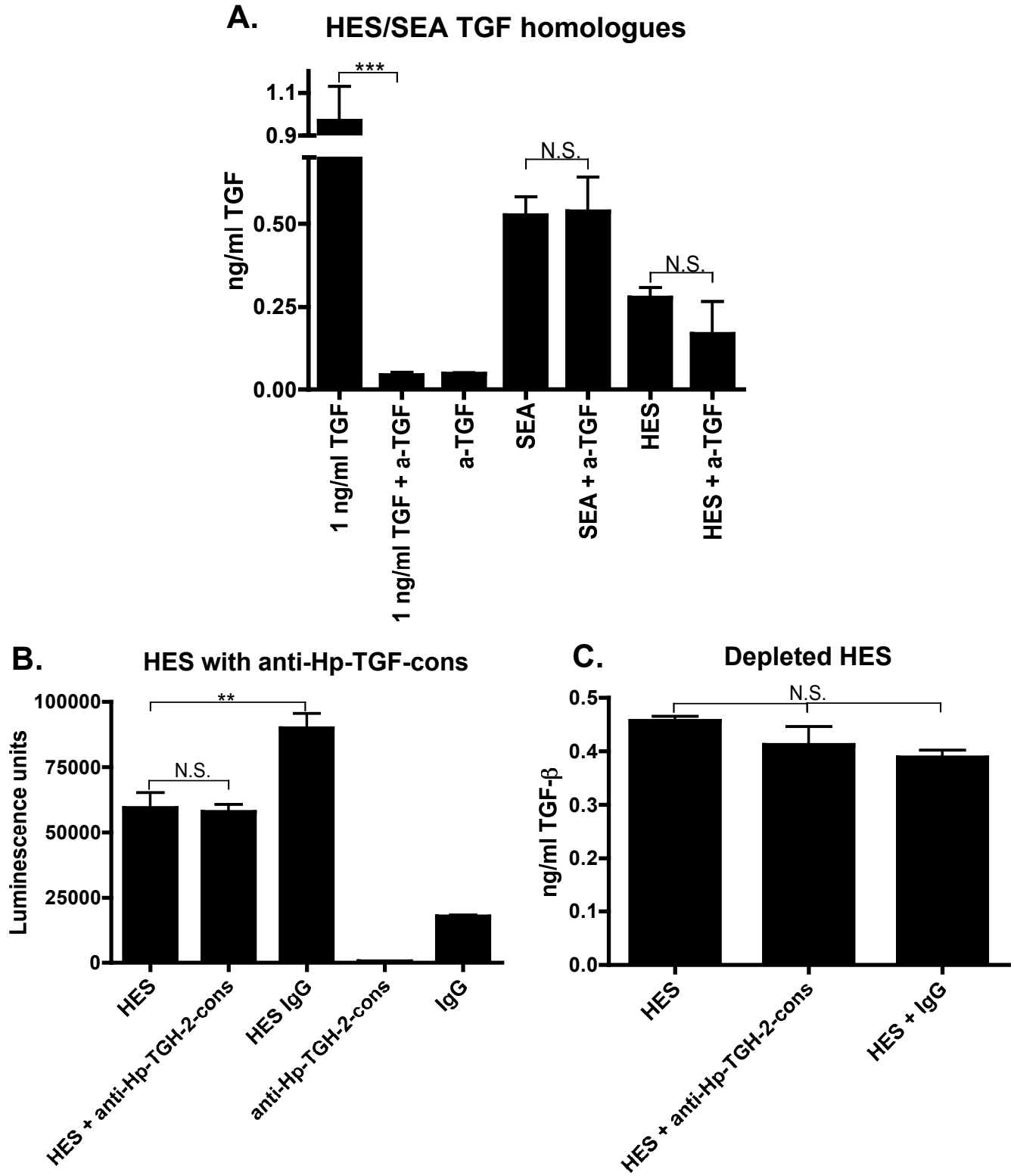

Figure 3.15: Attempts to block HES TGF-β activity.
SEA (25 μg/ml), HES (10 μg/ml) or TGF-β (1 ng/ml) with or without 1 μg/ml anti-TGF-β (clone 1D11) were assayed for TGF-β activity on the MFB-F11 TGF-β bioassay (A). Polyclonal antibody against the expressed conserved domain of Hp-TGH-2 (anti-Hp-TGH-2-cons) or a control of rat IgG (both at 100 μg/ml) were added to HES (10 μg/ml) on the MFB-F11 bioassay in an attempt to block binding to the TGF-β receptor (B). In an attempt to deplete the TGF-β signal from HES, anti-Hp-TGH-2 cons or rat IgG (both at 100 μg/ml) was incubated with HES at 37°C for 1 h, then at 4°C with protein G sepharose beads overnight. The bound antibody bound to the beads were then centrifuged out prior to addition of the supernatant to the MFB-F11 TGF-β bioassay (C).Values shown are calculated from a TGF-β standard curve (A and C), or luminescence units (B). Values in (B) were above TGF-β standard curve. Error bars are standard error of mean of three technical replicates. *** = P<0.001, ** = P<0.01, N.S. = Non significant.

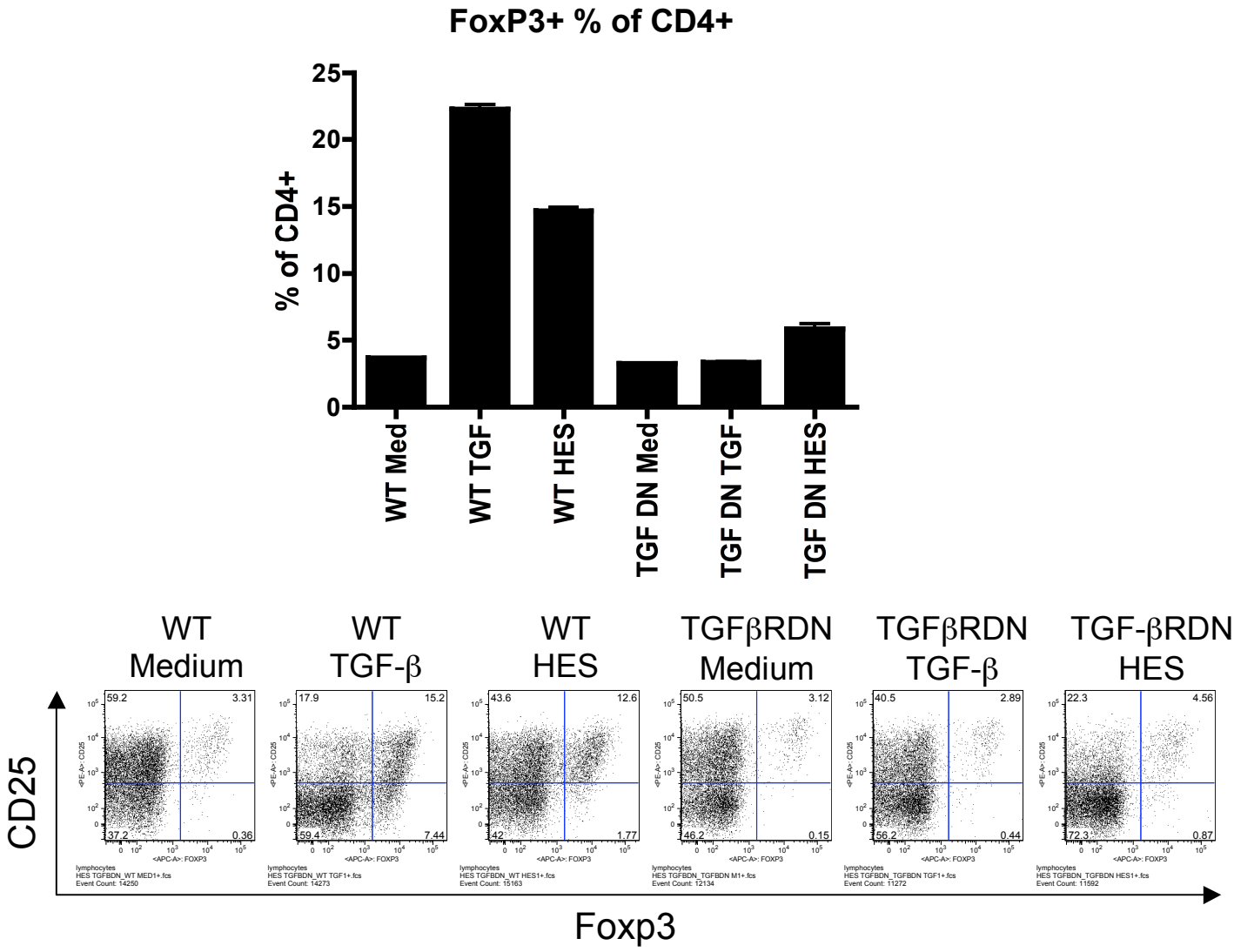

Figure 3.16: HES Foxp3 induction.
HES (10 μg/ml) or TGF-β (10 ng/ml) was applied to C57BL/6 or CD4-trophic TGF-βRII dominant negative (on a C57BL/6 background, the T cells from these mice are unable to respond to TGF-β) splenocytes in the presence of 2 μg/ml ConA for 3 days, then stained for CD4, CD25 and FoxP3 by flow cytometry. Graph shows $Foxp3^+$ proportion of the $CD4^+$ population, with error bars showing standard error of mean of triplicate cultures. Bivariate flow cytometry plots (bottom) show Foxp3 and CD25 staining on $CD4^+$-gated lymphocytes.

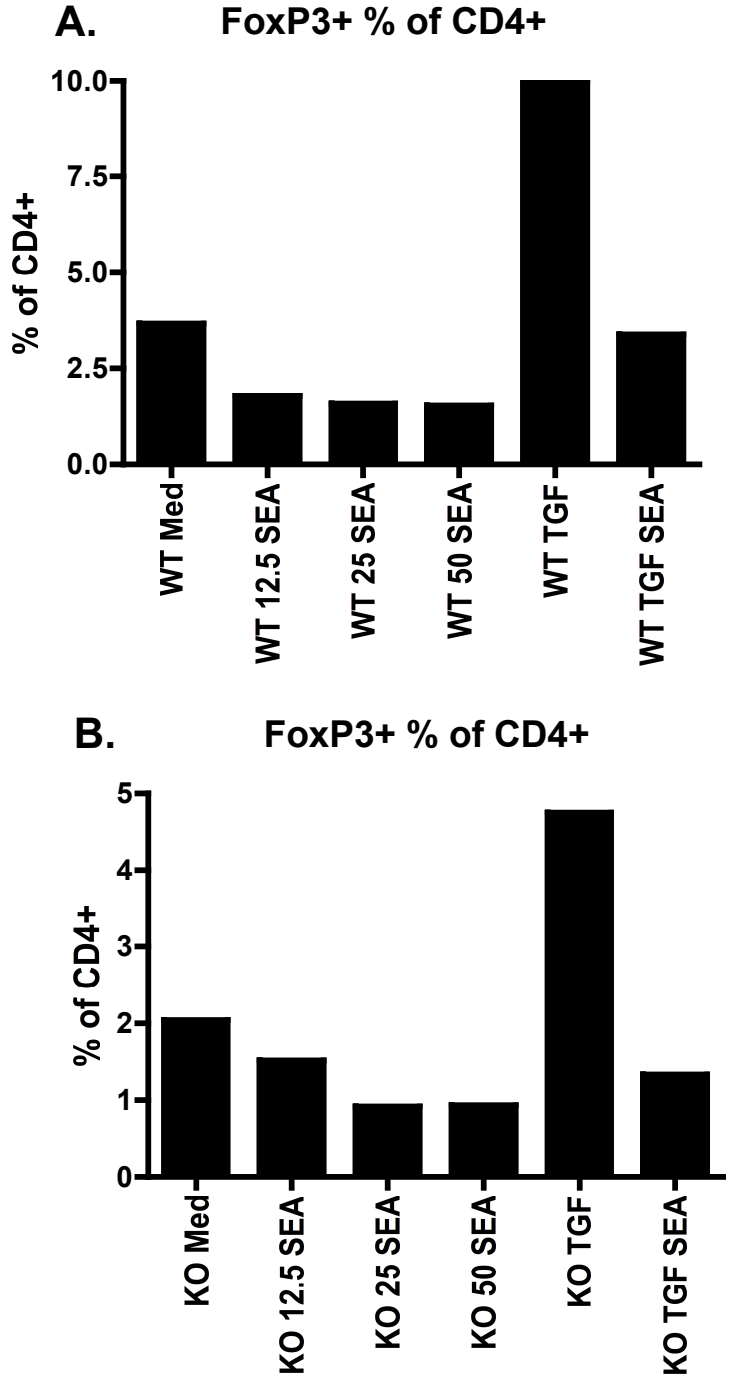

Figure 3.17: SEA cannot induce Foxp3 expression in wild-type or MyD88-deficient splenocytes.

SEA (12.5 μg/ml, 25 μg/ml or 50 μg/ml as indicated) or TGF-β (10 ng/ml), or 10 ng/ml TGF with 25 μg/ml SEA was applied to 1 x 10^6 C57BL/6 (A) or MyD88-deficient (C57BL/6 background) (B) splenocytes in the presence of 2 μg/ml ConA for 3 days, then stained for CD4 and Foxp3 by flow cytometry. Data shown is the $Foxp3^+$ proportion of the $CD4^+$ population. WT = C57BL/6 splenocytes, KO = MyD88-deficient splenocytes, Med = medium control, SEA = *S. mansoni* Soluble Egg Antigen added (preceding numbers indicate final concentration of SEA in μg/ml), TGF = TGF-β added, TGF SEA = TGF-β and SEA both added. All bars are single cultures

3.9. Discussion

In this chapter, I showed that TGF-β homologues are encoded by many intestinal parasites, and that TGF-β signals are present in parasite-derived products. Using molecular techniques I identified TGF-β homologues in *H. contortus*, *H. polygyrus*, *N. brasiliensis* and *T. circumcincta*. These TGF-β homologues were very similar to *A. caninum* Ac-TGH-2 showing they are highly conserved in intestinal nematodes. The real-time PCR data shows that in *H. contortus*, *H. polygyrus* and *N. brasiliensis* expression is highest in L3 larvae. This expression profile could indicate that parasites express TGF-β homologues prior to entry into the host, producing high levels of TGF-β which is then released on infection of the host, thus skewing the immune response towards tolerance at the earliest contact between the parasite and the host. In *T. circumcincta* however, the expression profile indicates low expression in the infective larvae, and highest expression in exsheathed (tissue-stage) L3 larvae and adults. This could indicate that *T. circumcincta* does not upregulate its TGF-β homologue until it enters the host, when it is in contact with the immune system. The high expression in adults is more difficult to explain, as once hookworms are adult they live in the lumen of the gut, external to the host immune system. These real-time PCR results are only a single experiment, and therefore should be repeated for confirmation. These experiments are currently in progress.

An alternative explanation of TGF-β homologue production in nematodes is that they have a role in development, as shown in *C. elegans* (95), *S. mansoni* (78), and *A. caninum* (76). They are associated with developmental arrest, for example in *C. elegans* dauer larvae, or *A. caninum* L3 larvae. Thus, the high levels of transcription of the *H. contortus*, *H. polygyrus* and *N. brasiliensis* TGF-β

homologues in the L3 larvae stage could indicate the TGF-β homologues are maintaining the arrested L3 state, and are downregulated when the parasite develops to later stages. Interestingly, *H. polygyrus* Hp-TGH-2 is again upregulated in the egg stage, which is also developmentally arrested. To study this further it would be useful to assess the transcription of the other TGF-β homologues in the egg stages of *H. contortus*, *N. brasiliensis* and *T. circumcincta*. A possible caveat of transcriptional results from the egg stage is that although all larval and adult stages are motile, the egg stages are not. As the housekeeping gene used here, actin, is involved in muscle contraction (208) it may be downregulated in the non-motile egg stage, giving a falsely high result for the relative TGF-β homologue expression.

The hypothesis that TGF-β homologues from parasites are involved in immunosuppression is supported by the fact that Hp-TGH-2 could be detected in HES, and that HES and the soluble egg antigens of *S. mansoni* (SEA) both produce a signal in the TGF-β bioassay. However, only HES can induce Tregs *in vitro*. The lack of Treg induction by SEA is intriguing, especially as a similar level of TGF-β activity is seen in SEA as in HES. As SEA is known to potently induce TH2 responses (209), the inhibitor of mammalian TGF-β Treg induction could be an activatory TH2 ligand. The fact that mammalian TGF-β Treg induction was still ablated by SEA in MyD88-deficient splenocytes indicates that the Treg inhibition is not dependent on TLR ligands, although it may depend on other Pathogen Associated Molecular Patterns (PAMPs) that act through other Pattern Recognition Receptors (PRRs). The inhibition of Treg induction may be due to the method by which SEA is prepared – eggs are taken from infected animals and homogenised, thus antigens which during infection would be sequestered inside the egg by the

surrounding granuloma are released in SEA. As it would be useful for the parasite to induce Tregs through TGF-β, it may be that the Treg inhibiting factor is an antigen which is not released from the egg during infection. To test this hypothesis, it would be interesting to study excretory/secretory products from *S. mansoni* live eggs or adults, and assess levels of TGF-β signalling and Treg induction.

We could not block the TGF-β signal in HES using rat antiserum, nor could we deplete HES of the TGF-β signal. Due to the fact that the antiserum was raised against bacterially expressed protein, it would not be surprising that it would not block binding of the protein to the receptor, as the bacterial protein would not have the same conformation as parasite-derived protein. This could also affect the affinity of the antiserum for the parasite protein. A low affinity antibody would also be less able to deplete the protein from the HES, which could explain why we were not able to reduce the HES TGF-β signal in the depletion experiment (Figure 3.15C). In order to investigate this further, it would be useful to produce functional *H. polygyrus* Hp-TGH-2 in another expression system such as insect cells, as described in chapter 4. Antibodies raised against functional protein would be more likely to block binding. It also may be that a very small proportion of the antibody present in rat polyclonal sera is specific to the TGF-β homologue, and so not enough specific antibody was present to block or deplete HES. Therefore a monoclonal antibody against *H. polygyrus* TGF-β would be useful for these studies, as the specific antibody would be at a known concentration and affinity.

Chapter 4:
Bm-TGH-2
Insect Cell Expression

4. Bm-TGH-2 Insect Cell Expression

4.1. Preparation of Baculovirus

4.1.1. Ce-DAF-7 Cloning

At the outset of the project, Bm-TGH-1 and Bm-TGH-2 had previously been cloned into the pBAC-1 vector (Novagen), and Ce-DAF-7 had been isolated from a *C. elegans* cDNA library, and had been cloned into pcDNA3 by N. Gomez-Escobar. It was amplified using PCR with specific primers containing overhanging StuI and XhoI restriction enzyme sites to allow restriction enzyme digestion, and sticky end cloning into the pBAC-1 vector. The primers used are shown below, with the restriction sites highlighted in blue, and the start codon highlighted in red:

Primer name	Sequence
StuI-DAF-7-for	5'-AAA**AGGCCT**A**TG**TTCATGGCATCTTCACTC-3'
DAF-7-rev-XhoI	5'-CCG**CTCGAG**TGAGCAACCGCATTTCTTGGC-3'

The PCR product was then purified using a gel purification kit (QIAGEN) and restriction digested with StuI and XhoI enzymes. The resulting fragment was then ligated into StuI/XhoI-digested pBAC-1 plasmid.

4.1.2. Recombinant Baculovirus Production

All three constructs were then transfected with bacPAK-6 into SF21 cells using the Clontech kit, allowing homologous recombination to occur, resulting in viable virus expressing the proteins of interest. Clones were plaque picked, purified and amplified to high titre in SF9 cells (Around 10^8/ml, depending on batch). Small-scale expressions of Bm-TGH-1, Bm-TGH-2 and Ce-DAF-7 were then carried out in SF21 and Hi5 cells over a 72 h timecourse, and supernatants assayed for expression

levels by Western blotting with anti-6-His antibody. No bands were visible in the Bm-TGH-1 6-His Western blots (data not shown), so these were re-probed with anti-Bm-TGH-1 mouse serum, where a faint band could be seen at the predicted size for the immature protein of 45 kDa (Figure 4.1A). Bm-TGH-1 in expressions after this point was only ever detectable at very low levels with anti-Bm-TGH-1 serum, and was never detectable by anti-6-His antibody. Therefore it was decided to abandon Bm-TGH-1, as Ce-DAF-7 was an adequate control for a nematode TGF-β homologue. The small scale expressions of Bm-TGH-2 and Ce-DAF-7 showed that homologues were present at the highest levels in SF21 cells after 72 h, with very low expression Hi5 cells at early timepoints (Figure 4.1B + C). Expression in Hi5 cells was attempted twice more without significant levels of expression being seen, so SF21 cells were used for all expressions.

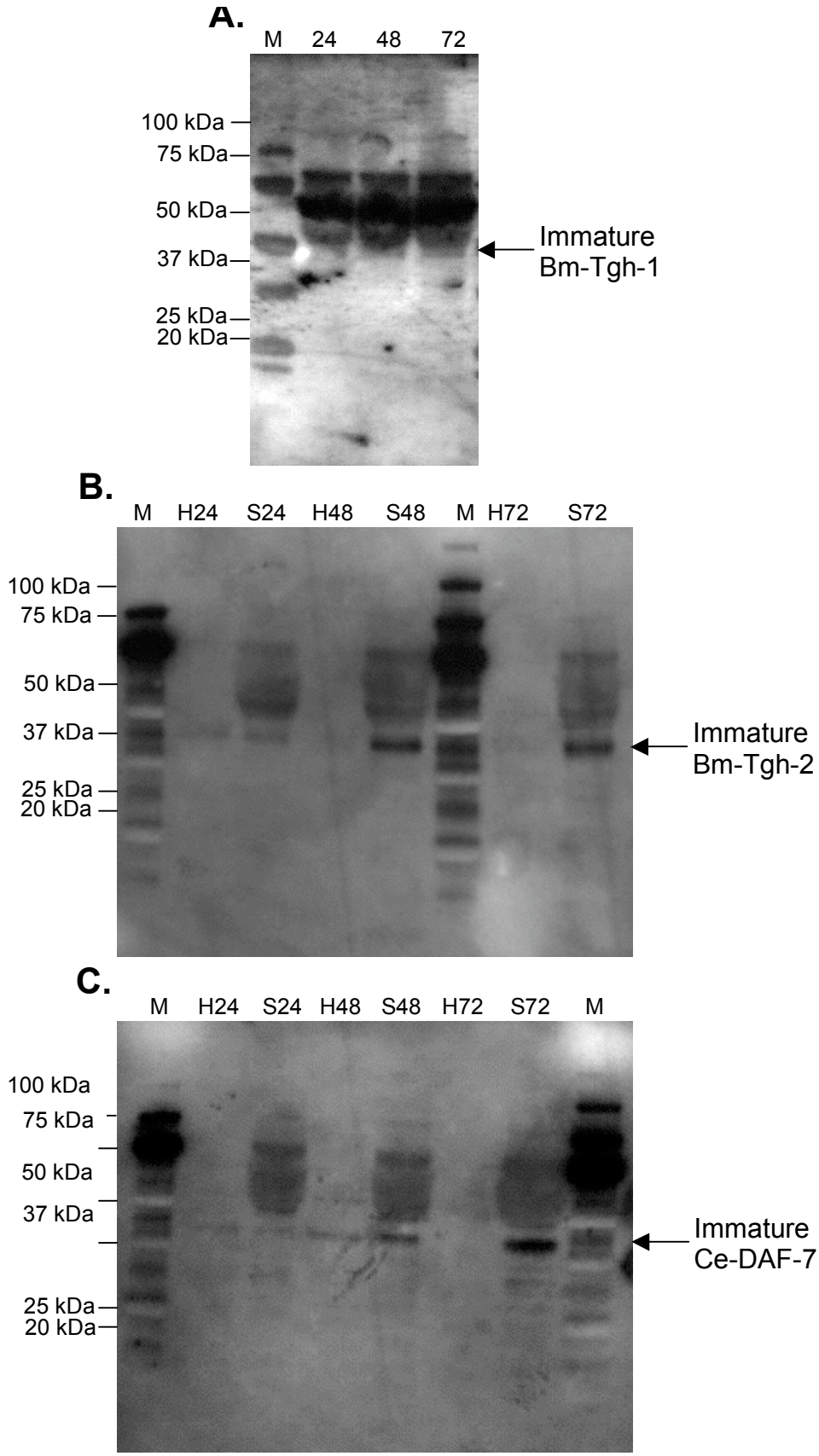

Figure 4.1: Small-scale expression timecourse of Bm-TGH-1, Bm-TGH-2 and Ce-DAF-7 in SF21 or Hi5 insect cells.

Expression time-course of Bm-TGH-1 (**A**), Bm-TGH-2 (**B**), and Ce-DAF-7 (**C**). Supernatants taken at 24, 48 and 72 h from small-scale expressions were probed in Western blots with 1/200 anti-Bm-TGH-1 serum, then 1/1000 anti-mouse IgG-HRP (A), or 1/2000 anti-6-His-HRP (B and C). M = marker, H/S 24/48/72 = cell line used for expression (H=Hi5, S = SF21) and time-point – hours after infection (e.g. S48 = SF21 cells at 48 h after infection).

4.2. Production of Recombinant Proteins

A large scale expression of Bm-TGH-2 and Ce-DAF-7 was then carried out in the presence of furin recombinant baculovirus (which was supplied at high titre by N. Gomez-Escobar), and the culture supernatants were purified using the AKTAprime. All eluted fractions were assayed for protein levels using a Bradford Assay and Coomassie stain. Positive fractions were pooled, dialysed against PBS, and probed with anti-6-His antibody on a Western blot (Figure 4.2). Representative Coomassie stains of purified TGH-2 and DAF-7 are shown in Figure 4.3.

The large scale expression of Bm-TGH-2 produced a strong band on the Western blot at approximately 14 kDa, which is similar to the expected size of 12kDa. The difference could be due to the His tag and glycosylation during the insect cell expression. There is still a dense band at ~45 kDa however, indicating that the immature form is still present. Thus not all protein produced was cleaved to the active form by the furin-expressing virus. It is difficult to tell what the smaller band at ~5 kDa is. However, it may be as a result of a further cleavage of the active Bm-TGH-2 by furin. None of the bands shown by Western blot were detectable by Coomassie stain, as far stronger bands of serum proteins mask them. Therefore although the recombinant proteins were 6-His purified, it seems the vast majority of protein present is of contaminants from the serum.

The large scale expression of Ce-DAF-7 shows a fainter band of approximately 12 kDa. However, this is also present in the flow-through, so may be a non-specific band from the serum in the media.

As a negative control of a non-TGF-β homologue, Bm-ALT-2 recombinant baculovirus was used (courtesy of J. Hewitson) and was amplified and expressed as

with Bm-TGH-2 and Ce-DAF-7, using SF21 cells. As can be seen from the Coomassie stain (Figure 4.3), the Bm-ALT-2 purification also resulted in a large amount of contaminating serum proteins being co-purified.

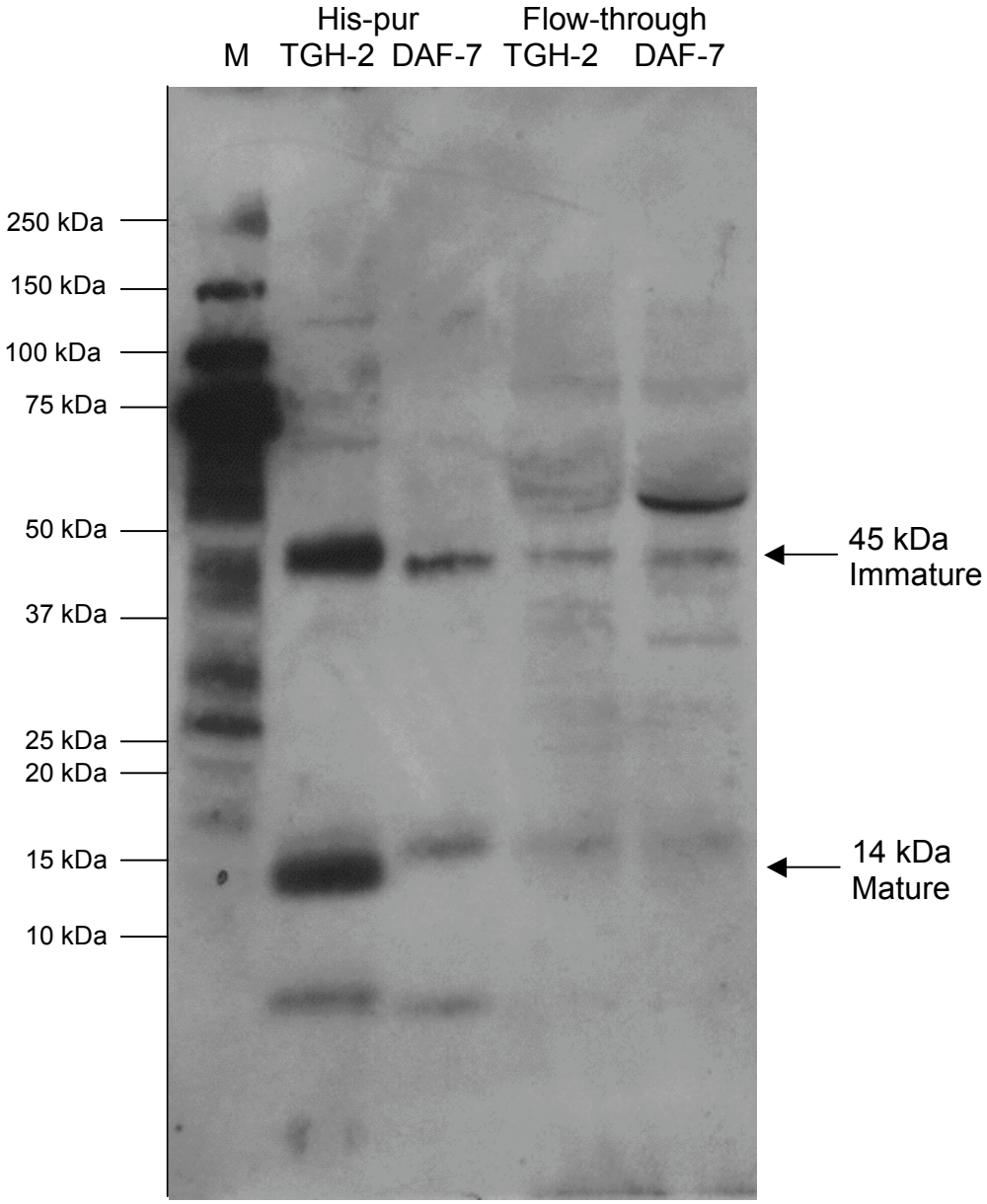

Figure 4.2: Purification of SF21-expressed Bm-TGH-2 and Ce-DAF-7.
Western blot of 6-His purified and AKTAprime flow-through for Bm-TGH-2 and Ce-DAF-7, probed with 1/2000 anti-6-His-HRP. Fractions taken from the AKTAprime were tested for the presence of protein by Bradford assay and Coomassie staining, and then positive fractions were pooled. Fractions were eluted in a rising concentration of imidazole from 10 mM to 500 mM, with Bm-TGH-2 eluted off in fractions 14 to 21 and Ce-DAF-7 in fractions 13 to 17 of 40 fractions collected.

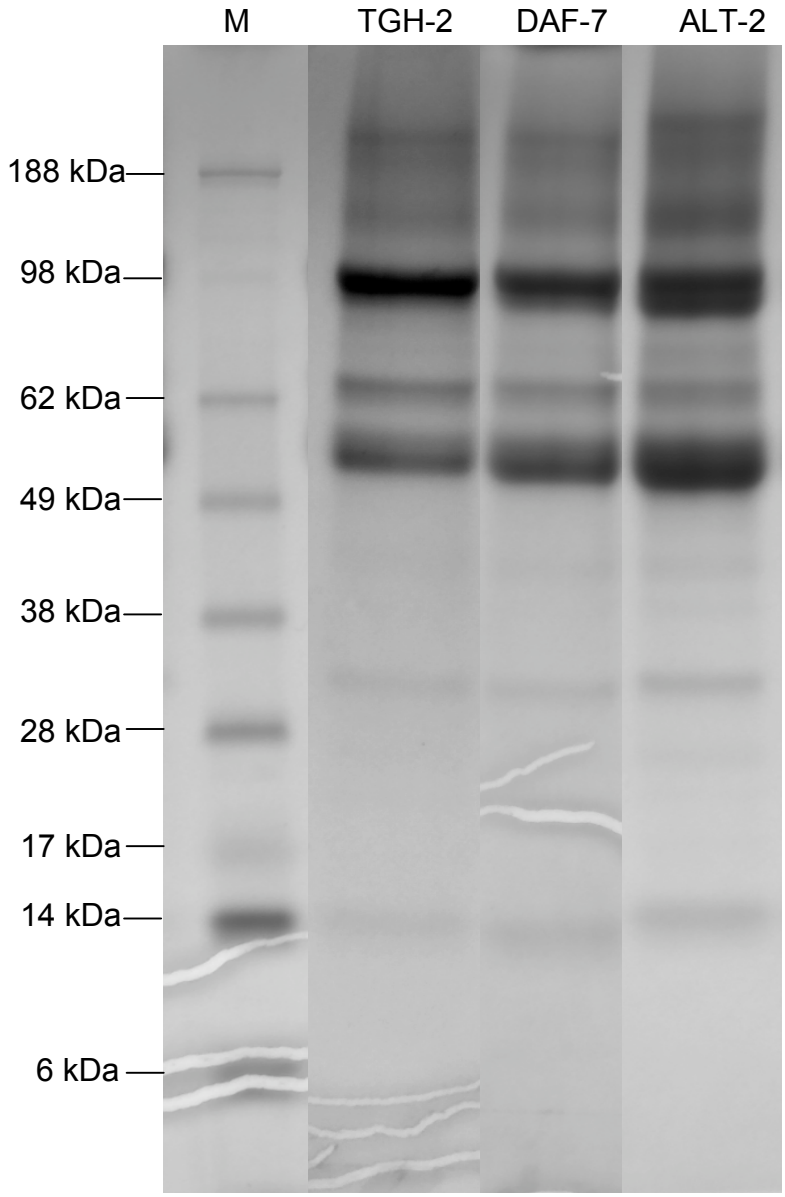

Figure 4.3: Coomassie stain of expressed proteins
Representative Coomassie stains of 6-His purified Bm-TGH-2, Ce-DAF-7 and Bm-ALT-2. Each protein was expressed in SF21 cells (in medium containing FCS), purified using the 6-His tag and 30 μl run on a 4-12 % SDS-PAGE gel in MES buffer, then Coomassie stained.
M = marker.

4.3. TGF-β Activity in Expressed Proteins

Endogenous or heat-activated samples of the expressed proteins were then used in the TGF-β bioasssay to check for TGF-β receptor binding (Figure 4.4A). It was decided it would not be possible to use similar concentrations of each protein as it was impossible to tell from the Bradford assay how much protein was present – the Coomassie stains clearly show most of the protein present is FCS proteins, rather than recombinant protein (Figure 4.3). Therefore 1 in 2 dilutions in media of neat samples of proteins were used to roughly compare. All proteins had similar levels of endogenous TGF-β receptor binding ability (around 1 ng/ml), with equivalently higher levels after heat-treatment (3-7 ng/ml), including the negative control of Bm-ALT-2 (a non-TGF-β homologue). Therefore the signal seen was thought to be TGF-β present in the FCS the proteins were expressed in, and had co-purified with the proteins. To investigate this further, neat samples of expressed proteins and a range of controls including FCS were added to the TGF-β bioassay (Figure 4.4B). As can be seen in Figure 4.4B, neat FCS contains roughly equivalent levels of TGF-β as is present in Bm-TGH-2 or Bm-ALT-2 expressed in SF21s. As this TGF-β signal is not present in Bm-ALT-2 expressed in Hi5 cells (an insect cell line that does not require FCS in the media), and no detectable signal can be seen in neat TC100 media containing 10 % FCS, the serum proteins including mammalian TGF-B must be being preferentially purified with the recombinant proteins, with almost pure FCS being purified from the AKTAprime.

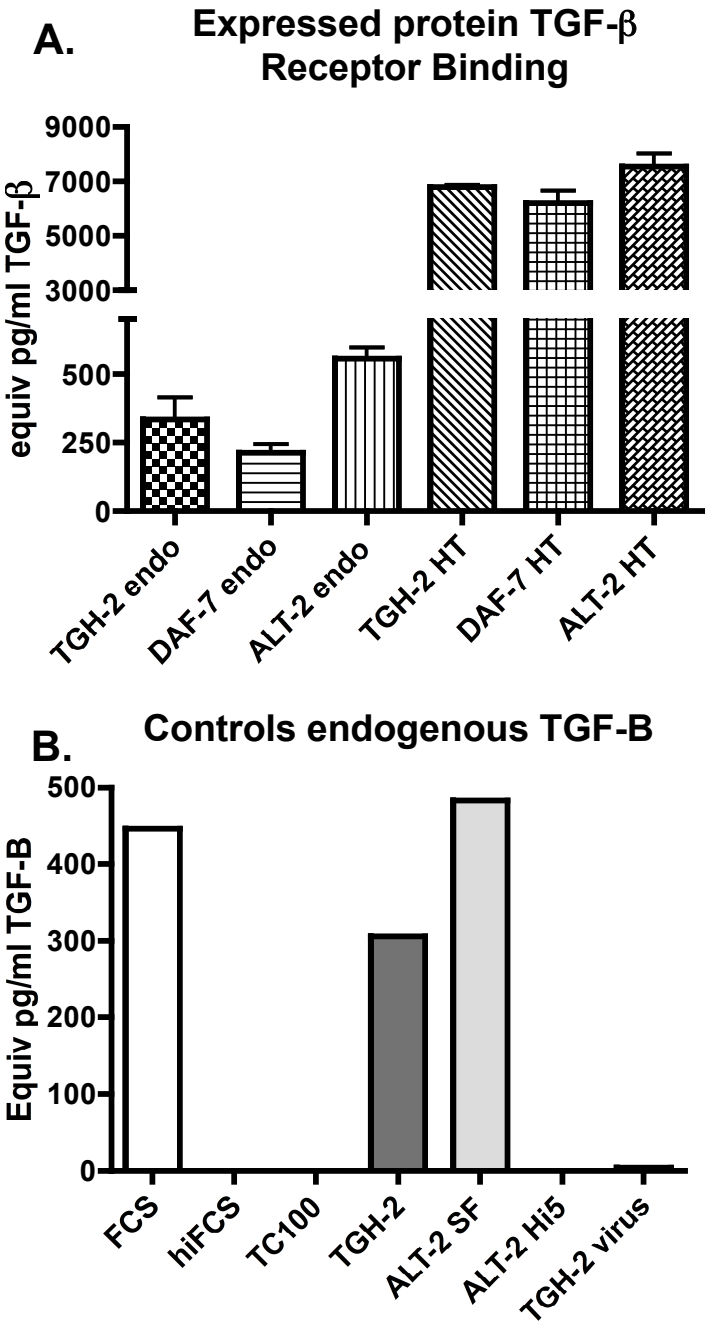

Figure 4.4: TGF-β activity in insect-cell expressed proteins or controls.
Expressed Bm-TGH-2, Ce-DAF-7 and Bm-ALT-2 from SF21 cells (expressed with FCS) infected in the presence of furin virus and purified using 6-His tag were diluted 1:2 in DMEM medium and added to the MLEC TGF-β bioassay either immediately to measure endogenous levels of TGF-β (endo), or after heat-treatment (85°C 5 min) to activate latent TGF-β (HT) (A). Controls of pure FCS, boiled FCS (hiFCS) TC100 media (containing 10% FCS), Bm-TGH-2 and Bm-ALT-2 (expressed as above), Bm-ALT-2 expressed in Hi5 cells (ALT-2 Hi5), and Bm-TGH-2 baculovirus, were also added to the MLEC TGF-β bioassay (B).

4.4. Protein Production without FCS

In order to avoid the problem of FCS-derived TGF-β activity, expression of all proteins was attempted with heat-inactivated (boiled for 30 min) FCS (hiFCS), which ablates any TGF-β activity (Figure 4.4B) however this proved to cross-link the FCS and resulted in a very viscous supernatant, which proved impossible to purify. Therefore small-scale expressions were attempted under several conditions: standard culture conditions (normal SF21 in TC100 media with 10% FCS); normal SF21 using TC100 media without FCS supplement; a new strain of SF21 cells, which do not require FCS in the media (SFM SF21); and normal SF21s in TC100 containing hiFCS. Under all conditions Bm-TGH-2 could be detected by Western blot with anti-Bm-TGH-2 sera (Figure 4.5). As would be expected Bm-TGH-2 was expressed best with FCS in the media (as SF21s have a much higher level of cell death without FCS in the media (data not shown)), however both the SFM SF21s and the normal SF21 in TC100 media without FCS produced some Bm-TGH-2. As the SFM SF21 cells grew at a much slower rate than the normal SF21 cells, it was decided to continue expressing in normal SF21 cells, washing the cells into TC100 without FCS just prior to infecting with the recombinant baculovirus.

Furin baculovirus was not coinfected with the TGF-β homologues as before as it could have been reducing the expression of the other proteins by competition for infection of the cells, and it had previously been shown that it was not cleaving the majority of the TGF-β homologue protein to activity (Figure 4.2). The TGF-β homologues could then be cleaved to activity after expression by either heat-, acid- or recombinant furin-cleavage. Examples of fractions of Ce-DAF-7 and Bm-TGH-2 eluted from the AKTAprime are shown in Figure 4.6. Bm-TGH-2 gives a pure single

band at around 45 kDa as expected from the Western blots. Ce-DAF-7 however gave bands at 70 kDa, 40 kDa, 30 kDa and 27 kDa as well as the expected band at 45 kDa. These may be cleavage products or contamination of insect cell proteins. The fractions containing bands at 45 kDa were pooled and dialysed against PBS and their concentrations calculated by Bradford assay.

In order to check that the Bm-TGH-2 protein expressed was not a contaminant, the 45 kDa Bm-TGH-2 band was excised from a Coomassie gel and sent to the SIRCAMs facility for matrix-assisted laser desorption/ionization (MALDI) Mass Spectrometry analysis. When the peptide fragment sizes were entered into the ProteinProspector MS-Fit tool (http://prospector.ucsf.edu), and searched against the NCB Inr *B. malayi* database, one match was returned – Bm-TGH-2, with a extremely significant score of 1.57×10^{14}. The peptide fragment sequences returned from the analysis are shown aligned with Bm-TGH-2 in Figure 4.7.

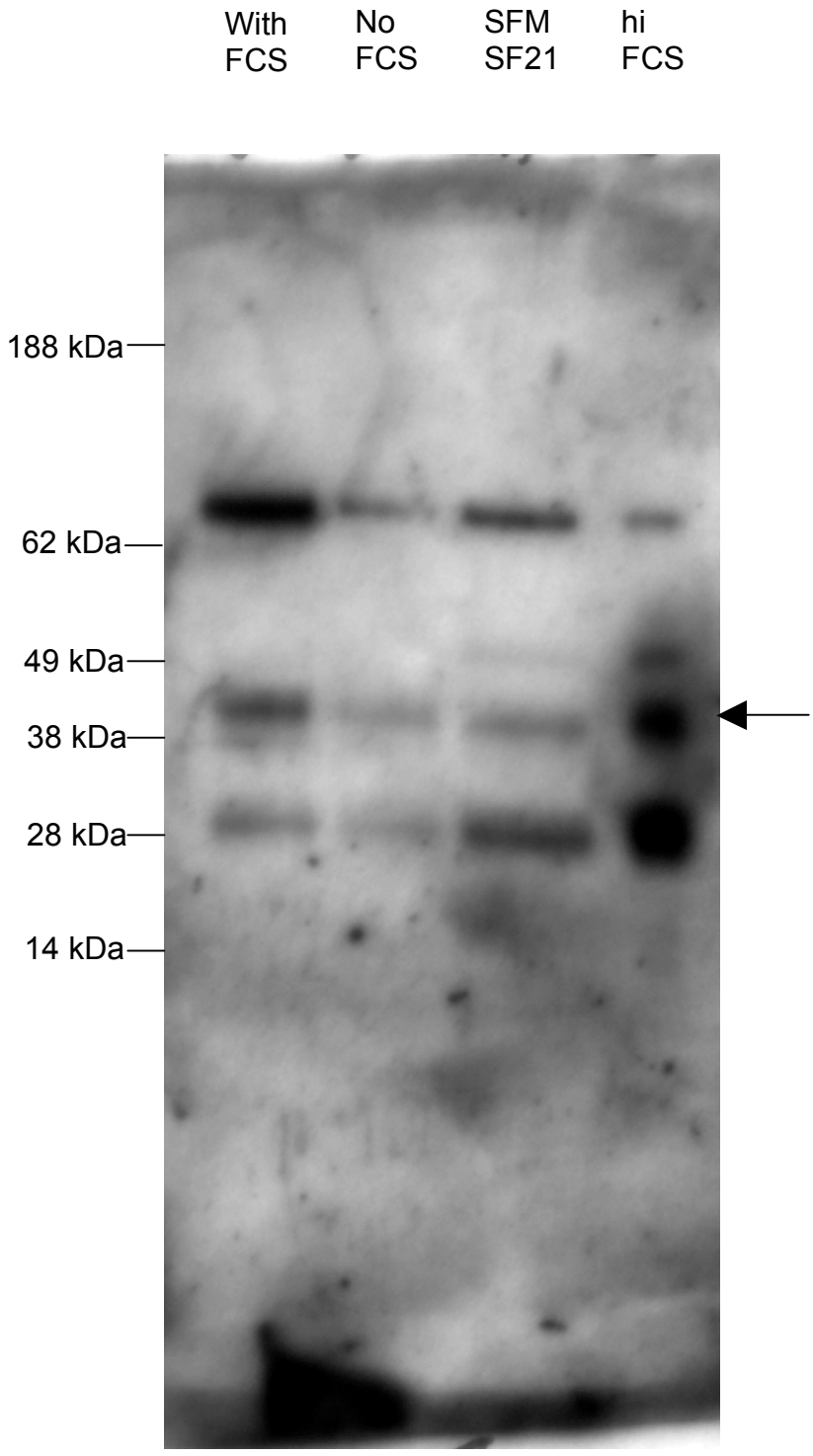

Figure 4.5: Expression of Bm-TGH-2 under conditions to minimise TGF-β from FCS
Western blot of supernatants from small-scale expressions of Bm-TGH-2, expressed in normal SF21 cells in TC100 with FCS or TC100 without FCS, in SF21 SFM cells (not requiring FCS in their media) or normal SF21 cells in TC100 media containing hiFCS, probed with 1/200 anti-Bm-TGH-2, then 1/1000 anti-mouse IgG-HRP. The expected size of Bm-TGH-2 is indicated by the arrow.

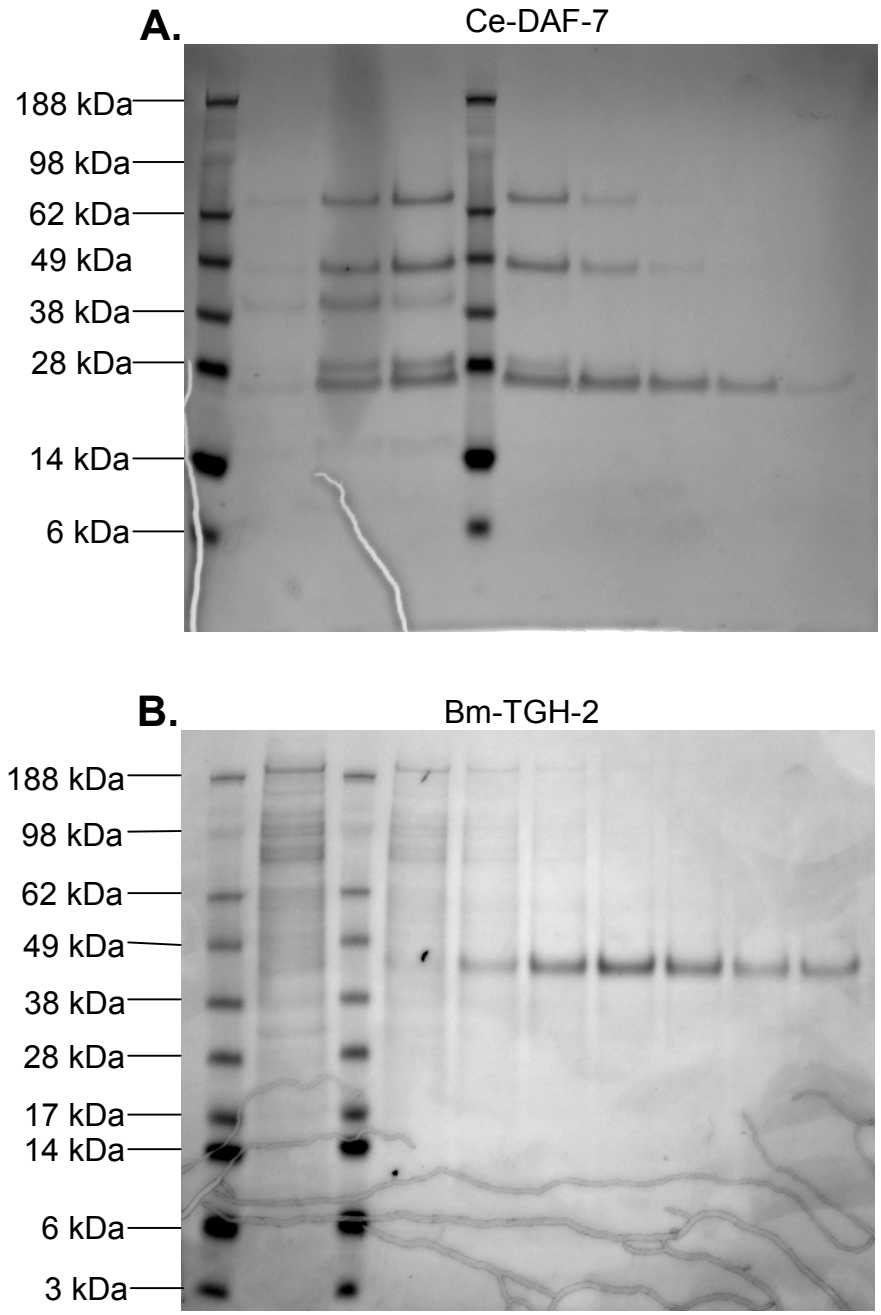

Figure 4.6: Coomassie stains of 6-His purified fractions of Ce-DAF-7 and Bm-TGH-2
Ce-DAF-7 (A) and Bm-TGH-2 (B) were expressed in SF21 cells in the absence of FCS, then purified using the 6-His tag on the AKTAprime in a rising concentration from 10 mM to 500 mM of imidazole.

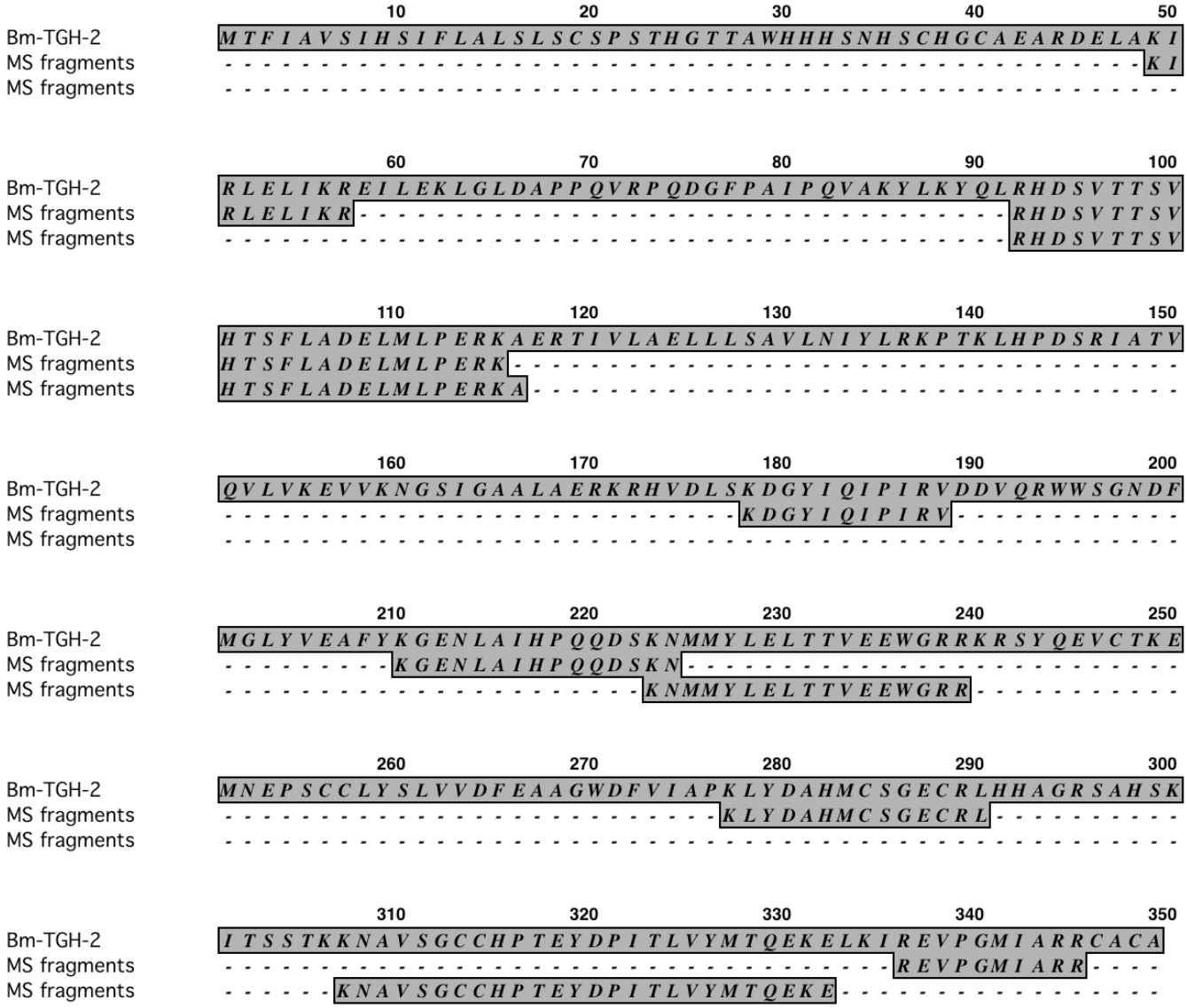

Figure 4.7: Mass spectrometry of Bm-TGH-2
Peptides predicted by MALDI-TOF mass spectrometry analysis of expressed Bm-TGH-2 aligned with full Bm-TGH-2 amino acid sequence.

4.5. TGF-β Activity in Serum-free Expressed Proteins

Bm-TGH-2 and Ce-DAF-7 were then used in the TGF-β bioassay at defined concentrations with a Bm-ALT-2 (also expressed in SF21s without FCS) negative control. In an attempt to activate the samples, they were either heat treated, acid treated or furin treated (2 units of recombinant furin (New England Biolabs) added and heated to 37 °C for 2 hours), any of which should have been capable of activating any latent TGF-β present. The levels of TGF-β activity seen are very low (close to the detection limit of the assay), and do not increase significantly when a greater concentration was added, therefore the signals seen are most likely artifactual (Figure 4.8).

A well-characterised action of TGF-β is the induction of Tregs when combined with a polyclonal stimulus. To test for induction of Tregs, purified Bm-TGH-2, Ce-DAF-7 and Bm-ALT-2 were used in cultures of BALB/c splenocytes stimulated with ConA, with a positive control of recombinant TGF-β (Figure 4.9). No Treg induction was seen by the any of the recombinant proteins.

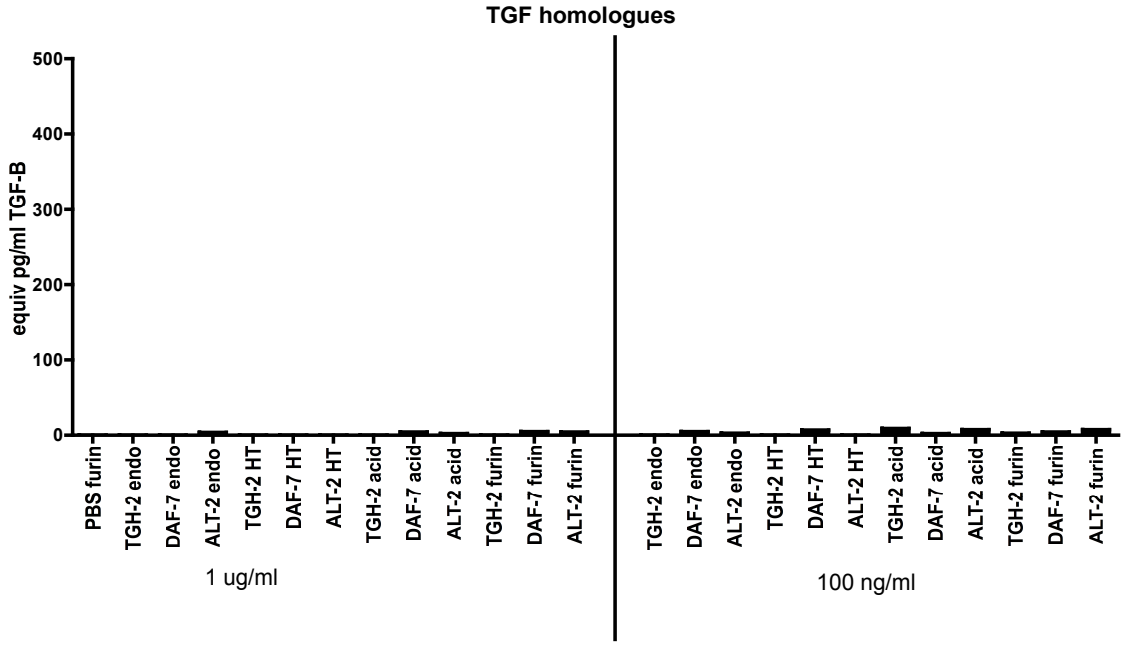

Figure 4.8: TGF-β activity of TGF-β homologues expressed in the absence of FCS
1 μg/ml or 100 ng/ml Bm-TGH-2, Ce-DAF-7 or Bm-ALT-2 (expressed in the absence of FCS), either endogenous (endo) or activated by heat-, acid- or furin-treatment were added to the MLEC TGF-β bioassay. Scale is set to the top of the standard curve (500 μg/ml).

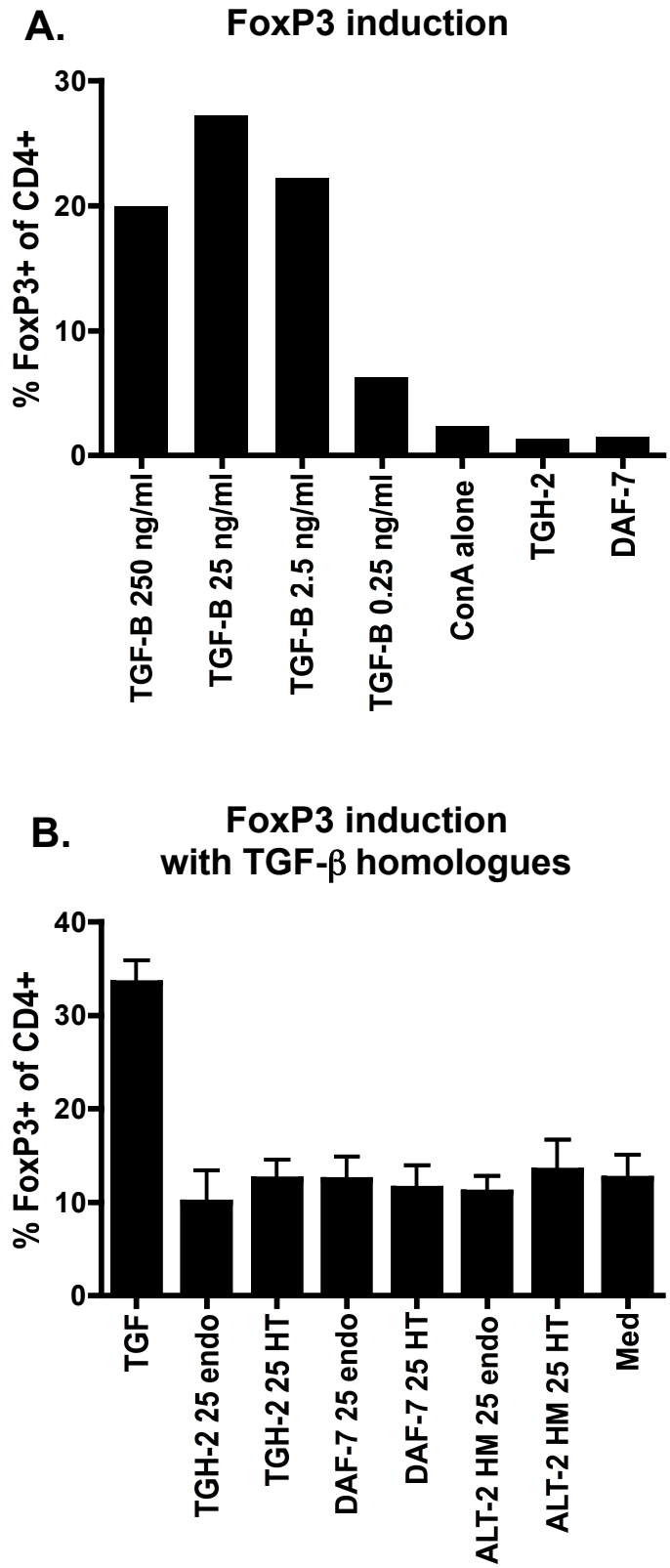

Figure 4.9: Foxp3 induction in BALB/c spenocytes by TGF-β or recombinant parasite products.

$1x10^6$ BALB/c splenocytes were stimulated with 2 μg/ml ConA and TGF-β or TGF-β homologues, then stained for CD4 and Foxp3 in 2 separate experiments. (A) Splenocytes stimulated in the presence of a range of TGF-β concentrations as shown, or Bm-TGH-2 or Ce-DAF-7 at 1 μg/ml. (B) Splenocytes stimulated in the presence of 25 ng/ml TGF-β or 2.5 ng/ml endogenous (endo) or heat-treated (HT - 85°c 5 min) Bm-TGH-2, Ce-DAF-7 or Bm-ALT-2.

4.6. Discussion:

In this chapter, I was able to purify the TGF-β homologues Bm-TGH-2 and Ce-DAF-7 from baculovirus-infected insect cells. As shown by N. Gomez-Escobar (96), Bm-TGH-2 expressed in insect cells can signal through the mammalian TGF-βR. However, in a very similar system used here highly pure TGH-2 could not produce a signal through the TGF-β bioassay, or induce Treg differentiation in a similar manner to mammalian TGF-β. As the DNA construct used to create the baculovirus was the same as the one used by N. Gomez-Escobar, the protein produced should have been identical. However, it was produced in a different cell line in these experiments (SF21 as opposed to Hi5), as when expression was attempted using the Hi5 cell line, very low levels of expressed protein were detected. The SF21 cell line may produce proteins with different post-translational modifications, which may have rendered the protein produced here non-functional. Other differences between the methods include a 6-His purification step in these experiments, while crude supernatant was used in N. Gomez-Escobar's paper. It could be that infection with the Bm-TGH-2 baculovirus was inducing the cells to produce a TGF-β homologue of their own, producing the published signal. However as controls of wild-type virus infected cell supernatant were used, which produced no signal, this is unlikey.

A previous study expressing mutants of mammalian TGF-β1 showed that addition of either a six-residue endoplasmic reticulum targetting sequence (SEKDEL), or a control non-functional 6-residue sequence (SEKDVS) to the C-terminus rendered the protein non-functional (210). The modified proteins could not produce a signal in a TGF-β bioassay, and could not dimerise or be proteolytically

cleaved to activity. Therefore the C-terminal of TGF-β appears to be extremely important for correct folding and processing, and any addition to the C-terminus can interfeer with this. This could be a possible explanation of the non-functional Bm-TGH-2 produced here, as the 6-residue Histidine tag added to the C-terminal could be interfering with functional protein production in a similar fashion. This however does not explain the disparity between the result shown here and the published result, as Bm-TGH-2 was previously expressed with a C-terminal 6-His tag. However as the protein produced by N. Gomez-Escobar was not 6-His purified, and no anti-6-His Western blots are shown in the published data, the possibility remains that a stop codon was introduced between the end of the protein and the 6-His tag, resulting in the production of functional protein.

In order to test the hypothesis that the His-tag is rendering the protein non-functional, the sequence could be altered to introduce a protease cleavage site between the end of the sequence and the His-tag, so that it could be cleaved off after expression, perhaps releasing functional protein. The proteins could alternatively be expressed without C-terminus tags and instead purified based on other physical properties such as size or charge. Another possible approach would be to add a N-terminal tag for purification of the proteins, however any correctly processed protein would lack the N-terminal pro-protein, and hence would have no tag. Any protein purified by this technique would thus be latent TGF-β, which could then be cleaved to activity by addition of proteases such as furin.

Insect cell expression may be a good system for expressing other TGF-β homologues, such as the novel TGF-β homologues identified in chapter 3, as it has been previously used to produce functional TGF-β (74, 211). However the problems

faced here should be borne in mind when expressing other proteins, such as the possibility of C-terminal tags interfering with processing, and mammalian TGF-β from FCS present in purified proteins.

Chapter 5:
Treg characterisation in *B. malayi* infection

5. Treg characterisation in *B. malayi* infection

5.1 *B. malayi* L3 larvae subcutaneous infection

My primary hypothesis was that Bm-TGH-2 produced by *B. malayi* signals through the host's TGF-β receptors, resulting in downregulation of the immune response through induction of Tregs. A previous paper (203) showed that 12 days after subcutaneous infection with *Brugia pahangi* L3, a $CD25^{+}CTLA\text{-}4^{+}$ T cell phenotype with increases in IL-10 and Foxp3 transcript levels could be seen in splenocytes upon restimulation with *B. pahangi* antigen. These data indicate a Treg induction by *B. pahangi* that is antigen specific and able to be seen after antigen restimulation of a secondary lymphoid organ.

At the time of the Gillan study, reagents for Foxp3 flow cytometric staining were not available, therefore I extended these experiments to measure Foxp3 expression by splenocytes *ex vivo* 12 days after subcutaneous injection of L3 *Brugia malayi* larvae. Infections were carried out twice in separate experiments, and as can be seen in Figure 5.1, a slight increase in the proportions of $Foxp3^{+}$ cells within the $CD4^{+}$ population, and $CD103^{+}$ cells in the $Foxp3^{+}$ population was seen in the first experiment, however this was not evident in the second experiment. As the spleen is a secondary lymphoid site, any response induced by the infection (for instance a Treg induction) will be diluted by the large numbers of naïve cells already present at steady state in the spleen. In order to more sensitively see changes induced by an infection it is preferable to study the draining lymph node, or ideally the infection site. To perform such studies, a model of *B. malayi* infection was used in which parasites are introduced into the peritoneal cavity, which can subsequently be lavaged to recover cells recruited to the site of infection (212).

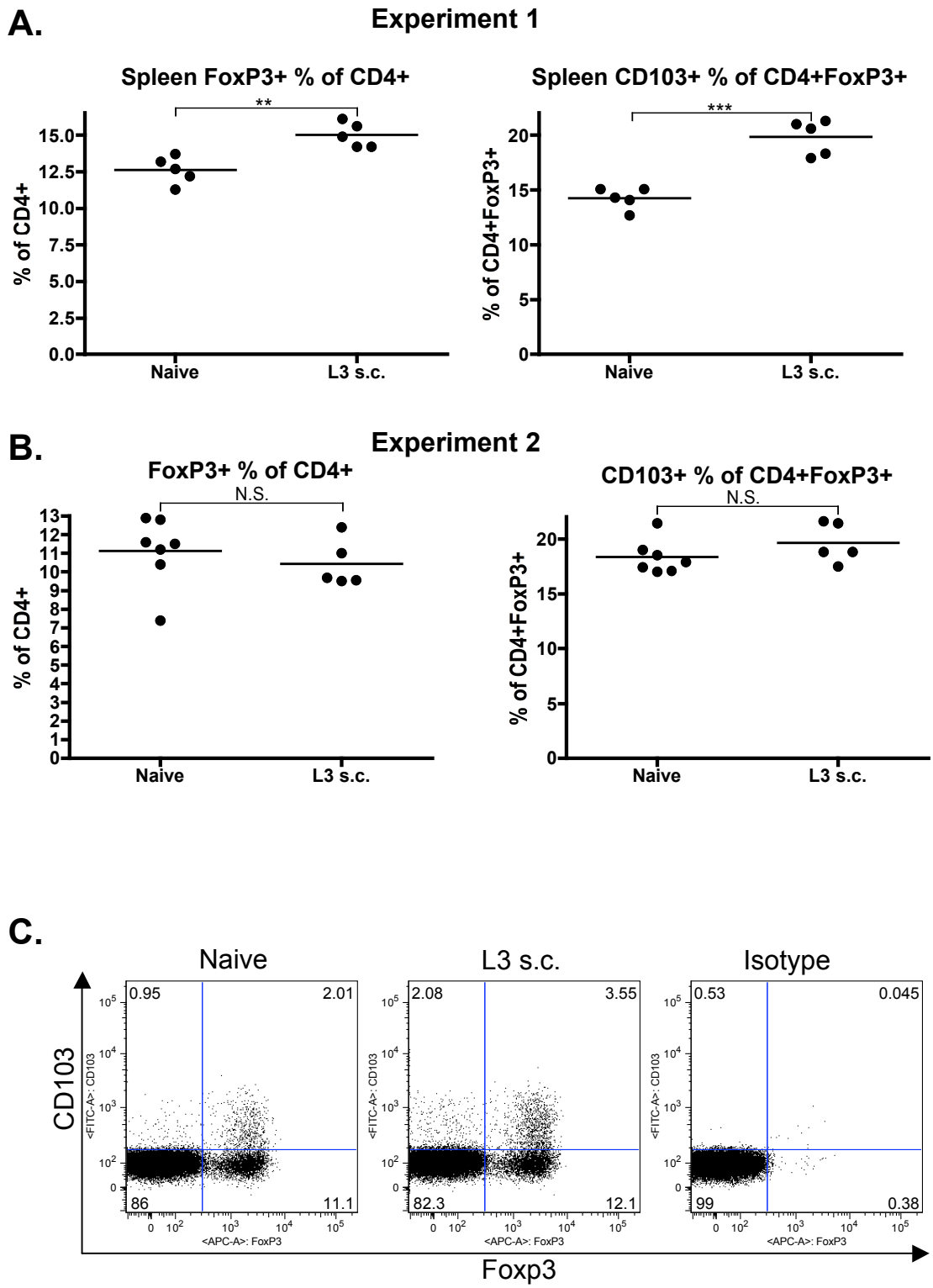

Figure 5.1: Tregs in the spleen following s.c. L3 *B. malayi* injection
BALB/c males were injected s.c. in the scruff with 50 *B. malayi* L3 larvae, and spleens taken 12 days later and analysed for expression of CD4, Foxp3 and CD103 by flow cytometry. (A) and (B) show 2 independent experiments. (C) shows bivariate plots from representative samples of experiment 1, and are gated on $CD4^+$ cells. N.S. = non-significant, ** = P<0.01, *** = P<0.001

5.2 Treg induction by intraperitoneal *Brugia malayi* L3

We hypothesised that *B. malayi* induces a Treg response during infection, and that this could be detected most sensitively at the infection site. In order to investigate this, mice were injected intraperitoneally with infective L3 larvae, and peritoneal lavages taken at various timepoints. These were analysed *ex vivo* by flow cytometry for Treg-associated markers.

5.2.1 Characterisation of day 7 *B. malayi* L3 peritoneal Tregs

Groups of male BALB/c mice were injected intraperitoneally with *B. malayi* L3, and peritoneal lavage cells taken at day 7 after infection. These were analysed by flow cytometry for expression of Treg associated markers (Figures 5.2 and 5.3). Significant increases in percentages of Foxp3 within the CD4 population, (Figure 5.2A and B) and CD103 in the $CD4^{+}Foxp3^{+}$ population (Figure 5.2C and D) were seen between *B. malayi* L3 i.p. infections and controls. The $CD4^{+}Foxp3^{+}$ cells also significantly upregulated expression of CD25 (Figure 5.3B and C), with a trend for an increase in CTLA-4 expression in this experiment (Figure 5.3E and F). The increase in CTLA-4 expression reached significance in most other experiments. Thus the induced Tregs were $CD4^{+}CD25^{hi}$CTLA-$4^{hi}Foxp3^{+}$ and a subset were $CD103^{+}$, and so resembled activated natural Tregs (135). Changes were also seen in the $CD4^{+}Foxp3^{-}$ T effector population, with significant decreases in proportions of $CD25^{+}$ cells (Figure 5.3A and C), and increases in CTLA-4^{+} cells (Figure 5.3D and F) in this population. CD103 staining on $Foxp3^{-}$ cells was almost undetectable (Figure 5.2D).

5.2.2. *B. malayi* L3 induce an increase in Treg cell numbers

The increase in cells expressing Treg associated markers was also seen in total cell numbers (Figure 5.4). In 4 repeat experiments, *B. malayi* L3 infected peritoneal lavages showed an increase of 4.5-fold, 5-fold, 13-fold and 5.5-fold in $Foxp3^+$ absolute cell numbers above controls (Figure 5.4C), whereas $CD4^+Foxp3^-$ cell numbers only showed an increase of 3-fold, 3-fold, 10-fold and 2.5-fold respectively (Figure 5.4E). These results show that the increase in proportion of $Foxp3^+$ cells within the $CD4^+$ population is not due to a reduction in $Foxp3^-$ cell numbers, but rather an overwhelming increase in numbers of $Foxp3^+$ Tregs, indicating that the Tregs are actively induced to proliferate or are recruited from elsewhere in the host.

5.2.3. *B. malayi* L3 i.p. infection timecourse

To appraise the kinetics of Treg expansion in the three weeks following infection, data were aggregated from a number of experiments in which mice were infected with *B. malayi* L3 larvae, in terms of $Foxp3^+$ proportions of the $CD4^+$ population (Figure 5.5A) and $CD103^+$ proportions of the $CD4^+Foxp3^+$ population (Figure 5.5B). At all timepoints studied, live L3 larvae could be recovered from the peritoneum of infected mice. Infection caused an increase in $Foxp3^+$ expression within the $CD4^+$ population at day 7, which decreased to control levels in later timepoints, continuing to negative values compared to controls at day 21, which reached significance in one of two repeat experiments (Figure 5.5A).

CD103 expression within the $CD4^+Foxp3^+$ population was increased significantly in infected mice at most timepoints (Figure 5.5B). These results

indicate that while the early increase in proportion of $Foxp3^+$ within the $CD4^+$ population is not sustained over time, the $Foxp3^+$ population retains higher CD103 expression, possibly indicating that a heightened state of Treg activation pertains throughout infection. Interestingly, CD103 expression on $Foxp3^+$ cells was highly significantly increased at later timepoints after infection, indicating CD103 expression is dynamic, and may reflect further activation of Tregs, or the requirement for their retention at the effector site.

Statistical analysis of these pooled data was not possible as control levels of Foxp3 expression were statistically different between experiments. Each experiment was analysed separately for differences between control and infected levels by Student's t test, with statistical significances for each replicate experiment separately shown in Table 5.1. All significant differences are increases from controls unless indicated.

Table 5.1: Individual statistics for each timepoint after L3 *B. malayi* infection

Timepoint	$Foxp3^+$ % of $CD4^+$ cells	$CD103^+$ % of $CD4^+Foxp3^+$ cells
Day 7 p.i.	Expt 1: ** = 0.0097 Expt 2: ** = 0.0011 Expt 3: ** = 0.0018 Expt 4: *** = 0.0000061	Expt 1: ** = 0.0058 Expt 2: *** = 0.00029 Expt 3: *** = 0.000027 Expt 4: N.S. = 0.11
Day 12 p.i.	Expt 1: ** = 0.0051 Expt 2: * = 0.042 Expt 3: N.S. = 0.29	Expt 1: ** = 0.0065 Expt 2: * = 0.048 Expt 3: N.S. = 0.29
Day 14 p.i.	Expt 1: N.S. = 0.32 Expt 2: N.S. 0.96	Expt 1: N.S. = 0.17 Expt 2: N.S. = 0.45
Day 21 p.i.	Expt 1: N.S. = 0.98 Expt 2: * = 0.022 (Decrease)	Expt 1: ** = 0.0085 Expt 2: ** = 0.0036

5.2.4. Dead *B. malayi* L3 control

It was important to ensure that the observed increase in $Foxp3^+$ cells was not due to any immune response taking place in the peritoneal cavity, therefore as the closest possible control to an anti-parasite response, *B. malayi* L3s were killed by heating to 65°C for 10 min before injecting intraperitoneally, and compared to live infection over a timecourse as before. Dead L3s were shown to induce a peritoneal response with no increases in proportions (Figure 5.6A) or numbers (Figure 5.6B) of $Foxp3^+$ cells over intraperitoneal media injections, unlike live L3s. Dead L3s did

induce a small effector response in the peritoneal cavity at day 7 after injection however, as total cell numbers (Figure 5.7A) increased, although $CD4^+$ cell numbers (Figure 5.7B) remained unchanged. Thus, the Treg induction seen in *B. malayi* infection is an active process as it depends on the presence of live parasites.

5.2.5. Characterisation of effector response induced by L3 *B. malayi* infection

At day 7 post-infection with either dead or live L3s, the total cell population recruited to the peritoneum was examined by flow cytometry. A trend for an increase in numbers (but not proportions) of $F4/80^+$ macrophages was seen in live L3 infection only (Figure 5.8A and B). This increase in macrophage numbers reached significance in some other L3 experiments, however this was very variable. Proportions and numbers of SIGLEC-F^+ eosinophils (Figure 5.8C and D) and $GR1^+$SIGLEC-F^- neutrophils (Figure 5.8E and F) were also significantly increased with live L3s only. Thus, only live L3 infection recruited a significant population of TH2 effector cells. The lack of a strong response seen in dead L3 *B. malayi* injection indicates that dead L3 are quickly cleared from the peritoneal cavity by innate immune mechanisms to which live parasites are not susceptible.

Splenocytes were also prepared from these mice, and restimulated for 72 h with *B. malayi* adult worm homogenate, then assayed for cytokines in the supernatants by ELISA. There was a specific response of the live L3-exposed splenocytes to adult *B. malayi* antigen, resulting in production of the TH2 cytokines IL-4 (Figure 5.9A), IL-5 (Figure 5.9B) and IL-13 (Figure 5.9C). Dead L3 injection did not result in a significant increase in the TH2 cytokines, but there was a small trend towards a TH2 response. Therefore, although dead L3s did appear to induce a

small TH2 response, with recruitment of cells to the peritoneum, this response is either smaller, or not as sustained, as the response induced by live parasites.

5.2.6. Splenic response to *B. malayi* L3 i.p. infection

The response in the spleen to i.p. L3 infection was also assayed *ex vivo* by flow cytometry. No significant differences in proportions of $Foxp3^+$ cells with the $CD4^+$ population (Figure 5.10A) or $CD103^+$ cells within the $CD4^+Foxp3^+$ population (Figure 5.10B) could be seen at any timepoint.

5.2.7. Summary of Treg induction by intraperitoneal *Brugia malayi* L3

The results above show that intraperitoneal *B. malayi* L3 injection induces a transient Treg induction at the infection site. However, as the mouse model is not fully tolerant to the *B. malayi* lifecycle, the effect of later lifecycle stages cannot be assessed using the L3 larvae infection model. In order to look at later lifecycle stages, a model of *B. malayi* infection where adult parasites were introduced to the peritoneal cavity was used.

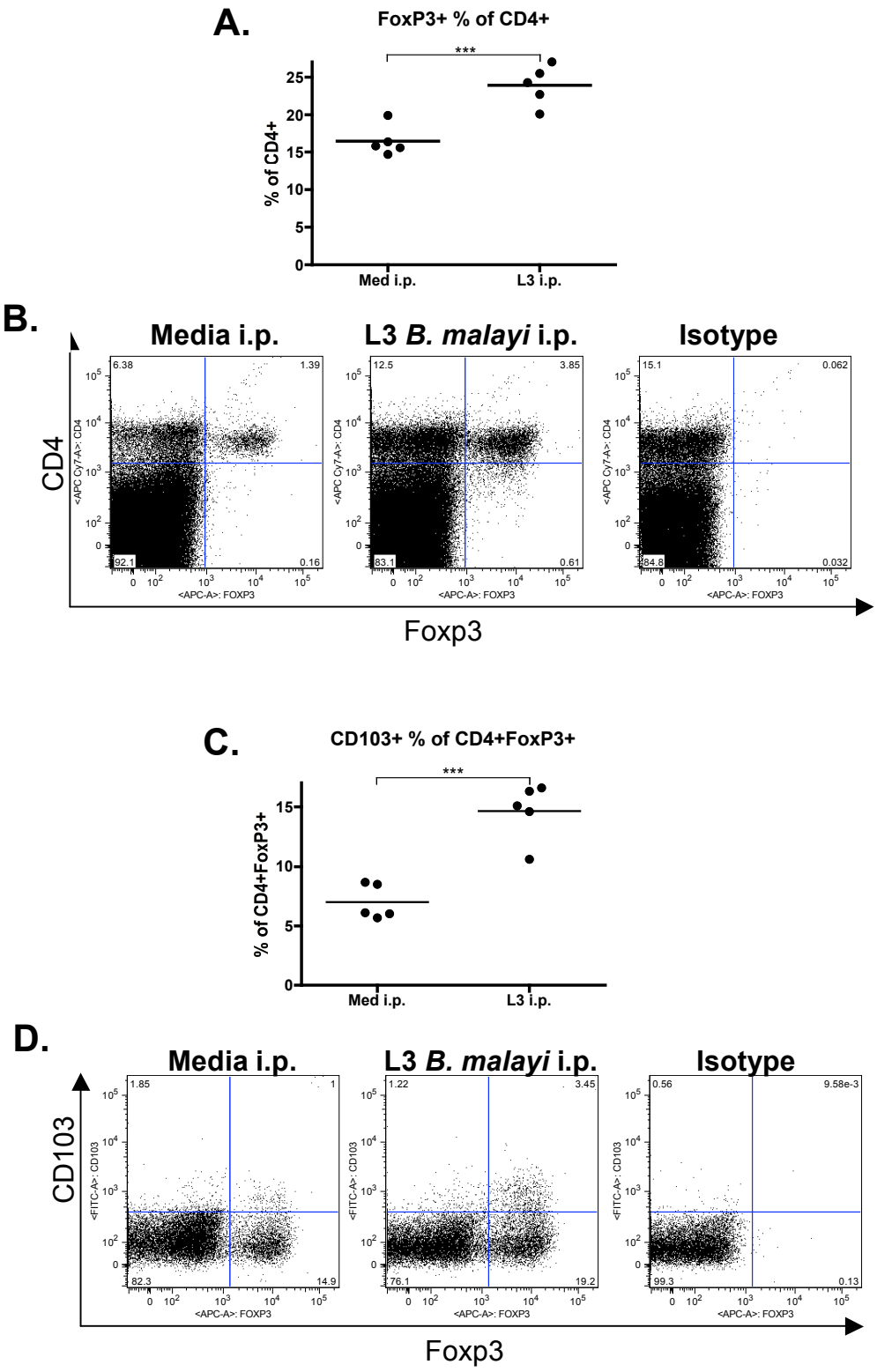

Figure 5.2: Treg markers in the PL 7 days after i.p. L3 *B. malayi* infection
Peritoneal lavage samples were taken from BALB/c males 7 days after injection of 50 L3 *B. malayi* or controls of media, then analysed by flow cytometry for expression of Treg markers. Graphs shown are 1 representative experiment of 4 repeats, showing $Foxp3^+$ % of $CD4^+$ cells (A), and $CD103^+$ % of $Foxp3^+$ (C) and bivariate plots shown are representative samples of experiment shown, showing CD4 vs Foxp3, gated on lymphocytes by FSC and SSC (B) and CD103 vs Foxp3, gated on $CD4^+$ cells (D). Isotype control shown for Foxp3 vs CD4 (B) contains anti-CD4 antibody to allow for gating on the $CD4^+$ population, and so is only a control for Foxp3 staining. *** = $P<0.001$.

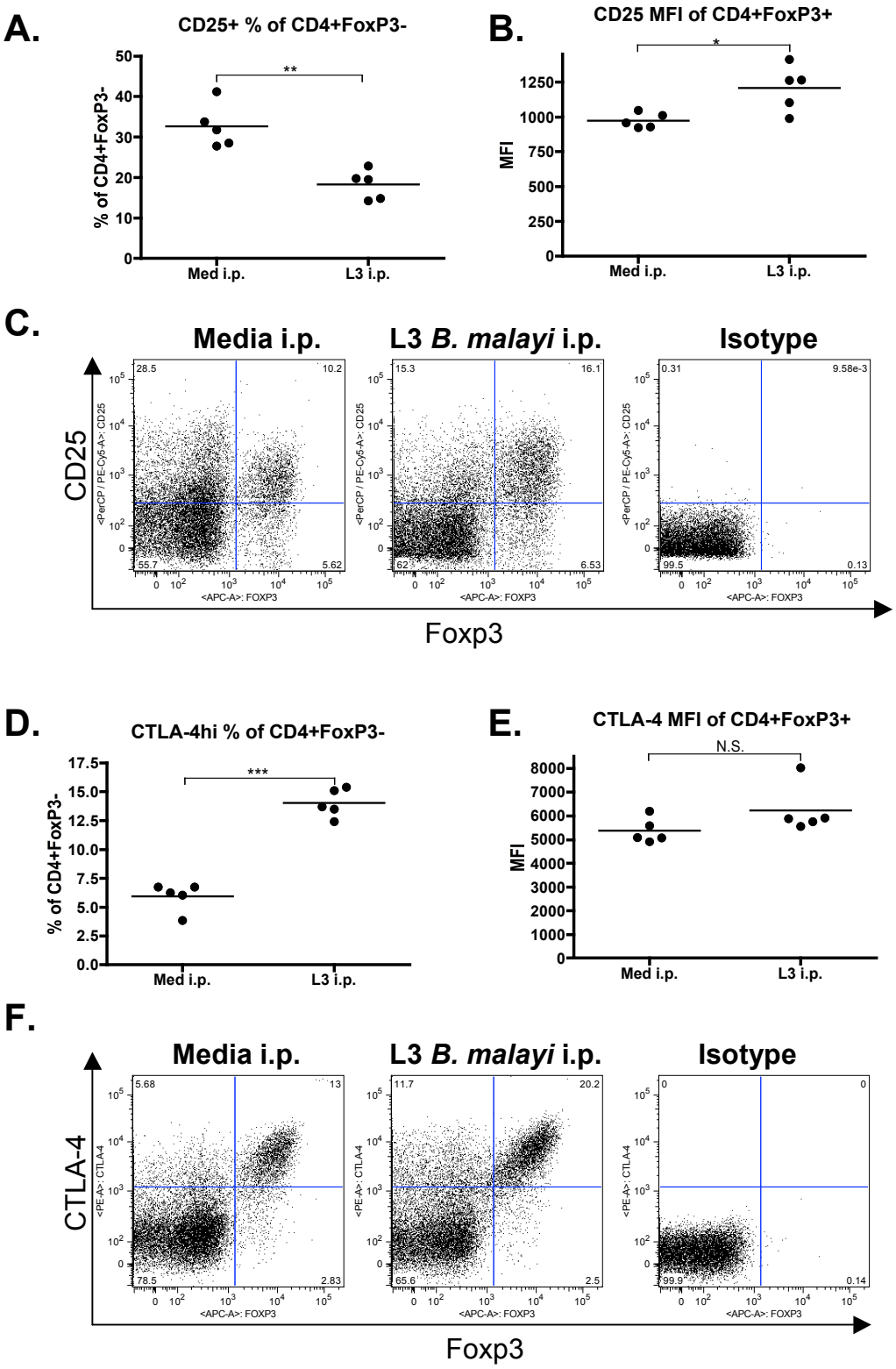

Figure 5.3: Treg markers in the PL 7 days after i.p. L3 *B. malayi* infection
Peritoneal lavage samples were taken from BALB/c males 7 days after injection of 50 L3 *B. malayi* or controls of media, then analysed by flow cytometry for expression of Treg markers. Graphs shown are 1 representative experiment of 4 repeats, showing $CD25^+$ % of $CD4^+Foxp3^-$ cells (A), CD25 MFI of $CD4^+Foxp3^+$ cells (B), CTLA-4^{hi} % of $CD4^+Foxp3^-$ (D) and CTLA-4 MFI of $CD4^+Foxp3^+$ cells (E). Bivariate plots shown are representative samples of experiment shown, showing CD25 vs Foxp3 (C), and CTLA-4 vs Foxp3 (F), gated on $CD4^+$ cells. *** = P<0.001, ** = P<0.01, * = P<0.05, N.S. = non-significant.

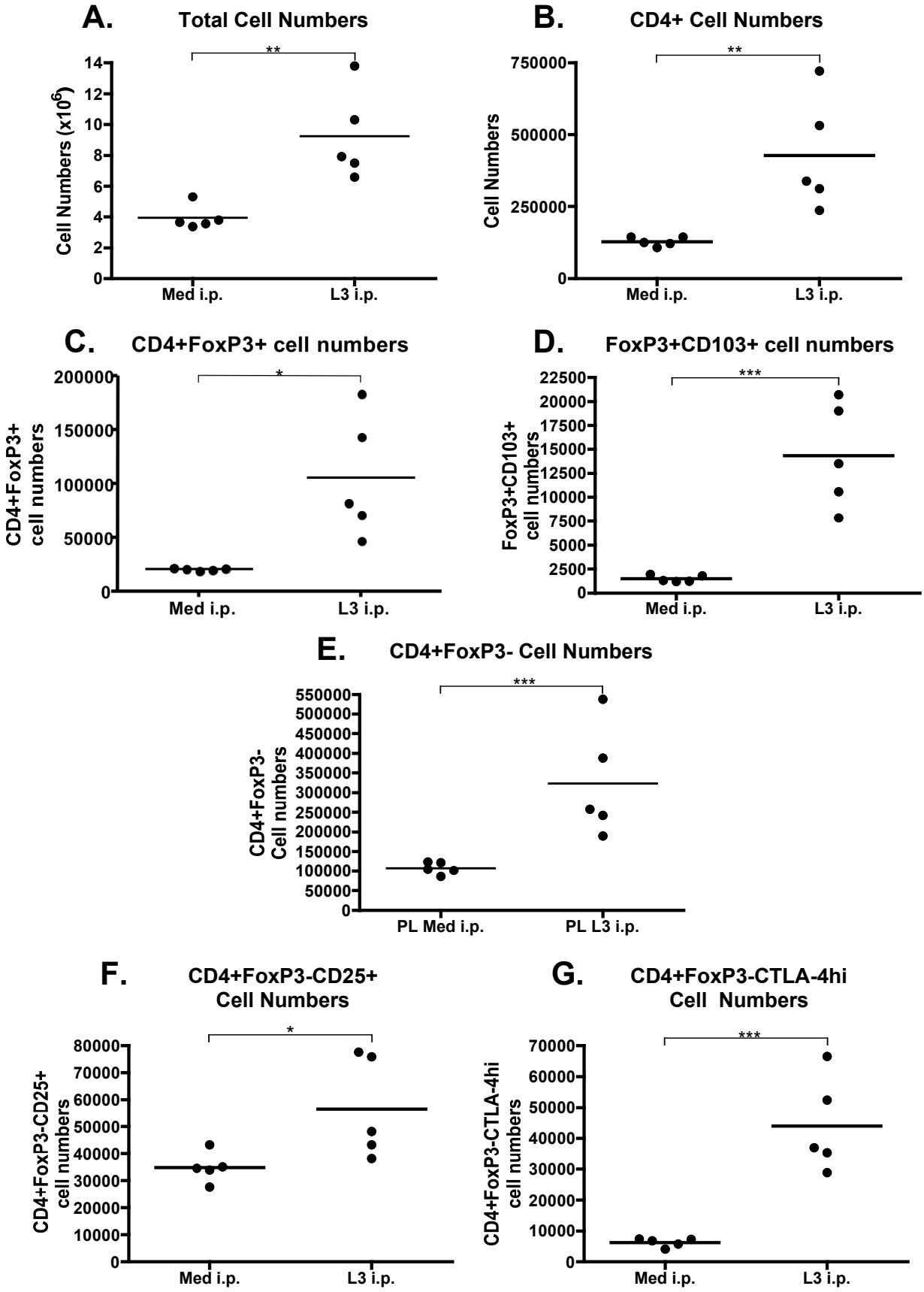

Figure 5.4: Treg numbers in the PL 7 days after i.p. L3 *B. malayi* infection
Peritoneal lavage samples were taken from BALB/c males 7 days after injection of L3 *B. malayi* or controls of media, then analysed by flow cytometry for expression of CD4, Foxp3 and CD103. Show are total PL cell numbers (A), and cell numbers of $CD4^+$ cells (B), $CD4^+Foxp3^+$ cells (C), $CD4^+Foxp3^+CD103^+$ cells (D), $CD4^+Foxp3^-$ cells (E), $CD4^+Foxp3^-CD25^+$ cells (F) and $CD4^+Foxp3^-$ CTLA-4^{hi} cells (G). Data shown is from a representative experiment of 4 repeats. * = $P<0.05$, ** = $P<0.01$, *** = $P<0.001$.

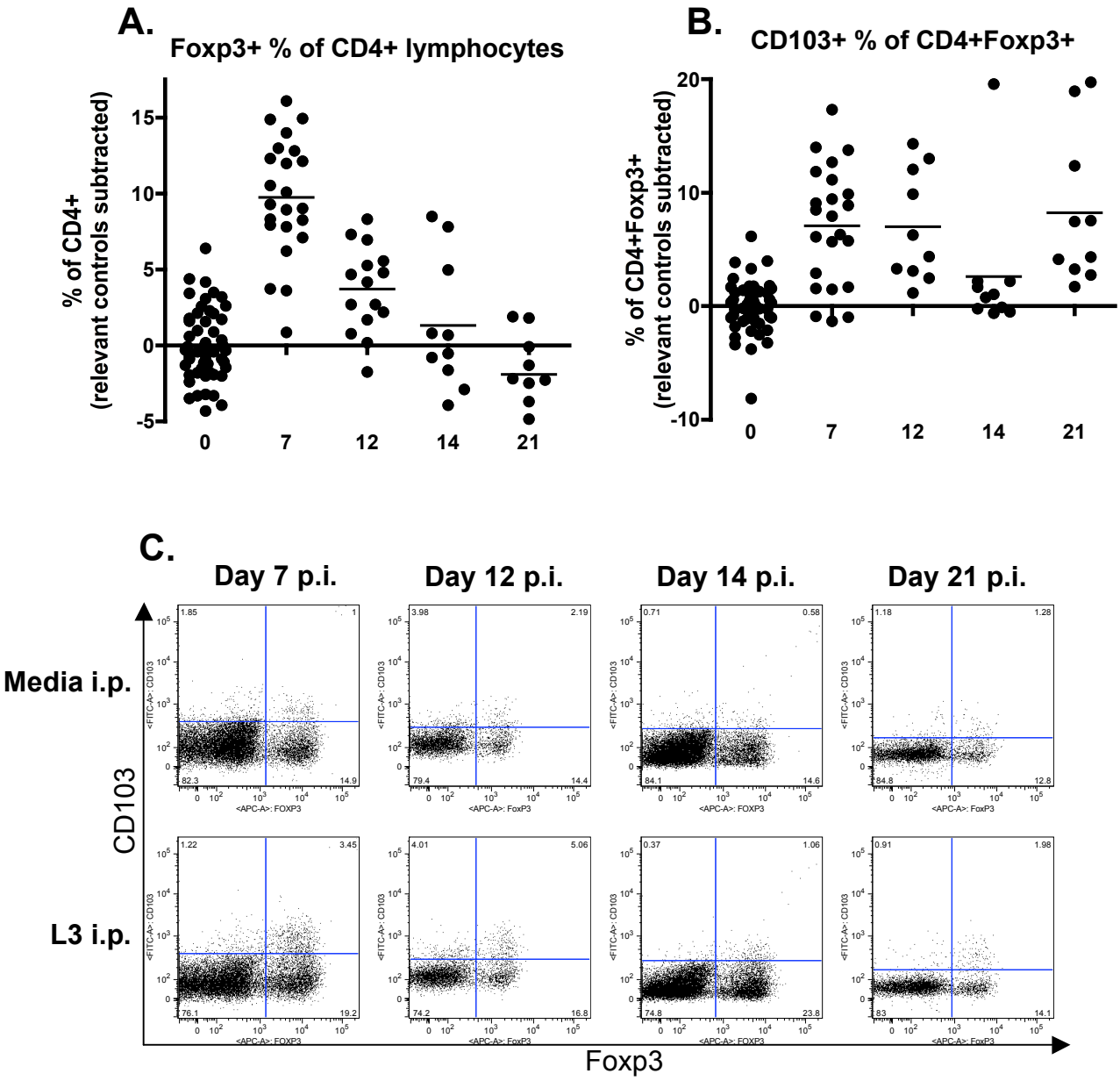

Figure 5.5: Timecourse of PL Tregs after L3 *B. malayi* infection
Peritoneal lavage samples were taken from BALB/c males at 7, 12, 14 and 21 days after injection with L3 *B. malayi* or controls of media, then analysed by flow cytometry for expression of CD4, Foxp3, and CD103. (A) shows timecourse of $Foxp3^+$ % in $CD4^+$ population, (B) shows timecourse of $CD103^+$ % in the $CD4^+Foxp3^+$ population. Graphs shown are the pooled results from 4 experiments for day 7, 3 experiments for day 12, a single experiment for days 14 and 2 experiments for day 21. The day 0 timepoint is a pool of controls from all timepoints. The average of each experiment controls was subtracted from all datapoints. (C) shows bivariate plots of Foxp3 vs CD103 median samples from representative experiments.

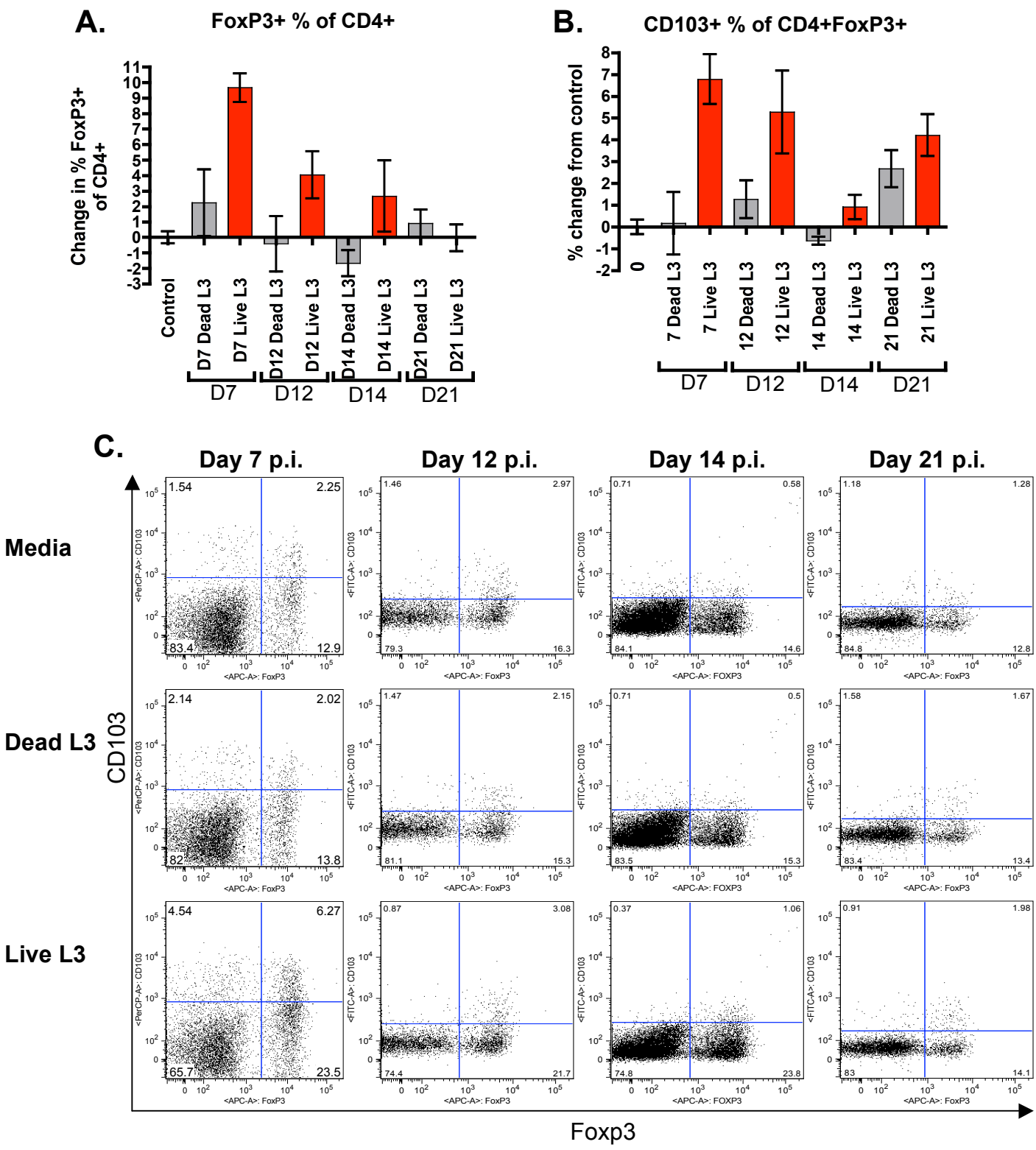

Figure 5.6: Timecourse of PL Tregs after dead or live L3 *B. malayi* infection
Peritoneal lavage samples were taken from BALB/c males at 7, 12, 14 and 21 days after injection with live or dead L3 *B. malayi* or controls of media, then analysed by flow cytometry for expression of CD4, Foxp3, and CD103. (A) shows a timecourse of $Foxp3^+$ % in $CD4^+$ population, (B) shows a timecourse of $CD103^+$ % in $CD4^+Foxp3^+$ population. Graphs shown are single experiments at each timepoint. D0 timepoint is a pool of controls from all timepoints, with average of each experiment controls subtracted, to show normal variation. (C) bivariate plots show CD4-gated Foxp3 vs CD103 median samples from representative experiments. * = P<0.05, ** = P<0.01, *** = P<0.001, N.S.=Non-Significant.

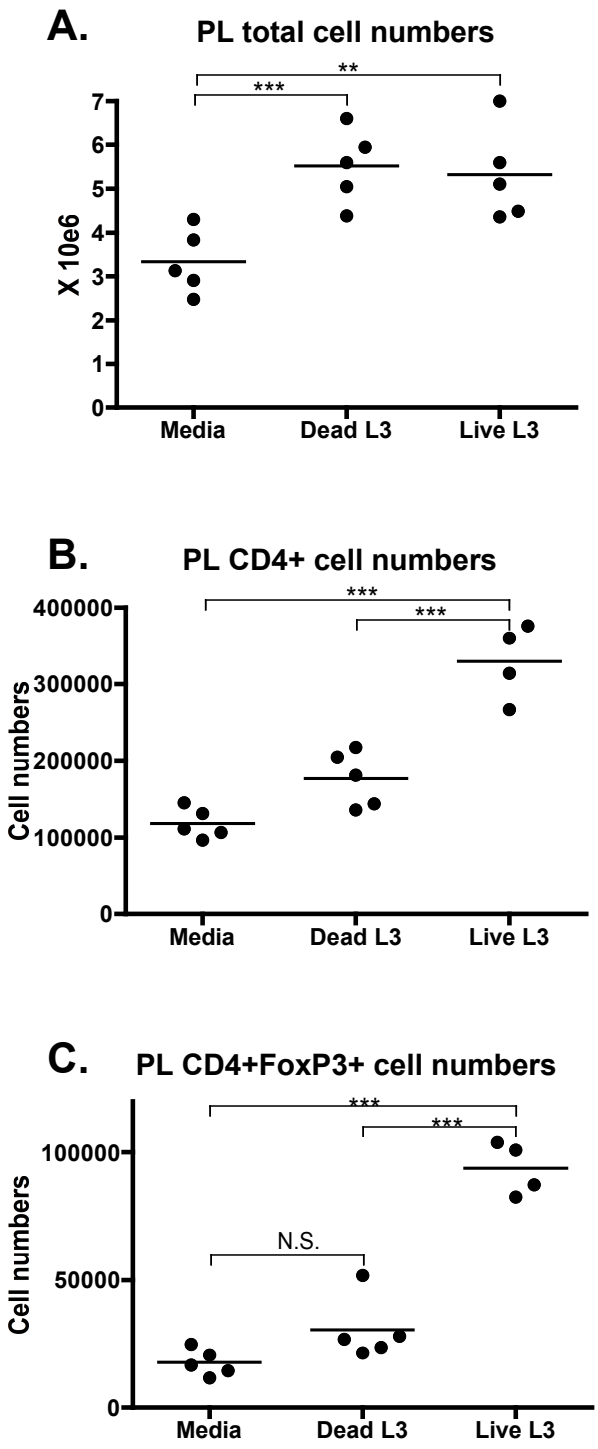

Figure 5.7: PL Treg cell numbers 7 days after live or dead L3 *B. malayi* injection
Peritoneal lavage samples were taken from BALB/c males 7 days after i.p. injection of media or, dead or live L3 *B. malayi*, then analysed by flow cytometry for expression of CD4 and Foxp3. Graphs show total cell numbers (A), $CD4^+$ cell numbers (B) and $CD4^+Foxp3^+$ cell numbers (C). N.S. = non-significant, ** = P<0.01, *** = P<0.001

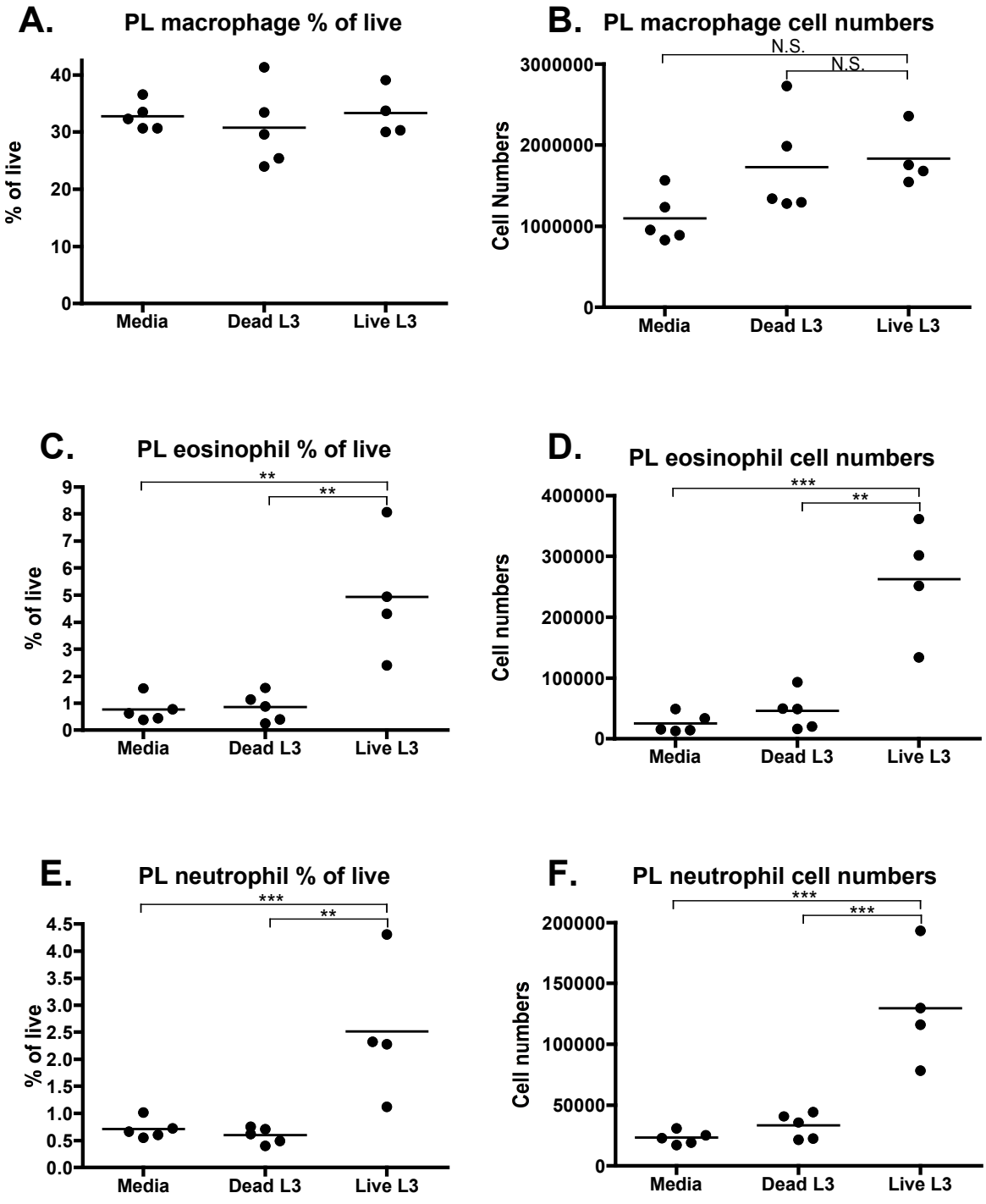

Figure 5.8: Innate immune cell recruitment after i.p. dead or live L3 *B. malayi* injection
Peritoneal lavage samples were taken from BALB/c males 7 days after i.p. injection of media or, dead or live L3 *B. malayi*, then analysed by flow cytometry for proportions and numbers of macrophages ($F4/80^{+}$) (A and B), eosinophils ($SIGLEC\text{-}F^{+}GR1^{+}$) (C and D), and neutrophils ($SIGLEC\text{-}F^{-}GR1^{+}$) (E and F), all shown as a percentage of live cells (gated on FSC/SSC to remove cell debris from calculations). ** = P<0.01, *** = P<0.001, N.S. = non-significant.

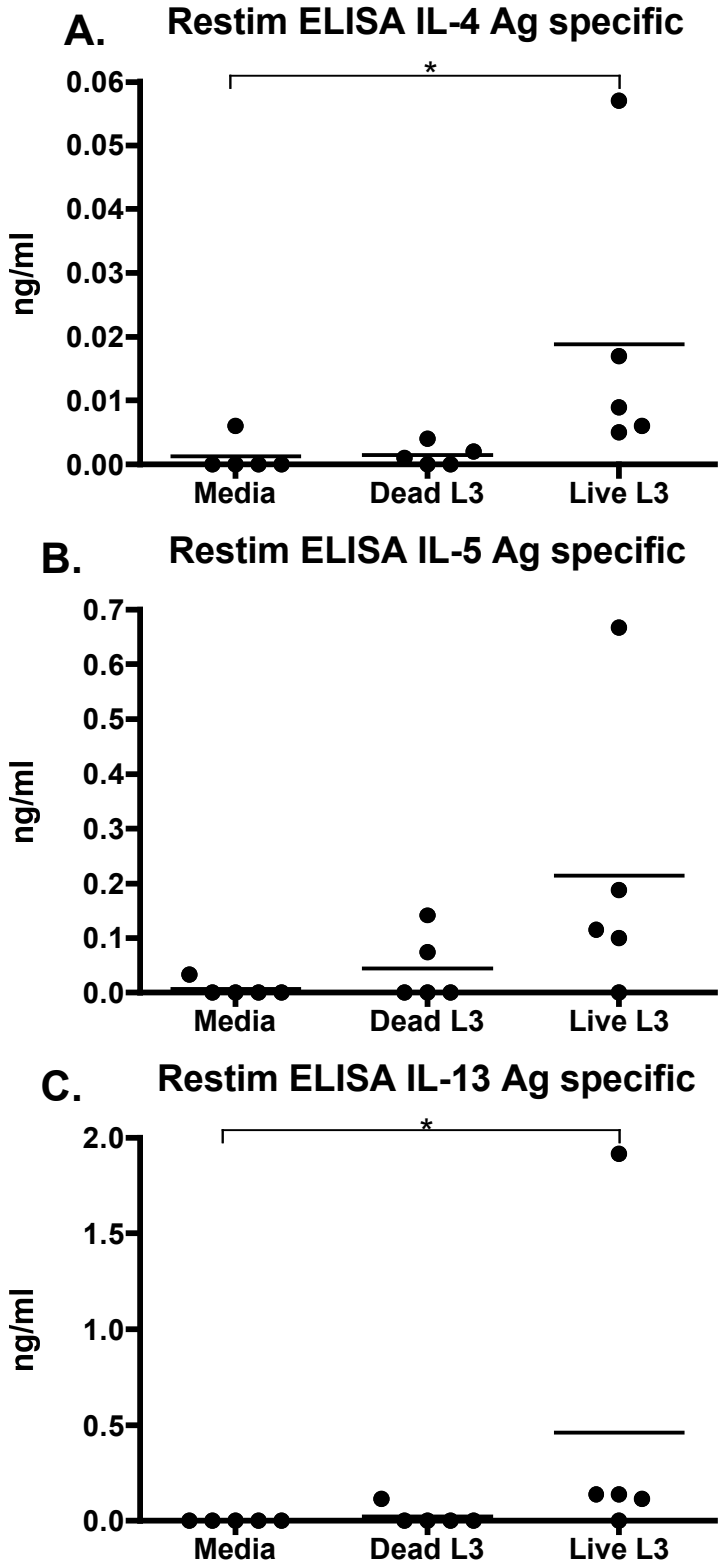

Figure 5.9: Restimulation cytokines after dead or live L3 *B. malayi* injection
Splenocytes were prepared from BALB/c male mice injected i.p. with medium, or dead or live L3 *B. malayi* 7 days previously, and restimulated with *B. malayi* antigen for 72 h. Supernatants were taken and used in cytokine ELISA. Shown is antigen-specific (unstimulated levels subtracted) production of IL-4 (A), IL-5 (B) and IL-13 (C).

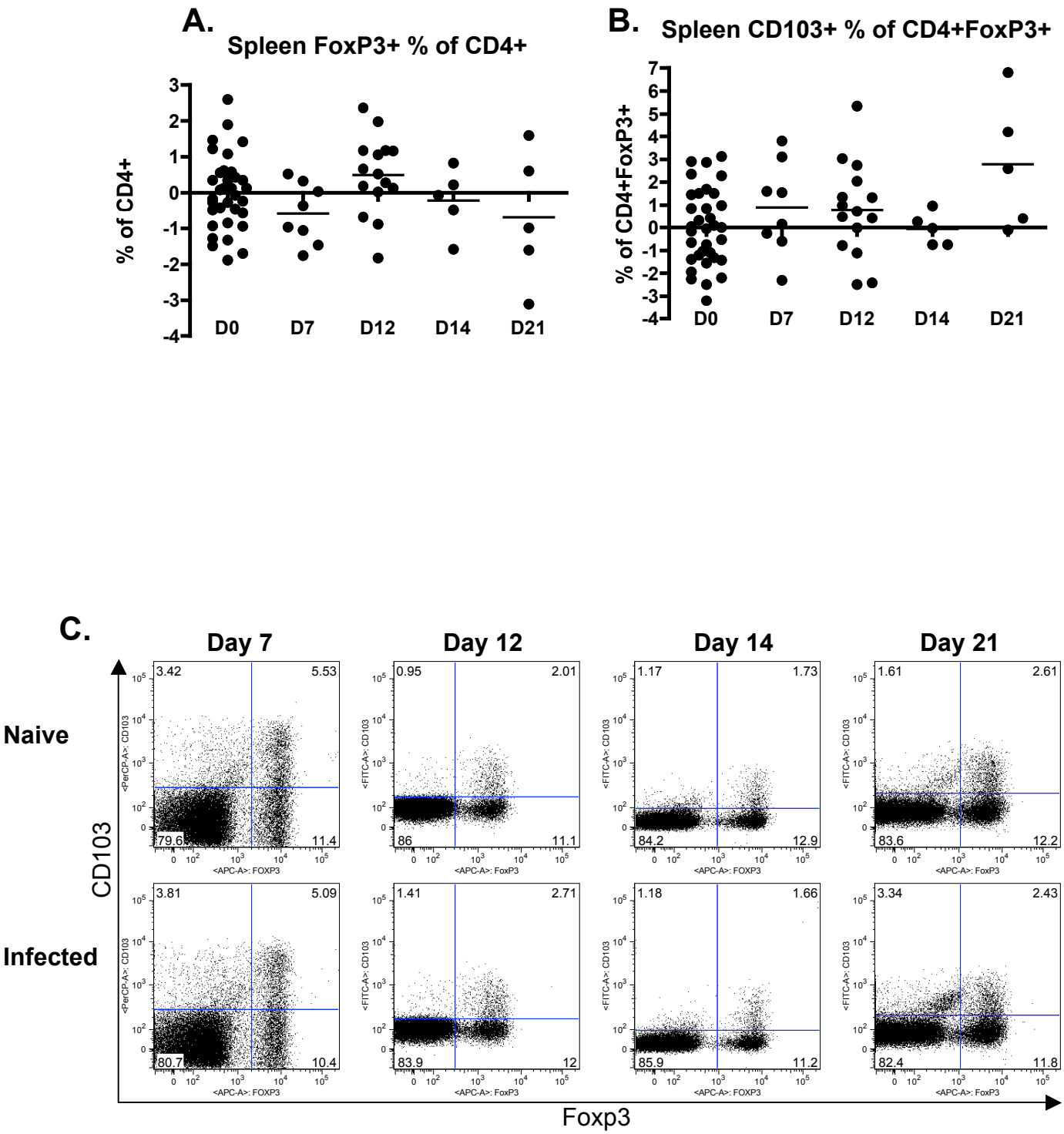

Figure 5.10: Tregs in the spleen after i.p. L3 *B. malayi* infection
Splenocytes were prepared from BALB/c males at 12, 14 and 21 days after injection with L3 *B. malayi* or controls of media, then analysed by flow cytometry for expression of CD4, Foxp3, and CD103. Graphs shown are the pooled results from 2 experiments at the D7 timepoint, 3 experiments at the D12 timepoint, and single experiments for the D14 and D21 timepoints. (A) shows Foxp3 % of $CD4^+$, (B) shows CD103 % of $CD4^+Foxp3^+$. (C) bivariate plots are representative of each timepoint, and are gated on $CD4^+$ lymphocytes. No significant differences were found.

5.3. Intraperitoneal adult *B. malayi* Treg induction

I wanted to study the effect of later *B. malayi* developmental stages of infection on the mouse model, using implantation of adult parasites into the peritoneal cavity. It has been previously shown that adult and L3 larvae of *B. malayi* induce similar downregulated TH2 responses in the mouse, characterised by suppressive macrophages. We hypothesised that a similar Treg induction would also be evident in adult infection.

5.3.1. Characterisation of day 7 *B. malayi* adult peritoneal Tregs

Adult *B. malayi* were implanted intraperitoneally in BALB/c mice, and again Treg associated markers on peritoneal lavage cells were assayed by flow cytometry at day 7 post-implantation. As in the L3 infection, an increase in percentages of $Foxp3^+$ cells in the $CD4^+$ population (Figure 5.11A and B), and $CD103^+$ cells within the $CD4^+Foxp3^+$ population (Figure 5.11C and D) was seen, indicating an expansion and activation of the Treg population. Both CD25 (Figure 5.12B and C) and CTLA-4 (Figure 5.12E and F) expression were increased on the $CD4^+Foxp3^+$ population. In the $CD4^+Foxp3^-$ population, a decrease in CD25 expression (Figure 5.12A and C), and an increase in CTLA-4 expression (Figure 5.12D and F) were seen.

Adult implant resulted in an increase in total (Figure 5.13A) and $CD4^+$ (Figure 5.13B) cell numbers. The increases in proportion of Treg markers were again reflected in cell numbers, as increases in $CD4^+Foxp3^+$ (Figure 5.13C) and $CD4^+Foxp3^+CD103^+$ (Figure 5.13D) cell numbers were seen.

5.3.2. *B. malayi* adult infection timecourse

A similar timecourse to L3 infection was run, with timepoints at days 7, 11, 12 and 20 post-implanation (Figure 5.14). Treg induction was seen in a similar manner to L3 infection, with a peak of Foxp3 proportions of the $CD4^+$ population at day 7, which is not sustained to later timepoints (Figure 5.14A). The percentage of $CD103^+$ cells within the $CD4^+Foxp3^+$ population was also increased with infection, and levels are significantly increased at every timepoint shown (Figure 5.14B), indicating the Tregs present are more active than at steady state, possibly due to the presence of host or parasite-derived TGF-β. As in section 5.2.2, control levels of Foxp3 expression were statistically different between experiments so data could not be statistically analysed as a pool, and so statistical significances for each replicate experiment were calculated separately using Student's t test, and are shown in Table 5.2.

Table 5.2: Individual statistics for each timepoint after adult *B. malayi* infection

Timepoint	$Foxp3^+$ % of $CD4^+$ cells	$CD103^+$ % of $CD4^+Foxp3^+$ cells
Day 7 p.i.	Expt 1: * = 0.032 Expt 2: ** = 0.0076 Expt 3: N.S. = 0.19	Expt 1: *** = 0.0000041 Expt 2: N.S. = 0.60 Expt 3: *** = <0.0001
Day 11 p.i.	Expt 1: N.S. = 0.25	Expt 1: * = 0.038
Day 12 p.i.	Expt 1: N.S. = 0.059	Expt 1: ** = 0.0086
Day 20 p.i.	Expt 1: N.S. = 0.15 Expt 2: N.S. = 0.71	Expt 1: *** = 0.00012 Expt 2: *** = <0.0001

5.3.3. Dead *B. malayi* adult control

A timecourse was also run using a control of dead parasites (adults killed by freeze-thawing), to day 20 with no Foxp3 induction seen if the parasites were dead (Figure 5.15A). However, at day 7 in the timecourse shown no $CD103^+$ induction on the $Foxp3^+$ Tregs was seen (Figure 5.15B), unlike other experiments (e.g. Figure 5.14B) in comparison of live adult implant to controls alone. At day 20, dead parasites caused an increase in $CD103^+$ proportions of the $CD4^+Foxp3^+$ population, unlike all other timepoints. This is at odds with the other data from dead parasite implants, and a repeat of the day 7 and 20 timepoints with dead parasite implantation is needed to confirm these results.

5.3.4. Summary of Intraperitoneal adult *B. malayi* Treg induction

Overall, the data from the adult implant model closely reflects that of the L3 infection model, indicating the same mechanism may be acting here.

In both models a transient activated Treg induction is seen ($CD103^+Foxp3^+CD4^+$) with a concurrent suppression of CD25 and induction of CTLA-4 on the $CD4^+Foxp3^-$ cells. The parasite must be alive in order to induce Tregs, indicating active processes, and we may infer that these may include the release of immunomodulatory molecules, such as TGF-β homologues.

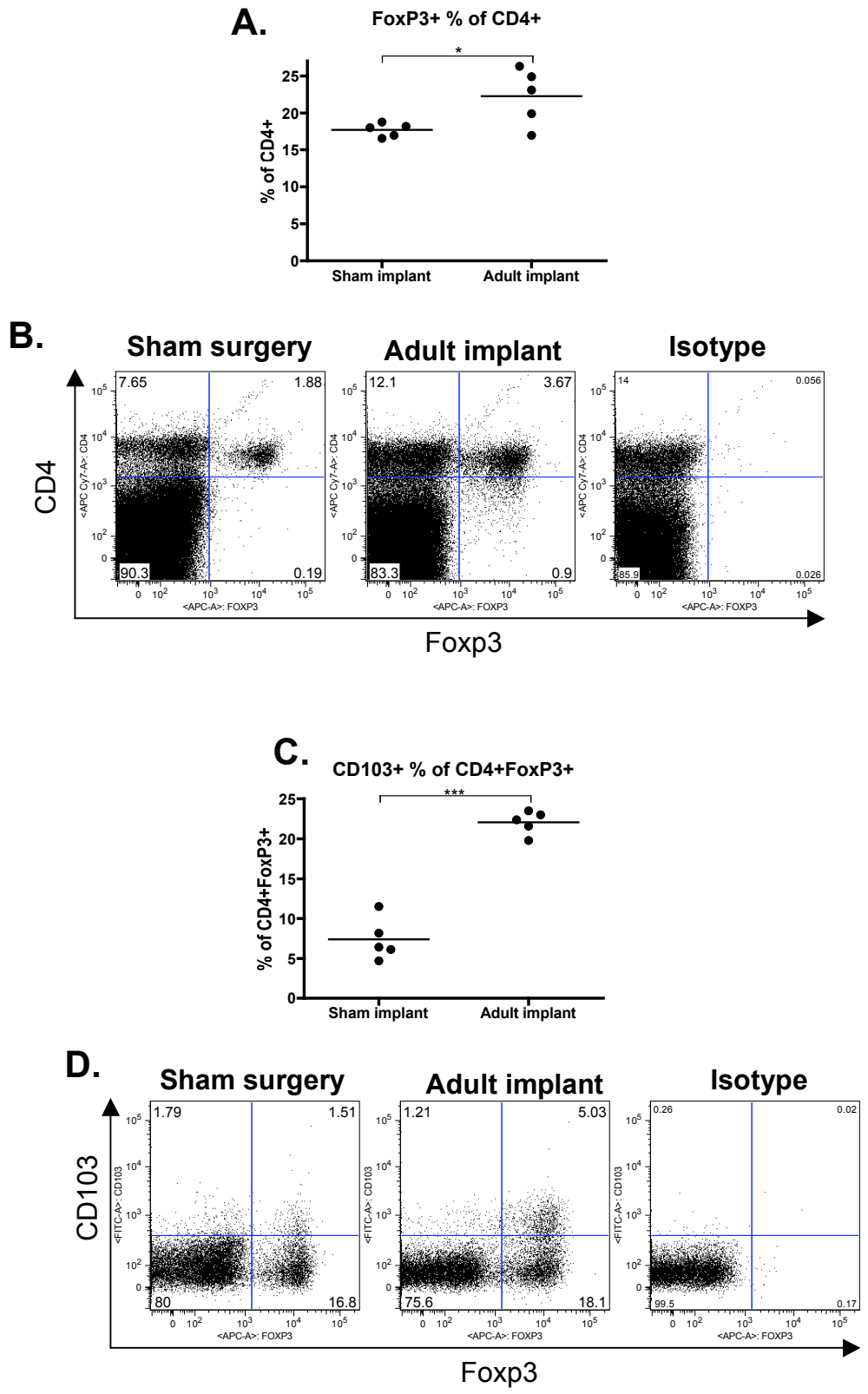

Figure 5.11: Treg markers in the PL 7 days after *B. malayi* adult implant
Peritoneal lavage samples were taken from BALB/c males 7 days after implantation of adult *B. malayi* or sham surgery controls, then analysed by flow cytometry for expression of Treg markers. (A) shows $Foxp3^+$ % in CD4 population, (B) shows representative plots of CD4 vs Foxp3 (gated on lymphocytes by FSC and SSC). (C) Shows CD103 in the $CD4^+Foxp3^+$ population, (D) shows representative plots of Foxp3 vs CD103 (gated on $CD4^+$ cells). A representative experiment of 3 repeats is shown here.. *** = P<0.001, ** = P<0.01, N.S. = Non-Significant.

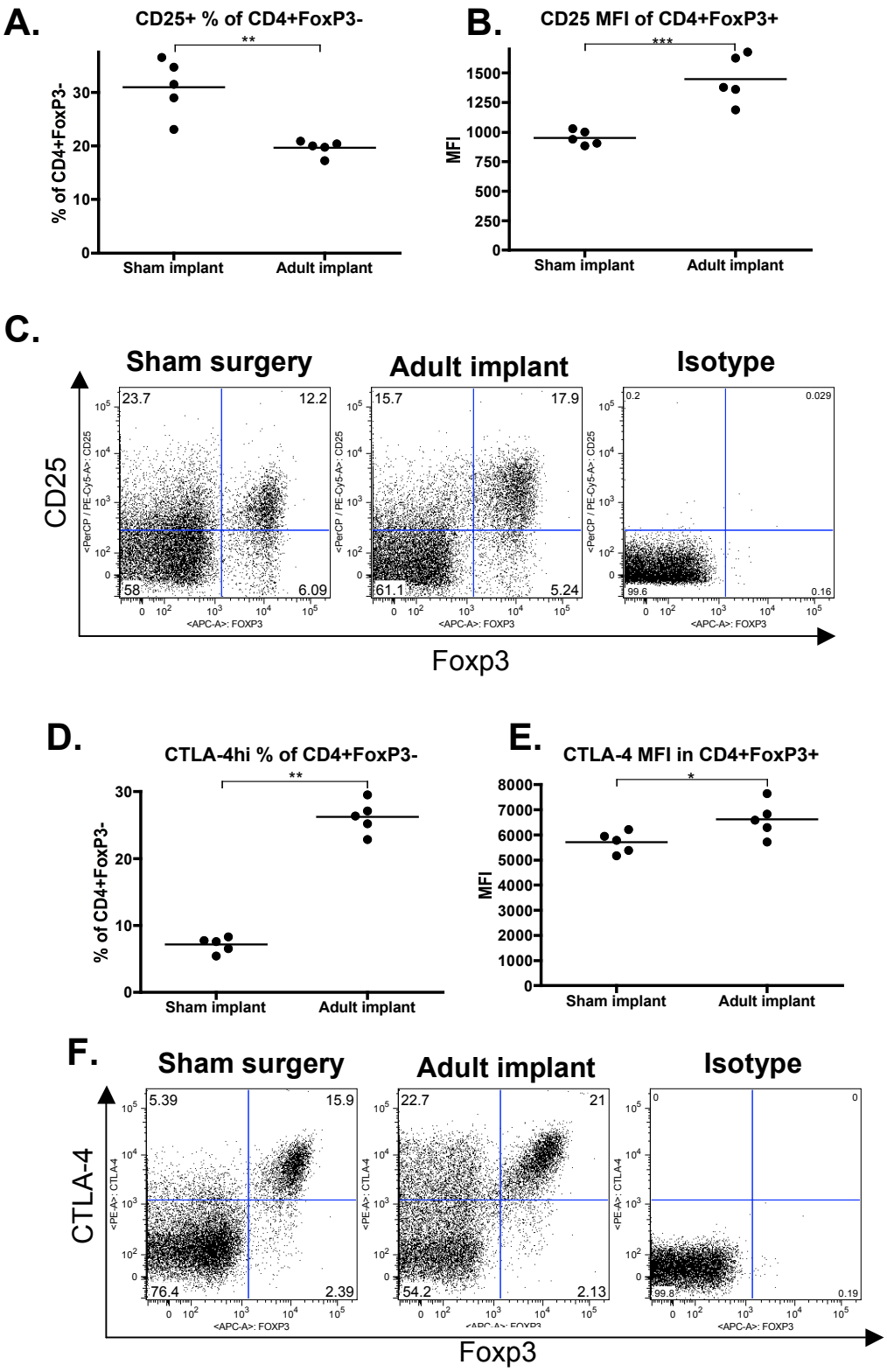

Figure 5.12: Treg markers in the PL 7 days after *B. malayi* adult implant
Peritoneal lavage samples were taken from BALB/c males 7 days after implantation of adult *B. malayi* or sham surgery controls, then analysed by flow cytometry for expression of Treg markers. (A) shows $CD25^+$ % in $Foxp3^-$ population, (B) shows CD25 MFI in the $CD4^+Foxp3^+$ population, and (C) shows representative plots of Foxp3 vs CD25 (gated on $CD4^+$ cells). (D) shows CTLA-4^{hi} in $CD4^+Foxp3^-$, (E) shows CTLA-4 MFI in the $CD4^+Foxp3^+$ population, and (F) shows representative plots of CTLA-4 vs Foxp3 (gated on $CD4^+$ cells). A representative experiment of 3 repeats is shown here. *** = P<0.001, ** = P<0.01, N.S. = Non-Significant.

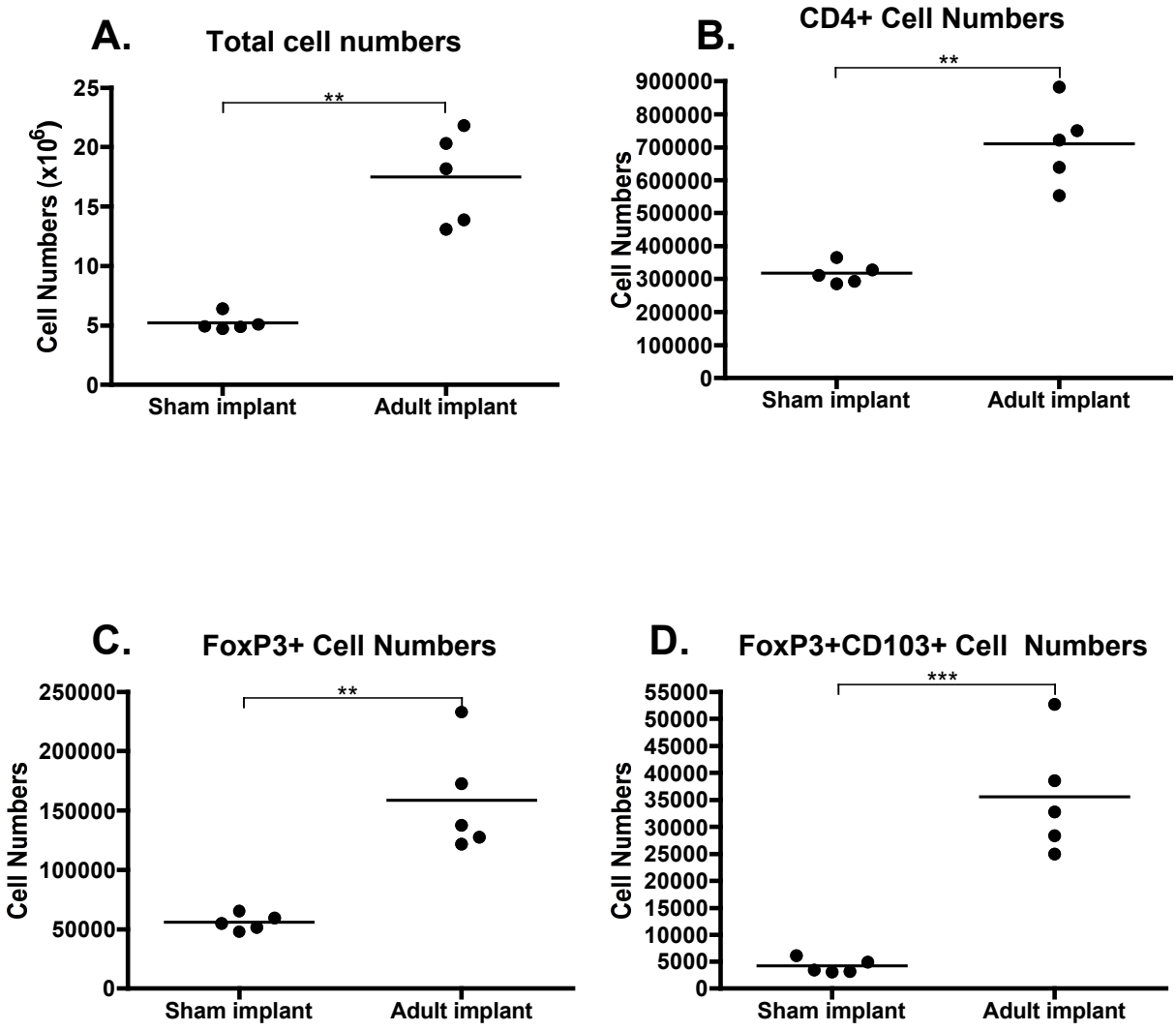

Figure 5.13: Treg numbers in the PL 7 days after *B. malayi* adult implant
Peritoneal lavage samples were taken from BALB/c males 7 days after adult *B. malayi* implant or sham surgery controls, then analysed by flow cytometry for expression of CD4, Foxp3 and CD103. Graphs show total PL cell numbers (A), $CD4^+$ cell numbers (B), $CD4^+Foxp3^+$ cell numbers (C) and $CD4^+Foxp3^+CD103^+$ cell numbers (D). Shown is a representative experiment of 3 repeats. * = P<0.05, ** = P<0.01, *** = P<0.001 (1-way ANOVA)

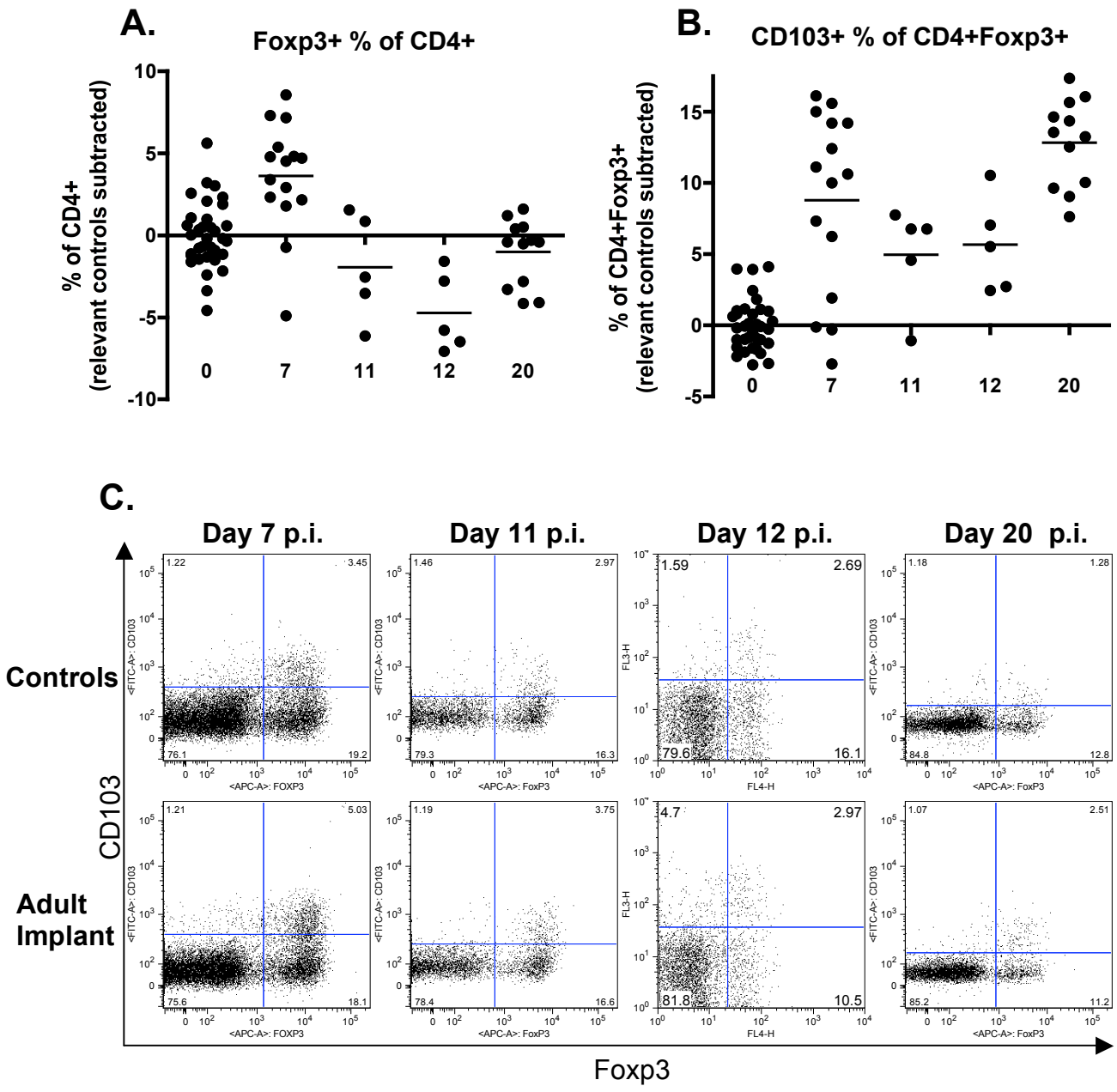

Figure 5.14: Timecourse of Treg markers in the PL after *B. malayi* adult implant
Peritoneal lavage samples were taken from BALB/c males at 7, 11, 12 and 20 days after implantation with adult *B. malayi* or control mice, then analysed by flow cytometry for expression of CD4, Foxp3, and CD103. At D7 and D12 timepoints controls are sham surgery, on D11 and D20 timepoints controls are naïve mice. (A) shows $Foxp3^+$ % of $CD4^+$ and (B) shows $CD103^+$ % of $CD4^+Foxp3^+$, timecourses are pooled results from 3 experiments for the day 7 timepoint, single experiments for days 11 and 12 and 2 experiments at day 20. (C) shows bivariate plots of CD103 vs Foxp3 of median samples from representative experiments, and are gated on $CD4^+$ lymphocytes.

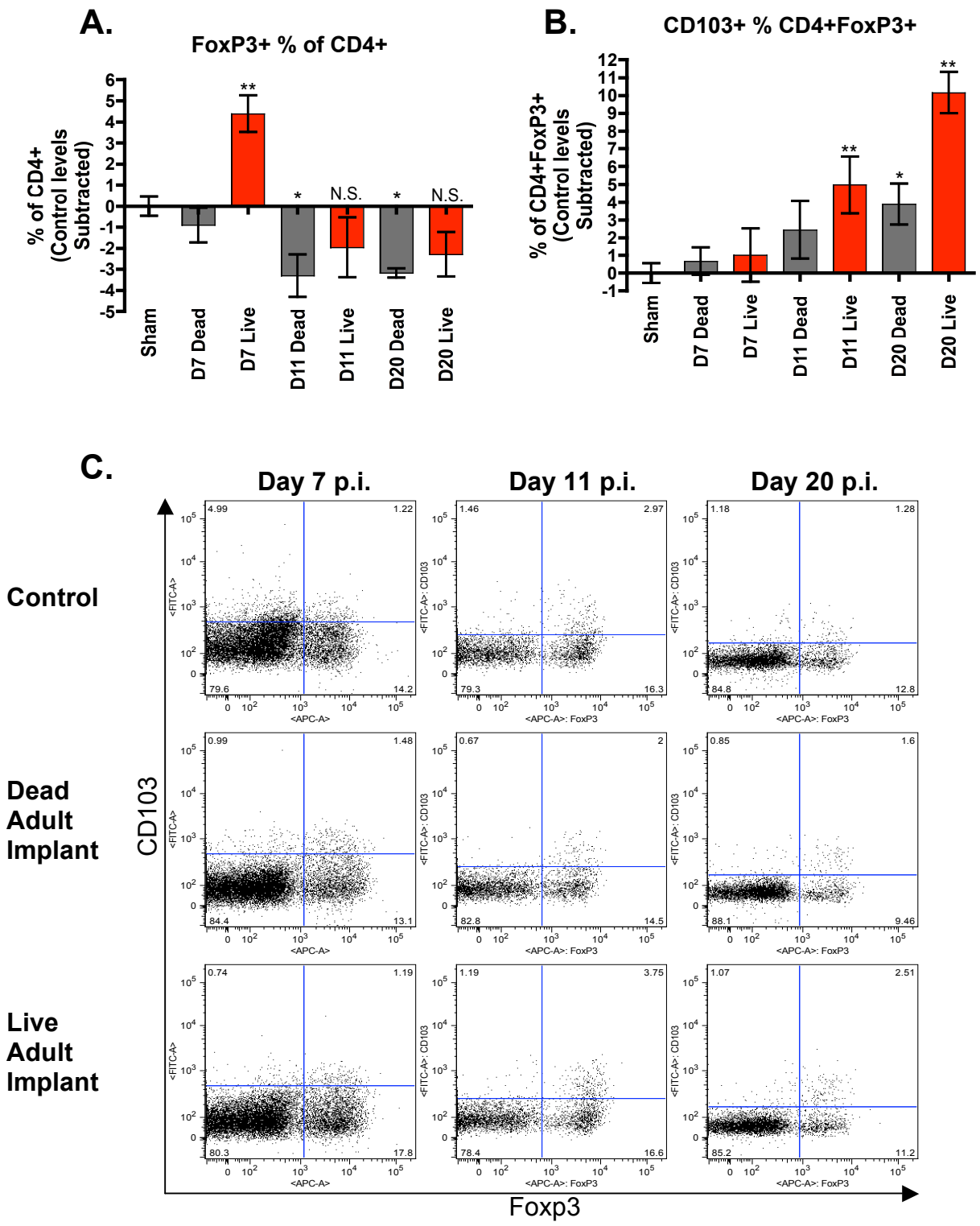

Figure 5.15: Timecourse of Treg markers after live or dead *B. malayi* implant
Peritoneal lavage samples were taken from BALB/c males at 7, 11, and 20 days after implantation with live or dead (freeze-thawed) adult *B. malayi* or controls of sham surgery, then analysed by flow cytometry for expression of CD4, Foxp3, and CD103. (A) shows $Foxp3^+$ % of $CD4^+$ cells and (B) shows $CD103^+$ % of $CD4^+Foxp3^+$ cells, shown are single experiments for each timepoint. (C) shows representative Foxp3 vs CD103 bivariate plots of each timepoint, gated on $CD4^+$ lymphocytes. * = P<0.05, ** = P<0.01, N.S.=Non-Significant.

5.4. Strain difference in tolerance of *B. malayi*

BALB/c mice tolerate *B. malayi* L3s longer than C57BL/6 mice (194), and male mice are more tolerant than females (213). To investigate whether these differences in susceptibility are due to differences in Treg induction, female C57BL/6 (least tolerant) and male BALB/c (most tolerant) mice were infected with L3 or adult *B. malayi* as in previous experiments.

In L3 infection, $Foxp3^+$ proportion of the $CD4^+$ population increased in both strains at day 7 post-infection (Figure 5.16A), but no increase was seen in C57BL/6 female mice at day 12 post-infection (Figure 5.16C), as opposed to BALB/c males at the same timepoint (Figure 5.16B). However, when the day 12 timepoint was repeated with C57BL/6 males, a similar increase in proportions $Foxp3^+$ cells within the $CD4^+$ population was seen.

In adult implant experiments, a significant increase in $Foxp3^+$ proportion of the $CD4^+$ population was seen in BALB/c males, but not in C57BL/6 females, at day 7 post-implantation (Figure 5.17A). When this experiment was repeated using C57BL/6 males, a trend for an increase in $Foxp3^+$ proportions of the $CD4^+$ population was seen in both BALB/c males and C57BL/6 males after implant (Figure 5.17B).

These results, although inconclusive, may indicate a spectrum of susceptibility to *B. malayi* that is reflected in Treg induction. BALB/c males are most susceptible to infection, and also have the most sustained Treg induction. C57BL/6 females are least susceptible, and have the least sustained Treg induction. In between these extremes are the C57BL/6 males (which in Figure 5.16A appear to have lower Treg induction than BALB/c males), and, we may hypothesise, the BALB/c females.

To investigate this further, infections of all the strains and sexes could be carried out. L3 larvae and microfilaria in the peritoneal lavage were not counted in the experiments shown here, and this data should be collected on repeats of these experiments.

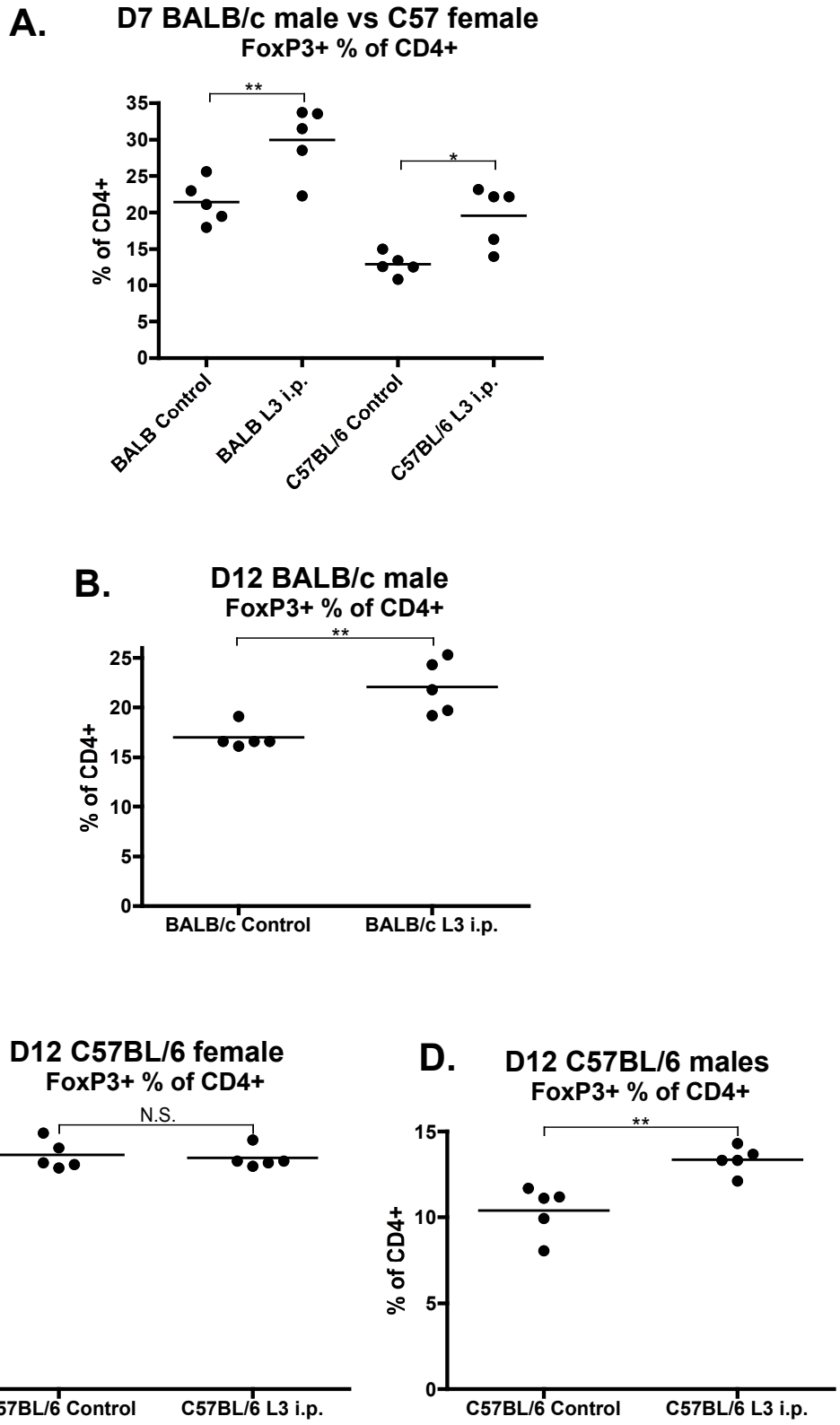

Figure 5.16: Tregs in PL after L3 *B. malayi* infection of BALB/c or C57BL/6 mice. Peritoneal lavage samples were taken after injection with L3 *B.malayi* or controls of media i.p., then analysed by flow cytometry for expression of CD4 and Foxp3. The graphs show Foxp3 proportions of the $CD4^+$ population in BALB/c males and C57 females 7 days after infection (A), BALB/c males 12 days after infection (B), C57BL/6 females 12 days after infection (C) and C57BL/6 males 12 days after infection (D) * = P<0.05, ** = P<0.01, N.S.=Non-Significant.

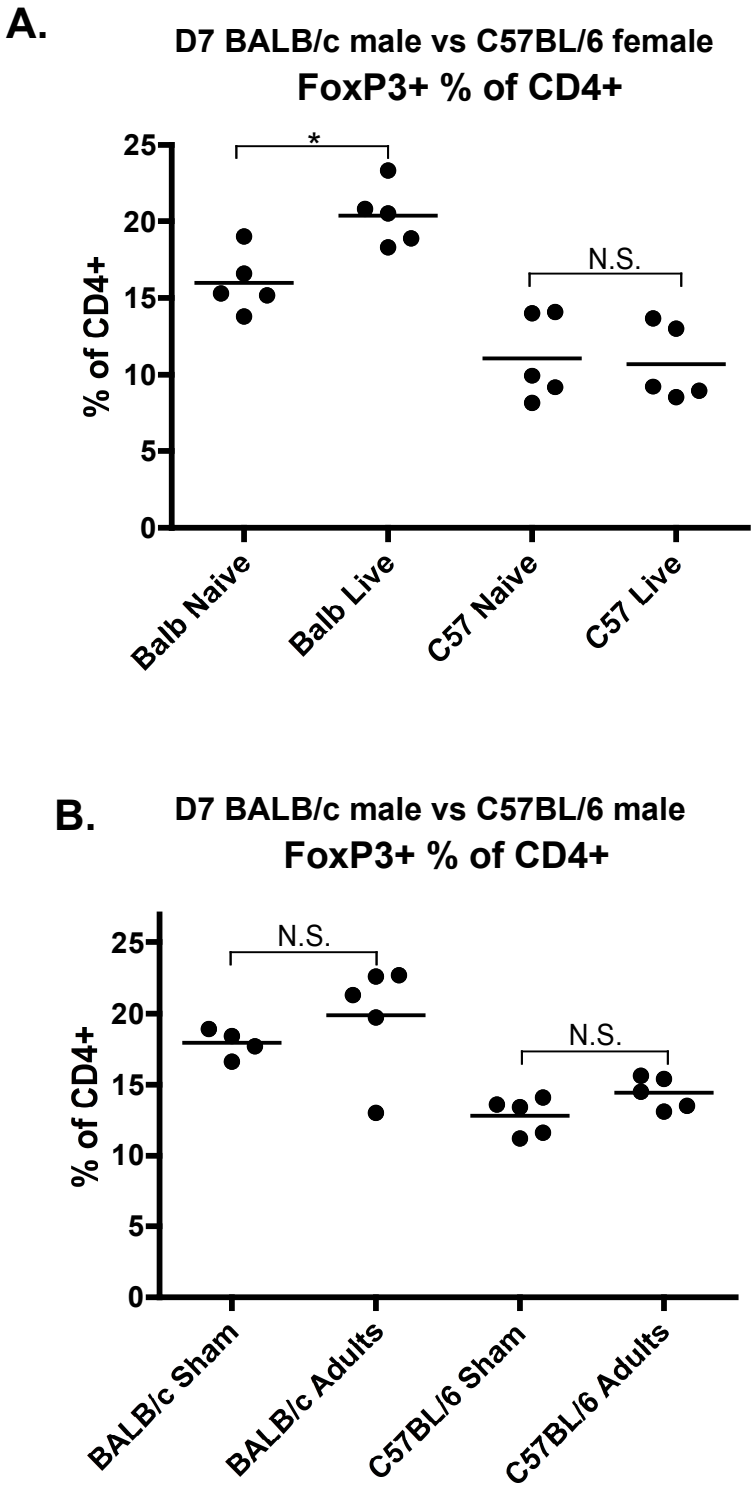

Figure 5.17: Tregs in PL after *B. malayi* adult implant in BALB/c or C57BL/6 mice. Peritoneal lavage samples were taken after implantation with *B. malayi* or controls as indicated, and analysed by flow cytometry for expression of CD4 and Foxp3. Graphs show $FoxP3^+$ proportions of the $CD4^+$ population 7 days after implantation of BALB/c males or C57BL/6 females (with naïve controls) (A) or BALB/c males and C57BL/6 males (with sham surgery controls) (B). * = $P<0.05$, N.S.=Non-Significant.

5.5. Proliferation history of peritoneal lavage Tregs

The increased percentage of Foxp3$^+$ Tregs within the CD4$^+$ peritoneal cavity population could be due to recruitment or expansion of existing Foxp3$^+$ Tregs, or induction of Foxp3 in Foxp3$^-$ naïve T cells. BrdU incorporation was used to investigate whether the Foxp3$^+$ cells in the peritoneal cavity had proliferated to a greater degree than those in naive animals. BrdU was administered by injection 24 hours before the animals were culled, to show within a defined period of time whether the Tregs or Teffectors were proliferating to a greater extent, at day 3, 6 and 7 post-infection timepoints. The levels of BrdU incorporation in the PL Foxp3$^+$ population were not significantly higher than controls in infected animals (Figure 5.18C), however neither were they higher in the Foxp3$^-$ population, except on day 6 (Figure 5.18B). This is surprising as during a productive immune response the effector cells proliferate to cognate antigen, and at the effector site it would be expected than the majority of effector cells were proliferating.

Although this data is inconclusive, it suggests the Foxp3$^+$ cells in the peritoneum have not proliferated to a greater extent than in the steady state, and therefore may either have been recruited from the existing Foxp3$^+$ natural Treg pool, or may have upregulated Foxp3 without proliferation.

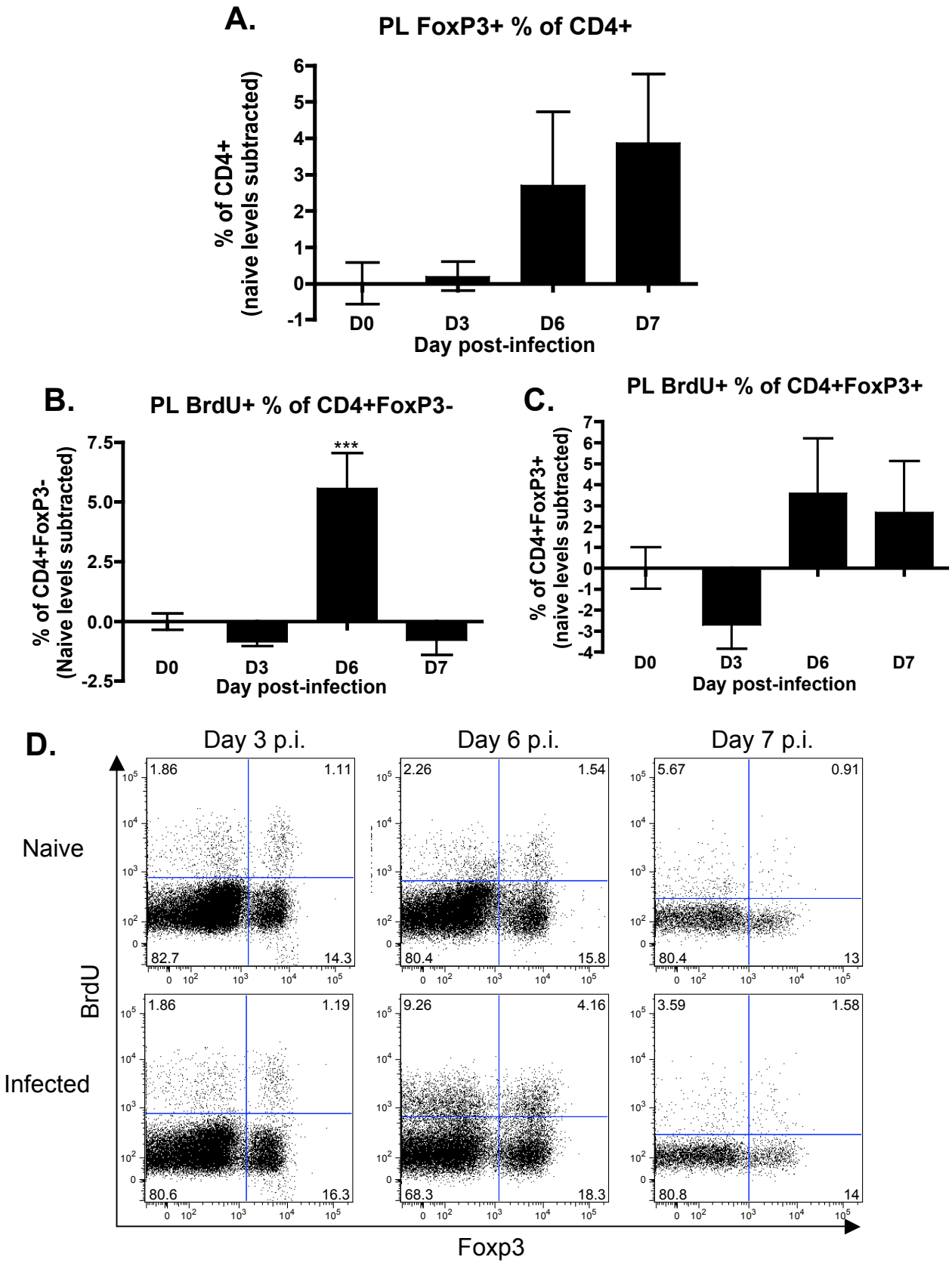

Figure 5.18: Proliferation history of PL T cells after L3 *B. malayi* infection
Peritoneal lavage samples were taken from BALB/c mice after infection with L3 *B. malayi*, with 1 mg BrdU injected i.p. 24 hours before culling. Samples were then analysed by flow cytometry for levels of BrdU, CD4 and Foxp3. Graphs show $Foxp3^+$ proportions of $CD4^+$ population (A), $BrdU^+$ proportion of $CD4^+Foxp3^-$ population (B) and $BrdU^+$ proportion of $CD4^+FoxP3^+$ population (C), with naïve control levels (from relevant timepoint) subtracted. Bivariate plots show representative samples from each timepoint, gated on CD4+ lymphocytes (D). *** = P<0.001

5.6. Suppressive capacity of peritoneal lavage Tregs

The functional suppressiveness of the recruited Tregs was then tested, using a suppression assay. $CD4^+CD25^+$ and $CD4^+CD25^-$ cells were sorted from the peritoneal lavage of infected BALB/c and a naïve spleen, by first positively purifying by MACS for $CD4^+$ cells, then FACS sorting for $CD4^+CD25^+$ cells and $CD4^+CD25^-$ cells. The spleen separations had higher purity of $Foxp3^+$ in the $CD4^+CD25^+$ and $Foxp3^-$ in the $CD4^+CD25^-$ than peritoneal lavage samples (see Figure 5.19) for a number of reasons. Firstly, the peritoneal lavage samples contain large numbers of activated cells, which are $CD25^+$ and $Foxp3^-$, and so would be purified in the $CD25^+$ population, reducing the proportion of $Foxp3^+$ cells here. Also, the $CD25^+$ staining in the peritoneal lavage was consistently weaker than in the spleen in all experiments, and so not all the $Foxp3^+$ cells would be separated out by the $CD25^+$ gate, resulting in some contamination of the $CD25^-$ population with $Foxp3^+$ cells.

$CD4^+CD25^-$ cells were then stained with CFSE and mixed at a 1:1 ratio with $CD4^+CD25^+$ cells in the presence of suboptimal levels of anti-CD3. After 4 days of restimulation, cells were analysed by flow cytometry and CFSE dilution used to gate each division. As can be seen in Figure 5.20, *B. malayi*-induced Tregs are equally as suppressive of splenic Teffectors as naïve splenic Tregs, but they appear to be slightly less suppressive than splenic Tregs when cultured with PL Teffectors.

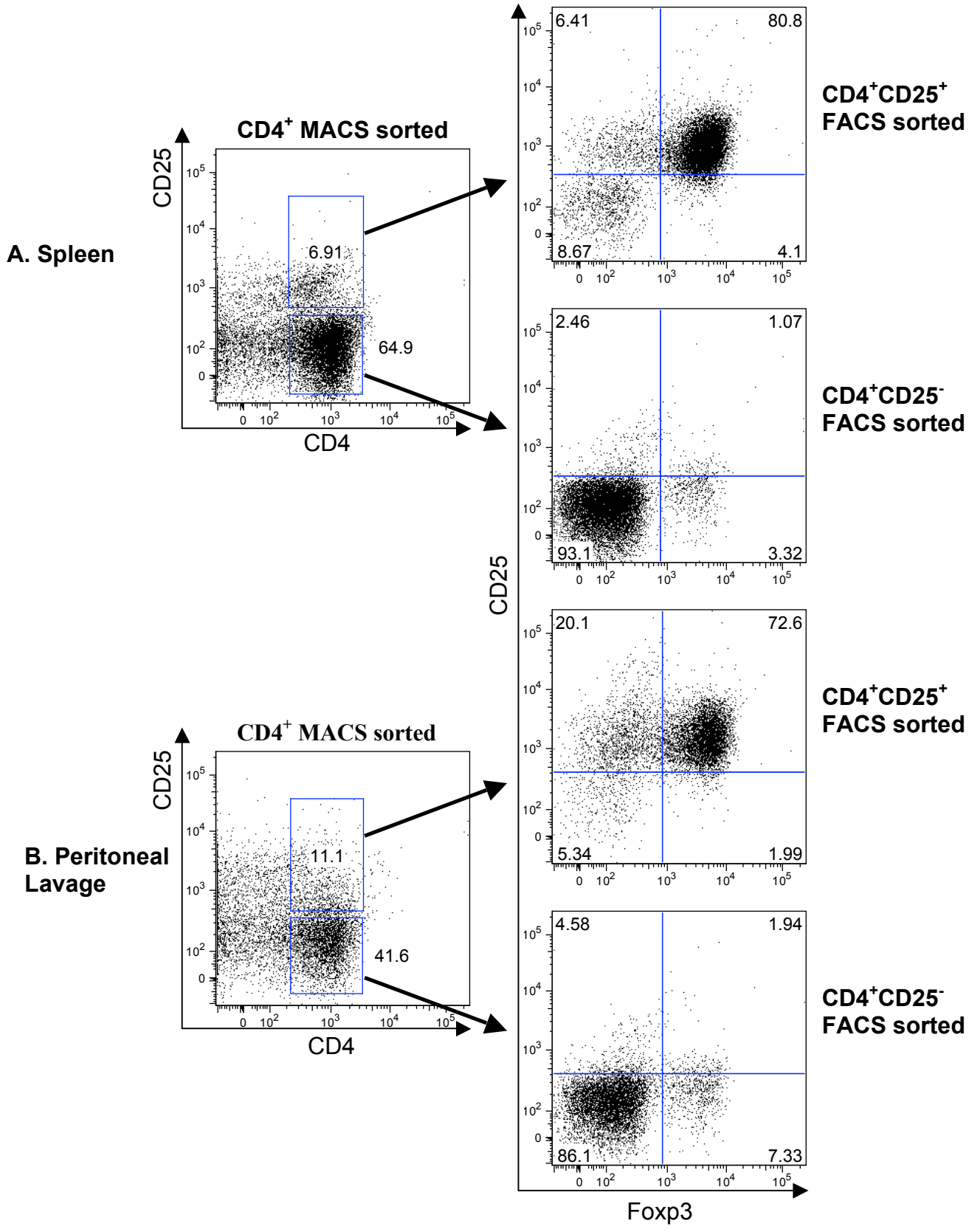

Figure 5.19: Separation of spleen and PL $CD4^+CD25^+$ and $CD4^+CD25^-$ cells
Naïve spleen cells (A) and peritoneal lavage samples (day 7 after *B. malayi* L3 infection, 15 mice pooled) (B) were positively selected for $CD4^+$ cells by MACS ($CD4^+$ cell plots), and sorted by FACS for $CD4^+CD25^+$ and $CD4^+CD25^-$ cells. Shown are bivariate plots gated on live cells (by FSC/SSC profile).

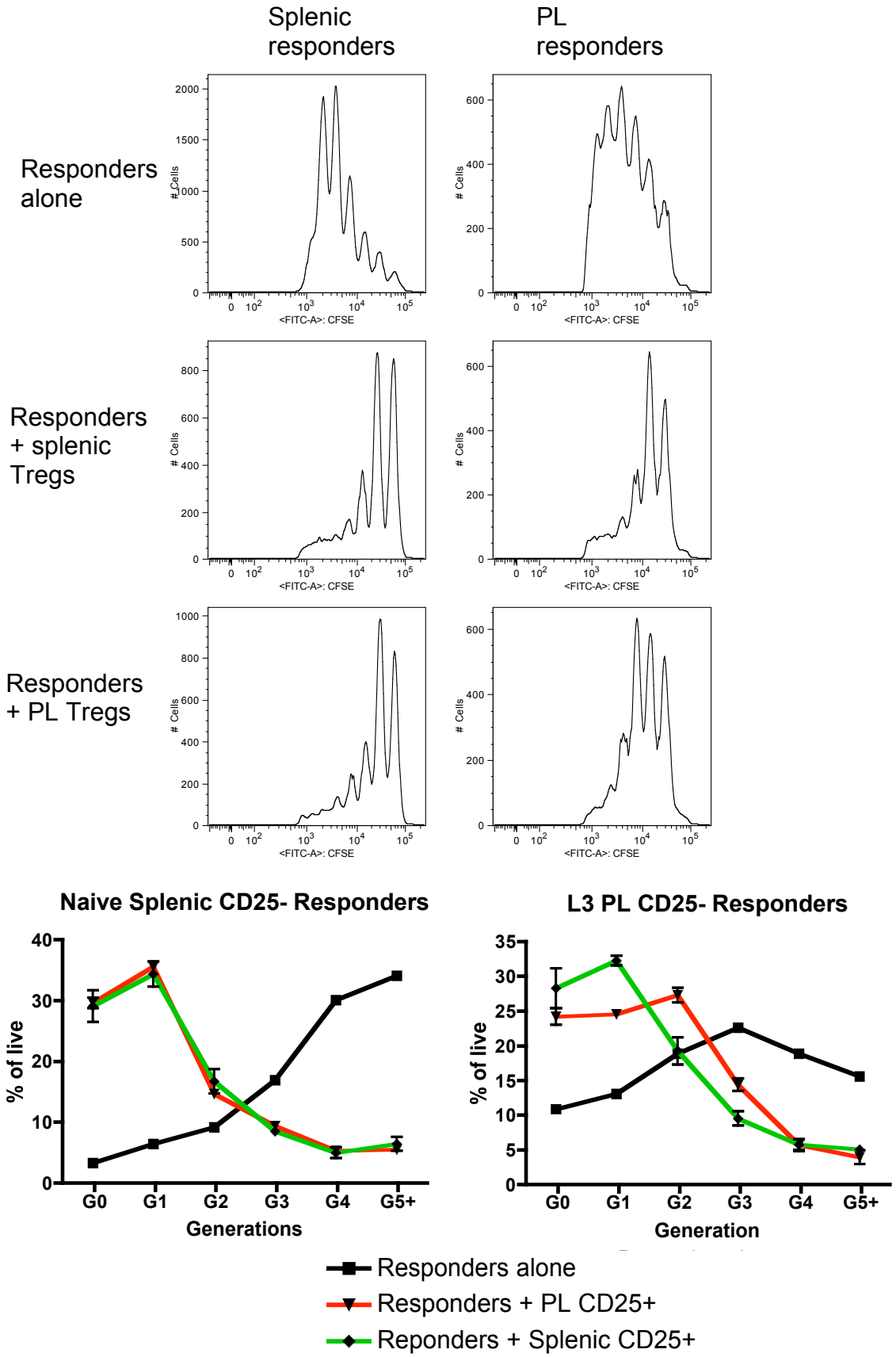

Figure 5.20: Suppression assay of splenic or PL Tregs
Lymphocytes were isolated from either a naïve BALB/c spleen or a pool of 15 live day 7 L3 *B. malayi* infected peritoneal lavages, then separated into $CD4^+CD25^+$ or $CD4^+CD25^-$ by MACS and FACS sorting. $CD4^+CD25^-$ cells were CFSE stained and stimulated with anti-CD3 for 4 days in presence or absence of $CD4^+CD25^+$ cells as indicated. Graphs show percentage of cells in each division based on CFSE dilution. FACS plots show CFSE staining on $CD4^+$ live cells, based on intermediate DAPI staining. Error bars indicate SEM of duplicate wells, where available.

5.7. Discussion

The data presented here support the hypothesis that helminth parasites amplify the host regulatory T cell network, postulated to be a key factor in the ability of parasites to evade host immunity (214, 215). I began by building on the results of Gillan *et al*, that s.c. infection with L3 *B. malayi* induces a Treg response in the spleen (159). My results indicate that if this population is detectable *ex vivo*, it is diluted in the spleen, a large lymphoid organ. Therefore, I moved on to a model where the T cell population recruited to the site of infection could be examined, in the peritoneal cavity.

Both the initial invasive stage (the L3 larvae), and the long-lived adult parasite elicit a significant expansion in Treg numbers, and stimulate upregulation of the activation-associated markers CD25, CTLA-4 and CD103. Enhancement of the regulatory population has also been observed in several other helminth infections, including the rodent filaria *L. sigmodontis* (160), the gastrointestinal nematode *H. polygyrus* (21, 216), and the trematode parasite of man, *S. mansoni* (217, 218). It is likely that an immunological challenge of any nature will induce some element of Treg activity, as a homeostatic guard against inappropriate responsiveness; however, in these infections I document a preferential expansion of the regulatory phenotype. Interestingly, the relative proportions of regulatory and effector cells may change over the course of infection (21, 164, 218, 219), perhaps allowing the responder population in due course to overcome regulation and eliminate the parasites.

Beyond numbers alone, however, both regulatory and non-regulatory populations show important qualitative differences in phenotype. The data presented in this chapter shows that Tregs following *B. malayi* infection show increased levels

of CD103, a marker associated with stronger suppressive activity (220), and retention of Treg at the site of infection (120). The data also indicate significant upregulation of CD25 and CTLA-4 on the $Foxp3^+$ population, and as these are variously described as either transient activation markers or regulatory T cell markers, this also indicates these Tregs may be activated. In addition, the nonregulatory ($Foxp3^-$) population also show higher CTLA-4 expression, as indeed observed in both *H. polygyrus* (21) and *L. sigmodontis* (160) infections. In the latter case anti-CTLA-4 treatment, in conjunction with anti-CD25 antibody, abrogates suppression and enhances parasite killing (221). It is notable that a very similar profile has been observed in human filarial infections, in which CTLA-4 expression is elevated on the peripheral T cell population, and anti-CTLA-4 antibody treatment uplifts cytokine responsiveness of T cells from filarial patients (45, 158). CTLA-4 expression on $CD4^+Foxp3^-$ T cells has also been shown to be necessary for Treg induction through the TGF-β pathway (127), and so a further possibility is that $CD4^+CTLA\text{-}4^+Foxp3^-$ T cells may be primed for Foxp3 induction later in the course of infection.

The fact that only live parasites can induce Foxp3 within the CD4 population is consistent with both field and laboratory data linking active infection to immune regulation. For example, in human studies, T cell responsiveness is regained after drug-induced parasite killing (38). Moreover, live L3 larvae have been shown to directly inhibit cytokine production by human lymphocytes *in vitro* (45). These results imply that immunomodulatory products of viable parasites are released within the infected host, possibly implicating Bm-TGH-2 in this process.

The proliferation history of the PL Tregs was assessed by BrdU staining. These data may indicate that Tregs at the site of infection are not proliferating at increased levels to naïve animals, despite their increased proportions at the site of infection. A possible explanation for this is that the Tregs have not proliferated in order to increase their numbers, but instead have been recruited from elsewhere in the host. If the Tregs in this model could be shown to be antigen specific, and to proliferate to antigen *in vitro* (such as in the *Leishamania major* model (155)) this would argue against a recruitment of natural Tregs, and instead argue for an antigen-specific induction. This experiment was also only carried out once, with variable BrdU staining (see Figure 5.18D), so should be repeated to confirm these results.

The Treg suppression assay results presented here show that the $Foxp3^+$ population is functional, and can suppress polyclonal responses *in vitro*. When compared to conventional naïve natural Tregs from the spleen, the levels of suppression seen were indistinguishable. This was surprising, as an increase in suppressive activity was hypothesised due to the activated/effector phenotype of the Tregs that accumulated in the PL ($CD4^+CD25^{hi}$CTLA-$4^{hi}CD103^+$). $CD103^+$ Tregs in particular are highly suppressive in some models (135). In *Heligmosomoides polygyrus* infection, Tregs in the draining mesenteric lymph node have higher per-cell suppressive ability than those in naïve animals (222), and these Tregs show a similar increase in CD103 expression to that seen in the *B. malayi* model. However, increased suppressive capacity seen in *H. polygyrus* infection was seen at later timepoints (day 28 after infection, when the infection has become patent) than those used here. Similarly to our data, increases in proportions of Treg markers within the $CD4^+$ population were only associated with early timepoints. Therefore it may be

that increased suppressive capacity is associated with patency, once proportions of Tregs have fallen to control levels. This model suggests a two-step process of Treg control of anti-parasite immune responses, where at early timepoints Tregs expand more quickly than the effector population, but retain normal levels of suppressive ability, followed at later timepoints by further activation and enhancement of suppressive ability of the Treg population without further expansion.

Thus, at early timepoints effector responses could be controlled by increased Treg to Teffector ratios, whilst at later timepoints the ratio would return to normal, but the Tregs could more potently suppress at a per-cell level. This could reflect the situation in Teffector responses which first expand rapidly to cognate antigen as TH0 cells, followed by commitment to a TH1 or TH2 pathway to best control an infection. Further experiments need to be carried out to test this hypothesis in the *B. malayi* infection model, including Treg suppression assays over a timecourse after infection, and identification of factors inducing the expansion and activation of Tregs. To repeat these experiments, the Foxp3-GFP mouse would be useful, as this enables FACS-sorting of Tregs by Foxp3 rather than the less reliable marker of CD25 used here. Due to the fact that the PL population contains $CD4^+Foxp3^-CD25^+$ effector cells, the $CD4^+CD25^+$ population contained a smaller proportion of $Foxp3^+$ cells than the naïve splenocyte $CD4^+CD25^+$ population, in which the only $CD25^+$ cells are Tregs.

In conclusion, the results presented here indicate that in a mouse model filarial parasites expand the frequency and activity of Foxp3-expressing T cells at the site of infection, and that these cells have functional *in vitro* suppressive capacity indicative of regulatory T cells. As the mouse is not fully susceptible to the parasite,

this result suggests that an initial immune subversion mechanism is accompanied by an effector cell response which can eventually outpace regulation and kill the filariae. If a similar dynamic relationship exists in human infections, with regulatory and effector mechanisms in contention, this may help explain the spectrum of immunological and pathological outcomes that ensue in filariasis. Furthermore, by understanding the factors which promote or impede regulatory mechanisms in helminth infection, intervention can aim to reverse this activity and generate an immunological cure for disease.

Chapter 6: Mechanism of Treg accumulation at the site of *B. malayi* infection

6. Mechanism of Treg accumulation at the site of *B. malayi* infection

6.1. Adoptive transfer model

6.1.1. *B. malayi* adult implants induce Foxp3 in a bystander response

As shown in chapter 5, *B. malayi* induces a Treg response at the effector site. To investigate the antigen specificity of the Tregs induced, adoptive transfer experiments were carried out, inducing a response to an irrelevant antigen in the context of an infection. DO11.10 splenocytes were transferred into naïve BALB/c males, which were then infected with *B. malayi*, followed by transfer of OVA peptide-loaded LPS-stimulated BMDCs.

In order to show that *B. malayi* antigens do not crossreact with the OVA-specific DO11.10 TcR, DO11.10s were transferred into BALB/c's with or without infection and with or without DC transfer (Figure 6.1). In both the spleen and the PL, the DO11.10 population did not expand in the absence of pOVA-loaded DC transfer, indicating *B. malayi* antigens do not cross-react with the DO11.10 TcR (Figure 6.1A and B). Adult *B. malayi* implant did not affect the expansion of DO11.10s to OVA peptide stimulation, as similar proportions of DO11.10 cells were present in controls or live implant (Figure 6.1A and B). However, within the DO11.10 population live *B. malayi* implant induced a higher proportion of $Foxp3^+$ cells (Figure 6.1C), suggesting the Treg induction by *B. malayi* can also affect bystander responses to irrelevant antigens.

6.1.2. Adult implant-induced TH2 switch in bystander effector response

Splenocytes from this experiment were restimulated with pOVA, and supernatants taken for the TH2 cytokines IL-4, IL-5 and IL-10 ELISA (Figure 6.2).

Implantation of live or dead parasites induced trends for increases in these cytokines, which reached significance in the IL-4 ELISA (Figure 6.2A). This suggests the DO11.10 response may have been skewed towards a TH2 response.

6.1.3. *B. malayi* L3 infection induces Foxp3 in a bystander response

The adoptive transfer experiment described in section 6.1.1 was repeated using *B. malayi* L3 larvae (Figure 6.3). A similar result as in the adult implant was obtained: the presence of live parasites led to a higher proportion of $Foxp3^+$ cells within the DO11.10 population in 2 repeat experiments (Figure 6.3B and D), with no difference in proportions of DO11.10 cells with *B. malayi* infection (Figure 6.3A and C).

6.1.4. L3 infection-induced TH2 switch in bystander effector response

In the second L3 adoptive transfer experiment, splenocytes were restimulated with pOVA and supernatants tested for the presence of IL-4, IL-10 and IFN-γ by cytokine ELISA (Figure 6.4). Although no significant differences were seen between groups, a trend for an increase was seen in IL-4 levels with the presence of live parasites (Figure 6.4A), and a trend for a decrease in IFN-γ levels (Figure 6.4C) was seen in the presence of live or dead parasites, again arguing for a switch to a TH2 response in the bystander DO11.10 response.

The peritoneal lavage cells in the second L3 adoptive transfer experiment were also stained for intracellular IL-4 and IFN-γ *ex vivo*, but no differences were seen between groups (Figure 6.5). The intracellular cytokine staining did not corroborate the switch to TH2 suggested by the splenocyte restimulation ELISA

data. This may be due to the PMA/Ionomycin stimulus used in the intracellular cytokine staining protocol, which is a very strong stimulus, and so could overcome the TH1/TH2 balance seen *in vivo*. This may also explain the large proportions of IL-4^{+}IFN-γ^{+} double positive cells (Figure 6.5C).

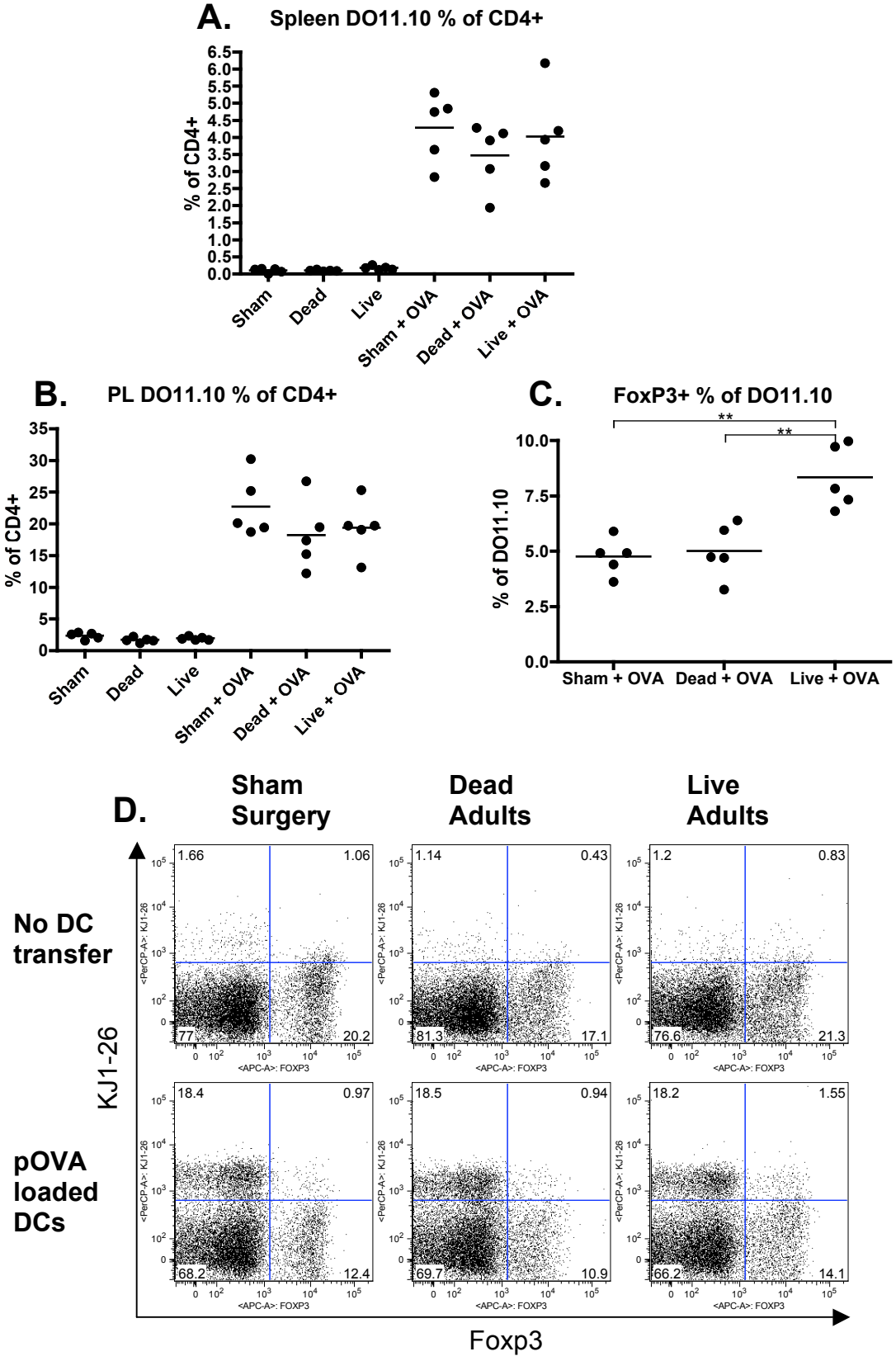

Figure 6.1: Foxp3 staining in adoptively transferred DO11.10 cells after *B. malayi* adult implant
5x10^6 DO11.10 splenocytes were injected i.p. in BALB/c males and 1 day later were implanted with live or dead adult *B. malayi*, or controls of sham surgery. A further day after implantation 3 groups were injected i.p. with 5x10^5 pOVA-loaded, mature DCs. At day 7 post-implantation, PL and spleens were taken and analysed by flow cytometry for expression of CD4, Foxp3 and KJ1-26 (DO11.10 TcR). Graphs show DO11.10 % within the CD4+ population in the spleen (A) and PL (B), and Foxp3$^+$ % of the PL CD4$^+$ population (C). Bivariate plots of Foxp3 against KJ1-26 (gated on CD4$^+$ cells) in (D) show representative samples of stained PL cells from each group. ** = P<0.01.

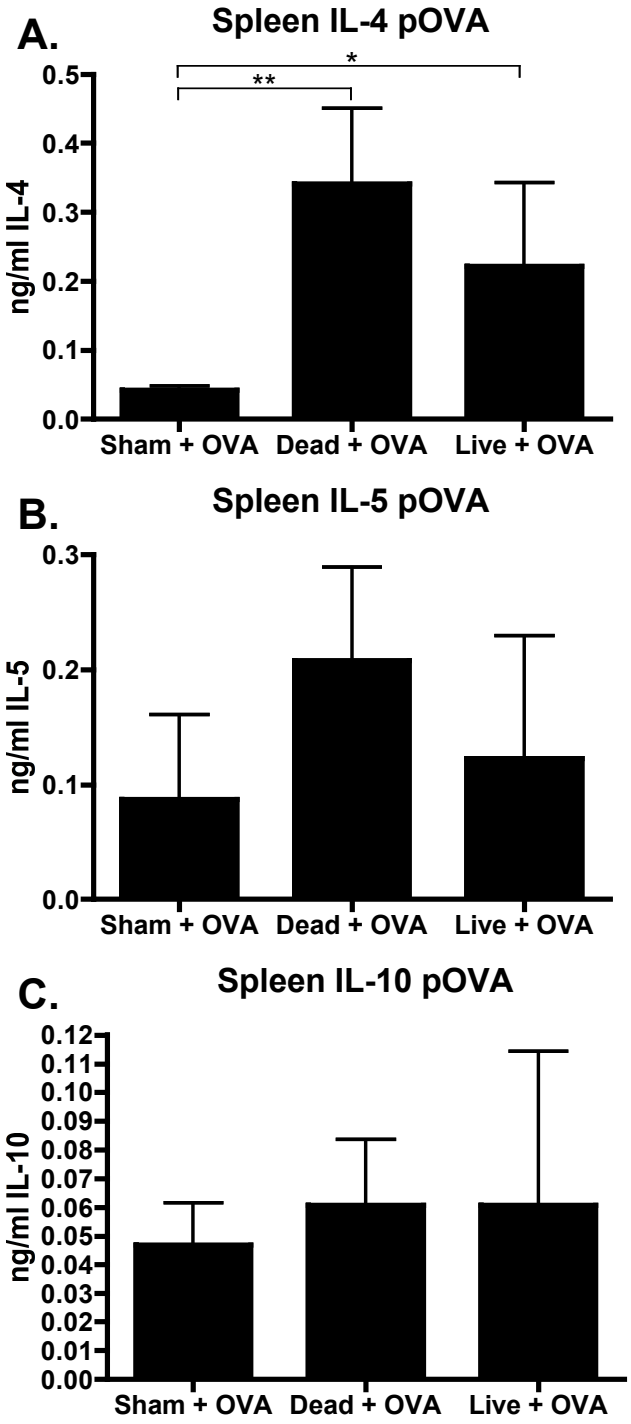

Figure 6.2: Splenocytes from D011.10 adoptive transfer produce increased IL-4 in the presence of adult implant

$5x10^6$ DO11.10 splenocytes were injected i.p. in BALB/c males and 1 day later were implanted with live or dead adult *B. malayi*, or controls of sham surgery. A further day after implantation 3 groups were injected i.p. with $5x10^5$ pOVA-loaded, mature DCs. Seven days after infection, splenocytes from these mice were prepared and stimulated with 1 μg/ml pOVA for 72 h, then supernatants taken and tested by ELISA for IL-4 (A), IL-5 (B) and IL-10 (C). Levels shown have unstimulated levels subtracted from stimulated levels for each sample. ** = $P<0.01$

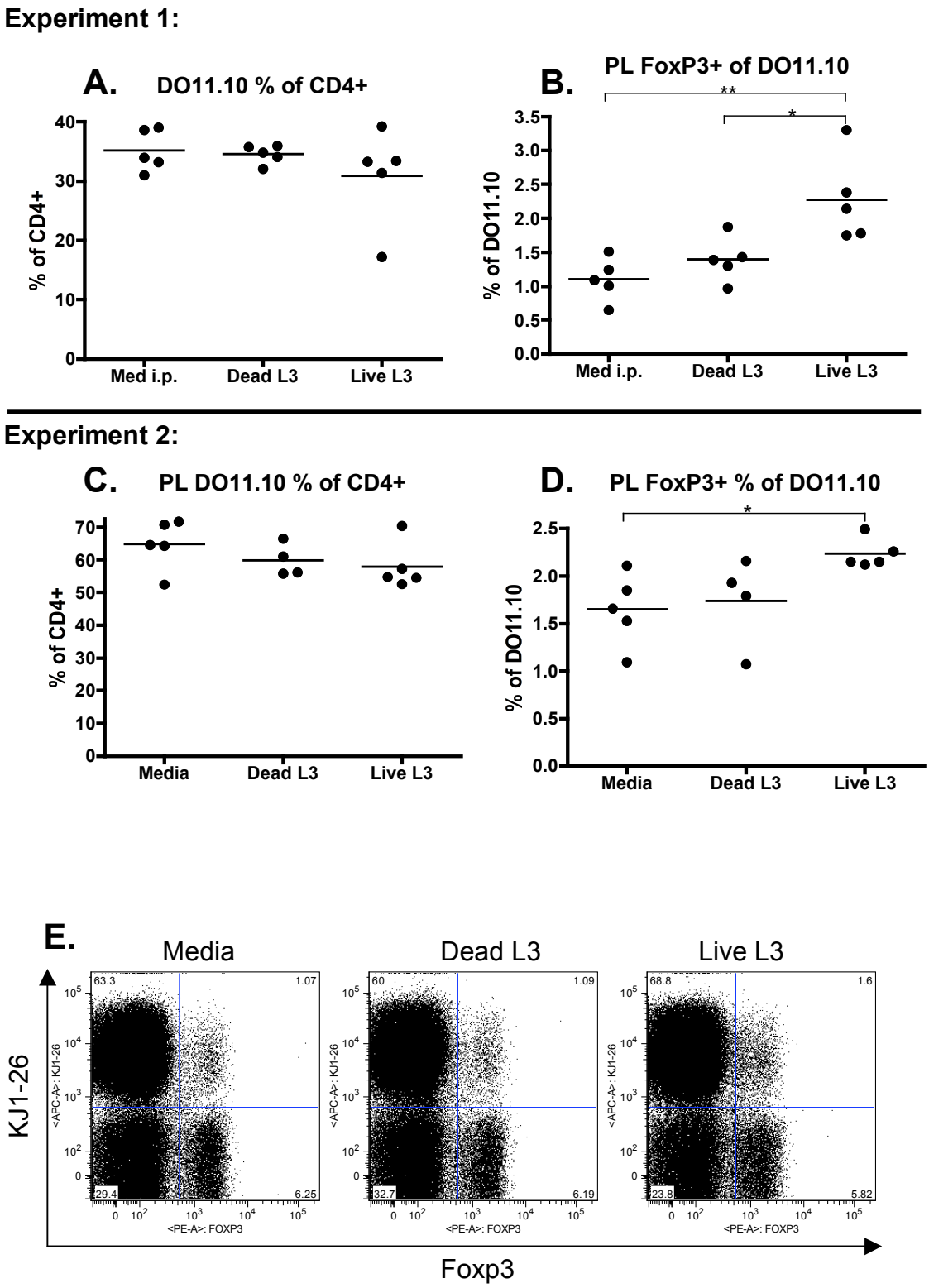

Figure 6.3: Foxp3 staining in adoptively transferred DO11.10 after i.p. L3 *B. malayi* infection

5x10^6 DO11.10 splenocytes were injected i.p. into BALB/c males, which 1 day later were injected i.p. with live or dead L3 *B. malayi*, or media. A further day after infection they were injected i.p. with 5x10^5 pOVA-loaded mature DCs. At day 7 post-infection, PL were taken and analysed by flow cytometry for expression of CD4, Foxp3 and KJ1-26 (DO11.10 TcR). Graphs in (A) and (C) show KJ1-26$^+$ % of CD4$^+$ population and (B) and (D) show Foxp3$^+$ % in the CD4$^+$KJ1-26$^+$ population. Bivariate plots in (E) show Foxp3 vs KJ1-26 on representative CD4$^+$-gated PL samples from each group in experiment 2. ** = P<0.01, * = P<0.05.

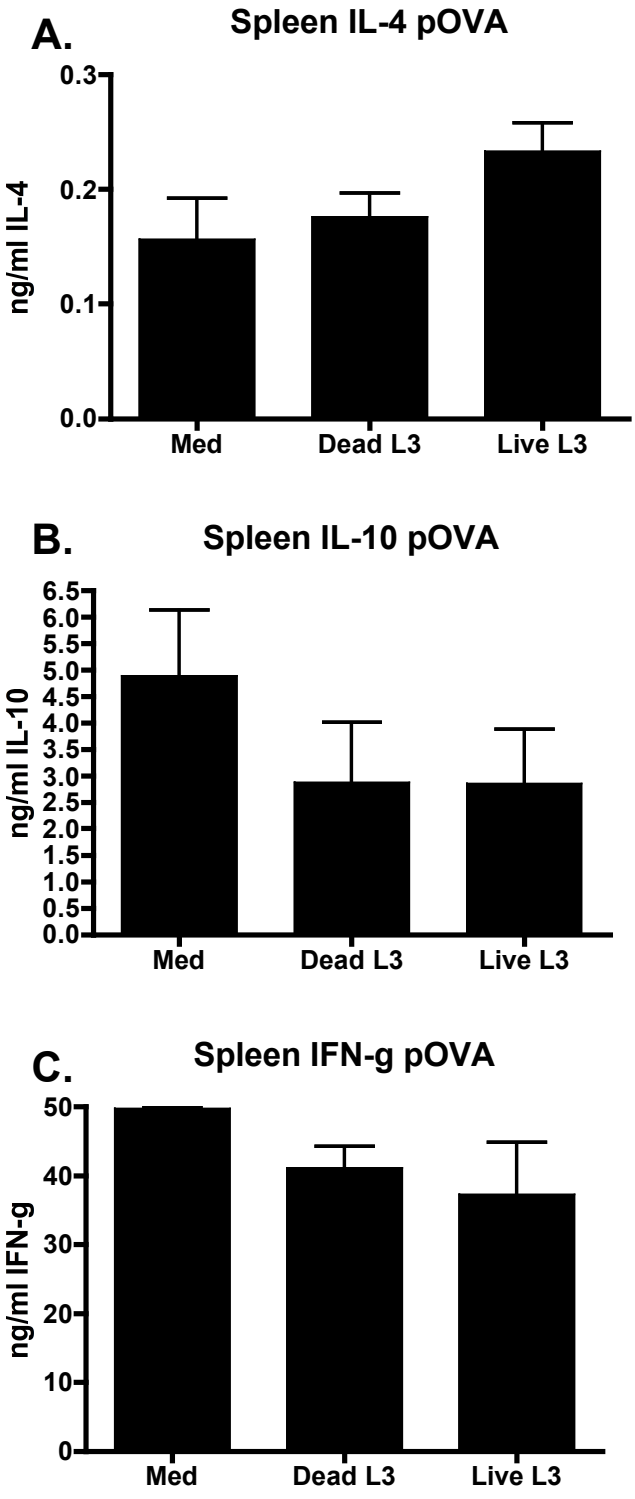

Figure 6.4: Restimulation cytokine production from bystander DO11.10 cells after L3 *B. malayi* infection

Splenocytes from mice from the experiment shown in Figure 6.3C-E were stimulated with 1 μg/ml pOVA for 72 h, then supernatants taken and tested by ELISA for IL-4 (A), IL-10 (B) and IFN-γ (C). Levels shown have unstimulated levels subtracted from stimulated levels for each sample.

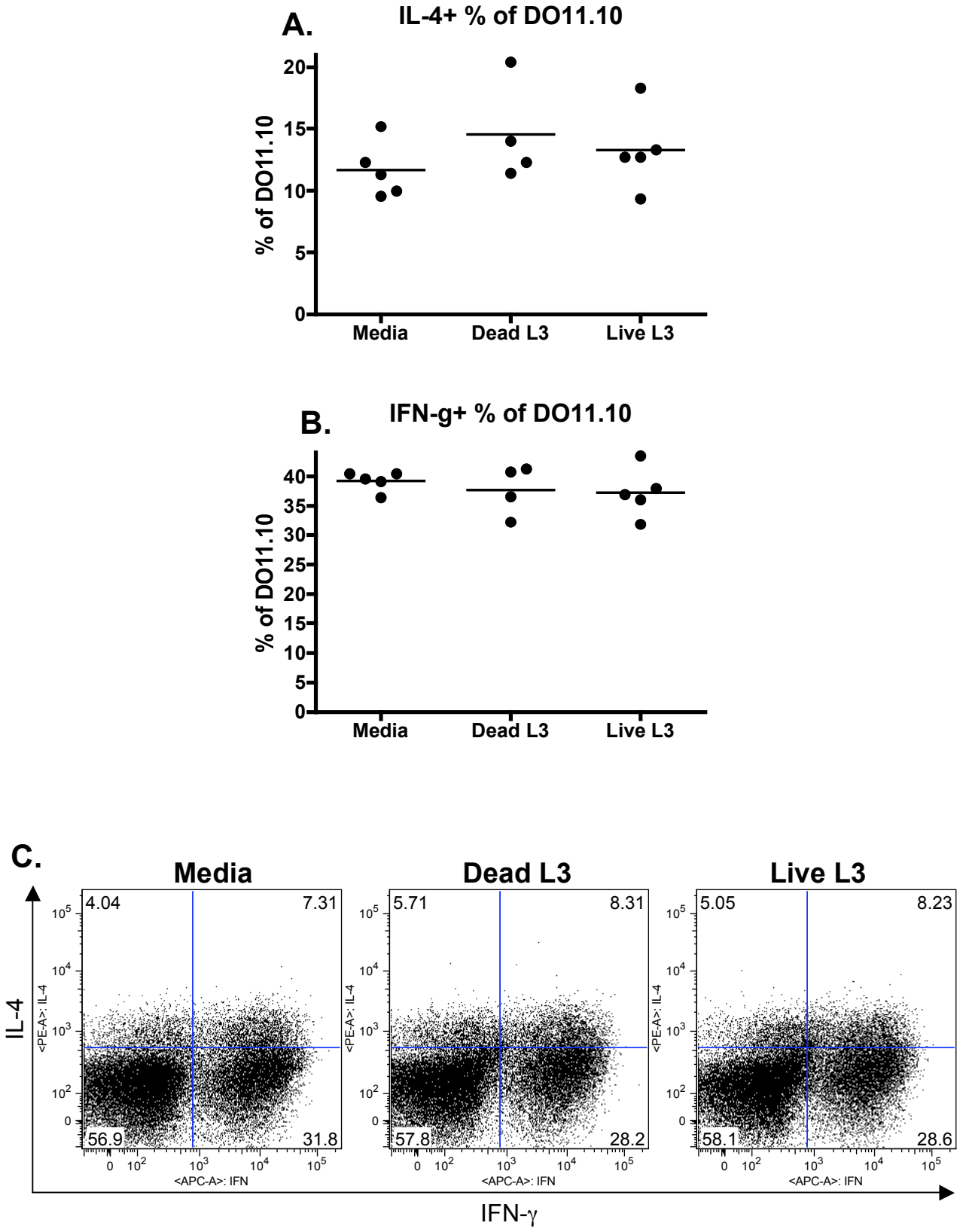

Figure 6.5: Intracellular cytokine staining of DO11.10 cells after i.p. L3 *B. malayi* infection
Peritoneal lavage cells from mice from the experiment shown in Figure 6.3C-E were intracellularly stained *ex vivo* for IL-4 (A) and IFN-γ (B). Representative plots of IFN-γ vs IL-4 are shown in (C), gated on $CD4^{+}KJ1\text{-}26^{+}$ (DO11.10) cells.

6.2. Host TGF-β blocking

I hypothesised that the Treg induction after *B. malayi* infection may be dependent on the *B. malayi* TGF-β homologue Bm-TGH-2, and that the activated Tregs induced may produce host TGF-β, thus feeding back and increasing the Treg induction. Therefore, I decided to block host TGF-β by injections of anti-TGF-β, to see if this reduced, or even ablated, *B. malayi* Treg induction.

6.2.1 Blocking host TGF-β does not ablate Treg induction

Male BALB/c mice were infected with L3 *B. malayi* as before, and anti-TGF-β monoclonal antibody (clone 1D11) was injected on days -1, 1, 3 and 5 from infection. Rat IgG was injected as a control, however the anti-TGF-β antibody is derived from mouse. Therefore the isotype groups are not good controls for the anti-TGF-β injections as the rat IgG will be recognised as non-self, whereas the mouse anti-TGF-β will not. However, even with this caveat, this experiment should be able to tell us something about the role of host TGF-β during infection.

Treg induction with *B. malayi* infection was evident in both rat IgG injections and anti-TGF-β groups, with increases seen in $Foxp3^+$ proportions of $CD4^+$ cells (Figure 6.6A) and $CD103^+$ proportions of $CD4^+Foxp3^+$ cells (Figure 6.6B). However, the rat IgG injections affected the peritoneal lavage population, as in the medium with rat IgG control group the proportion of $Foxp3^+$ cells was decreased from levels seen in other experiments (mean of 10.5% here, compared to a mean of 16.5% in a representative experiment). This was also decreased from the $Foxp3^+$ proportions of $CD4^+$ population in the anti-TGF-β control group. The $CD103^+$ proportion of the $Foxp3^+$ population was also low in both the anti-TGF-β groups,

which could be expected as TGF-β is known to induce CD103 (99). Alternatively, rat IgG in the control groups could induce artificially high levels of CD103 expression, especially as it was subsequently found to conatin TGF-β (Figure 3.15B)

Splenocytes from the mice were also stained *ex vivo* for Treg markers, and as can be seen in Figure 6.7, no change was seen in $Foxp3^+$ proportions of the $CD4^+$ population with infection in the rat IgG injections groups. However, in the anti-TGF-β injection groups, a decrease in $Foxp3^+$ proportions of the $CD4^+$ population was seen after infection compared to the control anti-TGF-β and sham surgery group, and both anti-TGF-β groups have increased levels of $Foxp3^+$ proportions of the $CD4^+$ population compared to the rat IgG injection groups (Figure 6.7A). The decrease in Foxp3 levels in rat IgG injection groups may again be due to the effector response against the rat IgG increasing levels of $Foxp3^-$ cells.

In the spleen, proportions of $CD103^+$ cells of the $CD4^+Foxp3^+$ population were decreased with anti-TGF-β injections, again corroborating that anti-TGF-β reduces CD103 expression. In both the rat IgG and the anti-TGF-β groups, infection induced an increase in the $CD103^+$ proportion of the $CD4^+Foxp3^+$ population (Figure 6.7B).

The above results from the PL and spleen are consistent with the hypothesis that the Treg induction in *B. malayi* infection is dependent on a parasite-derived TGF-β homologue, as this would not be blocked by anti-mammalian TGF-β antibody. There may be a role for host-derived TGF-β in exacerbating this effect, however in order to assess this, the experiment would have to be repeated with the correct controls, and larger sample sizes.

6.2.2. Blocking host TGF-β increases cytokine responses

Restimulations of mediastinal lymph node (the draining lymph node for the peritoneal cavity) cells were carried out for IL-4, IL-10, IL-5 and IL-13 cytokine ELISA, while the cells were pulsed with tritiated thymidine to assay proliferation to parasite antigen. As can be seen in Figure 6.8, increases in cytokine production to *B. malayi* antigen are increased with administration of anti-TGF-β, however this increase only reaches significance in IL-13 production (Figure 6.8H). In unstimulated cultures, spontaneous cytokine production was only seen with anti-TGF-β administration in *B. malayi* infection (Figure 6.8A, C, E and G). Therefore it can be hypothesised that host TGF-β controls the effector cell cytokine production. Background proliferation was also increased with administration of anti-TGF-β (Figure 6.8I), with a trend for an increase in antigen-specific proliferation (Figure 6.8J).

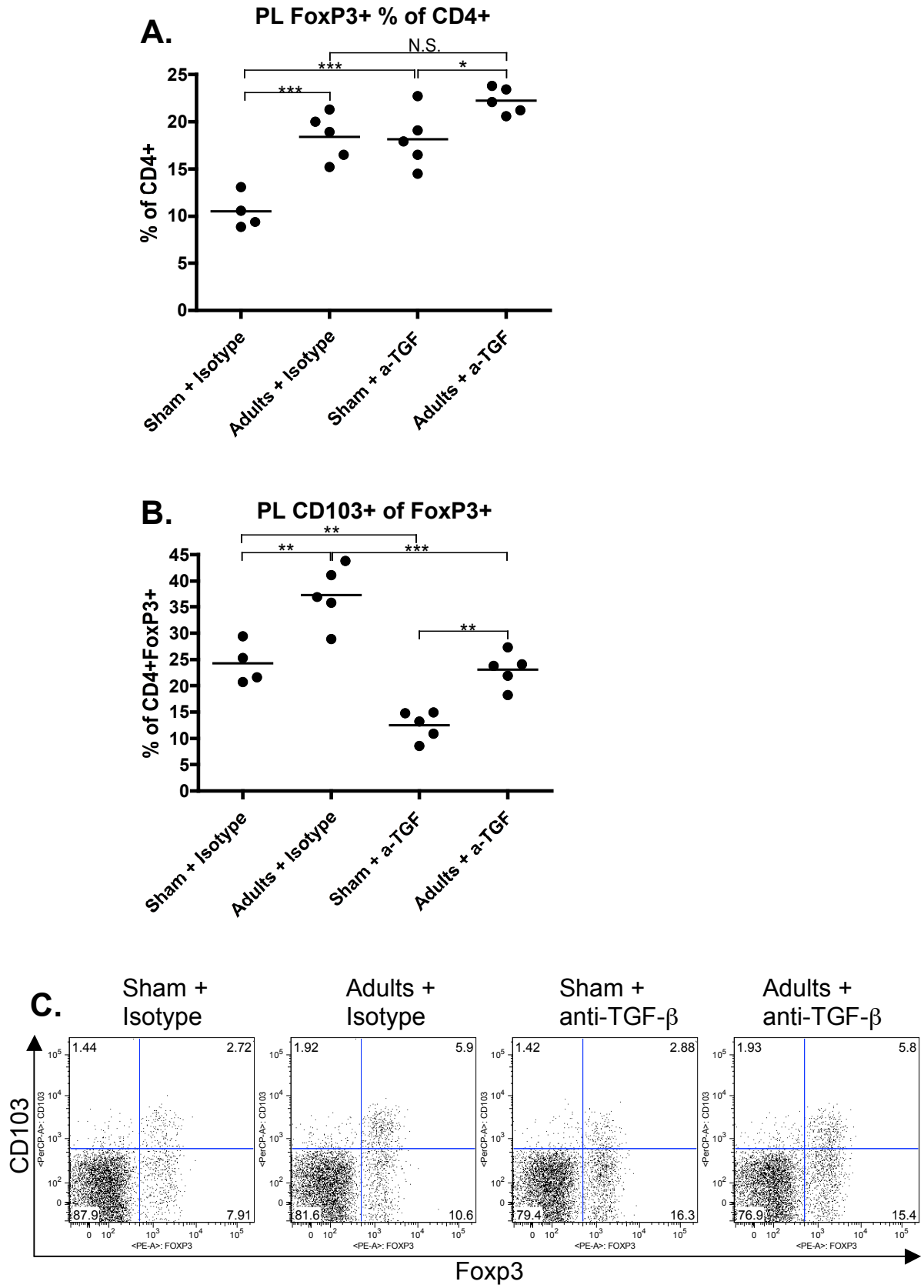

Figure 6.6: Foxp3$^+$ cells accumulate in the PL after *B. malayi* adult implant in presence of anti-TGF-β

Peritoneal lavage cells from BALB/c mice 7 days after adult *B. malayi* implant, with 100 μg anti-TGF-β or rat IgG administered i.p. on day -1, 1, 3 and 5 after infection were stained for flow cytometry with CD4, Foxp3 and CD103. Graphs shown are Foxp3$^+$ % of the CD4$^+$ population (A), and CD103$^+$ % of the CD4$^+$Foxp3$^+$ population (B). Shown in (C) are representative plots from each group of Foxp3 vs CD103, gated on the CD4$^+$ population. *** = P<0.001, ** = P<0.01, * = P<0.05.

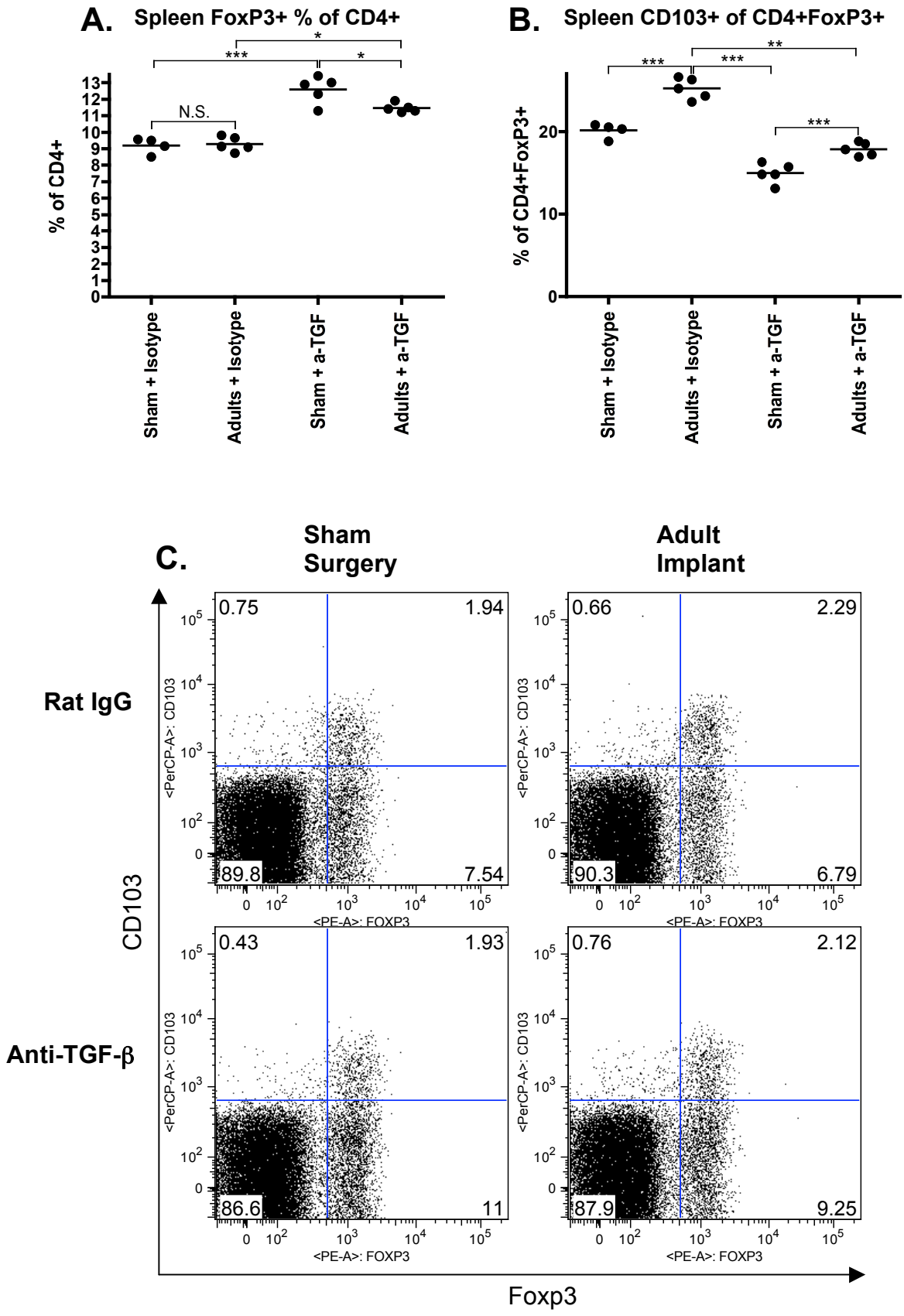

Figure 6.7: Foxp3 levels in spleen after anti-TGF-β treatment and adult *B. malayi* implant
Splenocytes were isolated from BALB/c mice 7 days after adult *B. malayi* implant, with 100 μg anti-TGF-β or rat IgG administered i.p. on day -1, 1, 3 and 5 after infection and were stained for flow cytometry with CD4, Foxp3 and CD103. Graphs shown are $Foxp3^+$ % of the $CD4^+$ population (A), and $CD103^+$ % of the $CD4^+Foxp3^+$ population (B). Shown in (C) are representative plots from each group of Foxp3 vs CD103, gated on the $CD4^+$ population. *** = P<0.001, ** = P<0.01, * = P<0.05, N.S. = Non-significant

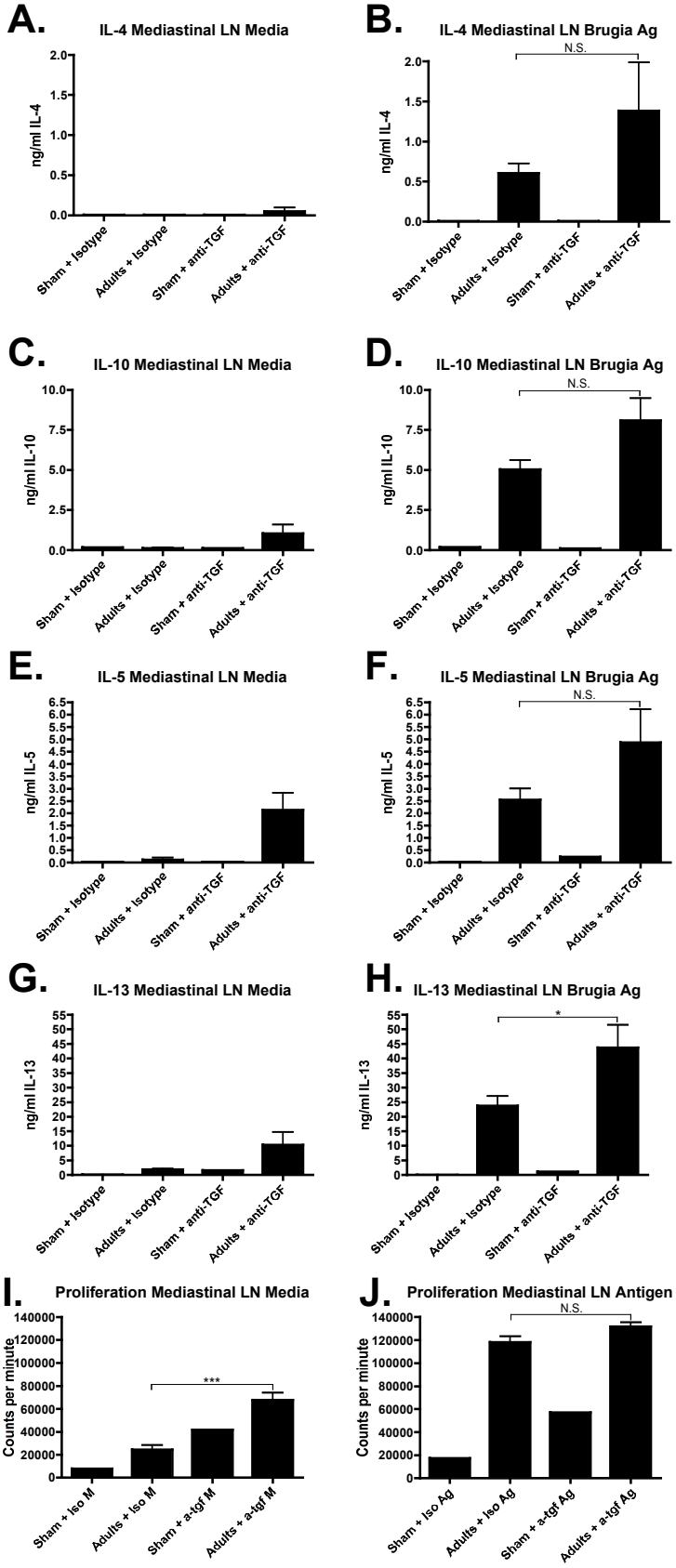

Figure 6.8: Restimulation of LN cells after *B. malayi* adult implant with anti-TGF-β administration

Mediastinal LN cells were isolated from mice from the experiment shown in Figure 6.6 and were stimulated for 72 h with media (A, C, E, G and I) or adult *B. malayi* antigen (B, D, F, H and J). Supernatants were then taken and tested by ELISA for IL-4 (A and B), IL-10 (C and D), IL-5 (E and H) and IL-13 (G and H). The LN cells were also pulsed with ^{3}H-thymidine overnight and read on a scintillation counter to show levels of proliferation (I and J). *** = P<0.001, ** = P<0.01, * = P<0.05, N.S. = Non-significant

6.3. Blocking TGF-β Signalling

We hypothesised that parasite-derived TGF-β (such as Bm-TGH-2) may induce Tregs to parasite antigens. As the Bm-TGH-2 mature domain is only 41% identical to human TGF-β (96), it would be very unlikely to be blocked by anti-mammalian TGF-β monoclonal antibody. To address this, the TGF-β signalling pathway can be interfered with, which should block both host and parasite-derived TGF-β signalling. I used SB-525334, a specific inhibitor of ALK-5 (the TGF-β type I receptor chain) (223). Mice were injected with either 200 μg/mouse SB-525334 in PBS:DMSO or vehicle (PBS:DMSO) s.c. in the flank 30 min before infection and boosts on day 2, 4 and 6 after infection with L3 *B. malayi*. Doses higher than this were found to be toxic (data not shown).

6.3.1. Subcutaneous Injection of ALK-5 Inhibitor

SB-525334 administration did not affect $Foxp3^+$ proportions of the $CD4^+$ T cell population (Figure 6.9A), or $CD103^+$ proportions of the $CD4^+Foxp3^+$ Treg population (Figure 6.9B), similarly to results seen in anti-TGF-β administration (Figure 6.6). In contrast with the anti-TGF-β restimulation cytokine results (Figure 6.8) however, blockade of the TGF-β pathway did not have any effect on restimulation cytokine levels (Figure 6.10).

6.3.2. Intraperitoneal Injection of ALK-5 Inhibitor

As none of the parameters measured changed with subcutaneous inhibitor administration, there is a possibility that the inhibitor could not affect cells in the peritoneal cavity when injected subcutaneously, although the closest possible

subcutaneous injection site to the peritoneal cavity was chosen (the flank, adjacent to the peritoneal membrane). Therefore, the experiment was repeated with intraperitoneal injections of inhibitor or vehicle. However, when the peritoneal lavage was taken from these mice, they were found to be highly contaminated with blood, indicating either the repeated injections, or the toxic nature of the vehicle DMSO, was causing damage to the peritoneal cavity. Therefore the peritoneal lavage cells were discarded, as any results received would be unreliable due to contamination of circulating leukocytes. The spleens from these mice were restimulated for cytokine ELISA, and showed increased levels of antigen-specific cytokine production, which reached significance compared to vehicle control groups in IL-5 and IL-13 levels (Figure 6.11).

From these results it is difficult to tell if blockade of TGF-β signaling prevents Treg induction in *B. malayi* infection. As no differences were seen with subcutaneous injection of inhibitor, the inhibitor may not have reached the peritoneal cavity. With intraperitoneal injection of inhibitor, although no data was retrieved from the peritoneal lavage cells, antigen-specific cytokine responses increased, reflecting the anti-mammalian TGF-β results. Therefore intraperitoneal injection of inhibitor may have been effective in blocking TGF-β signaling at the site of infection.

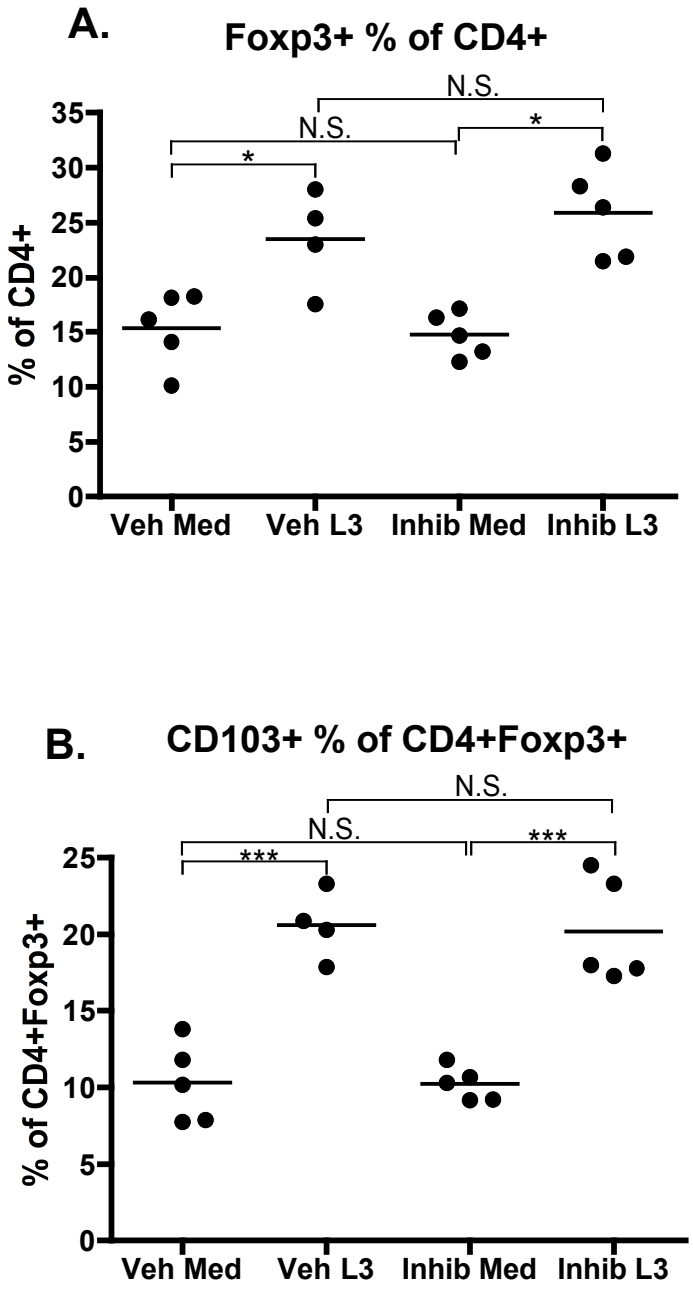

Figure 6.9: PL Treg markers after i.p. *B. malayi* infection and s.c. TGF-βR inhibitor administration

BALB/c mice were injected with L3 *B. malayi* i.p., and ALK-5 inhibitor (Inhib) or PBS:DMSO vehicle (Veh) injected s.c. on day 0, 2, 4 and 6 after infection. PL cells were stained for flow cytometric staining for CD4, Foxp3 and CD103. Graphs show $Foxp3^+$ proportions of the $CD4^+$ population (A) and $CD103^+$ proportions of the $CD4^+Foxp3^+$ population (B). *** = $P<0.001$, * = $P<0.05$.

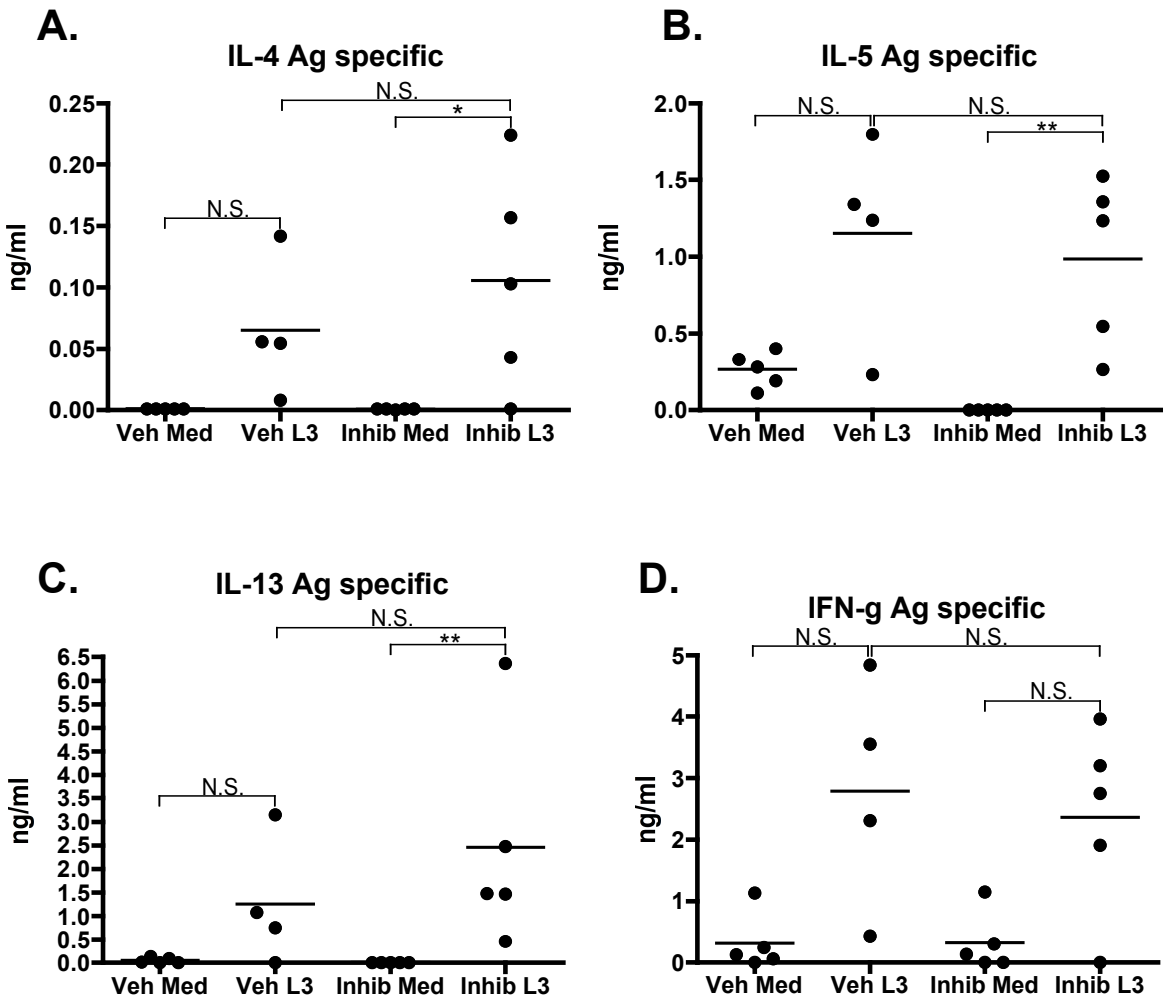

Figure 6.10: Restimulation cytokines after i.p. *B. malayi* infection and s.c. TGF-βR inhibitor administration

BALB/c mice were injected with L3 *B. malayi* i.p., and ALK-5 inhibitor (Inhib) or PBS:DMSO vehicle (Veh) injected s.c. on day 0, 2, 4 and 6 after infection. Splenocytes were stimulated with *B. malayi* adult antigen for 72 h, and supernatants used in cytokine ELISA for IL-4 (A), IL-5 (B), IL-13 (C) and IFN-γ (D). All graphs are antigen-specific, with unstimulated levels subtracted. ** = $P<0.01$, * = $P<0.05$, N.S. = non-significant.

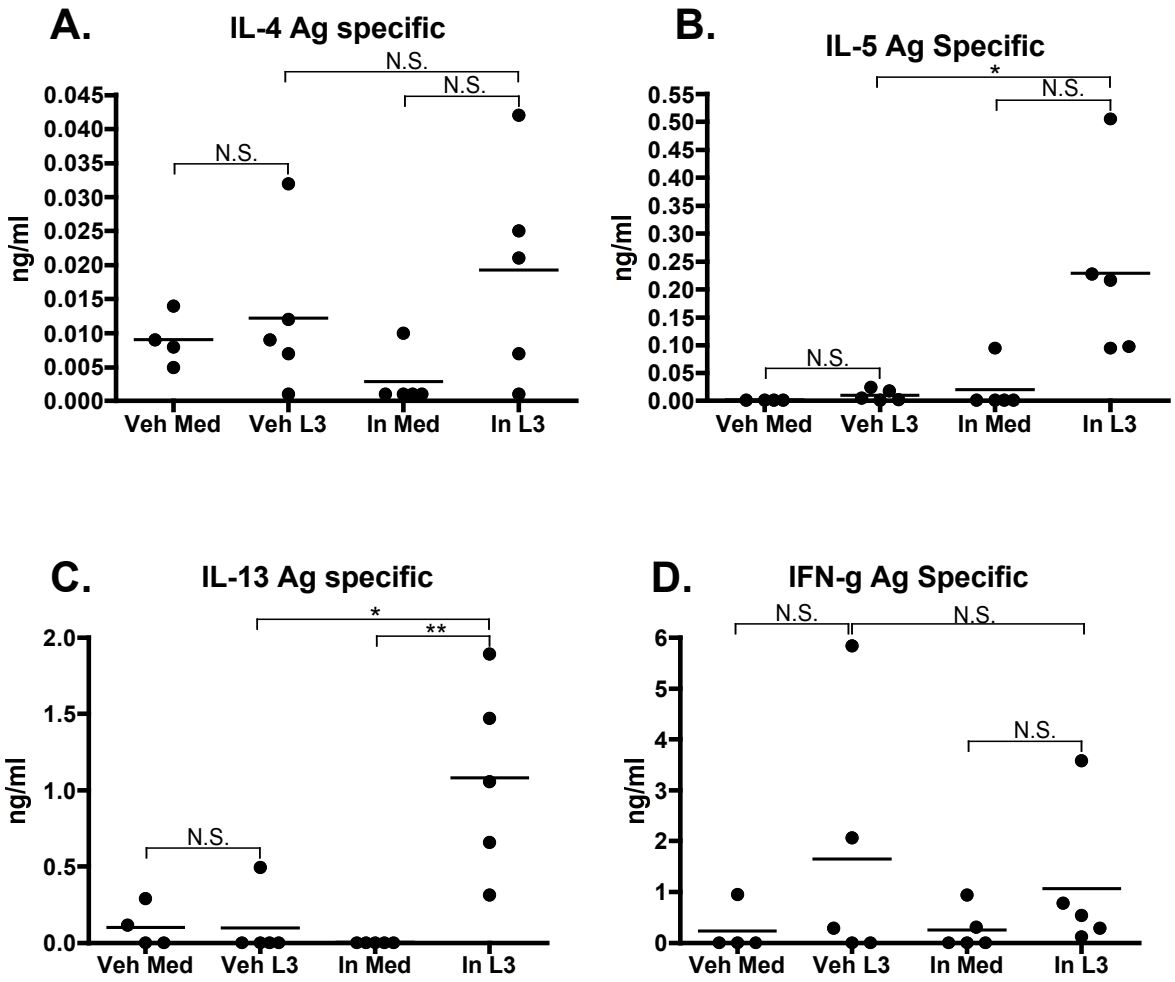

Figure 6.11: Restimulation cytokines after i.p. *B. malayi* infection and i.p. TGF-βR inhibitor administration

BALB/c mice were injected with L3 *B. malayi* i.p., and ALK-5 inhibitor (Inhib) or PBS:DMSO vehicle (Veh) injected i.p. on day 0, 2, 4 and 6 after infection. Splenocytes were stimulated with *B. malayi* adult antigen for 72 h, and supernatants used in cytokine ELISA for IL-4 (A), IL-5 (B), IL-13 (C) and IFN-γ (D). All graphs are antigen-specific, with unstimulated levels subtracted. ** = P<0.01, * = P<0.05, N.S. = non-significant.

6.4. Infection of IL-4R-deficient mice

The Treg respone in *B. malayi* infection shown here is associated with a TH2 effector response. IL-4R signalling is essential for a productive TH2 response (14, 15), and induction of suppressive macrophages (223). Therefore in its absence, it could be hypothesised that the TH2 effector response would be absent, and therefore could result in an increased proportion of $Foxp3^+$ cells remaining. Conversely, in the absence of IL-4R signalling and therefore suppressive macrophages, Treg induction could also be absent, as suppressive macrophages could induce Tregs. To look at this mechanism, IL-4R-deficient and wild-type mice were infected with *B. malayi*, and the macrophage and Treg populations were examined.

6.4.1. *B. malayi* Treg response in IL-4R-deficient mice

BALB/c wild-type or IL-4R-deficient mice on a BALB/c background were infected with L3 *B. malayi* and recruited cells assayed by *ex vivo* flow cytometry. As can be seen in Figure 6.12, WT and IL-4R-deficient mice both had similar levels of Treg induction (Figure 6.12A), however IL-4R-deficient mice had lost the recruitment of eosinophils seen in wild-type mice (Figure 6.12B). Interestingly, numbers of L3 *B. malayi* recovered in the PL were lower in IL-4R-deficient than wild-type mice (Figure 6.12C). This may reflect the situation in *L. sigmodontis* infection, where a mixed TH1/TH2 response is required for parasite killing, as IL-4-deficient mice cannot clear *L. sigmodontis* infection (170), and IL-5 and IFN-γ-deficient mice both have higher worm burdens than wild-type (171).

6.4.2. Loss of AAMac in IL-4R-deficient mice

AAMacs cannot be induced in IL-4R-deficient cells (178), and AAMacs induced in *B. malayi* infection are highly suppressive *in vitro* (212). As shown in Figure 6.13A, F4/80^{+} macrophage recruitment to the peritoneal cavity is lost in IL-4R-deficient mice. The macrophages present in the IL-4R-deficient PL were tested for suppressive capacity in an EL-4 (a continually proliferating thymoma cell line) suppression assay, and as shown in Figure 6.13B, IL-4R-deficient macrophages could not suppress proliferation. Therefore *B. malayi* AAMac induction is lost in the absence of the IL-4R.

6.4.3. Cytokine responses to antigen in IL-4R-deficient mice

Splenocytes were isolated and restimulated with *B. malayi* adult worm antigen. As can be seen in Figure 6.14A, IL-4 responses were increased in IL-4R-deficient mice, presumably as no IL-4R-mediated uptake of IL-4 produced by innate cells (e.g. NKT cells (202)) could occur. However the TH2 cytokines IL-5 (Figure 6.14B) and IL-13 (Figure 6.14D) were decreased in IL4R-deficient mice, indicating IL-4R-deficient mice lack a functional TH2 response, which is backed up by the lack of eosinophil recruitment (Figure 6.12B).

These results indicate that the Foxp3 induction seen in *B. malayi* infection is independent of the presence of AAMacs.

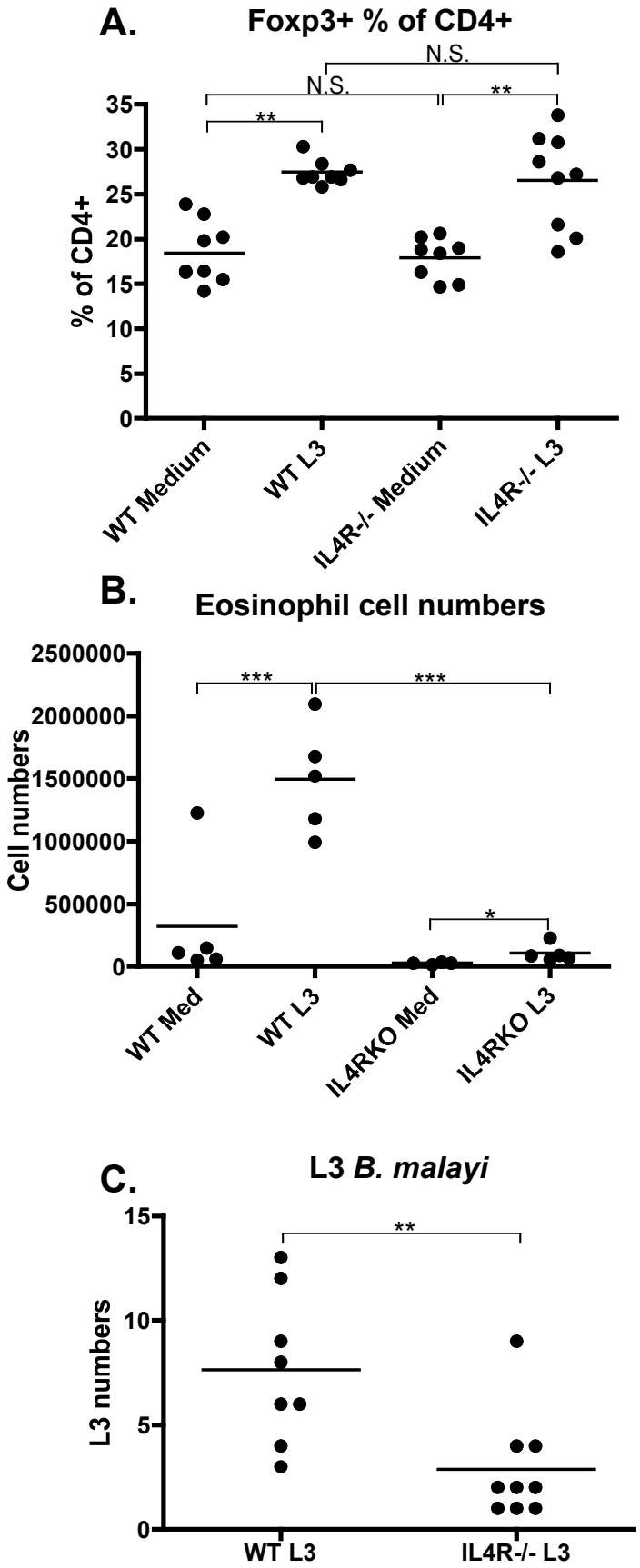

Figure 6.12: Response in PL after i.p. L3 *B. malayi* infection of WT or IL-4R-deficient mice
PL cells were taken from BALB/c or IL-4R-deficient mice 7 days after infection with 50 L3 *B. malayi* i.p. and stained for CD4, Foxp3 and SIGLEC-F for flow cytometric staining. Graphs show $Foxp3^+$ proportion of $CD4^+$ cells (A), SIGLEC-F^+ cell numbers (B) and numbers of L3 recovered in the PL (C). (A) and (C) are pooled data from 2 repeat experiments, (B) is a single representative experiment. *** = $P < 0.001$, ** = $P < 0.01$, * = $P < 0.05$

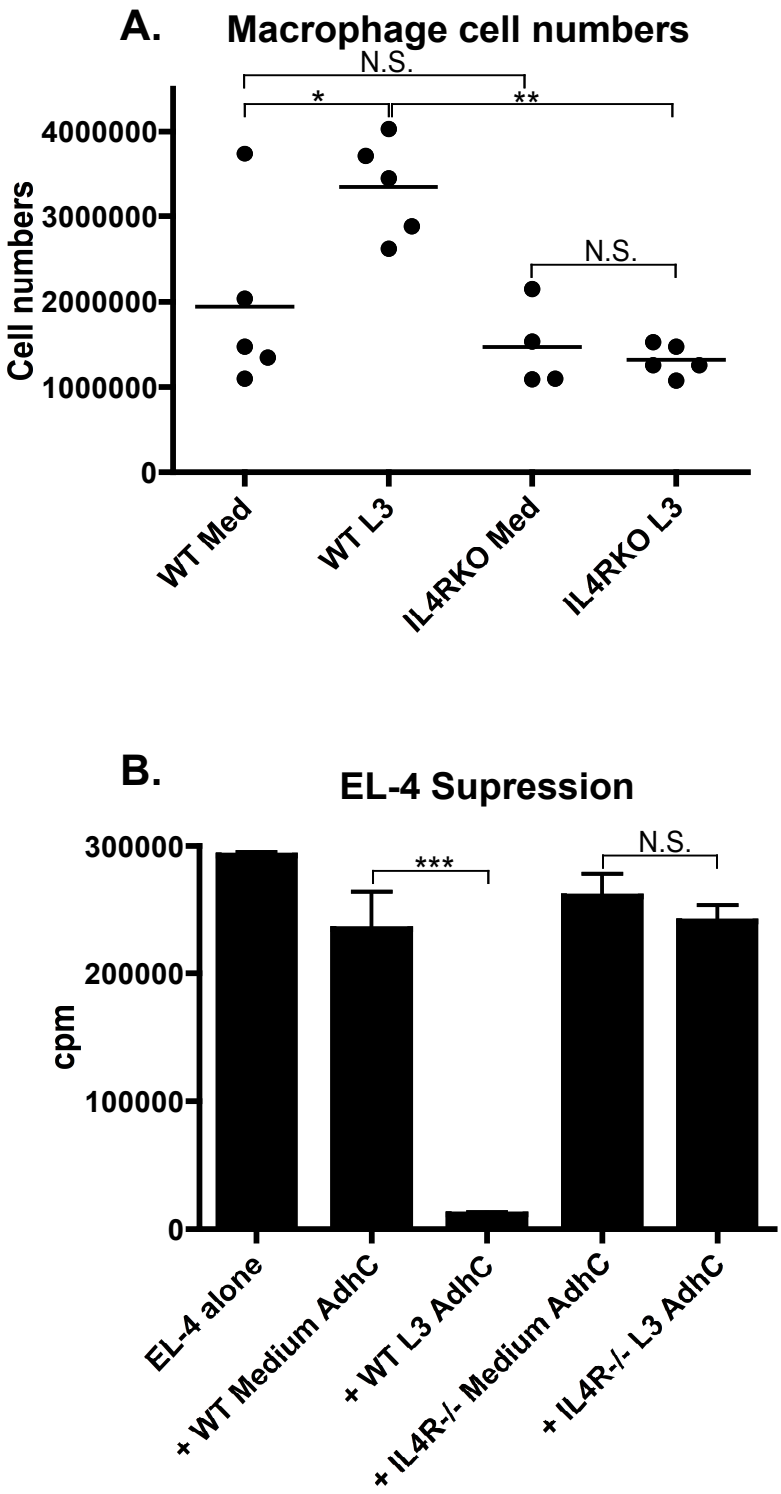

Figure 6.13: Macrophage phenotype in PL after i.p. L3 *B. malayi* infection of WT or IL-4R-deficient mice

PL cells were taken from BALB/c or IL-4R-deficient mice 7 days after infection with 50 L3 *B. malayi* i.p. and stained for F4/80 for flow cytometric staining. Graph (A) show $F4/80^{+}$ cell numbers. Adherent cells were purified from the PL, and cocultured with EL-4 cells. Graph (B) shows scintillation counts from a tritiated thymidine incorporation assay. *** = $P < 0.001$, ** = $P < 0.01$, N.S. = non-significant.

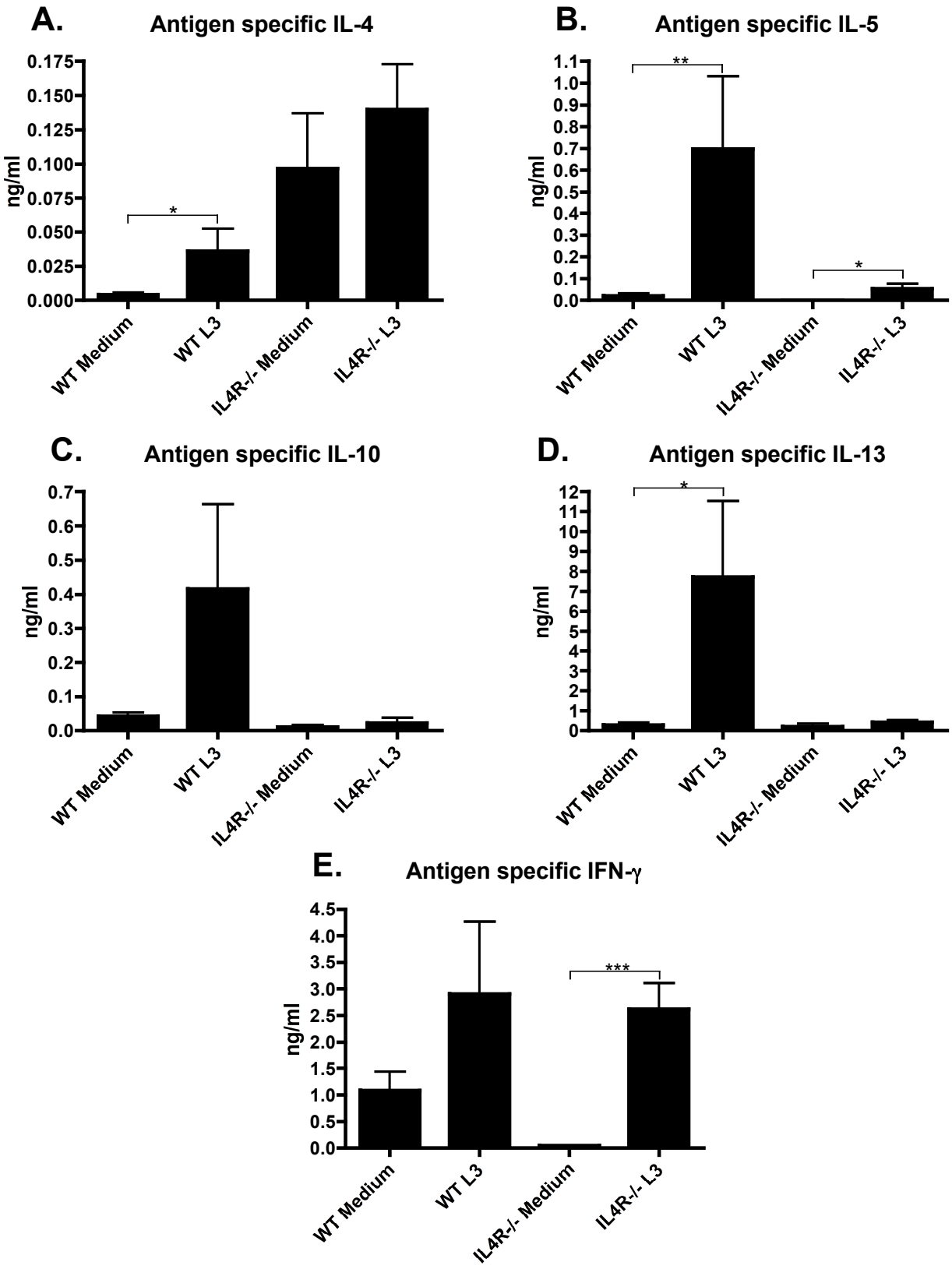

Figure 6.14: Restimulation cytokines after i.p. L3 *B. malayi* infection of WT or IL-4R-deficient mice

Splenocytes were prepared from BALB/c or IL-4R-deficient mice 7 days after infection with 50 L3 *B. malayi* i.p. and cultured for 72 h in media or 10 μg/ml *B. malayi* antigen. Supernatants were then tested for IL-4 (A), IL-5 (B), IL-10 (C), IL-13 (D) and IFN-γ (E) by cytokine ELISA. Graphs shown are antigen-specific cytokine with media levels subtracted, and are representative of 2 repeat experiments. ** = $P < 0.01$, * = $P < 0.05$.

6.5. *In vitro* Treg Induction

The data presented in chapter 5 and 6 shows that *B. malayi* L3 larvae can induce Tregs at the site of infection *in vivo*, and as shown in chapter 3, products of some parasitic nematodes contain significant levels of TGF-β. To test whether the *B. malayi* Treg response is due to release of a TGF-β homologue such as Bm-TGH-2 by L3 larvae, *B. malayi* L3 larvae were cultured *in vitro* in serum-free media, and supernatants used in the TGF-β bioassay. *B. malayi* L3 excretory/secretory products (Figure 6.15A), and ES prepared from L3 larvae, adult or Mf *B. malayi*, or *B. malayi* adult antigen (Figure 6.15B) do not produce an active or latent TGF-β signal.

As some of the downregulatory effects of culture with live L3 *B. malayi* are contact dependent (40), we cultured naive BALB/c splenocytes in the presence of live *B. malayi* L3 and polyclonal stimulus (Figure 6.16). No induction of Foxp3 was seen in the presence of live L3 *B. malayi*, indicating the larvae may not be releasing significant levels of TGF-β, or that the TGF-β released is below the detection limit of this assay.

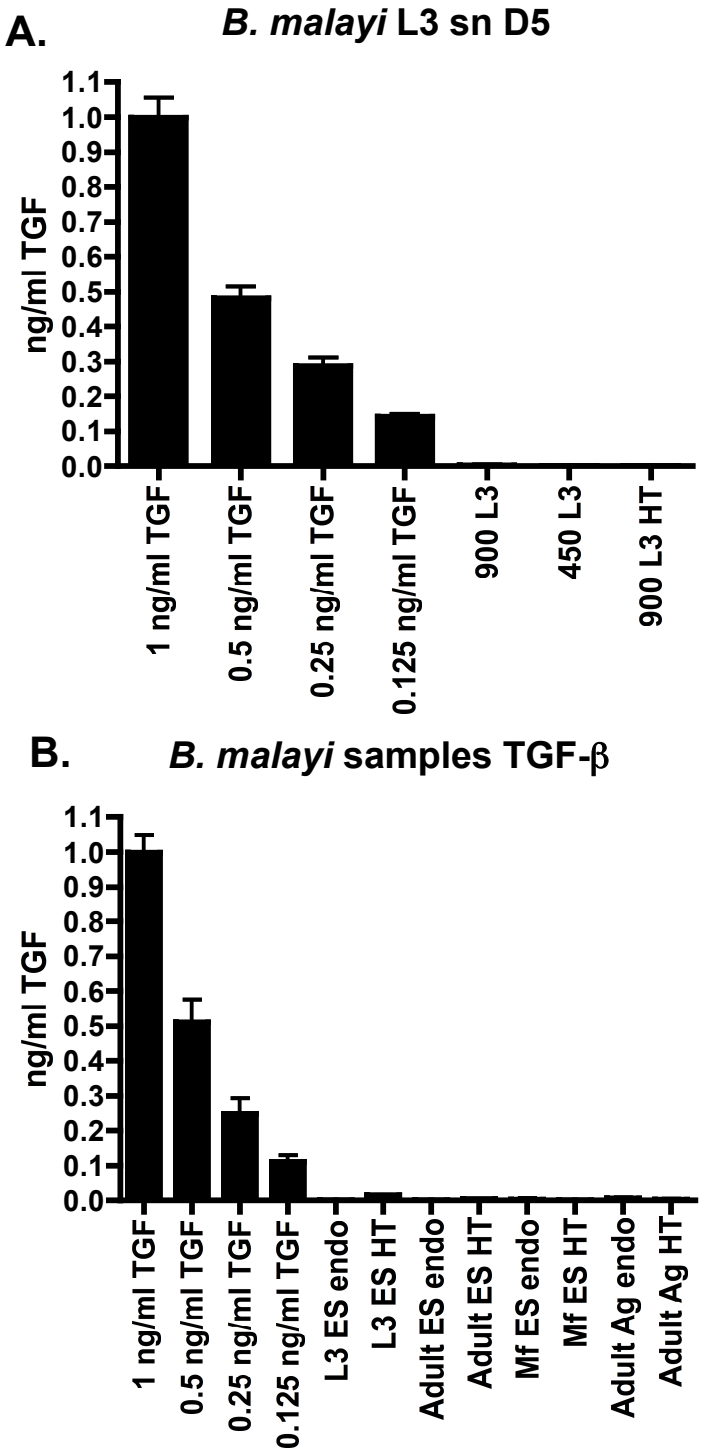

Figure 6.15: TGF-β activity of *in vitro* cultured L3 *B. malayi*
L3 *B. malayi* were cultured in serum-free medium for 5 days, then the supernatant collected and tested for TGF-β activity in the MLEC TGF-β bioassay (A), with some samples heat-treated to activate latent TGF-β (80 °C, 5 min.). Samples of ES from *B. malayi* L3, adults or Mf and adult *B. malayi* antigen were also added to the MLEC TGF-β bioassay (all at 10 μg/ml), with or without heat-treatment (B).

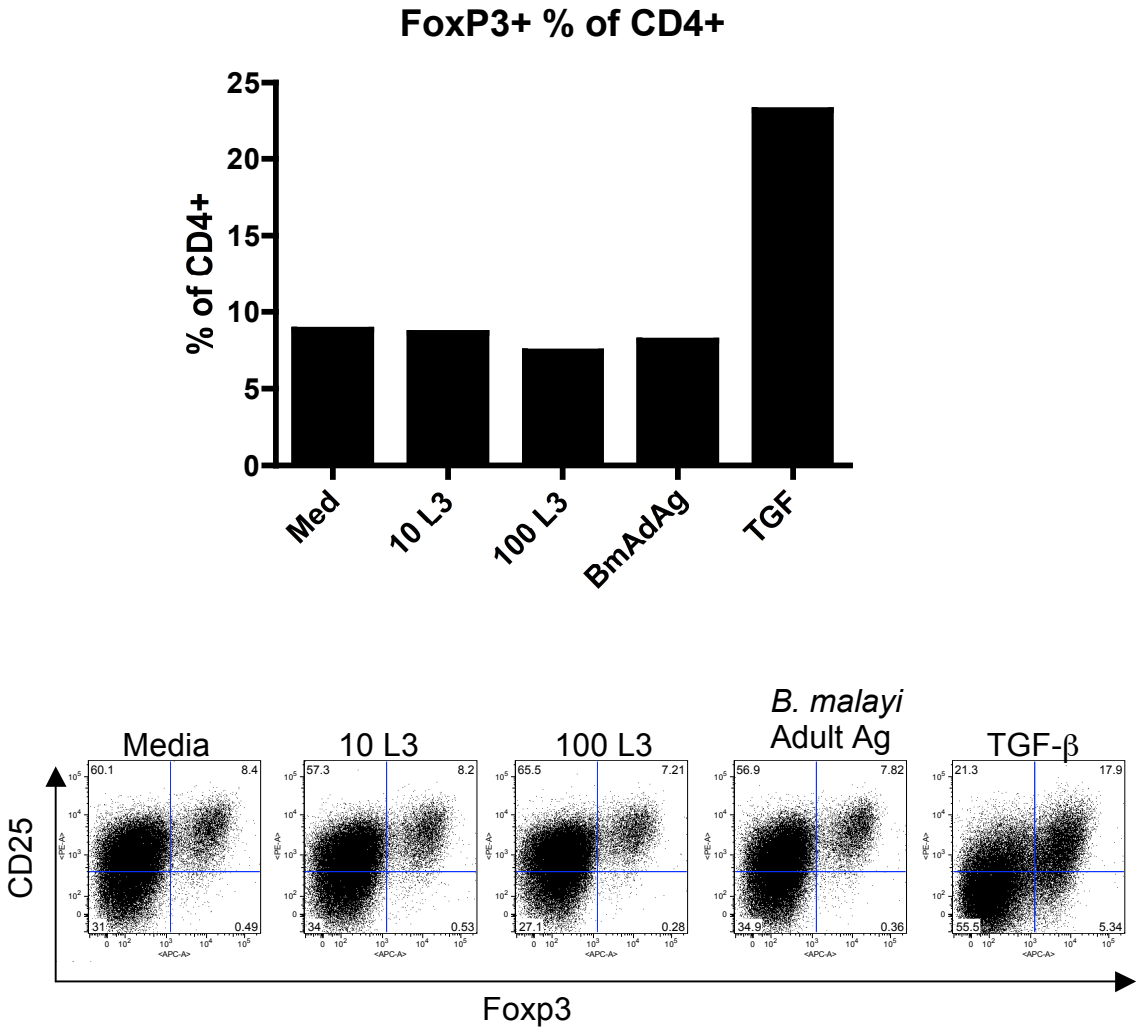

Figure 6.16: Foxp3 induction by *B. malayi* products
BALB/c splenocytes were cultured for 48 h in the presence of 0.01 μg/ml anti-CD3 and either 10 μg/ml *B. malayi* adult antigen or live L3 *B. malayi*, then stained for CD4, CD25 and Foxp3 for flow cytometric analysis. Graph shows the $Foxp3^+$ proportion of the $CD4^+$ population, bivariate plots are Foxp3 vs CD25, gated on $CD4^+$ cells.

6.6. Discussion

The data presented in this chapter show that Treg induction in a mouse model of *B. malayi* is not restricted to parasite antigen-specific T cells (as Treg induction was seen in a bystander response), and is not dependent on the presence of alternatively activated macrophages. Experiments using the anti-TGF-β antibody and a specific inhibitor of TGF-β signalling indicate TGF-β may not be involved in Treg induction, although these results are less conclusive. Finally, culture of live L3 *B.malayi in vitro* indicate they do not produce significant levels of TGF-β under the culture conditions used, and are incapable of inducing Tregs when cultured with polyclonally stimulated splenocytes.

The hygiene hypothesis states that downregulation of the host immune response by parasitic infections affect bystander antigens, suppressing inappropriate immune responses. In high-intensity human filarial infections, there is strong evidence that immune down-regulation extends beyond parasite specificities, spreading out to affect responses to vaccine antigens *in vivo* (224, 225) and T cell stimulation *in vitro* (226). In this context, it is important to know whether *B. malayi* can induce Treg activity beyond the parasite antigen-specific T cell population. Using an adoptive transfer model, DO11.10 T cells specific for a bystander, non-cross-reactive antigen, OVA, also showed expansion of Foxp3, even though the DO11.10 cells are strongly stimulated with mature BMDCs loaded with cognate peptide. The DO11.10 cells remained strongly TH1 polarised by intracellular cytokine staining, indicating that the Foxp3 induction could take place even in the presence of IFN-γ, surprising as it has been shown that both IFN-γ and IL-4

downregulate Foxp3 induction *in vitro* and in a DO11.10 adoptive transfer model (146). An important caveat of these results is the wild-type background of the DO11.10 cells used, where a small population of pre-existing $Foxp3^+$ T cells exist, due to low levels of endogenous TcR expression (227). Thus the induction of Foxp3 in the DO11.10 cells seen here may either be from expansion of a pre-existing $Foxp3^+$ subset, or induction of Foxp3 in naïve DO11.10 cells.

I investigated the role of host and parasite-derived TGF-β by using anti-mammalian TGF-β blocking antibody and an inhibitor of TGF-β signalling. The blocking antibody results have the caveat that isotype antibody from rat, rather than mouse, was used. However, with anti-TGF-β antibody administration an increase in proportions and activation of Tregs remained after *B. malayi* infection. Therefore, host TGF-β appears to be dispensable for Treg induction in our model, although it may be a Treg effector molecule, as antigen-specific TH2 cytokine production was increased in anti-TGF-β-treated animals.

The ALK-5 (TGF-β type I receptor) inhibitor experiments also assessed the impact of parasite-derived TGF-β where the anti-mammalian-TGF-β antibody experiment does not. However, this inhibitor has not been used previously in an intraperitoneal infection, so there is no evidence to what extent the inhibitor blocked TGF-β signalling, and whether subcutaneous injection in the flank will allow the inhibitor to access the peritoneal cavity. Intraperitoneal administration of the inhibitor however, appears to have had a significant effect on cytokine recall responses, reflecting administration of the anti-mammalian TGF-β antibody.

To interpret these results, it is important to know whether subcutaneous injection of ALK-5 inhibitor results in ablation of TGF-βR signalling in the peritoneal cavity (and systemically). To assess this in a repeat of the experiment, peritoneal lavage cells could be taken and levels of smad-7 transcription measured by real-time RT-PCR. Smad-7 is strongly upregulated by TGF-β signalling (91), so if the inhibitor were working correctly, it would be expected that smad-7 transcription would be reduced. However, as the antigen-specific cytokine recall responses in intraperitoneal inhibitor injection reflect the anti-mammalian TGF-β results, but not the subcutaneous injection results, it seems likely that subcutaneous injection of the inhibitor has negligible systemic effects.

If we presume that subcutaneous administration of the ALK-5 inhibitor did not affect the peritoneal population, we can make some interesting conclusions about the role of TGF-β in *B. malayi* infection. Host TGF-β seems not to be involved in induction of the Treg population (Figure 6.6), but in suppression of cytokine production by antigen-specific Teffectors (Figures 6.8 and 6.11). This would be consistent with a model of *B. malayi* Treg induction where Bm-TGH-2 is released by the parasite, resulting in accumulation of Tregs in the peritoneal cavity. These Tregs could then produce TGF-β to suppress Teffector responses.

To look further at the role of TGF-β in *B. malayi* Treg induction, the CD4-trophic TGF-βRIIDN transgenic mouse (228) could be used. These mice express both normal TGF-βR chains, but also transgenically express a truncated version of the TGF-βRII chain under the control of a modified CD4 promoter (with a regulatory region removed, to allow expression in both $CD4^+$ and $CD8^+$ T cells). The truncated

TGF-βRII lacks a signalling domain but can still bind to TGF-β and ALK-5, and so its expression results in formation of a non-functional receptor, ablating TGF-β signalling (228). This mouse is very useful, as the TGF-βR is present on many cell types and has many different effects, whereas in these mice only the role of TGF-β on T cells is assessed. Thus if the model of Treg induction by release of parasite-derived TGF-β holds true, no Treg induction would be seen in infection of these mice. We now have a colony of these mice, and these experiments are currently underway.

A well-documented result of *B. malayi* adult implantation is the recruitment of alternatively activated macrophages to the peritoneal cavity (177, 229). These have been shown to suppress proliferation of antigen-specific T cells through a contact-dependent mechanism (229), and induce TH2 responses through release of TGF-β (184). The experiments using IL-4R-deficient mice give more evidence on the role of AAMacs in this system. Alternatively-activated macrophages do not develop in filarial-infected IL-4R-deficient mice (J. E. Allen, personal communication), or in STAT-6-deficient animals infected with other helminths (185, 230). By showing that *B. malayi* induces Foxp3 within the T cell population even in the absence of IL-4R signalling, we have established that this process is independent of alternatively activated macrophages. In long-term *L. sigmodontis* infections, alternatively-activated macrophages are found together with both $Foxp3^+$ Tregs and CTLA-4^+ anergic effector T cells (221), although the inter-dependency of these populations has not been established. In the experiments shown here, CTLA-4 remained high on $Foxp3^-$ effector cells even in the IL-4R-deficient setting, while $CD4^+FoxP3^+$ cell expression of CD25, CD103 and CTLA-4 were indistinguishable

from wild-type (data not shown). Thus, we hypothesise that induction of Foxp3 may be a primary event in the infection process, leading subsequently to effector cell anergy and the generation of alternatively activated macrophages. The possibility that Tregs at the site of infection drive alternatively activated macrophage differentiation is supported by a recent paper showing that in humans, alternatively activated marcrophages are induced after culture in the presence of activated Tregs (186).

It is interesting to note the lower susceptibility of IL4R-deficient mice to L3 infection, with significantly lower numbers of larvae recovered from the peritoneal cavity. This is at odds with a previous study (231), which showed significantly higher worm recovery from L3 *B. malayi* infected IL-4R$^{-/-}$ mice. This discrepancy could be accounted for by differences in timing, as the difference seen previously was not significant until 7 weeks post-infection. Therefore the possibility remains of increased resistance in IL-4R-deficient mice at early timepoints after infection, followed by a less productive response at later timepoints. The curtailed IL-10 in the IL4R-deficient genotype draws a parallel with the doubly-deficient IL-4/IL-10 construct which was found (unlike IL-4 single deficiency) to be resistant to *L. sigmodontis* (170). This outcome could reflect a more potent immune response, in the absence for example of suppressive macrophages, although the lack of an increased neutrophil recruitment or increased TH1 cytokines argues against this. An alternative explanation reflects the known requirement of filarial worms for host-derived growth-factors, in which IL-5 has been shown to have a role (232), as IL-5 is greatly reduced in the IL-4R-deficient mouse.

In order to look at direct Treg induction by L3 larvae *in vitro*, we assessed supernatants from live L3 *B. malayi* culture, or coculture with live L3 larvae for TGF-β activity. These results show that no significant levels of TGF-β are released by *B. malayi* in culture. Possible caveats include the culture conditions used, as *B. malayi* may only release TGF-β in the host. Also, the levels of TGF-β release may be too low to be detected in the assays used here, but may have significant effects when released over a long period *in vivo*.

Taken together, the results from this chapter indicate that the Treg induction seen in *B. malayi* infection depends on context, rather than antigen specificity (as Foxp3 could be induced to an irrelevant antigen at the site of infection), and that it is not dependent on alternatively activated macrophages. The results shown here indicate that host TGF-β is dispensable for Treg induction in this model, but the role of parasite TGF-β is yet to be elucidated.

Chapter 7:
Discussion

7. Discussion

Chronic helminth infections are still amongst the most important public health issues worldwide, with significant mortality and morbidity in developing countries. They affect the majority of the world's population, and as such are highly successful pathogens. Data from human studies (18) and animal models (12, 14-16) shows that anti-parasite immunity is possible, so some degree of immunomodulation must be present in all chronic helmith infections, however our understanding of the mechanisms is incomplete. The lack of damage to the host in most chronic helminth infections may be seen as an example of successful coevolution: the helminth is allowed to maintain a productive infection whilst the host remains asymptomatic.

In many ways, downregulation of host anti-parasite immune responses may be advantageous for both the parasite and the host, as it acts to minimise the 'collateral damage' of immunopathology in the host, and allows the parasite to evade potentially fatal immune responses. Evidence from studies using mice deficient in components of immune suppression pathways shows that in *S. mansoni* infection, lack of the immunosuppressive cytokine IL-10 leads to increased immunity to reinfection (27) but also increased mortality in primary infection due to immunopathology (28). In *L. major* infection, lack of IL-10 results in sterile immunity being achieved, but without a small number of persisting parasites immunity to reinfection was also lost (157). Thus, a balance must be struck between potentially disadvantageous immunopathology and control of parasite infection.

The disappearance of parasitic infections in first world countries has been associated with increased prevalence of allergy and autoimmunity. This association led to various forms of the 'hygiene hypothesis', suggesting that parasitic infection

suppresses not only parasite-directed immunopathology but also inappropriate immune responses (such as allergy, autoimmunity and inflammatory gut disorders) to bystander specificities. Epidemiological (3-6, 9) and interventional (7, 8, 25) studies added weight to this hypothesis, and animal models have helped to dissect the mechanism of suppression (22, 23).

Production of immunomodulatory molecules by parasites is one explanation of the downregulation of the host immune response, and parasite-derived TGF-β is an attractive candidate for this. Release of parasite-derived TGF-β could increase the proportion of circulating Tregs without regard to antigen specificity, so that any developing immune responses (for instance against inhaled allergens) would be more likely to be skewed towards regulation and tolerance rather than immune reactivity.

Members of the TGF-β family are present in non-parasitic nematodes such as *C. elegans*, therefore when a group of nematodes evolved from free-living animals into parasites this pre-existing, primarily developmental, pathway could have been co-opted as an immune evasion mechanism. Developmental roles for TGF-β molecules in parasitic nematodes have been proposed in many species (74, 76, 78), and the differences (if any) between a developmental TGF-β family member and an immunomodulatory TGF-β homologue may be very subtle. A developmental TGF-β homologue would act on tissues within the parasite, and therefore would not necessarily be secreted, however an immunomodulatory TGF-β homologue would have to be secreted from the parasite in order to act on the host. An immunomodulatory TGF-β homologue would also need to signal through the mammalian TGF-β receptor, whereas a developmental TGF-β family member would signal through a parasite-encoded TGF-β receptor. However, the TGF-β signalling

pathway may be conserved to such a degree that all TGF-β homologues can signal through other TGF-β receptors: potentially a TGF-β homologue could signal through both host and parasite receptors fulfilling both roles. It would seem to be more logical for the parasite to encode different TGF-β homologues for each function as they may need to be transcriptionally controlled separately – development and immunomodulation may not occur concurrently. However, in analysing the B. malayi genome there does not appear to have been any expansion in the number of TGF-β homologue gene loci (70), arguing that if Bm-TGH-2 is immunomodulatory it may also have retained some developmental function within the parasite.

Expression profiles provide important information about the function of TGF-β homologues, as we would expect immunomodulatory TGF-β homologues to be expressed only in stages that live within the host. Therefore, although the transcription profiles of the novel TGF-β homologues shown in chapter 3 give us some information about their function, it would be useful in future experiments to assess their transcription profiles in the free-living larval stages stages (L1 and L2 larvae). Information from various timepoints within each stage (as shown in Bm-TGH-1 (74)) would also be useful, as then something could be inferred from upregulation of the homologues just prior to moults.

Control of the activation of TGF-β homologues may also tell us something about their function - in mammalian TGF-β, the pro-protein is essential for correct folding and localisation of the protein, and prevents TGF-β binding the receptor until latent TGF-β is cleaved. If parasitic TGF-β family members function to control the development of the parasite, their activity would be expected to be just as tightly controlled as their mammalian counterparts. Therefore a truncation of the N-terminal

pro-region could result in uncontrolled activation of the proteins, which could have disastrous consequences for the parasite – if they function similarly to the *C. elegans* TGF-β homologue Ce-DAF-7, constant signalling would prevent entry into the dauer hibernative state (94), which has been hypothesised to be similar to the arrested L3 larvae of parasitic nematodes (76). Thus, worms lacking the pro-region of their TGF-β homologue could never develop to infective L3 larvae. Clearly this is not the case in the *N. brasiliensis* homologue identified here, and *S. mansoni* SmInAct, which both lack the majority of the pro-region. If however these TGF-β homologues serve to suppress the host immune system, they may not have a cognate receptor encoded by the parasite, and therefore constitutive activity after release would not be deleterious. Future work on these TGF-β homologues should focus on these areas in an attempt to dissect their function.

The *B. malayi* TGF-β homologue Bm-TGH-2 was previously shown to bind to the mammalian TGF-β receptor. The data presented here could not replicate this result, possibly due to the slightly different method of expression. However it proved to be useful as a method of expressing highly pure protein, and if modified, could be used to express other TGF-β homologues (such as the novel TGF-β homologues identified in chapter 3) for functional studies.

The *B. malayi* infection model provides a great deal of data regarding the role of Tregs during helminth infection, and may serve as a good model to study immunomodulation by helminths. The chief criticism of the *B. malayi* mouse model is that the mouse is not a fully tolerant host for *B. malayi*, and therefore death of the parasites may occur due to a lack of correct growth factors. Furthermore, following intraperitoneal infection *B. malayi* stays within the peritoneal cavity, whereas in the

human infection it migrates to the lymphatics. Thus, while *B. malayi* infection in mice may give us only limited insight into immune mediated killing of filarial parasites, the data presented in Chapters 5 and 6 offer important new information about the role of Tregs in this model.

The data presented here using the *B malayi* mouse model shows an accumulation of Tregs at the site of infection in the presence of live parasites. An important control in this model was the lack of Treg induction with injection or implantation of dead parasites, indicating Treg induction is an active process, depending on viable parasites. This correlates with the data from human infection, where drug-mediated killing of parasites results in loss of the hypoproliferative defect (38). The Treg accumulation dependence on viability of parasites is compatible with release of parasite-derived immunomodulators.

The DO11.10 adoptive transfer experiments show that *B. malayi* can induce Tregs with specificity for bystander antigens. As the DO11.10 response occurred within the peritoneal cavity, in direct contact with the anti-parasite response, this non-antigen specific Treg response could also depend on parasite-derived immunomodulators. Alternatively it could depend on Tregs induced to *B. malayi* antigens, releasing TGF-β which in turn induces Foxp3 within the DO11.10 population. In this respect, it would be interesting to deplete host Tregs in this model, by using DEREG mice. These mice express a diptheria toxin receptor (which is not expressed in wild-type mice) under the control of the *foxp3* promoter, so administration of diptheria toxin ablates all Tregs (233). If the DO11.10 Foxp3 induction is dependent on host Tregs, it should be ablated in their absence, with diptheria toxin administration in this model.

The data from infection of IL-4R-deficient mice indicates that Treg induction is unchanged in the absence of alternatively activated macrophages. This implies that although some of the suppressive effects of alternatively activated macrophages are dependent on their release of TGF-β (184), they are not responsible for Treg induction in this model. The possibility remains that alternatively activated macrophage induction is dependent on Tregs, especially given the recent report showing Tregs can induce alternatively activated macrophages *in vitro* (186). In order look at the order of events in *B. malayi* infection, it would be interesting to look for the presence of alternatively activated macrophages and Tregs at early timepoints (prior to day 7 post-infection). If proportions of Tregs increase prior to induction of alternatively activated macrophages, it would be consistent with alternatively activated macrophage induction by Tregs. Treg depletion experiments would also be informative in this regard, as without Tregs, but in the presence of a productive TH2 response (which would presumably still be present in the absence of Tregs), the relative roles of IL-4 production and Treg cytokines could be dissected.

All the above data are consistent with release of parasite immunomodulators which induce Tregs in the *B. malayi* infection model. I hypothesised that this Treg induction is dependent on parasite-derived TGF-β production, however other candidate parasite immunomodulators have been proposed. An interesting candidate immunomodulator is the lipid metabolite PGE2. PGE2 induces Foxp3 in human T cells, and increases the suppressive ability of Tregs (69). The filarial nematode *O. volvulus* and the trematode *S. mansoni* both produce PGE2, therefore this may be a further pathway of parasite immunomodulation (66, 67).

The role of parasite-derived TGF-βs in Treg induction was addressed, indirectly, using blocking antibodies to mammalian TGF-β. Anti-TGF-β treatment did not ablate Treg induction, but increased antigen specific cytokine responses. Therefore host TGF-β appears to be responsible for suppression of Teffector responses, but not Treg induction. As antibodies did not block parasite-derived TGF-β, blocking TGF-β signaling would be useful as it would block the effects of both host and parasite TGF-β. The ALK-5 inhibitor is a useful tool for these experiments, however it proved to be too toxic when injected intraperitoneally to give reliable results in my hands.

In order to show a direct link between Bm-TGH-2 and Treg induction by *B. malayi*, a number of strategies could be used. Infection of CD4-trophic TGF-βRII dominant negative mice (228) would definitively show if Treg induction is dependent on TGF-β signalling on the responding T cells, although this would not differentiate between host and parasite derived TGF-β. To look more directly at Bm-TGH-2, a number of methods could be used to block its action. Firstly, if functional Bm-TGH-2 were produced in insect cells, monoclonal antibodies could be raised against it and tested for ability to block the binding to the mammalian TGF-βR. The blocking anti-Bm-TGH-2 monoclonal antibody could then be used *in vivo* to see if this could block the Treg induction.

It would be most informative to prevent the parasite from expressing Bm-TGH-2, as this would show whether its role is immunomodulatory or developmental. Studies of nematode parasites are problematic as conventional knock-out strategies cannot be used, due to a lack of techniques for selecting transgenics, a long generation time, their complex lifecycles and the difficulty in introducing transgenes

into the parasite (234). However, the reverse genetic technique of RNAi has recently enabled the manipulation of nematode gene transcription. It involves introduction of double-stranded RNA (dsRNA) into nematode cells, which results in specific reduction in transcription of the gene encoded by the dsRNA. This can be transmitted for several generations. The process is carried out by cell defence mechanisms against attack of the host genome by viruses or transposable elements of genetic material (235). Successful RNAi has been reported in *B. malayi* (234), and has also previously been used to prevent expression of *S. mansoni* SmInAct, showing a developmental role (78). Therefore this technique could also be used to investigate the function of the other TGF-β homologues identified here.

If a direct link can be shown between parasite-derived TGF-β and the suppression of inappropriate immune responses seen in parasitic infection, it would have major implications for the hygiene hypothesis. If the reason that our immune systems are prone to inappropriate immune responses in the absence of parasitic infection is an insufficiency of TGF-β that can be supplemented by parasite derived TGF-β, it could be possible to redress the balance therapeutically by administration of host or parasite-derived TGF-β. This would be a more directed strategy of controlling inappropriate immune responses than infection with parasites in humans (25). The disadvantage of using parasitic infection are the possible side-effects, and the unpalatable connotations of parasitic infection. TGF-β administration may be a hazardous strategy, however, as it may suppress other non-pathological immune responses, resulting in decreased tumour surveillance, and susceptibility to infection.

The data presented in this thesis clearly demonstrate that members of the TGF-β family are commonly expressed among parasitic nematodes. It is also shown

that parasitic infection (in this case a mouse *B. malayi* model) results in induction of Tregs. Although a link has not been directly established between these two pieces of data, it can be hypothesised that TGF-β homologue production is a powerful method by which parasitic nematodes induce Tregs, thus downregulating the anti-parasite immune response and preventing ejection or killing of the parasites. The role of TGF-β homologues in the development of parasites and immunomodulation of the host has been the subject of some scrutiny, but these roles are still insufficiently characterised. Further work in this area may give important insights into parasite immunomodulation, and the roles of parasites in the development of the mammalian immune system.

References

1. Strachan, D. P. 1989. Hay fever, hygiene, and household size. *BMJ (Clinical research ed* 299:1259-1260.
2. Weinstock, J. V., R. W. Summers, and D. E. Elliott. 2005. Role of helminths in regulating mucosal inflammation. *Springer seminars in immunopathology* 27:249-271.
3. Tezel, A., G. Dokmeci, M. Eskiocak, H. Umit, and A. R. Soylu. 2003. Epidemiological features of ulcerative colitis in Trakya, Turkey. *The Journal of international medical research* 31:141-148.
4. Blanchard, J. F., C. N. Bernstein, A. Wajda, and P. Rawsthorne. 2001. Small-area variations and sociodemographic correlates for the incidence of Crohn's disease and ulcerative colitis. *American journal of epidemiology* 154:328-335.
5. Bodansky, H. J., A. Staines, C. Stephenson, D. Haigh, and R. Cartwright. 1992. Evidence for an environmental effect in the aetiology of insulin dependent diabetes in a transmigratory population. *BMJ (Clinical research ed* 304:1020-1022.
6. Cardwell, C. R., D. J. Carson, and C. C. Patterson. 2007. Secular trends, disease maps and ecological analyses of the incidence of childhood onset Type 1 diabetes in Northern Ireland, 1989-2003. *Diabet Med* 24:289-295.
7. Lynch, N. R., I. Hagel, M. Perez, M. C. Di Prisco, R. Lopez, and N. Alvarez. 1993. Effect of anthelmintic treatment on the allergic reactivity of children in a tropical slum. *The Journal of allergy and clinical immunology* 92:404-411.
8. van den Biggelaar, A. H., L. C. Rodrigues, R. van Ree, J. S. van der Zee, Y. C. Hoeksma-Kruize, J. H. Souverijn, M. A. Missinou, S. Borrmann, P. G. Kremsner, and M. Yazdanbakhsh. 2004. Long-term treatment of intestinal helminths increases mite skin-test reactivity in Gabonese schoolchildren. *J Infect Dis* 189:892-900.
9. Wordemann, M., R. J. Diaz, L. M. Heredia, A. M. Collado Madurga, A. Ruiz Espinosa, R. C. Prado, I. A. Millan, A. Escobedo, L. Rojas Rivero, B. Gryseels, M. B. Gorbea, and K. Polman. 2008. Association of atopy, asthma, allergic rhinoconjunctivitis, atopic dermatitis and intestinal helminth infections in Cuban children. *Trop Med Int Health* 13:180-186.
10. Yazdanbakhsh, M. 1999. Common features of T cell reactivity in persistent helminth infections: lymphatic filariasis and schistosomiasis. *Immunology letters* 65:109-115.
11. Else, K. J. 2005. Have gastrointestinal nematodes outwitted the immune system? *Parasite Immunol* 27:407-415.
12. Urban, J. F., Jr., C. R. Maliszewski, K. B. Madden, I. M. Katona, and F. D. Finkelman. 1995. IL-4 treatment can cure established gastrointestinal nematode infections in immunocompetent and immunodeficient mice. *J Immunol* 154:4675-4684.
13. Garside, P., M. W. Kennedy, D. Wakelin, and C. E. Lawrence. 2000. Immunopathology of intestinal helminth infection. *Parasite Immunol* 22:605-612.
14. Maizels, R. M., and M. J. Holland. 1998. Parasite immunology: pathways for expelling intestinal helminths. *Curr Biol* 8:R711-714.

15. Finkelman, F. D., T. Shea-Donohue, S. C. Morris, L. Gildea, R. Strait, K. B. Madden, L. Schopf, and J. F. Urban, Jr. 2004. Interleukin-4- and interleukin-13-mediated host protection against intestinal nematode parasites. *Immunol Rev* 201:139-155.
16. Herbert, D. R., T. Orekov, C. Perkins, M. E. Rothenberg, and F. D. Finkelman. 2008. IL-4R{alpha} Expression by Bone Marrow-Derived Cells Is Necessary and Sufficient for Host Protection against Acute Schistosomiasis. *J Immunol* 180:4948-4955.
17. Urban, J. F., Jr., N. Noben-Trauth, L. Schopf, K. B. Madden, and F. D. Finkelman. 2001. Cutting edge: IL-4 receptor expression by non-bone marrow-derived cells is required to expel gastrointestinal nematode parasites. *J Immunol* 167:6078-6081.
18. Jackson, J. A., J. D. Turner, L. Rentoul, H. Faulkner, J. M. Behnke, M. Hoyle, R. K. Grencis, K. J. Else, J. Kamgno, M. Boussinesq, and J. E. Bradley. 2004. T helper cell type 2 responsiveness predicts future susceptibility to gastrointestinal nematodes in humans. *J Infect Dis* 190:1804-1811.
19. Forrester, D. J. 1971. Heligmosomoides polygyrus (=Nematospiroides dubius) from wild rodents of northern California: natural infections, host specificity, and strain characteristics. *The Journal of parasitology* 57:498-503.
20. Monroy, F. G., and F. J. Enriquez. 1992. Heligmosomoides polygyrus: a model for chronic gastrointestinal helminthiasis. *Parasitol Today* 8:49-54.
21. Finney, C. A., M. D. Taylor, M. S. Wilson, and R. M. Maizels. 2007. Expansion and activation of CD4(+)CD25(+) regulatory T cells in Heligmosomoides polygyrus infection. *Eur J Immunol* 37:1874-1886.
22. Wilson, M. S., M. D. Taylor, A. Balic, C. A. Finney, J. R. Lamb, and R. M. Maizels. 2005. Suppression of allergic airway inflammation by helminth-induced regulatory T cells. *J Exp Med* 202:1199-1212.
23. Elliott, D. E., T. Setiawan, A. Metwali, A. Blum, J. F. Urban, Jr., and J. V. Weinstock. 2004. Heligmosomoides polygyrus inhibits established colitis in IL-10-deficient mice. *Eur J Immunol* 34:2690-2698.
24. Weng, M., D. Huntley, I. F. Huang, O. Foye-Jackson, L. Wang, A. Sarkissian, Q. Zhou, W. A. Walker, B. J. Cherayil, and H. N. Shi. 2007. Alternatively activated macrophages in intestinal helminth infection: effects on concurrent bacterial colitis. *J Immunol* 179:4721-4731.
25. Summers, R. W., D. E. Elliott, K. Qadir, J. F. Urban, Jr., R. Thompson, and J. V. Weinstock. 2003. Trichuris suis seems to be safe and possibly effective in the treatment of inflammatory bowel disease. *The American journal of gastroenterology* 98:2034-2041.
26. Belkaid, Y., and B. T. Rouse. 2005. Natural regulatory T cells in infectious disease. *Nat Immunol* 6:353-360.
27. Hoffmann, K. F., S. L. James, A. W. Cheever, and T. A. Wynn. 1999. Studies with double cytokine-deficient mice reveal that highly polarized Th1- and Th2-type cytokine and antibody responses contribute equally to vaccine-induced immunity to Schistosoma mansoni. *J Immunol* 163:927-938.
28. Hoffmann, K. F., A. W. Cheever, and T. A. Wynn. 2000. IL-10 and the dangers of immune polarization: excessive type 1 and type 2 cytokine

responses induce distinct forms of lethal immunopathology in murine schistosomiasis. *J Immunol* 164:6406-6416.
29. Taylor, J. J., M. Mohrs, and E. J. Pearce. 2006. Regulatory T cell responses develop in parallel to Th responses and control the magnitude and phenotype of the Th effector population. *J Immunol* 176:5839-5847.
30. Melrose, W. D. 2002. Lymphatic filariasis: new insights into an old disease. *Int J Parasitol* 32:947-960.
31. Malhotra, I., J. H. Ouma, A. Wamachi, J. Kioko, P. Mungai, M. Njzovu, J. W. Kazura, and C. L. King. 2003. Influence of maternal filariasis on childhood infection and immunity to Wuchereria bancrofti in Kenya. *Infect Immun* 71:5231-5237.
32. Lawrence, R. A. 2001. Immunity to filarial nematodes. *Vet Parasitol* 100:33-44.
33. Rajagopalan, P. K., P. K. Das, S. Subramanian, P. Vanamail, and K. D. Ramaiah. 1989. Bancroftian filariasis in Pondicherry, south India: 1. Pre-control epidemiological observations. *Epidemiology and infection* 103:685-692.
34. Stolk, W. A., K. D. Ramaiah, G. J. Van Oortmarssen, P. K. Das, J. D. F. Habbema, and S. J. De Vlas. 2004. Meta-analysis of age-prevalence patterns in lymphatic filariasis: no decline in microfilaraemia prevalence in older age groups as predicted by models with acquired immunity. *Parasitology* 129:605-612.
35. Nutman, T. B., V. Kumaraswami, and E. A. Ottesen. 1987. Parasite-specific anergy in human filariasis. Insights after analysis of parasite antigen-driven lymphokine production. *Journal of Clinical Investigation* 79:1516-1523.
36. Piessens, W. F., P. B. McGreevy, P. W. Piessens, M. McGreevy, I. Koiman, J. S. Saroso, and D. T. Dennis. 1980. Immune responses in human infections with *Brugia malayi.* Specific cellular unresponsiveness to filarial antigens. *Journal of Clinical Investigation* 65:172-179.
37. King, C. L., V. Kumaraswami, R. W. Poindexter, S. Kumari, K. Jayaraman, D. W. Alling, E. A. Ottesen, and T. B. Nutman. 1992. Immunologic tolerance in lymphatic filariasis. Diminished parasite-specific T and B cell lymphocyte precursor frequency in the microfilaremic state. *Journal of Clinical Investigation* 89:1403-1410.
38. Sartono, E., Y. C. M. Kruize, A. Kurniawan, P. H. van der Meide, F. Partono, R. M. Maizels, and M. Yazdanbakhsh. 1995. Elevated cellular responses and interferon-γ release after long-term diethylcarbamazine treatment of patients with human lymphatic filariasis. *Journal of Infectious Diseases* 171:1683-1687.
39. Sartono, E., Y. C. M. Kruize, A. Kurniawan-Atmadja, R. M. Maizels, and M. Yazdanbakhsh. 1997. Depression of antigen-specific interleukin-5 and interferon-γ responses in human lymphatic filariasis as a function of clinical status and age. *Journal of Infectious Diseases* 175:1276-1280.
40. Semnani, R. T., M. Law, J. Kubofcik, and T. B. Nutman. 2004. Filaria-induced immune evasion: suppression by the infective stage of Brugia malayi at the earliest host-parasite interface. *J Immunol* 172:6229-6238.
41. Ohl, L., M. Mohaupt, N. Czeloth, G. Hintzen, Z. Kiafard, J. Zwirner, T. Blankenstein, G. Henning, and R. Forster. 2004. CCR7 governs skin dendritic

cell migration under inflammatory and steady-state conditions. *Immunity* 21:279-288.
42. O'Connor, R. A., J. S. Jenson, J. Osborne, and E. Devaney. 2003. An enduring association? Microfilariae and immunosuppression [correction of immunosupression] in lymphatic filariasis. *Trends Parasitol* 19:565-570.
43. Semnani, R. T., A. Y. Liu, H. Sabzevari, J. Kubofcik, J. Zhou, J. K. Gilden, and T. B. Nutman. 2003. Brugia malayi microfilariae induce cell death in human dendritic cells, inhibit their ability to make IL-12 and IL-10, and reduce their capacity to activate CD4+ T cells. *J Immunol* 171:1950-1960.
44. Babu, S., C. P. Blauvelt, and T. B. Nutman. 2007. Filarial parasites induce NK cell activation, type 1 and type 2 cytokine secretion, and subsequent apoptotic cell death. *J Immunol* 179:2445-2456.
45. Babu, S., C. P. Blauvelt, V. Kumaraswami, and T. B. Nutman. 2006. Regulatory networks induced by live parasites impair both Th1 and th2 pathways in patent lymphatic filariasis: implications for parasite persistence. *J Immunol* 176:3248-3256.
46. Miller, S., D. Schreuer, and B. Hammerberg. 1991. Inhibition of antigen-driven proliferative responses and enhancement of antibody production during infection with Brugia pahangi. *J Immunol* 147:1007-1013.
47. Allen, J. E., and A. S. MacDonald. 1998. Profound suppression of cellular proliferation mediated by the secretions of nematodes. *Parasite Immunol* 20:241-247.
48. Loke, P., M. G. Nair, J. Parkinson, D. Guiliano, M. Blaxter, and J. E. Allen. 2002. IL-4 dependent alternatively-activated macrophages have a distinctive in vivo gene expression phenotype. *BMC Immunol* 3:7.
49. Balic, A., Y. Harcus, M. J. Holland, and R. M. Maizels. 2004. Selective maturation of dendritic cells by Nippostrongylus brasiliensis-secreted proteins drives Th2 immune responses. *Eur J Immunol* 34:3047-3059.
50. Vieira, L. Q., G. Gazzinelli, J. R. Kusel, C. P. De Souza, and D. G. Colley. 1986. Inhibition of human peripheral blood mononuclear cell proliferative responses by released materials from Schistosoma mansoni cercariae. *Parasite Immunol* 8:333-343.
51. Jenkins, S. J., and A. P. Mountford. 2005. Dendritic cells activated with products released by schistosome larvae drive Th2-type immune responses, which can be inhibited by manipulation of CD40 costimulation. *Infect Immun* 73:395-402.
52. Wilson, E. H., M. R. Deehan, E. Katz, K. S. Brown, K. M. Houston, J. O'Grady, M. M. Harnett, and W. Harnett. 2003. Hyporesponsiveness of murine B lymphocytes exposed to the filarial nematode secreted product ES-62 in vivo. *Immunology* 109:238-245.
53. Harnett, W., M. R. Deehan, K. M. Houston, and M. M. Harnett. 1999. Immunomodulatory properties of a phosphorylcholine-containing secreted filarial glycoprotein. *Parasite Immunol* 21:601-608.
54. Lal, R. B., V. Kumaraswami, C. Steel, and T. B. Nutman. 1990. Phosphocholine-containing antigens of Brugia malayi nonspecifically suppress lymphocyte function. *The American journal of tropical medicine and hygiene* 42:56-64.

55. van der Kleij, D., E. Latz, J. F. Brouwers, Y. C. Kruize, M. Schmitz, E. A. Kurt-Jones, T. Espevik, E. C. de Jong, M. L. Kapsenberg, D. T. Golenbock, A. G. Tielens, and M. Yazdanbakhsh. 2002. A novel host-parasite lipid cross-talk. Schistosomal lyso-phosphatidylserine activates toll-like receptor 2 and affects immune polarization. *J Biol Chem* 277:48122-48129.
56. Maizels, R. M., M. L. Blaxter, and A. L. Scott. 2001. Immunological genomics of Brugia malayi: filarial genes implicated in immune evasion and protective immunity. *Parasite Immunol* 23:327-344.
57. Tang, L., K. Gounaris, C. Griffiths, and M. E. Selkirk. 1995. Heterologous expression and enzymatic properties of a selenium-independent glutathione peroxidase from the parasitic nematode Brugia pahangi. *J Biol Chem* 270:18313-18318.
58. Tang, L., X. Ou, K. Henkle-Duhrsen, and M. E. Selkirk. 1994. Extracellular and cytoplasmic CuZn superoxide dismutases from Brugia lymphatic filarial nematode parasites. *Infect Immun* 62:961-967.
59. Selkirk, M. E., V. P. Smith, G. R. Thomas, and K. Gounaris. 1998. Resistance of filarial nematode parasites to oxidative stress. *Int J Parasitol* 28:1315-1332.
60. Pastrana, D. V., N. Raghavan, P. FitzGerald, S. W. Eisinger, C. Metz, R. Bucala, R. P. Schleimer, C. Bickel, and A. L. Scott. 1998. Filarial nematode parasites secrete a homologue of the human cytokine macrophage migration inhibitory factor. *Infect Immun* 66:5955-5963.
61. Falcone, F. H., P. Loke, X. Zang, A. S. MacDonald, R. M. Maizels, and J. E. Allen. 2001. A Brugia malayi homolog of macrophage migration inhibitory factor reveals an important link between macrophages and eosinophil recruitment during nematode infection. *J Immunol* 167:5348-5354.
62. Manoury, B., W. F. Gregory, R. M. Maizels, and C. Watts. 2001. Bm-CPI-2, a cystatin homolog secreted by the filarial parasite Brugia malayi, inhibits class II MHC-restricted antigen processing. *Curr Biol* 11:447-451.
63. Schierack, P., R. Lucius, B. Sonnenburg, K. Schilling, and S. Hartmann. 2003. Parasite-specific immunomodulatory functions of filarial cystatin. *Infect Immun* 71:2422-2429.
64. Hartmann, S., and R. Lucius. 2003. Modulation of host immune responses by nematode cystatins. *Int J Parasitol* 33:1291-1302.
65. Herve, M., V. Angeli, E. Pinzar, R. Wintjens, C. Faveeuw, S. Narumiya, A. Capron, Y. Urade, M. Capron, G. Riveau, and F. Trottein. 2003. Pivotal roles of the parasite PGD2 synthase and of the host D prostanoid receptor 1 in schistosome immune evasion. *Eur J Immunol* 33:2764-2772.
66. Ramaswamy, K., P. Kumar, and Y. X. He. 2000. A role for parasite-induced PGE2 in IL-10-mediated host immunoregulation by skin stage schistosomula of Schistosoma mansoni. *J Immunol* 165:4567-4574.
67. Brattig, N. W., A. Schwohl, R. Rickert, and D. W. Buttner. 2006. The filarial parasite Onchocerca volvulus generates the lipid mediator prostaglandin E(2). *Microbes Infect* 8:873-879.
68. von Bergwelt-Baildon, M. S., A. Popov, T. Saric, J. Chemnitz, S. Classen, M. S. Stoffel, F. Fiore, U. Roth, M. Beyer, S. Debey, C. Wickenhauser, F. G. Hanisch, and J. L. Schultze. 2006. CD25 and indoleamine 2,3-dioxygenase are up-regulated by prostaglandin E2 and expressed by tumor-associated

dendritic cells in vivo: additional mechanisms of T-cell inhibition. *Blood* 108:228-237.

69. Baratelli, F., Y. Lin, L. Zhu, S. C. Yang, N. Heuze-Vourc'h, G. Zeng, K. Reckamp, M. Dohadwala, S. Sharma, and S. M. Dubinett. 2005. Prostaglandin E2 induces FOXP3 gene expression and T regulatory cell function in human CD4+ T cells. *J Immunol* 175:1483-1490.
70. Ghedin, E., S. Wang, D. Spiro, E. Caler, Q. Zhao, J. Crabtree, J. E. Allen, A. L. Delcher, D. B. Guiliano, D. Miranda-Saavedra, S. V. Angiuoli, T. Creasy, P. Amedeo, B. Haas, N. M. El-Sayed, J. R. Wortman, T. Feldblyum, L. Tallon, M. Schatz, M. Shumway, H. Koo, S. L. Salzberg, S. Schobel, M. Pertea, M. Pop, O. White, G. J. Barton, C. K. Carlow, M. J. Crawford, J. Daub, M. W. Dimmic, C. F. Estes, J. M. Foster, M. Ganatra, W. F. Gregory, N. M. Johnson, J. Jin, R. Komuniecki, I. Korf, S. Kumar, S. Laney, B. W. Li, W. Li, T. H. Lindblom, S. Lustigman, D. Ma, C. V. Maina, D. M. Martin, J. P. McCarter, L. McReynolds, M. Mitreva, T. B. Nutman, J. Parkinson, J. M. Peregrin-Alvarez, C. Poole, Q. Ren, L. Saunders, A. E. Sluder, K. Smith, M. Stanke, T. R. Unnasch, J. Ware, A. D. Wei, G. Weil, D. J. Williams, Y. Zhang, S. A. Williams, C. Fraser-Liggett, B. Slatko, M. L. Blaxter, and A. L. Scott. 2007. Draft genome of the filarial nematode parasite Brugia malayi. *Science* 317:1756-1760.
71. Haas, B. J., M. Berriman, H. Hirai, G. G. Cerqueira, P. T. Loverde, and N. M. El-Sayed. 2007. Schistosoma mansoni genome: closing in on a final gene set. *Exp Parasitol* 117:225-228.
72. Mucida, D., Y. Park, G. Kim, O. Turovskaya, I. Scott, M. Kronenberg, and H. Cheroutre. 2007. Reciprocal TH17 and regulatory T cell differentiation mediated by retinoic acid. *Science* 317:256-260.
73. Toscano, M. A., G. A. Bianco, J. M. Ilarregui, D. O. Croci, J. Correale, J. D. Hernandez, N. W. Zwirner, F. Poirier, E. M. Riley, L. G. Baum, and G. A. Rabinovich. 2007. Differential glycosylation of TH1, TH2 and TH-17 effector cells selectively regulates susceptibility to cell death. *Nat Immunol* 8:825-834.
74. Gomez-Escobar, N., E. Lewis, and R. M. Maizels. 1998. A novel member of the transforming growth factor-beta (TGF-beta) superfamily from the filarial nematodes Brugia malayi and B. pahangi. *Exp Parasitol* 88:200-209.
75. Gomez-Escobar, N., W. F. Gregory, and R. M. Maizels. 2000. Identification of *Bm-tgh-2*, a filarial nematode homolog of *C.elegans daf-7* and human TGF-β, expressed in microfilarial and adult stages of *Brugia malayi. Infection and Immunity* 68:6402-6410.
76. Freitas, T. C., and P. Arasu. 2005. Cloning and characterisation of genes encoding two transforming growth factor-beta-like ligands from the hookworm, Ancylostoma caninum. *Int J Parasitol* 35:1477-1487.
77. Massey, H. C., M. L. Castelletto, V. M. Bhopale, G. A. Schad, and J. B. Lok. 2005. Sst-tgh-1 from Strongyloides stercoralis encodes a proposed ortholog of daf-7 in Caenorhabditis elegans. *Mol Biochem Parasitol* 142:116-120.
78. Freitas, T. C., E. Jung, and E. J. Pearce. 2007. TGF-beta Signaling Controls Embryo Development in the Parasitic Flatworm Schistosoma mansoni. *PLoS Pathog* 3:e52.

79. Moses, H. L., E. L. Branum, J. A. Proper, and R. A. Robinson. 1981. Transforming growth factor production by chemically transformed cells. *Cancer research* 41:2842-2848.
80. Anzano, M. A., A. B. Roberts, J. M. Smith, M. B. Sporn, and J. E. De Larco. 1983. Sarcoma growth factor from conditioned medium of virally transformed cells is composed of both type alpha and type beta transforming growth factors. *Proceedings of the National Academy of Sciences of the United States of America* 80:6264-6268.
81. Assoian, R. K., A. Komoriya, C. A. Meyers, D. M. Miller, and M. B. Sporn. 1983. Transforming growth factor-beta in human platelets. Identification of a major storage site, purification, and characterization. *J Biol Chem* 258:7155-7160.
82. Massague, J. 1990. The transforming growth factor-beta family. *Annual review of cell biology* 6:597-641.
83. Rahimi, R. A., and E. B. Leof. 2007. TGF-beta signaling: A tale of two responses. *Journal of cellular biochemistry* 102:593-608.
84. Wahl, S. M., J. Wen, and N. Moutsopoulos. 2006. TGF-beta: a mobile purveyor of immune privilege. *Immunol Rev* 213:213-227.
85. Annes, J. P., J. S. Munger, and D. B. Rifkin. 2003. Making sense of latent TGFbeta activation. *Journal of cell science* 116:217-224.
86. Cheifetz, S., A. Bassols, K. Stanley, M. Ohta, J. Greenberger, and J. Massague. 1988. Heterodimeric transforming growth factor beta. Biological properties and interaction with three types of cell surface receptors. *J Biol Chem* 263:10783-10789.
87. Yang, Z., Z. Mu, B. Dabovic, V. Jurukovski, D. Yu, J. Sung, X. Xiong, and J. S. Munger. 2007. Absence of integrin-mediated TGFbeta1 activation in vivo recapitulates the phenotype of TGFbeta1-null mice. *The Journal of cell biology* 176:787-793.
88. Lawler, J., M. Sunday, V. Thibert, M. Duquette, E. L. George, H. Rayburn, and R. O. Hynes. 1998. Thrombospondin-1 is required for normal murine pulmonary homeostasis and its absence causes pneumonia. *J Clin Invest* 101:982-992.
89. Travis, M. A., B. Reizis, A. C. Melton, E. Masteller, Q. Tang, J. M. Proctor, Y. Wang, X. Bernstein, X. Huang, L. F. Reichardt, J. A. Bluestone, and D. Sheppard. 2007. Loss of integrin alpha(v)beta8 on dendritic cells causes autoimmunity and colitis in mice. *Nature* 449:361-365.
90. ten Dijke, P., and C. S. Hill. 2004. New insights into TGF-beta-Smad signalling. *Trends Biochem Sci* 29:265-273.
91. Nakao, A., M. Afrakhte, A. Moren, T. Nakayama, J. L. Christian, R. Heuchel, S. Itoh, M. Kawabata, N. E. Heldin, C. H. Heldin, and P. ten Dijke. 1997. Identification of Smad7, a TGFbeta-inducible antagonist of TGF-beta signalling. *Nature* 389:631-635.
92. Wan, Y. Y., and R. A. Flavell. 2007. 'Yin-Yang' functions of transforming growth factor-beta and T regulatory cells in immune regulation. *Immunol Rev* 220:199-213.
93. Oshima, Y., T. Sakamoto, T. Hisatomi, C. Tsutsumi, H. Ueno, and T. Ishibashi. 2002. Gene transfer of soluble TGF-beta type II receptor inhibits experimental proliferative vitreoretinopathy. *Gene therapy* 9:1214-1220.

94. Savage-Dunn, C. 2005. TGF-beta signaling. *WormBook*:1-12.
95. Ren, P., C. S. Lim, R. Johnsen, P. S. Albert, D. Pilgrim, and D. L. Riddle. 1996. Control of C. elegans larval development by neuronal expression of a TGF-beta homolog. *Science* 274:1389-1391.
96. Gomez-Escobar, N., W. F. Gregory, and R. M. Maizels. 2000. Identification of tgh-2, a filarial nematode homolog of Caenorhabditis elegans daf-7 and human transforming growth factor beta, expressed in microfilarial and adult stages of Brugia malayi. *Infect Immun* 68:6402-6410.
97. Arasu, P. 2001. In vitro reactivation of Ancylostoma caninum tissue-arrested third-stage larvae by transforming growth factor-beta. *The Journal of parasitology* 87:733-738.
98. Islam, K. B., L. Nilsson, P. Sideras, L. Hammarstrom, and C. I. Smith. 1991. TGF-beta 1 induces germ-line transcripts of both IgA subclasses in human B lymphocytes. *Int Immunol* 3:1099-1106.
99. Robinson, P. W., S. J. Green, C. Carter, J. Coadwell, and P. J. Kilshaw. 2001. Studies on transcriptional regulation of the mucosal T-cell integrin alphaEbeta7 (CD103). *Immunology* 103:146-154.
100. Laouar, Y., F. S. Sutterwala, L. Gorelik, and R. A. Flavell. 2005. Transforming growth factor-beta controls T helper type 1 cell development through regulation of natural killer cell interferon-gamma. *Nat Immunol* 6:600-607.
101. Naiki, Y., K. S. Michelsen, W. Zhang, S. Chen, T. M. Doherty, and M. Arditi. 2005. Transforming growth factor-beta differentially inhibits MyD88-dependent, but not TRAM- and TRIF-dependent, lipopolysaccharide-induced TLR4 signaling. *J Biol Chem* 280:5491-5495.
102. Mendez-Samperio, P., M. Hernandez-Garay, and E. Garcia-Martinez. 2000. Induction of apoptosis in bacillus Calmette-Guerin-activated T cells by transforming growth factor-beta. *Cell Immunol* 202:103-112.
103. Fu, S., N. Zhang, A. C. Yopp, D. Chen, M. Mao, H. Zhang, Y. Ding, and J. S. Bromberg. 2004. TGF-beta Induces Foxp3 + T-Regulatory Cells from CD4 + CD25 - Precursors. *Am J Transplant* 4:1614-1627.
104. Bettelli, E., Y. Carrier, W. Gao, T. Korn, T. B. Strom, M. Oukka, H. L. Weiner, and V. K. Kuchroo. 2006. Reciprocal developmental pathways for the generation of pathogenic effector TH17 and regulatory T cells. *Nature* 441:235-238.
105. Ahmadzadeh, M., and S. A. Rosenberg. 2005. TGF-beta 1 attenuates the acquisition and expression of effector function by tumor antigen-specific human memory CD8 T cells. *J Immunol* 174:5215-5223.
106. Smyth, M. J., S. L. Strobl, H. A. Young, J. R. Ortaldo, and A. C. Ochoa. 1991. Regulation of lymphokine-activated killer activity and pore-forming protein gene expression in human peripheral blood CD8+ T lymphocytes. Inhibition by transforming growth factor-beta. *J Immunol* 146:3289-3297.
107. Kleinschek, M. A., A. M. Owyang, B. Joyce-Shaikh, C. L. Langrish, Y. Chen, D. M. Gorman, W. M. Blumenschein, T. McClanahan, F. Brombacher, S. D. Hurst, R. A. Kastelein, and D. J. Cua. 2007. IL-25 regulates Th17 function in autoimmune inflammation. *J Exp Med* 204:161-170.
108. Mangan, P. R., L. E. Harrington, D. B. O'Quinn, W. S. Helms, D. C. Bullard, C. O. Elson, R. D. Hatton, S. M. Wahl, T. R. Schoeb, and C. T. Weaver.

2006. Transforming growth factor-beta induces development of the T(H)17 lineage. *Nature* 441:231-234.
109. Hue, S., P. Ahern, S. Buonocore, M. C. Kullberg, D. J. Cua, B. S. McKenzie, F. Powrie, and K. J. Maloy. 2006. Interleukin-23 drives innate and T cell-mediated intestinal inflammation. *J Exp Med* 203:2473-2483.
110. Gershon, R. K., and K. Kondo. 1970. Cell interactions in the induction of tolerance: the role of thymic lymphocytes. *Immunology* 18:723-737.
111. Nishizuka, Y., and T. Sakakura. 1969. Thymus and reproduction: sex-linked dysgenesia of the gonad after neonatal thymectomy in mice. *Science* 166:753-755.
112. Asano, M., M. Toda, N. Sakaguchi, and S. Sakaguchi. 1996. Autoimmune disease as a consequence of developmental abnormality of a T cell subpopulation. *J Exp Med* 184:387-396.
113. Sakaguchi, S., K. Wing, and M. Miyara. 2007. Regulatory T cells - a brief history and perspective. *Eur J Immunol* 37 Suppl 1:S116-123.
114. Asseman, C., S. Fowler, and F. Powrie. 2000. Control of experimental inflammatory bowel disease by regulatory T cells. *Am J Respir Crit Care Med* 162:S185-189.
115. Takahashi, T., T. Tagami, S. Yamazaki, T. Uede, J. Shimizu, N. Sakaguchi, T. W. Mak, and S. Sakaguchi. 2000. Immunologic self-tolerance maintained by CD25(+)CD4(+) regulatory T cells constitutively expressing cytotoxic T lymphocyte-associated antigen 4. *J Exp Med* 192:303-310.
116. Nakamura, K., A. Kitani, and W. Strober. 2001. Cell contact-dependent immunosuppression by CD4(+)CD25(+) regulatory T cells is mediated by cell surface-bound transforming growth factor beta. *J Exp Med* 194:629-644.
117. Shimizu, J., S. Yamazaki, T. Takahashi, Y. Ishida, and S. Sakaguchi. 2002. Stimulation of CD25(+)CD4(+) regulatory T cells through GITR breaks immunological self-tolerance. *Nat Immunol* 3:135-142.
118. Hori, S., T. Nomura, and S. Sakaguchi. 2003. Control of regulatory T cell development by the transcription factor Foxp3. *Science* 299:1057-1061.
119. Huang, C. T., C. J. Workman, D. Flies, X. Pan, A. L. Marson, G. Zhou, E. L. Hipkiss, S. Ravi, J. Kowalski, H. I. Levitsky, J. D. Powell, D. M. Pardoll, C. G. Drake, and D. A. Vignali. 2004. Role of LAG-3 in Regulatory T Cells. *Immunity* 21:503-513.
120. Suffia, I., S. K. Reckling, G. Salay, and Y. Belkaid. 2005. A role for CD103 in the retention of CD4+CD25+ Treg and control of Leishmania major infection. *J Immunol* 174:5444-5455.
121. Raimondi, G., W. J. Shufesky, D. Tokita, A. E. Morelli, and A. W. Thomson. 2006. Regulated compartmentalization of programmed cell death-1 discriminates CD4+CD25+ resting regulatory T cells from activated T cells. *J Immunol* 176:2808-2816.
122. Collison, L. W., C. J. Workman, T. T. Kuo, K. Boyd, Y. Wang, K. M. Vignali, R. Cross, D. Sehy, R. S. Blumberg, and D. A. Vignali. 2007. The inhibitory cytokine IL-35 contributes to regulatory T-cell function. *Nature* 450:566-569.
123. Waterhouse, P., J. M. Penninger, E. Timms, A. Wakeham, A. Shahinian, K. P. Lee, C. B. Thompson, H. Griesser, and T. W. Mak. 1995.

Lymphoproliferative disorders with early lethality in mice deficient in Ctla-4. *Science* 270:985-988.

124. Piganelli, J. D., M. Poulin, T. Martin, J. P. Allison, and K. Haskins. 2000. Cytotoxic T lymphocyte antigen 4 (CD152) regulates self-reactive T cells in BALB/c but not in the autoimmune NOD mouse. *Journal of autoimmunity* 14:123-131.
125. Li, R., N. Perez, S. Karumuthil-Melethil, B. S. Prabhakar, M. J. Holterman, and C. Vasu. 2007. Enhanced engagement of CTLA-4 induces antigen-specific CD4+CD25+Foxp3+ and CD4+CD25 TGF-beta1+ adaptive regulatory T cells. *J Immunol* 179:5191-5203.
126. Mellor, A. L., and D. H. Munn. 2004. Ido expression by dendritic cells: tolerance and tryptophan catabolism. *Nat Rev Immunol* 4:762-774.
127. Zheng, S. G., J. H. Wang, W. Stohl, K. S. Kim, J. D. Gray, and D. A. Horwitz. 2006. TGF-beta Requires CTLA-4 Early after T Cell Activation to Induce FoxP3 and Generate Adaptive CD4+CD25+ Regulatory Cells. *J Immunol* 176:3321-3329.
128. Stephens, G. L., R. S. McHugh, M. J. Whitters, D. A. Young, D. Luxenberg, B. M. Carreno, M. Collins, and E. M. Shevach. 2004. Engagement of glucocorticoid-induced TNFR family-related receptor on effector T cells by its ligand mediates resistance to suppression by CD4+CD25+ T cells. *J Immunol* 173:5008-5020.
129. Ji, H. B., G. Liao, W. A. Faubion, A. C. Abadia-Molina, C. Cozzo, F. S. Laroux, A. Caton, and C. Terhorst. 2004. Cutting edge: the natural ligand for glucocorticoid-induced TNF receptor-related protein abrogates regulatory T cell suppression. *J Immunol* 172:5823-5827.
130. Brunkow, M. E., E. W. Jeffery, K. A. Hjerrild, B. Paeper, L. B. Clark, S. A. Yasayko, J. E. Wilkinson, D. Galas, S. F. Ziegler, and F. Ramsdell. 2001. Disruption of a new forkhead/winged-helix protein, scurfin, results in the fatal lymphoproliferative disorder of the scurfy mouse. *Nature genetics* 27:68-73.
131. Walker, M. R., D. J. Kasprowicz, V. H. Gersuk, A. Benard, M. Van Landeghen, J. H. Buckner, and S. F. Ziegler. 2003. Induction of FoxP3 and acquisition of T regulatory activity by stimulated human CD4+CD25- T cells. *J Clin Invest* 112:1437-1443.
132. Wu, Y., M. Borde, V. Heissmeyer, M. Feuerer, A. D. Lapan, J. C. Stroud, D. L. Bates, L. Guo, A. Han, S. F. Ziegler, D. Mathis, C. Benoist, L. Chen, and A. Rao. 2006. FOXP3 controls regulatory T cell function through cooperation with NFAT. *Cell* 126:375-387.
133. Li, N., Y. Wang, K. Forbes, K. M. Vignali, B. S. Heale, P. Saftig, D. Hartmann, R. A. Black, J. J. Rossi, C. P. Blobel, P. J. Dempsey, C. J. Workman, and D. A. Vignali. 2007. Metalloproteases regulate T-cell proliferation and effector function via LAG-3. *The EMBO journal* 26:494-504.
134. Schon, M. P., M. Schon, H. B. Warren, J. P. Donohue, and C. M. Parker. 2000. Cutaneous inflammatory disorder in integrin alphaE (CD103)-deficient mice. *J Immunol* 165:6583-6589.
135. Banz, A., A. Peixoto, C. Pontoux, C. Cordier, B. Rocha, and M. Papiernik. 2003. A unique subpopulation of CD4+ regulatory T cells controls wasting

disease, IL-10 secretion and T cell homeostasis. *Eur J Immunol* 33:2419-2428.
136. Okazaki, T., Y. Iwai, and T. Honjo. 2002. New regulatory co-receptors: inducible co-stimulator and PD-1. *Current opinion in immunology* 14:779-782.
137. Maloy, K. J., and F. Powrie. 2005. Fueling regulation: IL-2 keeps CD4+ Treg cells fit. *Nat Immunol* 6:1071-1072.
138. Soper, D. M., D. J. Kasprowicz, and S. F. Ziegler. 2007. IL-2Rbeta links IL-2R signaling with Foxp3 expression. *Eur J Immunol* 37:1817-1826.
139. Walker, L. S. 2004. CD4+ CD25+ Treg: divide and rule? *Immunology* 111:129-137.
140. Shevach, E. M. 2002. CD4+ CD25+ suppressor T cells: more questions than answers. *Nat Rev Immunol* 2:389-400.
141. Jordan, M. S., A. Boesteanu, A. J. Reed, A. L. Petrone, A. E. Holenbeck, M. A. Lerman, A. Naji, and A. J. Caton. 2001. Thymic selection of CD4+CD25+ regulatory T cells induced by an agonist self-peptide. *Nat Immunol* 2:301-306.
142. Hsieh, C. S., Y. Liang, A. J. Tyznik, S. G. Self, D. Liggitt, and A. Y. Rudensky. 2004. Recognition of the peripheral self by naturally arising CD25+ CD4+ T cell receptors. *Immunity* 21:267-277.
143. Pacholczyk, R., J. Kern, N. Singh, M. Iwashima, P. Kraj, and L. Ignatowicz. 2007. Nonself-antigens are the cognate specificities of Foxp3+ regulatory T cells. *Immunity* 27:493-504.
144. Chen, W., W. Jin, N. Hardegen, K. J. Lei, L. Li, N. Marinos, G. McGrady, and S. M. Wahl. 2003. Conversion of peripheral CD4+CD25- naive T cells to CD4+CD25+ regulatory T cells by TGF-beta induction of transcription factor Foxp3. *J Exp Med* 198:1875-1886.
145. Peng, Y., Y. Laouar, M. O. Li, E. A. Green, and R. A. Flavell. 2004. TGF-beta regulates in vivo expansion of Foxp3-expressing CD4+CD25+ regulatory T cells responsible for protection against diabetes. *Proceedings of the National Academy of Sciences of the United States of America* 101:4572-4577.
146. Wei, J., O. Duramad, O. A. Perng, S. L. Reiner, Y. J. Liu, and F. X. Qin. 2007. Antagonistic nature of T helper 1/2 developmental programs in opposing peripheral induction of Foxp3+ regulatory T cells. *Proceedings of the National Academy of Sciences of the United States of America* 104:18169-18174.
147. Rouse, B. T., and S. Suvas. 2004. Regulatory cells and infectious agents: detentes cordiale and contraire. *J Immunol* 173:2211-2215.
148. Zhou, Y. 2008. Regulatory T cells and viral infections. *Front Biosci* 13:1152-1170.
149. Luhn, K., C. P. Simmons, E. Moran, N. T. Dung, T. N. Chau, N. T. Quyen, T. T. Thao le, T. Van Ngoc, N. M. Dung, B. Wills, J. Farrar, A. J. McMichael, T. Dong, and S. Rowland-Jones. 2007. Increased frequencies of CD4+ CD25(high) regulatory T cells in acute dengue infection. *J Exp Med* 204:979-985.
150. Iwashiro, M., R. J. Messer, K. E. Peterson, I. M. Stromnes, T. Sugie, and K. J. Hasenkrug. 2001. Immunosuppression by CD4+ regulatory T cells induced

by chronic retroviral infection. *Proceedings of the National Academy of Sciences of the United States of America* 98:9226-9230.
151. Franzese, O., P. T. Kennedy, A. J. Gehring, J. Gotto, R. Williams, M. K. Maini, and A. Bertoletti. 2005. Modulation of the CD8+-T-cell response by CD4+ CD25+ regulatory T cells in patients with hepatitis B virus infection. *Journal of virology* 79:3322-3328.
152. Cabrera, R., Z. Tu, Y. Xu, R. J. Firpi, H. R. Rosen, C. Liu, and D. R. Nelson. 2004. An immunomodulatory role for CD4(+)CD25(+) regulatory T lymphocytes in hepatitis C virus infection. *Hepatology (Baltimore, Md* 40:1062-1071.
153. Chen, X., B. Zhou, M. Li, Q. Deng, X. Wu, X. Le, C. Wu, N. Larmonier, W. Zhang, H. Zhang, H. Wang, and E. Katsanis. 2007. CD4(+)CD25(+)FoxP3(+) regulatory T cells suppress Mycobacterium tuberculosis immunity in patients with active disease. *Clinical immunology (Orlando, Fla* 123:50-59.
154. Lundgren, A., E. Suri-Payer, K. Enarsson, A. M. Svennerholm, and B. S. Lundin. 2003. Helicobacter pylori-specific CD4+ CD25high regulatory T cells suppress memory T-cell responses to H. pylori in infected individuals. *Infect Immun* 71:1755-1762.
155. Suffia, I. J., S. K. Reckling, C. A. Piccirillo, R. S. Goldszmid, and Y. Belkaid. 2006. Infected site-restricted Foxp3+ natural regulatory T cells are specific for microbial antigens. *J Exp Med* 203:777-788.
156. Amante, F. H., A. C. Stanley, L. M. Randall, Y. Zhou, A. Haque, K. McSweeney, A. P. Waters, C. J. Janse, M. F. Good, G. R. Hill, and C. R. Engwerda. 2007. A role for natural regulatory T cells in the pathogenesis of experimental cerebral malaria. *The American journal of pathology* 171:548-559.
157. Belkaid, Y., C. A. Piccirillo, S. Mendez, E. M. Shevach, and D. L. Sacks. 2002. CD4+CD25+ regulatory T cells control Leishmania major persistence and immunity. *Nature* 420:502-507.
158. Steel, C., and T. B. Nutman. 2003. CTLA-4 in filarial infections: implications for a role in diminished T cell reactivity. *J Immunol* 170:1930-1938.
159. Gillan, V., and E. Devaney. 2005. Regulatory T cells modulate Th2 responses induced by Brugia pahangi third-stage larvae. *Infect Immun* 73:4034-4042.
160. Taylor, M. D., L. LeGoff, A. Harris, E. Malone, J. E. Allen, and R. M. Maizels. 2005. Removal of regulatory T cell activity reverses hyporesponsiveness and leads to filarial parasite clearance in vivo. *J Immunol* 174:4924-4933.
161. Beiting, D. P., L. F. Gagliardo, M. Hesse, S. K. Bliss, D. Meskill, and J. A. Appleton. 2007. Coordinated control of immunity to muscle stage Trichinella spiralis by IL-10, regulatory T cells, and TGF-beta. *J Immunol* 178:1039-1047.
162. Doetze, A., J. Satoguina, G. Burchard, T. Rau, C. Loliger, B. Fleischer, and A. Hoerauf. 2000. Antigen-specific cellular hyporesponsiveness in a chronic human helminth infection is mediated by T(h)3/T(r)1-type cytokines IL-10 and transforming growth factor-beta but not by a T(h)1 to T(h)2 shift. *Int Immunol* 12:623-630.

163. Singh, K. P., H. C. Gerard, A. P. Hudson, T. R. Reddy, and D. L. Boros. 2005. Retroviral Foxp3 gene transfer ameliorates liver granuloma pathology in Schistosoma mansoni infected mice. *Immunology* 114:410-417.
164. Rausch, S., J. Huehn, D. Kirchhoff, J. Rzepecka, C. Schnoeller, S. Pillai, C. Loddenkemper, A. Scheffold, A. Hamann, R. Lucius, and S. Hartmann. 2008. Functional Analysis of Effector and Regulatory T cells in a Parasitic Nematode Infection. *Infect Immun* 76:1908-1919
165. Baumgart, M., F. Tompkins, J. Leng, and M. Hesse. 2006. Naturally occurring CD4+Foxp3+ regulatory T cells are an essential, IL-10-independent part of the immunoregulatory network in Schistosoma mansoni egg-induced inflammation. *J Immunol* 176:5374-5387.
166. Baker, C. A., R. Clark, F. Ventura, N. G. Jones, D. Guzman, D. R. Bangsberg, and H. Cao. 2007. Peripheral CD4 loss of regulatory T cells is associated with persistent viraemia in chronic HIV infection. *Clin Exp Immunol* 147:533-539.
167. Suvas, S., A. K. Azkur, B. S. Kim, U. Kumaraguru, and B. T. Rouse. 2004. CD4+CD25+ regulatory T cells control the severity of viral immunoinflammatory lesions. *J Immunol* 172:4123-4132.
168. Kaviratne, M., M. Hesse, M. Leusink, A. W. Cheever, S. J. Davies, J. H. McKerrow, L. M. Wakefield, J. J. Letterio, and T. A. Wynn. 2004. IL-13 activates a mechanism of tissue fibrosis that is completely TGF-beta independent. *J Immunol* 173:4020-4029.
169. Hoffmann, W., G. Petit, H. Schulz-Key, D. Taylor, O. Bain, and L. Le Goff. 2000. Litomosoides sigmodontis in mice: reappraisal of an old model for filarial research. *Parasitol Today* 16:387-389.
170. Specht, S., L. Volkmann, T. Wynn, and A. Hoerauf. 2004. Interleukin-10 (IL-10) counterregulates IL-4-dependent effector mechanisms in Murine Filariasis. *Infect Immun* 72:6287-6293.
171. Saeftel, M., M. Arndt, S. Specht, L. Volkmann, and A. Hoerauf. 2003. Synergism of gamma interferon and interleukin-5 in the control of murine filariasis. *Infect Immun* 71:6978-6985.
172. Babayan, S., M. N. Ungeheuer, C. Martin, T. Attout, E. Belnoue, G. Snounou, L. Renia, M. Korenaga, and O. Bain. 2003. Resistance and susceptibility to filarial infection with Litomosoides sigmodontis are associated with early differences in parasite development and in localized immune reactions. *Infect Immun* 71:6820-6829.
173. Taubert, A., and H. Zahner. 2001. Cellular immune responses of filaria (Litomosoides sigmodontis) infected BALB/c mice detected on the level of cytokine transcription. *Parasite Immunol* 23:453-462.
174. Hoffmann, W. H., A. W. Pfaff, H. Schulz-Key, and P. T. Soboslay. 2001. Determinants for resistance and susceptibility to microfilaraemia in Litomosoides sigmodontis filariasis. *Parasitology* 122:641-649.
175. Lammie, P. J., and S. P. Katz. 1983. Immunoregulation in experimental filariasis. I. In vitro suppression of mitogen-induced blastogenesis by adherent cells from Jirds chronically infected with Brugia pahangi. *J Immunol* 130:1381-1385.

176. Osborne, J., and E. Devaney. 1999. Interleukin-10 and antigen-presenting cells actively suppress Th1 cells in BALB/c mice infected with the filarial parasite Brugia pahangi. *Infect Immun* 67:1599-1605.
177. MacDonald, A. S., R. M. Maizels, R. A. Lawrence, I. Dransfield, and J. E. Allen. 1998. Requirement for in vivo production of IL-4, but not IL-10, in the induction of proliferative suppression by filarial parasites. *J Immunol* 160:4124-4132.
178. Reyes, J. L., and L. I. Terrazas. 2007. The divergent roles of alternatively activated macrophages in helminthic infections. *Parasite Immunol* 29:609-619.
179. Stein, M., S. Keshav, N. Harris, and S. Gordon. 1992. Interleukin 4 potently enhances murine macrophage mannose receptor activity: a marker of alternative immunologic macrophage activation. *J Exp Med* 176:287-292.
180. Loke, P., M. G. Nair, J. Parkinson, D. Guiliano, M. Blaxter, and J. E. Allen. 2002. IL-4 dependent alternatively-activated macrophages have a distinctive in vivo gene expression phenotype. *BMC Immunol* 3:7.
181. Loke, P., I. Gallagher, M. G. Nair, X. Zang, F. Brombacher, M. Mohrs, J. P. Allison, and J. E. Allen. 2007. Alternative activation is an innate response to injury that requires CD4+ T cells to be sustained during chronic infection. *J Immunol* 179:3926-3936.
182. Liu, Y., J. A. Van Ginderachter, L. Brys, P. De Baetselier, G. Raes, and A. B. Geldhof. 2003. Nitric oxide-independent CTL suppression during tumor progression: association with arginase-producing (M2) myeloid cells. *J Immunol* 170:5064-5074.
183. Anthony, R. M., J. F. Urban, Jr., F. Alem, H. A. Hamed, C. T. Rozo, J. L. Boucher, N. Van Rooijen, and W. C. Gause. 2006. Memory T(H)2 cells induce alternatively activated macrophages to mediate protection against nematode parasites. *Nat Med* 12:955-960.
184. Loke, P., A. S. MacDonald, and J. E. Allen. 2000. Antigen-presenting cells recruited by Brugia malayi induce Th2 differentiation of naive CD4(+) T cells. *Eur J Immunol* 30:1127-1135.
185. Herbert, D. R., C. Hölscher, M. Mohrs, B. Arendse, A. Schwegmann, M. Radwanska, M. Leeto, R. Kirsch, P. Hall, H. Mossmann, B. Claussen, I. Förster, and F. Brombacher. 2004. Alternative macrophage activation is essential for survival during schistosomiasis and downmodulates T helper 1 responses and immunopathology. *Immunity* 20:623-635.
186. Tiemessen, M. M., A. L. Jagger, H. G. Evans, M. J. van Herwijnen, S. John, and L. S. Taams. 2007. CD4+CD25+Foxp3+ regulatory T cells induce alternative activation of human monocytes/macrophages. *Proceedings of the National Academy of Sciences of the United States of America* 104:19446-19451
187. Michael, E., B. T. Grenfell, V. S. Isham, D. A. Denham, and D. A. Bundy. 1998. Modelling variability in lymphatic filariasis: macrofilarial dynamics in the Brugia pahangi--cat model. *Proceedings* 265:155-165.
188. Porthouse, K. H., S. R. Chirgwin, S. U. Coleman, H. W. Taylor, and T. R. Klei. 2006. Inflammatory responses to migrating Brugia pahangi third-stage larvae. *Infect Immun* 74:2366-2372.

189. Lawrence, R. A. 1996. Lymphatic filariasis: what mice can tell us. *Parasitology Today* 12:267-271.
190. Cruickshank, J. K., K. M. Price, C. D. Mackenzie, C. J. Spry, and D. A. Denham. 1983. Infection of inbred and nude (athymic) rats with Brugia spp. *Parasite Immunol* 5:527-537.
191. Giambartolomei, G. H., B. L. Lasater, F. Villinger, and V. A. Dennis. 2001. Diminished expression of the costimulatory ligand CD80 (B7.1) gene correlates with antigen-specific cellular unresponsiveness in rhesus monkeys with lymphatic filariasis. *Acta Trop* 78:67-71.
192. Wang, P. Y., T. M. Zhen, Z. Z. Wang, Z. F. Gu, S. P. Ren, L. H. Liu, L. W. Hou, and J. L. Liu. 1994. A ten-year observation on experimental infection of periodic Brugia malayi in man. *The Journal of tropical medicine and hygiene* 97:269-276.
193. Lawrence, R. A. 1996. Lymphatic filariasis: What mice can tell us. *Parasitol Today* 12:267-271.
194. Rajan, T. V., L. Ganley, N. Paciorkowski, L. Spencer, T. R. Klei, and L. D. Shultz. 2002. Brugian infections in the peritoneal cavities of laboratory mice: kinetics of infection and cellular responses. *Exp Parasitol* 100:235-247.
195. Suswillo, R. R., D. G. Owen, and D. A. Denham. 1980. Infections of Brugia pahangi in conventional and nude (athymic) mice. *Acta Trop* 37:327-335.
196. Babu, S., L. M. Ganley, T. R. Klei, L. D. Shultz, and T. V. Rajan. 2000. Role of gamma interferon and interleukin-4 in host defense against the human filarial parasite Brugia malayi. *Infect Immun* 68:3034-3035.
197. Devaney, E., V. Gillan, I. Wheatley, J. Jenson, R. O'Connor, and P. Balmer. 2002. Interleukin-4 influences the production of microfilariae in a mouse model of Brugia infection. *Parasite Immunol* 24:29-37.
198. Ramalingam, T., L. Ganley-Leal, P. Porte, and T. V. Rajan. 2003. Impaired clearance of primary but not secondary Brugia infections in IL-5 deficient mice. *Exp Parasitol* 105:131-139.
199. Gillan, V., R. A. Lawrence, and E. Devaney. 2005. B cells play a regulatory role in mice infected with the L3 of Brugia pahangi. *Int Immunol* 17:373-382.
200. Lawrence, R. A., and E. Devaney. 2001. Lymphatic filariasis: parallels between the immunology of infection in humans and mice. *Parasite Immunol* 23:353-361.
201. Osborne, J., and E. Devaney. 1998. The L3 of Brugia induces a Th2-polarized response following activation of an IL-4-producing CD4-CD8-alphabeta T cell population. *Int Immunol* 10:1583-1590.
202. Balmer, P., and E. Devaney. 2002. NK T cells are a source of early interleukin-4 following infection with third-stage larvae of the filarial nematode *Brugia pahangi. Infection and Immunity* 70:2215-2219.
203. Gillan, V., and E. Devaney. 2005. Regulatory T cells modulate Th2 responses induced by *Brugia pahangi* third-stage larvae. *Infect Immun* 73:4034-4042.
204. Gupta, R., K. Tyagi, S. K. Jain, and S. Misra-Bhattacharya. 2003. Brugia malayi: establishment in inbred and outbred strains of mice. *Exp Parasitol* 103:57-60.
205. Knox, D. P., and D. G. Jones. 1990. Studies on the presence and release of proteolytic enzymes (proteinases) in gastro-intestinal nematodes of ruminants. *Int J Parasitol* 20:243-249.

206. Tesseur, I., K. Zou, E. Berber, H. Zhang, and T. Wyss-Coray. 2006. Highly sensitive and specific bioassay for measuring bioactive TGF-beta. *BMC cell biology* 7:15.
207. Grainger, D. J., L. Wakefield, H. W. Bethell, R. W. Farndale, and J. C. Metcalfe. 1995. Release and activation of platelet latent TGF-beta in blood clots during dissolution with plasmin. *Nat Med* 1:932-937.
208. Velarde, N., K. C. Gunsalus, and F. Piano. 2007. Diverse roles of actin in C. elegans early embryogenesis. *BMC developmental biology* 7:142.
209. Cervi, L., A. S. MacDonald, C. Kane, F. Dzierszinski, and E. J. Pearce. 2004. Cutting edge: dendritic cells copulsed with microbial and helminth antigens undergo modified maturation, segregate the antigens to distinct intracellular compartments, and concurrently induce microbe-specific Th1 and helminth-specific Th2 responses. *J Immunol* 172:2016-2020.
210. Wakefield, L. M., P. Kondaiah, R. S. Hollands, T. S. Winokur, and M. B. Sporn. 1991. Addition of a C-terminal extension sequence to transforming growth factor-beta 1 interferes with biosynthetic processing and abolishes biological activity. *Growth factors (Chur, Switzerland)* 5:243-253.
211. Laprise, M. H., F. Grondin, and C. M. Dubois. 1998. Enhanced TGFbeta1 maturation in high five cells coinfected with recombinant baculovirus encoding the convertase furin/pace: improved technology for the production of recombinant proproteins in insect cells. *Biotechnol Bioeng* 58:85-91.
212. Allen, J. E., R. A. Lawrence, and R. M. Maizels. 1996. APC from mice harbouring the filarial nematode, Brugia malayi, prevent cellular proliferation but not cytokine production. *Int Immunol* 8:143-151.
213. Furman, A., and L. R. Ash. 1983. Parameters influencing the susceptibility of neonate mice to infection with Brugia pahangi. *The Journal of parasitology* 69:1038-1042.
214. Hoerauf, A., and N. Brattig. 2002. Resistance and susceptibility in human onchocerciasis--beyond Th1 vs. Th2. *Trends Parasitol* 18:25-31.
215. Maizels, R. M., and M. Yazdanbakhsh. 2003. Regulation of the immune response by helminth parasites: cellular and molecular mechanisms. *Nature Reviews Immunology* 3:733-743.
216. Wilson, M. S., M. Taylor, A. Balic, C. A. M. Finney, J. R. Lamb, and R. M. Maizels. 2005. Suppression of allergic airway inflammation by helminth-induced regulatory T cells. *J Exp Med* 202:1199-1212.
217. Hesse, M., C. A. Piccirillo, Y. Belkaid, J. Prufer, M. Mentink-Kane, M. Leusink, A. W. Cheever, E. M. Shevach, and T. A. Wynn. 2004. The pathogenesis of schistosomiasis is controlled by cooperating IL-10-producing innate effector and regulatory T cells. *Journal of Immunology* 172:3157-3166.
218. Taylor, J. J., M. Mohrs, and E. J. Pearce. 2006. Regulatory T cell responses develop in parallel to Th responses, and control the magnitude and phenotype of the Th effector population. *Journal of Immunology* 176:5839-5847.
219. Taylor, M., L. Le Goff, A. Harris, E. Malone, J. E. Allen, and R. M. Maizels. 2005. Removal of regulatory T cell activity reverses hyporesponsiveness and leads to filarial parasite clearance in vivo. *Journal of Immunology* 174:4924-4933.

220. Huehn, J., K. Siegmund, J. C. Lehmann, C. Siewert, U. Haubold, M. Feuerer, G. F. Debes, J. Lauber, O. Frey, G. K. Przybylski, U. Niesner, M. de la Rosa, C. A. Schmidt, R. Brauer, J. Buer, A. Scheffold, and A. Hamann. 2004. Developmental stage, phenotype, and migration distinguish naive- and effector/memory-like CD4+ regulatory T cells. *J Exp Med* 199:303-313.
221. Taylor, M. D., A. Harris, S. Babayan, O. Bain, A. Culshaw, J. E. Allen, and R. M. Maizels. 2007. CTLA-4^+ and $CD4^+CD25^+$ regulatory T cells inhibit protective immunity to filarial parasites in vivo. *J Immunol* 179:4626-4634.
222. Finney, C. A., M. D. Taylor, M. S. Wilson, and R. M. Maizels. 2007. Expansion and activation of $CD4^+$CD25+ regulatory T cells in *Heligmosomoides polygyrus* infection. *Eur J Immunol* 37:1874-1886.
223. Grygielko, E. T., W. M. Martin, C. Tweed, P. Thornton, J. Harling, D. P. Brooks, and N. J. Laping. 2005. Inhibition of gene markers of fibrosis with a novel inhibitor of transforming growth factor-beta type I receptor kinase in puromycin-induced nephritis. *The Journal of pharmacology and experimental therapeutics* 313:943-951.
224. Kilian, H. D., and G. Nielsen. 1989. Cell-mediated and humoral immune response to tetanus vaccinations in onchocerciasis patients. *Tropical Medicine and Parasitology* 40:285-291.
225. Kilian, H. D., and G. Nielsen. 1989. Cell-mediated and humoral immune response to BCG and rubella vaccinations and to recall antigens in onchocerciasis patients. *Tropical Medicine and Parasitology* 40:445-453.
226. Greene, B. M., M. M. Fanning, and J. J. Ellner. 1983. Non-specific suppression of antigen-induced lymphocyte blastogenesis in *Onchocerca volvulus* infection in man. *Clinical and Experimental Immunology* 52:259-265.
227. Saparov, A., L. A. Kraus, Y. Cong, J. Marwill, X. Y. Xu, C. O. Elson, and C. T. Weaver. 1999. Memory/effector T cells in TCR transgenic mice develop via recognition of enteric antigens by a second, endogenous TCR. *Int Immunol* 11:1253-1264.
228. Gorelik, L., and R. A. Flavell. 2000. Abrogation of TGFbeta signaling in T cells leads to spontaneous T cell differentiation and autoimmune disease. *Immunity* 12:171-181.
229. Loke, P., A. S. MacDonald, A. Robb, R. M. Maizels, and J. E. Allen. 2000. Alternatively activated macrophages induced by nematode infection inhibit proliferation via cell to cell contact. *European Journal of Immunology* 30:2669-2678.
230. Rodríguez-Sosa, M., A. R. Satoskar, R. Calderón, L. Gomez-Garcia, R. Saavedra, R. Bojalil, and L. I. Terrazas. 2002. Chronic helminth infection induces alternatively activated macrophages expressing high levels of CCR5 with low interleukin-12 production and Th2-biasing ability. *Infection and Immunity* 70:3656-3664.
231. Spencer, L., L. Shultz, and T. V. Rajan. 2001. Interleukin-4 receptor-Stat6 signaling in murine infections with a tissue-dwelling nematode parasite. *Infect Immun* 69:7743-7752.
232. Martin, C., L. Le Goff, M. N. Ungeheuer, P. N. Vuong, and O. Bain. 2000. Drastic reduction of a filarial infection in eosinophilic interleukin-5 transgenic mice. *Infect Immun* 68:3651-3656.

233. Lahl, K., C. Loddenkemper, C. Drouin, J. Freyer, J. Arnason, G. Eberl, A. Hamann, H. Wagner, J. Huehn, and T. Sparwasser. 2007. Selective depletion of Foxp3+ regulatory T cells induces a scurfy-like disease. *J Exp Med* 204:57-63.
234. Aboobaker, A. A., and M. L. Blaxter. 2003. Use of RNA interference to investigate gene function in the human filarial nematode parasite Brugia malayi. *Mol Biochem Parasitol* 129:41-51.
235. Agrawal, N., P. V. Dasaradhi, A. Mohmmed, P. Malhotra, R. K. Bhatnagar, and S. K. Mukherjee. 2003. RNA interference: biology, mechanism, and applications. *Microbiol Mol Biol Rev* 67:657-685.